Control of sporulation-specific cell division in *Streptomyces coelicolor*

Elke Elza Eduarda Noens

Control of sporulation-specific cell division in *Streptomyces coelicolor*

PROEFSCHRIFT

ter verkrijging van
de graad van Doctor aan de Universiteit Leiden,
op gezag van Rector Magnificus prof. mr. P. F. van der Heijden,
volgens besluit van het College voor Promoties
te verdedigen op dinsdag 25 september 2007
klokke 15.00 uur

door
Elke Elza Eduarda Noens
geboren te Kapellen, België
op 3 april 1979

PROMOTIECOMMISSIE

Promotor	Prof. dr. C.W.A. Pleij
Co-Promotor	Dr. H.K. Koerten
	Dr. G.P. van Wezel
Referent	Prof. dr. H.A.B. Wösten (Universiteit Utrecht)
Overige Leden	Prof. dr. J. Brouwer
	Prof. dr. J.P. Abrahams
	Prof. dr. H.P. Spaink

Printing of this thesis was financially supported by the *Stichting tot Bevordering van de Electronenmicroscopie in Nederland* and the *J.E. Jurriaanse Stichting*.

Printed by Ponsen & Looijen BV, Wageningen, the Netherlands

“Do not go where the path may lead, go instead
where there is no path and leave a trail.”
Ralph Waldo Emerson

CONTENTS

1

Cell division during growth and development
The cytoskeleton

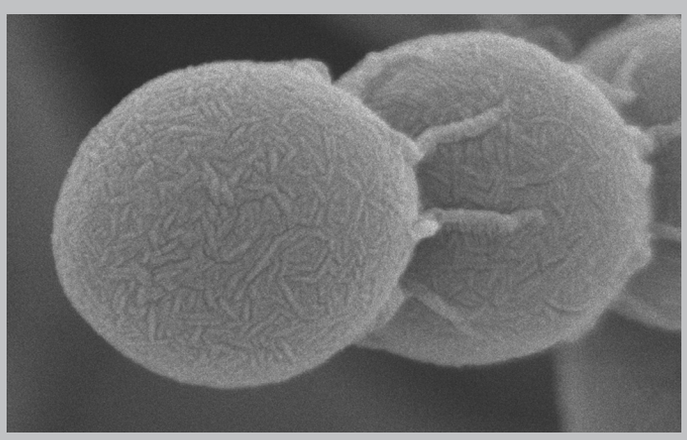

Table of contents

Introduction

Actinomycetes are gram-positive soil-dwelling bacteria whose DNA usually has a high GC content. Their natural habitat is very broad ranging from deep-sea deposits to soil and compost and they have even been detected living in symbiosis with ants (Currie *et al.,* 1999; Schultz *et al.,* 1999). They are producers of a long list of secondary metabolites, including the majority of antibiotics used today in medicine, making them extremely relevant for biotechnology. One of the best-identified genera among the actinomycetes is *Streptomyces*, with *Streptomyces coelicolor* as model system for this genus and the main organism of choice for most experiments in this thesis. Recently, the complete genome sequence of *Streptomyces coelicolor* (Bentley *et al.*, 2002) and *Streptomyces avermitilis* (Ikeda *et al.*, 2003) and a part of *Streptomyces scabies* (http://www.sanger.ac.uk/Projects/S_scabies) have become available.

In most prokaryotic species, cell division happens by binary fission; a mother cell will be divided in two equivalent daughter cells by the formation of a division septum at midcell. After completion of chromosome replication and segregation into the two future cells, the division septum will be build at a predetermined site and two progeny cells are created. During the complex life cycle of the gram-positive soil bacterium *S. coelicolor*, cell division consists of two, apparently different events (Fig. 1). *Streptomycetes* produce a mycelium network of branched hyphae, similar to that of filamentous fungi. In these branching vegetative hyphae, cross-walls are occasionally produced to generate multinucleoid compartments (Wildermuth, 1970). Development takes place after an environmental trigger, usually nutrient depletion, and aerial hyphae will grow upwards from the vegetative mycelium and break through the water-air interface. When sporulation starts, a ladder of septa is simultaneously produced at regular intervals (± 1 μm) in the aerial hyphae, dividing the hyphae into prespores, each containing one chromosome. The prespores mature and the mature spores are separated by autolysis.

Streptomycetes are a very good model for the study of bacterial development and cell division. One of the reasons is that cell division is dispensable for growth, which makes this organism an interesting model to study the functional, structural and regulatory aspects of cell division. In this chapter, we focus on all aspects of cell division in relation to growth and development of Streptomyces. The difference in the two types of septa will be presented, as well as the presence or absence of known and new cell division proteins, supported by the genome sequence.

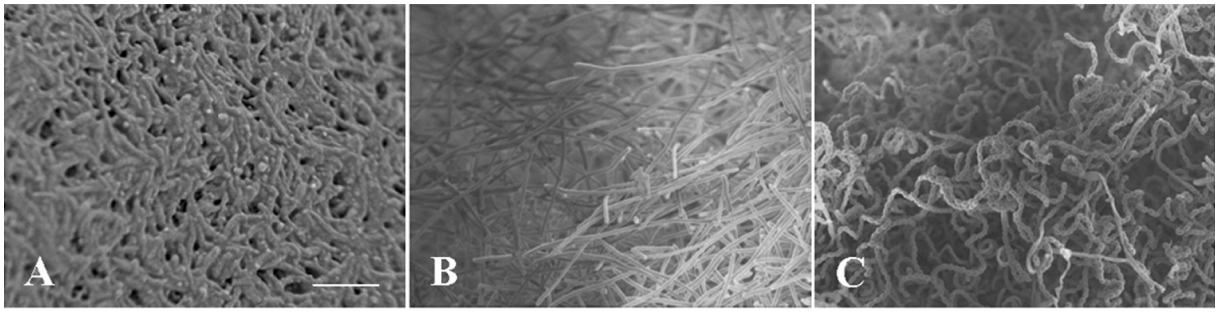

Figure 1*:* Life cycle of *S. coelicolor* grown on solid media. After spore germination, a dense network of branched vegetative mycelium is formed (**A**). During development, aerial hyphae will grow upwards (**B**). Eventually spore septa will divide the hyphae into spores (**C**). Bar = 10 μm.

Growth and vegetative division

Growth of *S. coelicolor* starts with one spore, originated from a place where nutrients are deficient and transported by wind, water or insects as dormant spores to germinate in a more favourable environment. The pleiotropic transcription factor Crp, a cAMP receptor protein, is most likely the key biomolecule responsible for the expression of proteins involved in the shift from dormant to germinating spores (Derouaux *et al.*, 2004; Piette *et al.*, 2005). During germination, one or more germ tubes emerge from the spore, which will grow and branch to form a vegetative or substrate mycelium (Chater and Losick, 1997). Fluorescently labelled vancomycin or radiolabelled N-acetylglucosamine, both incorporated into newly synthesised peptidoglycan, were used to visualise sites of nascent peptidoglycan insertion into the cell wall. In this way, peptidoglycan biosynthetic activity was primarly localised at hyphal tips and branching sites (Daniel and Errington, 2003; Gray *et al.*, 1990; Young, 2003). In *S. coelicolor*, DivIVA is an essential protein for polar growth and morphogenesis and was the first protein to be specifically localised at the tips of growing hyphae and lateral branches (Flärdh, 2003). Partial deletion results in a phenotype with irregular curly vegetative hyphae and apical branching, similar to that of many tip growth mutants in fungi, while overexpression altered cell shape and affected tip extension, causing hyperbranching (Flärdh, 2003). In *B. subtilis*, DivIVA was found to have two functions. Firstly, it is required for the stable polar localisation of MinCD and, therefore, functions as a functional analogue of the MinE protein in *E. coli* (see below) (Edwards and Errington, 1997; Fu *et al.*, 2001). Secondly, DivIVA has a role in localising or attaching the *oriC* region of the chromosome to the cell pole during sporulation (Errington, 2001). Tip growth, hyphal branching and hyphal breakage result in an exponential growth, giving rise to a complex mycelium network (Locci, 1980). In this mycelium, cell division gives rise to the formation of septa or cross-walls, often around

the middle of the growing apical cell when it reaches a certain length (Prosser and Tough, 1991). The two newly created compartments remain attached, although double membranes separate them and, therefore, no physical separation of the cells takes place. Our preliminary data show that these cross walls are more than a physical barrier as pore-like structures are visible, thus communication between the different compartments may be possible. This results in a multicellular mycelium harbouring multinucleoid compartments divided by cross-walls that are infrequently placed between varying numbers of chromosomes in the hyphae. To enlarge the dimensions of the subapical daughter cell, a new lateral branch is created, which usually occurs near a cross-wall and in this way reduces hyphal strength, suggesting some form of coordination between cell division and branching (Wardell *et al.*, 2002). The frequency of branching depends on the growth conditions: when sufficient nutrients are available, the formation of branching is supported to optimally take up the nutrients available, whereas in poor growth conditions, branching is reduced and tip extension is the dominant form of growth, resulting in the formation of "searching hyphae" (Bushell, 1988).

Proteins of the divisome of unicellular bacteria

How mysterious cell division seems to be, it is a very regular and strictly controlled event. In rod-shaped bacteria such as *E. coli*, division involves the invagination of the cell membrane, closely followed by septation, for which a change in direction of peptidoglycan synthesis is necessary. In *E. coli*, these processes involve the assembly of a multiprotein complex at the division site, called the divisome or the septosome (Table 1) (Fig. 2).

The FtsZ-ring

The earliest known component to be targeted to the cell division site is the key cell division protein, FtsZ, a structural homologue of eukaryotic tubulin and well conserved in nearly all bacteria, archaea and some eukaryotic organelles (Erickson *et al.*, 1996). FtsZ is missing in some groups of wall-less bacteria, indicating that cell division has changed in some bacteria during evolution (Vicente *et al.*, 2006). At the division site, FtsZ polymerises into a cytokinetic ring in a GTP-dependent fashion. This so-called Z-ring is located at the inner surface of the cytoplasmic membrane (Bramhill and Thompson, 1994).

The Z-ring acts as a scaffold and recruits other proteins to form a cytokinetic ring, which is also called the septasome or divisome (Fig. 2). At least 15 genes in *E. coli* are known

Table 1: Cell division-related genes in *E. coli, B. subtilis, S. coelicolor* and *S. avermitilis*.

E. coli	*B. subtilis*	*S. coelicolor*		*S. avermitilis*
gene	**gene**	**gene**	**database nr**	**database nr**
ftsA	*ftsA*	NP		NP
ftsB	NP	NP		NP
ftsE	*ftsE*	*ftsE*	SCO2969	SAV6104
ftsI	*ftsI*	*ftsI*	SCO2090	SAV6116
ftsK	*SpoIIIE*	*ftsK*	SCO5750	SAV4542
ftsL	*ftsL*	*ftsL*	SCO2091	SAV6115
ftsN	NP	NP		NP
ftsQ	*divIB*	*ftsQ*	SCO2083	SAV 6123
ftsW	*ftsW*	*ftsW**	SCO2085	SAV 6121
ftsX	*ftsX*	*ftsX*	SCO2968	SAV6105
ftsZ	*ftsZ*	*ftsZ*	SCO2082	SAV6124
zipA	NP	NP		NP
zapA	*zapA*	NP		NP
NP	*ezrA*	NP		NP
NP	*divIC*	*divIC*	SCO3085	SAV3532
minC	*minC*	NP		NP
minD	*minD*	*minD*	SCO5006	SAV3255
			SCO3557	SAV4605
minE	*NP*	NP		NP
NP	*divIVA*	*divIVA*	SCO2077	SAV6129
NP	NP	*ssgA*	SCO3926	SAV4267
		ssgR	SCO3925	SAV4268
NP	NP	*ssgB*	SCO1541	SAV6810
NP	NP	*ssgC*	SCO7289	NP
NP	NP	*ssgD*	SCO7622	SAV1687
NP	NP	*ssgE*	SCO3158	SAV3605
NP	NP	*ssgF*	SCO7175	NP
NP	NP	*ssgG*	SCO2924	NP
mreB	*mreB*	*mreB*	SCO2611	SAV5455
		mbl	SCO2451	SAV5720
NP	*mbl*			
mreC	*mreC*	*mreC*	SCO2610	SAV5456
mreD	*mreD*	mreD	SCO2609	SAV5457
NP	*mreBH*	NP		
parA	*soj*	*parA*	SCO3886	SAV4309
			SCO1772	SAV7508
parB	*spoOJ*	*parB*	SCO3887	SAV4308

NP: not present.

*: other *ftsW*-like genes: SCO2607 (SAV5459), SCO3846 (SAV4340), SCO5302 (SAV2951).

to be involved in septation: *ftsA, -B, -E, -I, -K, -L, -N, -Q, -W, -X, -Z, zipA, zapA, amiC, and envC* (Errington *et al.*, 2003) (Table 1). These division genes are well conserved among bacteria, indicating that most bacterial groups share common division machinery and mechanisms. However, not every protein is present in all the groups, suggesting a flexible cell division machinery, which has adapted to the diversity of bacterial cell envelopes, cell shapes and life cycles (e.g. FtsZ).

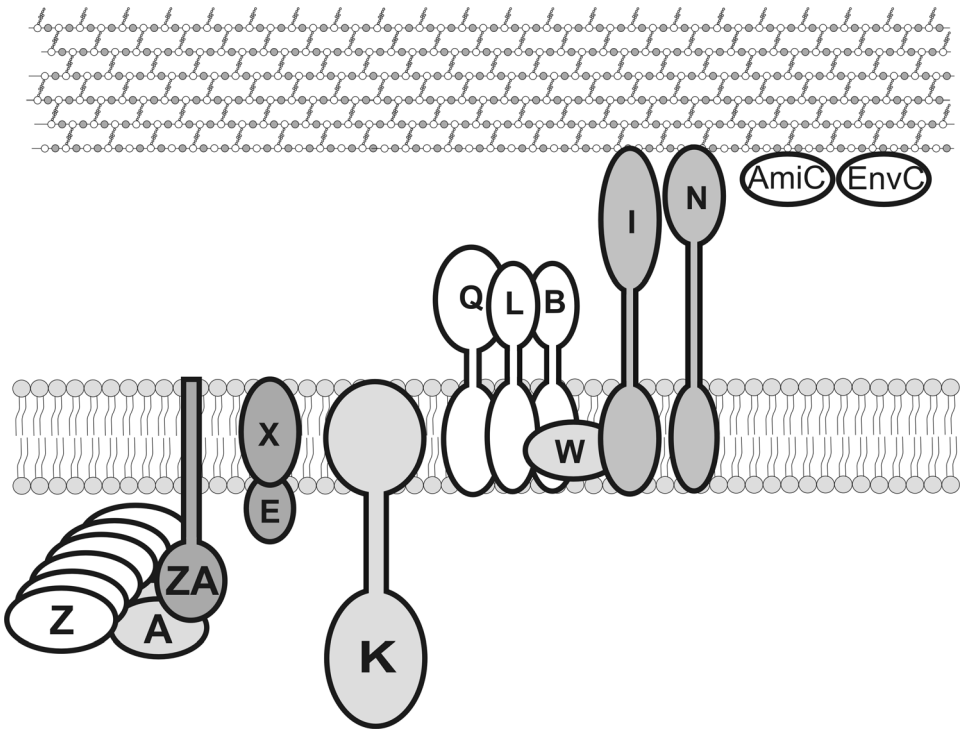

Figure 2: Proteins of the divisome of *E. coli*. Schematic overview of the order of recruitment of the proteins forming the cytokinetic ring. The proteins are ordered from left to right according to the order of assembly, taking the latest model of assembly in a concerted mode (Goehring *et al.*, 2005; Goehring *et al.*, 2006) into consideration. Protein names have been abbreviated by excluding "Fts" from them, except from ZA (ZipA), AmiC and EnvC.

Proteins involved in the early assembly of the cytokinetic ring

ftsA is conserved in most bacterial groups and the gene product belongs to the actin/Hsp70/sugar kinase superfamily and assembles at the Z-ring at an early stage, by directly interacting with FtsZ and stabilising the Z-ring (Bork *et al.*, 1992; Sanchez *et al.*, 1994).

Assembly of FtsZ in *E. coli* depends on either FtsA or ZipA or both. These proteins are bound to the inner cell membrane and are dependent on FtsZ for their localisation. They are most likely involved in linking the Z-ring to the cytoplasmic membrane (Pichoff and Lutkenhaus, 2002). Additionally, the widely conserved, though not essential protein ZapA might positively modulate Z-ring assembly *in vivo* by binding FtsZ polymers (Gueiros-Filho and Losick, 2002). *B. subtilis* harbours a negative assembly regulator, called EzrA, which modulates the frequency and positions of Z-ring formation by destabalising FtsZ polymers (Levin *et al.*, 1999).

Assembly of the downstream proteins

After the assembly of the proteins involved in linking the Z-ring to the membrane, FtsE and FtsX are recruited to the divisome. These two proteins are related to the ABC family of transporters with FtsE resembling the ATP-binding cassette interacting with the membrane component FtsX (de Leeuw *et al*; Schmidt *et al.*, 2004). The exact role of FtsE and FtsX remains unclear, although a role during constriction is suggested (Schmidt *et al.*, 2004). In most bacteria, *ftsEX* are in an operon with *ftsY*, encoding the receptor of the signal recognition particle and responsible for the correct insertion of FtsE, FtsQ, FtsX and ZipA into the *E. coli* inner membrane (de Leeuw *et al.*, 1999; Du and Arvidson, 2003).

Subsequently, FtsK, a large multifunctional membrane protein containing three cytoplasmic domains, will be assembled in the divisome. The essential N-terminal region and the intermediate linker domain have a role in cell division, while the C-terminal domain is an ATP-dependent DNA translocase functioning in chromosome dimer resolution and segregation of the chromosomes into the daughter cells (Bigot *et al.*, 2004). The *B. subtilis* homologue SpoIIIE "pumps" one of the chromosomes into the prespore compartment during the asymmetric cell division, leading to sporulation (Bath *et al.*, 2000). FtsQ assembles with FtsL and FtsB into a trimeric protein complex before localising to the septosome. However, the specific function of FtsQ is not known (Buddelmeijer and Beckwith, 2004). All three proteins harbour a transmembrane domain with the major C-terminal domain oriented on the outside of the membrane. The next proteins assembled into the divisome are FtsI and FtsW, both involved in peptidoglycan synthesis during cell division. FtsW is an integral membrane protein and belongs to FtsW/RodA/SpoVE family of proteins. The genes, encoding for these proteins, are usually paired with a gene, coding for a class B penicillin-binding protein (PBP). FtsW is proposed to act together with FtsI, a PBP3 with transpeptidase activity and responsible for synthesis of septal peptidoglycan, exactly like RodA and PBP2 do in cell elongation (Henriques *et al.*, 1998; Matsuhashi *et al.*, 1990). The last membrane protein involved in the assembly of the septosome of *E. coli*, is FtsN, which spans the periplasma and has a peptidoglycan-binding domain (Addinall *et al.*, 1997). Although the function of this protein is poorly understood, there is limited sequence similarity with cell wall amidases, suggesting a possible role in hydrolysis (Errington *et al.*, 2003). Requirement in both early and late phases of assembly is also hypothesised (Corbin *et al.*, 2004; Goehring *et al.*, 2005). Finally, the first completely periplasmic protein AmiC is recruited to the *E. coli* divisome. Its recruitment is dependent on FtsN. AmiC is an N-acetylmuroamoyl-L-alanine amidase that

specifically cleaves the bond between the peptide moiety and N-acetylmuramic acid in septal peptidoglycan to allow constriction of the septum and separation of the daughter cells (Bernhardt and de Boer, 2003). Another protein to play a direct role in septal peptidoglycan cleavage is EnvC, a lysostaphin-like, metallo-endopeptidase, which has peptidoglycan hydrolytic activity (Bernhardt and de Boer, 2004).

The recruitment of the cell division proteins to the Z-ring in *E. coli* is hypothesised to take place in a hierarchical linear order (Buddelmeijer and Beckwith, 2002) (Fig. 2). However, recent work suggests that assembly of the divisome in *E. coli* involves the formation of complexes, which are assembled in a concerted mode (Goehring *et al.*, 2005; Goehring *et al.*, 2006). In this way, a proto-ring is first formed on the cytoplasmic membrane by interactions between FtsZ, FtsA and ZipA, followed by the addition of FtsK to form the cytoplasmic ring. Later, FtsQ, FtsB and FtsL form the periplasmic connector. Subsequently, FtsW and FtsI, involved in synthesis of septal peptidoglycan are added, followed by FtsN as a ring oriented in the periplasm and connecting with the peptidoglycan (Vicente and Rico, 2006). In *B. subtilis* on the other hand, similar division proteins are cooperative in their recruitment to the division site and they are all completely interdependent for assembly (Errington *et al.*, 2003). Hence, the mode of division ring assembly is quite similar in these two bacteria.

The divisome of S. coelicolor

The genome sequences of *S. coelicolor* (Bentley *et al.*, 2002) and *S. avermitilis* (Ikeda *et al.*, 2003) allowed searching for *Streptomyces* homologues of known cell division proteins identified in other bacteria (Table 1) (Flärdh and van Wezel, 2003).

Not surprisingly, *S. coelicolor* harbours an FtsZ homologue, which is required for cell division, as in other bacteria. However, unlike in most other bacteria, *S. coelicolor* FtsZ is not essential for viability (McCormick *et al.*, 1994). *ftsZ* null mutants of *S. coelicolor* are blocked in septum formation, supporting the central role of FtsZ in cell division (McCormick *et al.*, 1994). As these strains could be sub-cultured, non-septated hyphae could be broken off without loss of viability. *S. coelicolor* is untill now the only FtsZ-containing organism that does not need FtsZ for its growth (McCormick *et al.*, 1994).

The way of recruitment of cell division proteins to the Z-ring in *S. coelicolor* is until now not known. However, certain events of sporulation-specific cell division occur in a

different order as in, for example, *E. coli*, suggesting that the cell division proteins will be differently recruited to the Z-ring in *S. coelicolor*.

Most of the membrane proteins involved in linking the Z-ring with septal peptidoglycan synthesis are present in *Streptomyces*, indicating that the basic mechanism of cell division is similar to that in most other bacteria. On the other hand, the proteins, responsible for the stability (FtsA, ZipA) and bundling of FtsZ protofilaments (ZapA, EzrA) are absent in the genomes of *S. coelicolor* and *S. avermitilis*, raising the important question as to how the Z-ring localises and attaches to the membrane. This suggests that new important division proteins, involved in these processes still need to be found in streptomycetes (Flärdh and van Wezel, 2003).

In *S. coelicolor* and other actinomycetes, *ftsEX* form an operon but *ftsY* is located elsewhere on the chromosome. It is not clear if FtsY is still involved in the membrane topology of these proteins. In chapter 6 of this thesis, the role of FtsE and FtsX is further discussed.

The genome of *S. coelicolor* harbours one clear homologue of FtsK, which has a similar function in chromosome segregation (Wang *et al.*, 2007). Chromosome segregation happens in *S. coelicolor* prior to septum closure during sporulation, while in *E. coli*, this occurs before the start of septum synthesis. This suggests that FtsK will be recruited to the divisome at a different time.

The *ftsQ* homologue of *S. coelicolor*, immediately upstream of *ftsZ*, is not essential and was not absolutely required for septation. Hyphal cross-wall formation was not completely blocked but reduced by 90-95% in an *ftsQ* null mutant, resulting in a phenotype less severe than that observed in an *ftsZ* null mutant (McCormick and Losick, 1996). An *ftsL* homologue, with conserved genomic position is present in the genome of *S. coelicolor*, while FtsB is not present (Flärdh and van Wezel, 2003). Nevertheless, *S. coelicolor* harbours a homologue of DivIC, which interacts with DivIB (FtsQ homologue) and FtsL in *B. subtilis* and most likely has a similar function as FtsB (Daniel *et al.*, 2006).

The *S. coelicolor* genome harbours four genes, whose products belong to the FtsW/RodA/SpoVE family of proteins. All of these genes are genetically paired with a gene, coding for a class B PBP. *ftsW* (SCO2085) is linked with *ftsI* (SCO2090), which act together in septal peptidoglycan synthesis (Bennet *et al.,* 2002) while *sfr* (SCO2607, *rodA* homologue) most likely acts together with PBP2 (SCO2608) in cell elongation (Burger *et al.*, 2000).

Another protein that is not present in *S. coelicolor* and the function of which is until now not clear, is FtsN. This is not surprising, as so far FtsN homologues have only been identified in Gram-negative bacteria.

In *S. coelicolor*, only sporulation-specific cell division results in physical separation of the cells (*i.e.* spores) and the genome harbours several lytic enzymes with a possible role in this process. Our microarray data revealed that for example, SCO5466, encoding a lysozyme-like hydrolase and SCO4132, coding for a lytic secreted transglycosylase (SLT), are transcribed in a developmental way, suggesting a role for these enzymes in spore separation.

Spatial control of the placement of the bacterial division site

One of the most important aspects of cell division is the correct timing and localisation of the septum. DNA must be segregated prior to septum closure to avoid guillotining the chromosome. For this, the correct localisation of FtsZ depends on two inhibitory mechanisms, namely the Min system and nucleoid occlusion (NO).

In *E. coli* as well as in many other bacteria, the Min system consists of the *minCDE* locus (Table 1). MinC is the division inhibitor, interacting with FtsZ to prevent formation of stable FtsZ rings, although it does not show site specificity. MinE is the topological specificity factor and gives, therefore, site specificity to MinC, limiting its activity to sites away from midcell. The membrane association of MinC and MinE is carried out by MinD, member of the large MinD/ParA superfamily of cytoskeletal proteins characterised by altered Walker A-type ATPase motif (Koonin, 1993). The result is a pole-to-pole oscillation, prevented from extending past midcell by the MinE-ring (Hu and Lutkenhaus, 1999; Rothfield *et al.*, 2005). *B. subtilis* and other gram-positive bacteria lack MinE, although DivIVA partly fulfils its role (Errington *et al.*, 2003). *S. coelicolor* does not harbour homologues of MinC and MinE. The function of its two MinD homologues, which lack motifs that are conserved in most other MinDs, is unclear, as *minD* null mutants have no obvious phenotype (McCormick and van Wezel, unpublished data). There is no evidence that *S. coelicolor* DivIVA plays a role in the Min system.

Cells lacking the Min system and cells in which nucleoid replication or segregation is defective have a second mechanism of negative regulation, called nucleoid occlusion (NO), which prevents septation over the nucleoids. Recently, two proteins that have a rol in NO have been identified: SlmA in *E. coli* (Bernhardt and de Boer, 2005) and Noc in *B. subtilis*

(Wu and Errington, 2004) and are essential for cell division in cells where the Min system is non-functional. In the absence of both Min and SlmA or Noc, cells fail to septate.

Two important observations make it very likely that *S. coelicolor* uses a different system for septum site selection. Firstly, the placement of the septa in both vegetative and aerial hyphae is not necessarily at midcell. Secondly, the segregation of the chromosomes into the prespores is carried out prior to septum closure, indicating that the divisome is built over the chromosomes.

The bacterial cytoskeleton

Although the major determinant of the bacterial cell shape is the bacterial cell wall, bacteria possess clear homologues of all three major types of eukaryotic cytoskeletons, which function in the determination of the cell wall architecture and have strong impacts on cell shape. As discussed above, FtsZ is a tubulin homologue and the earliest component of the division machinery to be targeted to the site of cell division site, linking the divisome with septal peptidoglycan synthesis (Erickson *et al.*, 1996). Crescentin, a bacterial equivalent of eukaryotic intermediate filament proteins, produces intermediate filament-like elements in *Caulobacter crescentus*, which maintain its curved shape (Ausmees *et al.*, 2003). The HSP70-actin-sugar kinase superfamily, including MreB, Hsp70, FtsA and ParM, are actin homologues (Bork *et al.*, 1992). Bacterial cells contain another group of cytoskeletal proteins, belonging to the large MinD/ParA superfamily, which have no homology to eukaryotic cytoskeletal elements (Barilla *et al.*, 2005; Shih *et al.*, 2003). They contain unusual Walker A-type ATPase motifs (Koonin, 1993) and are organised in filamentous structures within the cells (Suefuji *et al.*, 2002).

The bacterial actin mreB

MreB is present in Gram-positive and Gram-negative bacteria with nonspherical shapes but is absent from most bacteria displaying coccoid or spherical morphologies (Jones *et al.*, 2001). Gram-negative bacteria usually harbour only one copy of the *mreB* gene, while Gram-positive organisms often have multiple copies (Table 1). For example, *B. subtilis* has three *mreB*-like genes, called *mreB, mbl* and *mreBH*, whereas the genome of *S. coelicolor* contains two copies, *mreB* and *mbl*. MreB appears to be essential in all bacteria studied so far, including *E. coli*, *B. subtilis* and *C. crescentus*. Depletion of MreB in *E. coli, B. subtilis* and *C. crescentus* induced the formation of enlarged cells with extreme morphological defects and, finally,

resulted in cell lysis (Figge *et al.*, 2004; Jones *et al.*, 2001; Kruse and Gerdes, 2005). MreB homologues of *E. coli, B. subtilis* and *C. crescentus* all form helical-like structures underneath the cell envelope (Figge *et al.*, 2004; Jones *et al.*, 2001; Shih *et al.*, 2003; Soufo and Graumann, 2003). The use of a fluorescent derivative of vancomycin that labels nascent PG in gram-positive bacteria, revealed that the insertion of new cell wall material occurred in a helical pattern over the cylindrical part of the cell in *B. subtilis* and that Mbl is required for this lateral wall biosynthesis (Daniel and Errington, 2003). Several PBPs have been shown to display a helical distribution over the lateral wall and the localisation of PBP2 (a PG synthase) (Dye *et al.*, 2005) and LytE (a PG hydrolase) (Carballido-Lopez *et al.*, 2006) were shown to be MreB-dependent, indicating that mreB and its homologues govern cell wall morphogenesis by localisation of PG synthases and hydrolases. Other putative functions of MreB homologues include roles in correct chromosome segregation (Gitai *et al.*, 2005; Kruse *et al.*, 2003; Soufo and Graumann, 2003) and cell polarity (Gitai *et al.*, 2004).

The genome of *S. coelicolor* contains two homologues of *mreB*. One of them is located in a cluster with *mreC* and *mreD*, while the other one is located elsewhere (Burger *et al.*, 2000). In chapter 5 of this thesis, a role of these proteins in *S. coelicolor* is discussed.

The switch to development in *S. coelicolor*

When the time has come to go to a more favourable environment, motile bacteria move using a flagellum, bacterial gliding, twitching motility or changes of buoyancy. The multicellular mycelial streptomycetes are sessile microorganisms that have to go down a different alley.

In nutrient-limiting conditions, vegetative mycelium supports the development of non-branched hydrophobic aerial hyphae, which will break through the water-air surface to serve as a template for spore formation. The nutrients necessary for the production of an aerial mycelium are most likely provided by the lysis of the vegetative mycelium (Mendez *et al.*, 1985). This is one of the reasons why development goes together with antibiotic production, to kill microorganisms that are attracted by the pool of nutrients as a result of cell wall lysis.

DasR, sensing the nutritional state

Nutrient deprivation is an important signal for the onset of development. Recently, it was shown that N-acetylglucosamine (GlcNAc), derivative in nature from the polymer chitin and component of the peptidoglycan layer, is a crucial nutritional signal, whose extracellular concentration determines the choice between vegetative growth and the formation of aerial

mycelium (Rigali *et al.*, 2006). The metabolic regulator DasR, a member of the GntR-family and part of this nutrient-sensing system, controls the GlcNac regulon, including the *pts* genes *ptsH, ptsI* and *crr*, which are necessary for the uptake of GlcNAc (Rigali *et al.*, 2004). A high concentration of GlcNAc prevents the formation of aerial mycelium, while a low concentration of GlcNAc in the presence of glucose results in the phosphorylation by the intracellular components of the sugar phosphotransferase system (PTS) of specific target proteins, including WhiG. This will trigger the switch to development (Rigali *et al.*, 2006).

Mutants blocked in the formation of aerial mycelium (bld)

Mutants, most of them generated by random mutagenesis, that fail to produce the fluffy aerial mycelium are called 'bald' (*bld*) mutants because of their shiny, bald appearance. Several of the *S. coelicolor bld* mutants are often also disturbed in their primary and secondary metabolism and, therefore, lack the characteristic pigmentation of wild type substrate hyphae (Merrick, 1976; Pope *et al.*, 1996). Pope *et al.* (1996) showed that most of the *bld* mutants were affected in the regulation of carbon utilisation, suggesting that these *bld* genes are not involved in morphogenesis *per se*, but instead play a central role in the ability of these organisms to sense and/or signal starvation. Although the precise role of most of the *bld* genes is unclear, several genes encode regulatory proteins (Chater, 2001). Table 2 shows an overview of the *bld* genes in *S. coelicolor* with their possible function.

The best known *bld* gene is *bldA*, encoding a leucyl tRNA, which is necessary for the efficient translation of UUA, the rarest codon in the GC-rich *S. coelicolor* (Leskiw *et al.*, 1991a; Leskiw *et al.*, 1991b). About 150 genes of the *S. coelicolor* genome harbour one or more UUA codon (Bentley *et al.*, 2002). In this way, the translational efficiency of these genes is regulated by the expression of *bldA*. *bldA* mutants are completely defective in sporulation and antibiotic biosynthesis, the last is the result of the presence of a UUA codon in the activators of the undecylprodigiosin (Red) and actinorhodin (Act) biosynthetic clusters (*redZ* and *actII*-ORF4, respectively) (Fernandez-Moreno *et al.*, 1991; White and Bibb, 1997). An important gene that is *bldA*-dependent is *adpA* or *bldH*, the main target through which *bldA* affects differentiation (Nguyen *et al.*, 2003; Takano *et al.*, 2003). AdpA is a pleiotropic regulator belonging to the AraC family. In *S. griseus*, the expression of *adpA* is induced by A-factor, a γ-butyrolactone. This compound binds to the A-factor receptor protein (ArpA), which results in its dissociation from the *adpA* promoter. This causes the induction of the transcription of a number of genes by AdpA. Genes of the AdpA regulon involved in aerial

mycelium formation are *adsA*, the *S. coelicolor bldN* orthologue and encoding a ECF sigma factor (Bibb *et al.*, 2000; Yamazaki *et al.*, 2000), *sgmA*, encoding an extracellular metallopeptidase involved in the lysis of substrate hyphae during aerial hyphae formation (Kato *et al.*, 2002) and *amfR*, the orthologue of *S. coelicolor ramR*, resulting in production of an AmfS derivative, which is similar to SapB (Ueda *et al.*, 2002). Another important gene in *S. griseus*, dependent on AdpA is *ssgA*, a 15-kDa acidic protein involved in spore septum formation in both *S. griseus* (Jiang and Kendrick, 2000) and *S. coelicolor* (van Wezel *et al.*, 2000a). AdpA is also responsible for the regulation of several genes involved in secondary metabolism (Ohnishi *et al.*, 1999). In contract, *S. coelicolor scbA*, which produces the A-factor-like γ-butyrolactone SCB1, has no effect on the expression of *adpA* (Takano *et al.*, 2005). *S. coelicolor ssgA* is fully dependent on SsgR, although the typical upregulation of *ssgA* transcription towards the onset of sporulation was not visible in an *adpA* mutant (Traag *et al.*, 2004). Little is known about other genes present in the AdpA regulon in *S. coelicolor*.

Table 2: the *bld* genes in *S. coelicolor*.

Gene	Gene product	References
bldA	Leucyl tRNA for UUA codon	(Lawlor *et al.*, 1987) (Leskiw *et al.*, 1991b)
bldB	Small DNA-binding protein	(Pope *et al.*, 1998)
bldC	Small DNA-binding protein related to MerR transcriptional activators	(Hunt *et al.*, 2005)
bldD	Small DNA-binding protein repressing *bldN, whiG* and *sigH*	(Eccleston *et al.*, 2002; Elliot *et al.*, 1998; Elliot and Leskiw, 1999; Elliot *et al.*, 2001; Kelemen *et al.*, 2001)
bldG	Anti-anti-sigma factor	(Bignell *et al.*, 2000)
bldH	Pleiotropic regulator of the AraC family	(Nguyen *et al.*, 2003) (Takano *et al.*, 2003)
bldI	Unknown	(Leskiw and Mah, 1995)
bldJ	Unknown	(Nodwell and Losick, 1998)
bldK	Oligopeptide permease	(Nodwell *et al.*, 1996)
bldL	Unknown	(Nodwell *et al.*, 1999)
bldM	Response regulator	(Bibb *et al.*, 2000) (Molle and Buttner, 2000)
bldN	Extracytoplasmic function (ECF) sigma factor, required for the transcription of one of the two promoters of *bldM*	(Bibb *et al.*, 2000)

Although the *bld* genes have an essential role in the formation of aerial mycelium, our microarray data show that most of the *bld* genes are upregulated during sporulation or highly expressed during the whole lifecycle, which suggests that the products of these genes are necessary during more than one stage of development. Some *bldM* and *bldN* mutants result in a white aerial mycelium phenotype, which underlines this theory (Ryding *et al.*, 1999).

Mutants defective in sporulation

The first morphological change during development is the production of white, unbranched aerial hyphae, which will coil, cease to grow and serve as a template for spore formation in later stages of development. Mutants that produce aerial hyphae but fail to produce mature grey-pigmented spores are called 'white' (*whi*) mutants. The early *whi* genes (*whiA-B-G-H-I-J*) are involved in early sporulation events while the late white genes (*whiD-E-L-M-O*) function in septation and spore maturation.

1. Early *whi* genes

From the phenotypes of early *whi* mutants, it can be concluded that they are not blocked at a certain stage during spore differentiation. However, particular growth and/or morphological processes continue after the point at which they are blocked, resulting in mutation-specific terminal phenotypes (Flärdh *et al.*, 1999).

whiG, needed for the earliest stages of spore formation in aerial hyphae, encodes for an RNA polymerase sigma factor, similar to sigma factors involved in motility and chemotaxis (Chater *et al.*, 1989; Tan *et al.*, 1998). A *whiG* null mutant produces long, straight aerial hyphae containing septa with a distance similar to that of vegetative septa. Physicall cell separation was not seen in this mutant (Chater, 1972; Flärdh *et al.*, 1999). Overexpression of WhiG causes hypersporulation of aerial hyphae on solid media and ectopic sporulation of vegetative hyphae on solid and in liquid media (Chater *et al.*, 1989). Although *whiG* expression is repressed by BldD (Elliot *et al.*, 2001), *whiG* transcripts were detected during the whole life-cycle, suggesting post-transcriptional regulation (Kelemen *et al.*, 1996). Interestingly, proteome analysis showed that WhiG depends on the global components PtsH, PtsI and Crr of the PTS, suggesting a link between nutrient utilisation and development (Rigali *et al.*, 2006). The transcription of both *whiH* and *whiI* is regulated by WhiG (Kelemen *et al.*, 1996; Ryding *et al.*, 1998). Mutants of *whiH* display loosely coiled aerial hyphae that are divided into spore-like fragments, harbouring an unequal distribution of condensed DNA into bodies of variable sizes (Flärdh *et al.*, 1999). WhiH is a transcriptional regulator belonging to the GntR family and has autorepressor activity (Kelemen *et al.*, 1996; Ryding *et al.*, 1998). WhiI resembles the response regulators associated with a bacterial two-component system, although there is no histidine sensor kinase present and the phosphorylation domain found in WhiI is not present in most response regulators. This suggests that signals may be sensed through a more complex mechanism and that changes of the active state of WhiI may

depend on an atypical phosphorylation process or other post-translational modifications/activations. *whiI* null mutants produced moderately coiled aerial hyphae with few sporulation septa (Ainsa *et al.*, 1999). *whiA* and *whiB* have unusually long and curly aerial hyphae without any sporulation septa, suggesting WhiA and WhiB are required to stop aerial growth and allow sporulation to occur. *whiA* encodes a protein of unknown function with orthologues in most other Gram-positive bacteria (Ainsa *et al.*, 2000). WhiB belongs to a group of small putative transcription factors containing four conserved cysteines, only occurring in actinomycetes (Davis and Chater, 1992). Several paralogues of WhiB are present in the genome of *S. coelicolor*, including WhiD (Molle *et al.*, 2000). Expression of *parAB*, encoding chromosome partitioning proteins, depends absolutely on WhiA and WhiB (Jakimowicz *et al.*, 2006). *whiJ* mutants produce low numbers of normal spore chains. The product of this gene contains a lambda repressor-like DNA-binding domain at its N-terminus (Ryding *et al.*, 1999).

2. Late *whi* genes

In the final stage of development, the aerial hyphae are divided into unigenomic compartments by spore septa that subsequently develop into grey heat-resistant spores.

The sigma factor encoded by *sigF* is required for the later stages of sporulation. No *sigF* transcripts were detected in the early *whi* mutants, the reason for this is unknown. A *sigF* mutant displays a white phenotype although spores were produced. These spores were smaller than wild type spores with irregular shapes, a thin spore wall and uncondensed DNA. Targets, whose transcription depends on SigF have, until now not been discovered (Kelemen *et al.*, 1996; Potuckova *et al.*, 1995). *whiD* null mutants have a similar phenotype as *sigF* mutants. WhiD belongs to the wbl (WhiB-like) group (Molle *et al.*, 2000). *whiE* consists of a cluster of eight genes, encoding proteins responsible for the production of the grey spore pigment (Davis and Chater, 1992; Kelemen *et al.*, 1998). Mutations in *whiL, whiM* and *whiO* result in a disturbed sporulation-specific cell division but the gene products have not yet been identified (Ryding *et al.*, 1999). *whiK* and *whiN* were later renamed to *bldM* and *bldN*, respectively, after the discovery that null mutants of these genes were bald (Bibb *et al.*, 2000; Molle and Buttner, 2000).

Sporulation septation, Z ring assembly and segregation of the chromosomes

Both vegetative cross-walls and sporulation septa require FtsZ, FtsQ and most other cell division proteins and, therefore, most likely share a basic cell division machinery (Flärdh *et al.*, 2000; Grantcharova *et al.*, 2003; McCormick *et al.*, 1994; McCormick and Losick, 1996). However, there are some crucial differences between the two types of septa (Fig. 3). Sporulation septa are thick and separate into individual spores, while vegetative cross-walls are thinner and form connected compartments. Vegetative cross-walls are laid down with an average distance of 10 μm, often close to the middle of a hyphal cell resulting in multinucleoid compartments, whereas up to one hundred sporulation septa are produced simultaneously in one aerial hypha, at a distance of around 1 μm, creating uninucleoid spore compartments (Wildermuth and Hopwood, 1970).

The first event in sporulation-specific cell division of *S. coelicolor* is the formation of a ladder of regularly spaced FtsZ-rings in sporogenic aerial hyphae. This enormous assembly of Z-rings needs a high number of FtsZ molecules. This is provided by the upregulation of the developmentally regulated promoter of *ftsZ*, ftsZ2p, which is dependent on the early *whi* genes (Flärdh *et al.*, 2000). FtsZ-ring formation and septum synthesis in aerial hyphae occurs over non-segregated chromosomes, which will move to the prespore compartments prior to septum closure (Schwedock *et al.*, 1997). The negative effect of the nucleoid on Z-ring assembly, as in *E. coli* and *B. subtilis*, is obviously not present in *S. coelicolor*. Without a Min system or a system of nucleoid occlusion, it remains unknown how the ladder of FtsZ rings results in uniformly sized prespores, containing one single chromosome. An interesting fact is that *Streptomyces* FtsZ begins by forming spiral-shaped intermediates along the hypha, which will be remodelled into the regularly spaced Z-rings. The positioning of the chromosomes could influence this remodelling or, alternatively, the Z-rings or the synthesised septa could guide the segregation of the chromosomes (Grantcharova *et al.*, 2005). Interestingly, *ftsZΔ2p, ftsZ17* (Spo) and *whiH* mutants fail to make sporulation septa and have condensed but irregularly segregated chromosomes, suggesting a role for septation in the localisation of the nucleoids (Flärdh *et al.*, 1999; Flärdh *et al.*, 2000; Grantcharova *et al.*, 2003). Several proteins have been identified that play a role in chromosome segregation during sporulation-specific cell division in *S. coelicolor*. Developmental control of the second promoter of *parAB*, encoding chromosome-partitioning proteins, is required for the assembly of regularly spaced ParB complexes in the aerial hyphae, which are necessary for efficient chromosome segregation (Jakimowicz *et al.*, 2005; Jakimowicz *et al.*, 2006). *S. coelicolor* has also a

homologue of FtsK, a DNA translocator, which couples the completion of cell division and chromosome segregation in *E. coli* and is localised as part of the divisome (Yu *et al.*, 1998). FtsK helps in the ParB-mediated partitioning of the chromosomes to ensure that the whole moves into the prespore compartment (Wang *et al.*, 2007). The closest homologue of FtsK in *B. subtilis* is SpoIIIE. This protein is essential for sporulation as it translocates the chromosome into the asymmetric prespore complex (Bath *et al.*, 2000).

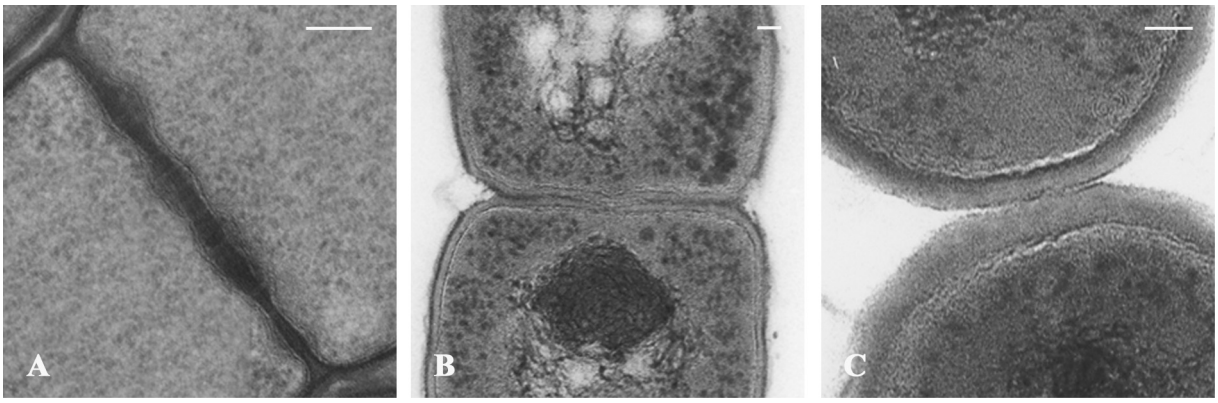

Figure 3: The difference between cross wall and sporulation septa. (**A**) a vegetative septum forming a non-physical separation between the two compartments, while pore-like structures still provide a connection. Immature spore septum (**B**) and mature spore septum (**C**). Bar = 100 μm.

Novel genes involved in development

Chaplins/rodlins

bld mutants that lack aerial hyphae, do not produce and secrete SapB. This small, hydrophobic, lantibiotic-like peptide is derived by posttranslational modification from the product of *rams*, which is part of the *ramCSAB* operon and is regulated by RamR (Keijser *et al.*, 2002). SapB can reduce the water surface tension, helping the hyphae to leave the aqueous environment of the vegetative mycelium and grow into the air. Addition of purified SapB to *S. coelicolor bld* mutants restores the formation of aerial hyphae but not sporulation (Tillotson *et al.*, 1998). After the formation of aerial hyphae, SapB was only detected in the medium and never at the surface of aerial hyphae and spores. SapB was only produced on rich media but not on minimal media containing mannitol (Willey *et al.*, 1991). Therefore, other molecules have to be present to fulfil a similar role to SapB on poor media and be responsible for the modulation of surface characteristics in accordance with environmental conditions.

Recently, two classes of structural proteins, called chaplins (Claessen *et al.*, 2003; Elliot *et al.*, 2003) and rodlins (Claessen *et al.*, 2002) were identified, which are involved in

the formation of aerial hyphae. The interplay between rodlins and chaplins results in the formation of a hydrophobic rodlet layer (Claessen *et al.*, 2004).

Deletion of the rodlin genes *rdlA* and/or *rdlB* resulted in the absence of the typical rodlet layer and the presence of fine fibrils coating the surface of aerial hyphae. Loss of the rodlins does not affect the growth or the hydrophobicity of aerial hyphae (Claessen *et al.*, 2002). The chaplins, a family of hydrophobic proteins consisting of eight members, are inserted into the cell wall of aerial hyphae of cultures grown on any media as a requirement for the aerial hyphae to escape into the air. Deletion of all eight *chp* genes (Δ*chpABCDEFGH*) resulted in a strain where formation of aerial hyphae was strongly affected, lacking both the rodlet layer and the fibrils. Addition of purified chaplins rescued the formation of aerial hyphae by lowering the water surface tension (Claessen *et al.*, 2003; Elliot *et al.*, 2003). Chaplins are assembled into small fibrils that are randomly distributed in the absence of the rodlins. In the presence of both rodlins, these fibrils are aligned into rodlets, containing two rods of each two fibrils, resulting in the hydrophobic layer (Claessen *et al.*, 2004).

SsgA-like proteins

The family of the SsgA-like proteins (SALPs), which are unique to sporulating actinomycetes, consists of seven homologues in *S. coelicolor* (SsgA-G) (Bentley *et al.*, 2002) and six in *S. avermitilis* (Ikeda *et al.*, 2003) (Table 1). All SALPs are small proteins (125-142 aa) with an average amino acid similarity of 30-40% (Keijser *et al.*, 2003).

The highest conservation is found in two sections of the proteins, corresponding to amino acid residues 13-30 and 40-65 of SsgA (Fig. 4). In total, 20 amino acid residues (15 % of the protein) are fully conserved among all 19 SALPs identified so far. Unfortunately, there are no sequences in these proteins that have similarity with known functional motifs (van Wezel and Vijgenboom, 2004).

Figure 4: Alignment of amino acid sequences of the SsgA-like proteins in *S. coelicolor*. Amino acids marked with black or grey boxes indicate sequence identity or similarity, respectively. The dashes indicate the gaps introduced to optimise the alignment.

The best-studied protein is SsgA, which was originally identified as an effector of cell division in *S. griseus* (Kawamoto and Ensign, 1995) and *S. coelicolor* (van Wezel *et al.*, 2000a). *ssgA* mutants produce normal vegetative septa but are defective in sporulation, although some viable spores are produced on mannitol-containing media (Fig 5A), indicating that SsgA only plays a role in sporulation-specific cell division (Jiang and Kendrick, 2000; van Wezel *et al.*, 2000a). SsgA has an activating role in the production of sporulation septa, as its enhanced expression in *S. coelicolor* submerged cultures results in fragmentation of the mycelia and a strong increase in the formation of septa, which were extremely thick and irregular and in this way produced spore-like compartments at high frequency (van Wezel *et al.*, 2000a). In *S.coelicolor*, no *ssgA* transcripts were detected in submerged cultures under normal conditions, while *ssgA* is strongly expressed in liquid cultures of *S. griseus* (Kawamoto *et al.*, 1997; van Wezel *et al.*, 2000a; van Wezel *et al.*, 2000b), which may explain why *S. griseus* is able to sporulate in submerged cultures but not *S. coelicolor*. Another difference between the two streptomycetes is the regulation of *ssgA*. While transcription of *ssgA* in *S. griseus* is fully dependent on AdpA (Ohnishi *et al.*, 2002), it is the upstream-located *ssgR*, a member of the family of *iclR*-type regulatory genes, which is responsible for the transcription of *ssgA* in *S. coelicolor* (Traag *et al.*, 2004). Transcription of *ssgA* and *ssgR*, both strongly upregulated during the onset of sporulation, is not dependent on the early *whi* genes in *S. coelicolor*. A possible reason for the *whi* gene-independent expression of *ssgAR* is the involvement of SsgA in the activation of submerged sporulation-specific cell division without the formation of aerial mycelium (Traag *et al.*, 2004).

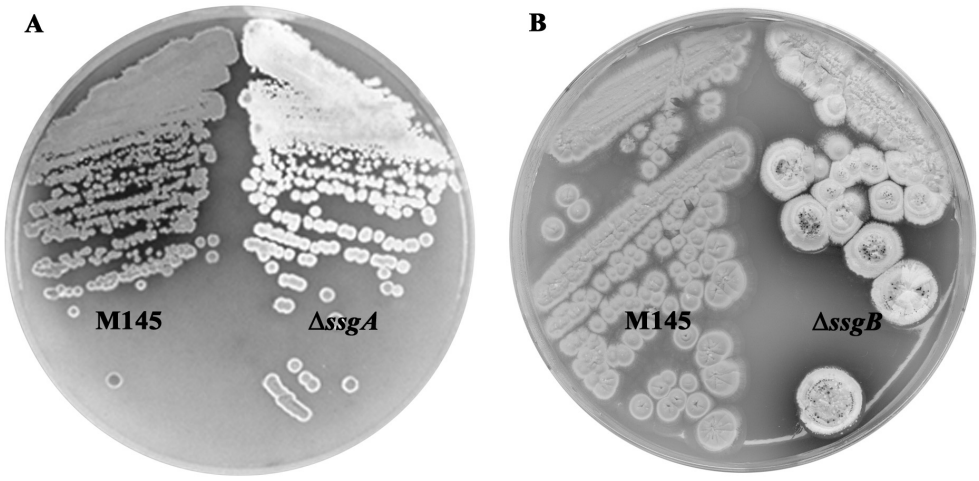

Figure 5: Effect of deletion of *ssgA* and *ssgB* on sporulation. Phenotypes of the *ssgA* mutant (A) and the *ssgB* mutant (B) and their congenic parent *S. coelicolor* M145.

Another member of the family, SsgB, is also identified to be essential for sporulation, as *ssgB* mutants resulted in a strict non-sporulating white phenotype, producing very large white colonies (Fig. 5B) (Keijser *et al.*, 2003; Kormanec and Sevcikova, 2002). *SsgB* is the only *whi* gene that is not a transcriptional regulator (Keijser *et al.*, 2003). Transcription of SsgB corresponds with aerial mycelium formation and depends on the developmental σ^H (Kormanec and Sevcikova, 2002), a sigma factor with a role in stress responses (Kelemen *et al.*, 2001). Chapter 2, 3 and 4 of this thesis go more deeply into this family of proteins.

Outline of this thesis

The study of the two types of cell division and development in *S. coelicolor* is the main focus of this thesis. An important part of the thesis regards the role of the SALPs in these processes.

In **chapter 2**, the mutants for each of the individual SALPs were created and analysed using electron and fluorescence microscopy, revealing various defects in the build-up and the degradation of peptidoglycan during sporulation. This underlines that the SALPs have an important function in the control of the sporulation process, from septum-site selection to spore separation. Using microarray analysis, the expression patterns of PBPs and autolysins present in the genome of *S. coelicolor* were checked to gain insight which one has a possible function during sporulation. In this way, certain PBPs and autolysins could be functionally related to the SALPs.

In **chapter 3**, the possible functions of the SALPs are analysed in more detail. SsgG showed a dynamic localisation, but could be found ultimately at positions resembling the sites for septum synthesis. FtsZ ladders were produced but Z-rings were regularly missing, therefore creating the typical longer spores in an *ssgG* mutant. From these observations, the important role of SsgG in septum-site selection was deduced. The importance of SsgB in the proper onset of sporulation-specific cell division of *S. coelicolor* is shown by the occasional formation of Z-rings in an *ssgB* mutant and the specific localisation of SsgB as an open ring at the sporulation septa. The conditional white phenotype of an *ssgA* mutant is most likely due to the presence of SsgC.

Chapter 4 shows the effect of a deletion of *ssgA* and *ssgR* mutant in global gene expression, using microarray analysis. The array results of the two mutants looked very similar, confirming our earlier data that *ssgA* is most likely the only gene regulated by SsgR. Many changes in gene expression in the *ssgA* mutant compared with the parental strain could be linked to phenotypical defects of an *ssgA* mutant. SsgA could be localised in a dynamically way during development, most likely at places where changes in local cell wall morphogenesis are required.

In **chapter 5,** analysis of null mutants deleted for either *mreB, mreC, mreD* and *mbl*, which encode actin-like cytoskeletal proteins, and for *pbp2*, encoding a PBP involved in lateral cell wall synthesis, were subjected to an intensive study using electron microsocpy. MreB could be localised at the septa of sporulating aerial hyphae, as bipolar foci in young spores, and as a ring- or shell-like pattern inside mature spores. Evidence is provided that all components play an important role in the control of the shape of aerial hyphae and spores.

In **chapter 6**, the function of two cell division proteins FtsE and FtsX, which are recruited to the divisome during sporulation, was studied in detail using mutational analysis and localisation studies. From our observations, we conclude that FtsEX participate in septum constriction, where they are most likely involved in the import of autolytically produced PG subunits for recycling.

In **chapter 7**, the results described in this thesis are summarised and discussed.

2

SsgA-like proteins determine the fate of peptidoglycan during sporulation of *Streptomyces coelicolor*

Elke E. E. Noens, Vassilis Mersinias, Bjørn A. Traag,
Colin P. Smith, Henk K. Koerten and Gilles P. van Wezel

Mol Microbiol (2005) 58: 929-944

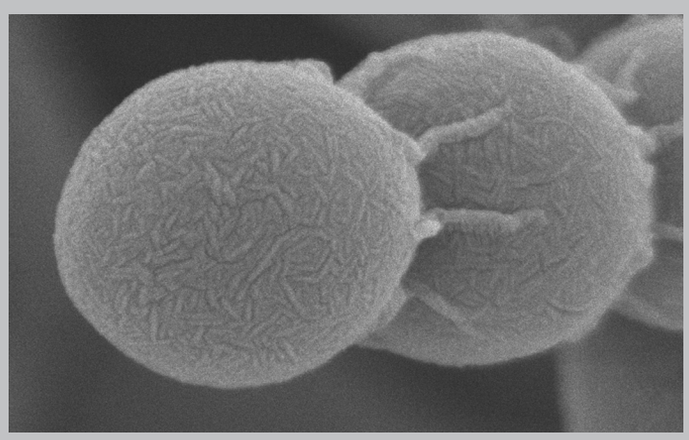

ABSTRACT

During developmental cell division in sporulation-committed aerial hyphae of streptomycetes, up to a hundred septa are simultaneously produced, in close harmony with synchromous chromosome condensation and segregation. Several unique protein families are involved in the control of this process in actinomycetes, including that of the SsgA-like proteins (SALPs). Mutants for each of the individual SALP genes were obtained, and high resolution and fluorescence imaging revealed that each plays an important and highly specific role in the control of the sporulation process, and their function relates to the build-up and degradation of septal and spore-wall peptidoglycan. While SsgA and SsgB are essential for sporulation-specific cell division in *S. coelicolor*, SsgC-G are responsible for correct DNA segregation/condensation (SsgC), spore wall synthesis (SsgD), autolytic spore separation (SsgE, SsgF), or exact septum localisation (SsgG). Our experiments paint a picture of a novel protein family that acts through timing and localisation of the activity of PBPs and autolysins, thus controlling important steps during the initiation and the completion of sporulation in actinomycetes.

INTRODUCTION

Cell division is a highly dynamic process of cell wall synthesis and breakdown, and its correct timing and localisation is one of the most studied topics in modern microbial cell biology. In *E. coli*, such control mechanisms include localisation of the septal ring exactly at the mid-cell position, mediated through the *minCDE* and *sulA* SOS systems (Autret and Errington, 2001; Justice *et al.*, 2000), coordinated peptidoglycan synthesis by penicillin-binding proteins (PBPs; reviewed in (Errington *et al.*, 2003; Holtje, 1998)), and timely DNA duplication and segregation (Errington, 2001; Sharpe and Errington, 1999). While in most bacteria a single septum is formed, that forms the cleavage furrow dividing the mother cell into the daugther cells, during sporulation of the Gram-positive mycelial bacterium *Streptomyces* many septa are simultaneously produced to form long chains of spores. In fact, *Streptomyces* undergoes two apparently different cell division events (Flärdh *et al.*, 2000; McCormick *et al.*, 1994). *Streptomyces* growth on solid media starts with the germination of a single spore that develops into a complex vegetative mycelium of branching hyphae (Chater and Losick, 1997). These vegetative hyphae are divided into connected multinucleoid compartments by vegetative septa or cross-walls. Environmental signals such as nutrient depletion result in the development of initially aseptate aerial hyphae while part of the vegetative mycelium lyses. Eventually, the aerial hyphae are dissected into spores by specialised sporulation septa, producing chains of connected uninucleoid spores (Chater, 2001), which are subsequently separated by a poorly understood process of autolytic cleavage, to produce mature spores. In contrast to cross-walls, sporulation septa are produced simultaneously and in a highly coordinated way. Another important difference with the generally accepted view of microbial cell division is the apparent lack of relatives of FtsA and ZipA, which anchor the spiral ring to the membrane (Errington *et al.*, 2003), and of homologues of *minC, minE,* and *sulA*. Therefore, the hunt is on for the discovery of novel proteins that facilitate the complex mechanism of cell division in *Streptomyces*.

The most well-known group of developmental genes is that of the *whi* genes, which were discovered by their ability to complement the White phenotype of non-sporulating and/or non-pigmented aerial hyphae (Chater, 1972; Chater, 1998). In more recent years, several important new families of developmental proteins were discovered, including the rodlins ((Claessen *et al.*, 2002)) and chaplins (Claessen *et al.*, 2003; Elliot *et al.*, 2003), hydrophobins and hydrophobin-like proteins respectively providing a water-repellant sheath

around the aerial hyphae, and the WhiB-like (Wbl) proteins, a family of small regulatory proteins with diverse targets that are also found in non-sporulating actinomycetes such as *Mycobacterium* (Soliveri *et al.*, 2000).

An emerging group of novel developmental regulators is that of the SsgA-like proteins (SALPs), which occur exclusively in sporulating actinomycetes (reviewed in (van Wezel and Vijgenboom, 2004)). Seven homologues occur in *S. coelicolor* (designated SsgA-G), and six in *S. avermitilis* ((van Wezel and Vijgenboom, 2004)). All SALPs are relatively small (125-142 aa) proteins ((Keijser *et al.*, 2003)), sharing an average amino acid similarity of 30-40%. The two members that have been studied so far, SsgA and SsgB, are essential for sporulation. The best-studied example is SsgA, which was originally identified as an effecter of cell division in *S. griseus* ((Kawamoto and Ensign, 1995), and specifically stimulates sporulation-specific cell division (van Wezel *et al.*, 2000). *ssgA* null mutants show strongly reduced sporulation, although some viable spores are produced on mannitol-containing media (Jiang and Kendrick, 2000; van Wezel *et al.*, 2000). The different timing and expression of *ssgA* explains some of the major differences in developmental control between the phylogenetically divergent species *S. coelicolor* and *S. griseus*, such as the ability of the latter strain to produce submerged spores, and the more dominant developmental role of γ-butyrolactones in this organism (Traag *et al.*, 2004; Yamazaki *et al.*, 2003). Mutation of *ssgB* resulted in a non-sporulating phenotype under all conditions, producing very large white colonies (Keijser *et al.*, 2003; Kormanec and Sevcikova, 2002)

The non-sporulating phenotypes of the *ssgA* and *ssgB* null mutants, and the fact that they occur exclusively in sporulating actinomycetes, suggested a role for the SALPs specifically during sporulation. We addressed this issue by the creation and intensive study of knock-out mutants of all *ssgA*-like genes of *S. coelicolor*, showing that each SALP is involved in a specific step in the sporulation process, from septum-site selection to the ultimate stages of spore maturation. A working model as to when and how these proteins carry out their function is proposed.

MATERIALS AND METHODS

Bacterial strains and media

The bacterial strains described in this work are listed in Table 1. *E. coli* K-12 strains JM109 (Sambrook *et al.*, 1989) and ET12567 (MacNeil *et al.*, 1992) were used for plasmid propagation, and were grown and transformed by standard procedures (Sambrook *et al.*, 1989). *E. coli* BW25113 (Datsenko and Wanner, 2000) was used to create and propagate the *S. coelicolor* cosmids used for the creation of knock-out mutants of *S. coelicolor* M145. *E. coli* ET12567 containing pUZ8002 was used for conjugation to *S. coelicolor* using the procedure described by Flett *et al*., (1997). Transformants were selected in L broth containing the appropriate antibiotics.

S. coelicolor A3(2) M145 was obtained from the John Innes Centre strain collection, and was the parent for the previously created *ssgA* mutant GSA3 (van Wezel *et al.*, 2000) and *ssgB* mutant GSB1 (Keijser *et al.*, 2003), and for the *ssgC-G* mutants described in this paper. All media and routine *Streptomyces* techniques are described in the *Streptomyces* manual (Kieser *et al.*, 2000). Soy Flour Mannitol (SFM) medium was used for making spore suspensions and R2YE agar plates for regeneration of protoplasts and, after the addition of the appropriate antibiotic, for selecting recombinants. Phenotypic characterisation of mutants was done on SFM, on R2YE (not shown) and on minimal medium agar plates (not shown) with glucose (MMgluc) or mannitol (MMman) as the sole carbon source (Kieser *et al.*, 2000).

Table 1: Bacterial strains.

Bacterial strain	Genotype	Reference
S. coelicolor A3(2)	$SCP1^+$ $SCP2^+$	(Kieser *et al.*, 2000)
S. coelicolor A3(2) M145	$SCP1^-$ $SCP2^-$	(Kieser *et al.*, 2000)
S. coelicolor A3(2) MT1110	$SCP1^-$ $SCP2^-$	(Kieser *et al.*, 2000)
GSA3	M145 Δ*ssgA* (::*aadA*)	(van Wezel *et al.*, 2000)
GSB1	M145 Δ*ssgB* (::*aac(3)IV*)	(Keijser *et al.*, 2003)
GSC1	M145 Δ*ssgC* (::*aac(3)IV*)	This chapter
GSD1	M145 Δ*ssgD* (::*aac(3)IV*)	This chapter
GSE1	M145 Δ*ssgE* (::*aac(3)IV*)	This chapter
GSF1	M145 Δ*ssgF* (::*aac(3)IV*)	This chapter
GSG1	M145 Δ*ssgG* (::*aac(3)IV*)	This chapter
E. coli JM109	See reference	(Sambrook *et al.*, 1989)
E. coli ET12567	See reference	(MacNeil *et al.*, 1992)
E. coli BW25311	See reference	(Gust *et al.*, 2003)
E. coli ET 12567/pUZ8002	See reference	(Gust *et al.*, 2003)

Plasmids, constructs and oligonucleotides

All plasmids and constructs are summarised in Table 2. Required PCRs were done with *Pfu* polymerase (Stratagene), in the presence of 10% (v/v) DMSO, with an annealing temperature of 58^0C. The oligonucleotides are listed in Table S1 (Noens *et al.*, 2005).

Table 2: Plasmids and constructs.

Plasmid/ Cosmid	Description	Reference
pHJL401	*Streptomyces/E. coli* shuttle vector (5-10 and around 100 copies per genome, respectively)	(Larson and Hershberger, 1986)
pIJ2925	Derivative of pUC19 (high copy number) with *Bgl*II sites flanking its multiple cloning site	(Janssen and Bibb, 1993)
pBR322	*E. coli* plasmid with *E. coli* ori (around 50 copies per chromosome)	(Covarrubias *et al.*, 1981)
pBR-KO	Derivative of pBR322 with engineered multiple cloning site and *tsr* gene	(Keijser *et al.*, 2003)
5F2A	Cosmid clone containing *ssgD*	(Bentley *et al.*, 2002)
E87	Cosmid clone containing *ssgE*	(Bentley *et al.*, 2002)
8A11	Cosmid clone containing *ssgF*	(Bentley *et al.*, 2002)
E19A	Cosmid clone containing *ssgG*	(Bentley *et al.*, 2002)
pGWS112	pHJL401 with 1.8 kb fragment harbouring *ssgC* (-1075/+894, relative to *ssgC*)	This chapter
pGWS122	pHJL401 with 900 bp fragment harbouring *ssgD* (-291/+608, relative to *ssgD*)	This chapter
pGWS108	pHJL401 with 1.8 kb fragment harbouring *ssgE* (-732/+1027, relative to *ssgE*)	This chapter
pGWS119	pHJL401 with 1 kb fragment harbouring *ssgF* (-404/+595, relative to *ssgF*)	This chapter
pGWS121	pHJL401 with 1.2 kb fragment harbouring *ssgG* (-459/+679, relative to *ssgG*)	This chapter
pGWS124	pBR-KO with 1.7 kb fragment harbouring the last 228 bp of *ssgE* and the last 1127 bp of SCO3157	This chapter
p*ΔssgC*	Construct for disruption of *S. coelicolor ssgC*	This chapter
p*ΔssgD*	Construct for disruption of *S. coelicolor ssgD*	This chapter
E87/*ΔssgE*	Mutant cosmid with coding region of *S. coelicolor ssgE* replaced by *aac(3)IV*, for gene replacement of *ssgE*	This chapter
8A11/*ΔssgF*	As E87/*ΔssgE*, but for *S. coelicolor ssgF*	This chapter
E19A/*ΔssgG*	As E87/*ΔssgE*, but for *S. coelicolor ssgG*	This chapter

General cloning vectors

pIJ2925 (Janssen and Bibb, 1993) is a pUC19-derived plasmid used for routine subcloning. pBR-KO is a PBR322-based vector for gene disruption in streptomycetes, which has the *Eco*RI-*Hin*dIII section replaced by the multiple cloning site of pUC18, and *tsr* ($Thio^R$) inserted into the *Bam*HI site (Keijser *et al.*, 2003). For cloning in *Streptomyces* we used the shuttle vector pHJL401 (Larson and Hershberger, 1986), which has the pUC19 *ori* for maintenance in *E. coli* and SCP2* *ori* (around 5 copies per chromosome) for maintenance in *S. coelicolor*.

Constructs for the deletion of ssgA-*like genes*

For the creation of vectors for the gene replacement of *ssgC*, *ssgD*, *ssgE*, *ssgF*, and *ssgG*, different strategies were deployed, all resulting in gene replacement constructs where (part of) the coding regions were replaced by the apramycin resistance cassette *aac(3)IV* (Blondelet-Rouault *et al.*, 1997). The coding sequences of the respective genes that were replaced by *aac(3)IV* were: -5/+102 for *ssgC*, +57/+270 for *ssgD*, and the entire coding regions of *ssgE*, *ssgF*, and *ssgG*. For details on the disruption constructs, for constructs for the complementation of the SALP mutants and for the creation of the SALP mutants, see Supplementary Materials and Methods (Noens *et al*,. 2005).

RNA isolation and DNA microarray analysis

S. coelicolor MT1110, an SCP1$^-$, SCP2$^-$ derivative of the wild type prototrophic strain 1147, was grown on Oxoid Nutrient Agar plates (Kieser et al., 2000) and mycelia were collected at 16, 18, 20, 21, 22, 23, 24, 25, 39 and 67 hours after inoculation. The time course sampling was repeated with a new set of cultures for biological replication. Biomass accumulation occurred with two clearly distinguishable phases of logarithmic growth, interceded by a short period (corresponding to sample 4, 21 h after inoculation) marking the transition from vegetative (samples 1-4) to aerial growth (samples 4-8). Spores had already been produced at 39 h, coinciding with growth cessation, and corresponded to the last two time points (samples 9 & 10, 39 h and 67 h after inoculation). For each time point RNA stabilisation, extraction and purification was carried out by methods described at http://www.surrey.ac.uk/SBMS/Fgenomics/Microarrays. For microarray hybridisation each RNA sample was reverse transcribed into Cy3-dCTP-labelled cDNA and co-hybridised with Cy5-dCTP-labelled genomic DNA from *S. coelicolor* M145, as common reference, on *S. coelicolor* M145 PCR-based microarrays. The data from the two biological replicates were averaged. Signal intensities were detected with an Affymetrix 428 laser scanner.

Computer analysis.

The 16-bit TIFF microarray images were analysed with BlueFuse (BlueGnome) spot quantification software and the generated raw data files were imported into GeneSpring^{TM} (Agilent Technologies) for normalisation and analysis of gene expression profiles. Data were normalised per spot (ratio of cDNA to genomic DNA signals) and per chip (ratios divided by the 50th percentile of the ratios within the array). Only data that scored a spot quality

confidence value >0.30 (a parameter calculated by the BlueFuse software) were included in the gene expression analysis. Expression profiles were analysed by hierarchical clustering using the Spearman correlation, which clustered the genes based on profile similarity regardless of their relative expression levels.

The TMPred program (http://www.ch.embnet.org/software/TMPRED_form.html) was used for the prediction of transmembrane domains in proteins and Clustal (Higgins et al., 1996) for multiple protein alignment and for the creation of the phylogenetic tree. Adobe Photoshop^{TM} was used for management of all microscopy images.

Microscopy

Electron microscopy

Morphological studies of surface-grown aerial hyphae and spores of *S. coelicolor* M145 and mutant derivatives by cryo-scanning electron microscopy (cryo-SEM) was performed as described previously, using a JEOL JSM6700F scanning electron microscope (Keijser *et al.*, 2003). Transmission electron microscopy (TEM) for the analysis of cross-sections of hyphae and spores was performed with a Philips EM410 transmission electron microscope as described previously (van Wezel *et al.*, 2000),

Confocal fluorescence microscopy

Impression preparations from the surface of 6-day-old colonies on SFM plates were taken and fixed with methanol. For staining of the DNA, the coverslips were incubated with propidium iodide (1μg ml^{-1}) (Sigma) in the dark for 15 min at room temperature, allowed to air dry and positioned on a microscope slide containing a drop of 20% glycerol, mycelium facing downwards. Staining of the cell wall was performed in 25mM borate buffer pH8, 0.9% sodium chloride + 2mg ml^{-1} BSA, 5μl ml^{-1} FITC-wheat germ agglutinin (Biomedica) for 15 min in the dark at room temperature, allowed to air dry and positioned in a drop of 20% glycerol on a microscope slide. Samples were analysed with a Leica TCS-SP2 confocal fluorescence microscope, equipped with an oil-immersed 100 × Planapo objective and a CCD camera. Digital images were assembled using ADOBE PhotoShop software.

RESULTS

Phylogenetic analysis of SALPs

The *ssgA*-like genes have so far only been identified in actinomycetes that undergo extensive morphological development, and predominantly in streptomycetes. We identified a homologue of *ssgB* in the partial genome sequences of the actinomycetes *Thermobifido fusca* and *Kineococcus radiotolerans*, but it is absent from *Mycobacterium*, *Corynebacterium, Nocardia* and *Rhodococcus*. The streptomycetes whose genome sequence has been completed (*S. coelicolor* and *S. avermitilis*) or almost completed (*S. scabies*) contain six or seven *ssgA*-like genes, and on the basis of hybridization and genomics data we ascertained that *S.lividans* contains the same 7 SALPs as *S. coelicolor* (*i.e.* SsgA-G). Phylogenetic analysis of all known SALP protein sequences revealed three main branches, namely the SsgA branch, the SsgBG branch and the SsgDE branch (Fig. 1). SsgC and SsgF of *S. coelicolor* do not cluster with any of the other proteins, thus forming separate branches, and we have so far only identified homologues of these proteins in *S. lividans*. Analysis of a zoo blot of various streptomycetes (*S. albus, S. fradiae, S. lividans* 1326, *S. coelicolor, S. griseus, S. ramocissimus, S. mobarense, S. cinnamoneus*) revealed homologues of SsgA, SsgB, SsgD, SsgE in all streptomyces species analysed, and typically also SsgG (though absent from *S. avermitilis*), suggesting they constitute the core set of SALPs, which is supplemented by 2-3 additional proteins in probably all streptomycetes.

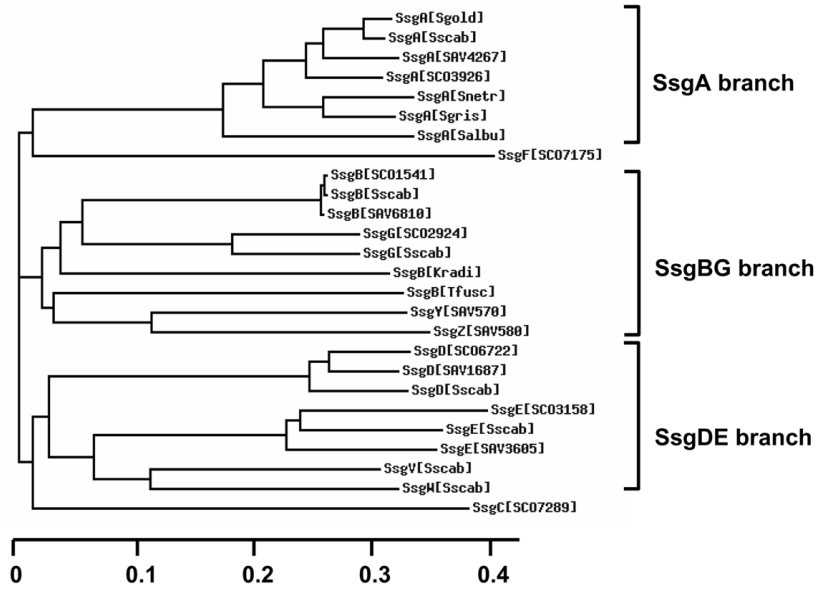

Figure 1: Phylogeny of the SALP protein family. Phylogenetic tree analysis of SsgA-like proteins (SALPs) was done using the ClustalX program. All proteins shown in the figure are listed in Noens *et al.,* 2005, Table S2.

Construction of mutants

The genomic organisation around *ssgC* (SCO7289), *ssgD* (SCO6722), *ssgE* (SCO3158), *ssgF* (SCO7175) and *ssgG* (SCO2924) is shown in Fig. 2. Considering that the genes located downstream of *ssgC*-*ssgG* are divergently transcribed, polar effects due to insertional gene replacements were not anticipated. The individual mutants for each of these genes were created using targeted gene replacement strategies, which are detailed in the Supplementary Materials and Methods (Noens *et al*., 2005). For all individual mutants multiple independent recombinants were obtained, and the correct recombination event was verified by PCR and Southern hybridisation (data not shown). The exact sections of the genes that were replaced by the apramycin resistance cassette *aac(3)IV* were (relative to the translational start): -5/+102 of *ssgC*, +57/+270 of *ssgD*, and precisely the coding regions of *ssgE*, *ssgF* and *ssgG* genes. Since *ssgE* partially overlaps the divergently transcribed ORF SCO3157, which encodes a putative penicillin-binding protein, the latter ORF was restored by integration of plasmid pGWS124, resulting in a wild type SCO3157, but still mutant *ssgE*. This mutant, called GSE1*, was studied alongside GSE1 to ensure that the *ssgE* mutant phenotype was solely due to the replacement of *ssgE* itself and not (entirely or partly) to the disruption of SCO3157. All mutants were restored to the phenotype of the parental strain by the introduction of a low copy-number vector harbouring the relevant *ssgA*-like gene and its promoter sequences. In all experiments described in this paper, we simultaneously analysed the mutants and their genetically complemented derivatives, to verify that all observed abnormalities were due solely to the gene replacement and not to a second-site mutation.

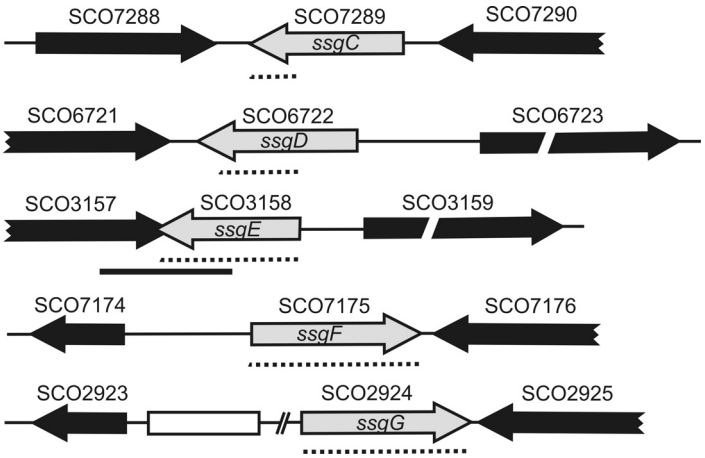

Figure 2: Genetic organisation of the *ssgA*-like genes. *ssgA*-like genes are shown as grey arrows while adjacent genes are shown as black arrows. Above the gene arrows are the corresponding SCO numbers. The dotted line under the *ssgA*-like genes represents (part of) the sequence which is replaced by the apramycine resistance cassette *aac(3)IV* in the knock out mutants. The fragment used for restoration of SCO3157 in the *ssgE* mutant is shown by a bold line.

Phenotypes of the mutants

All seven individual SALP mutants of *S. coelicolor* were plated on various media together with the parental strain M145 (Fig. 3). Sporulation was then assessed visually (spores are grey-pigmented), and verified by phase contrast microscopy and viable counts. The *ssgA* mutant GSA3 had a non-sporulating (White) phenotype on glucose-containing media, while it produced a small amount of spores on the mannitol-containing medium SFM (Fig. 3), in accordance with our earlier observations (van Wezel *et al.*, 2000). The *ssgB* mutant GSB1 displayed the typical unconditional non-sporulating phenotype (Fig. 3) (Keijser *et al.*, 2003).

The new SALP mutants Δ*ssgC-G* all produced grey-pigmented spores after 6 days, although *ssgG* - which is phylogenetically related to *ssgB* - produced significantly fewer spores, highlighted by its light grey appearance (Fig. 3). SsgG belongs to the SsgBG branch of the phylogenetic tree, and both proteins are important for the early stages of septum formation (Keijser *et al.*, 2003) and below). Both the *ssgE* mutant and *ssgF* mutant hyper-sporulated on mannitol-containing media, while there was no significant difference on glucose-containing media (data not shown). Analysis of impression prints by phase contrast microscopy showed that both mutants produced short spore chains, consisting of mostly three or four spores in the *ssgF* mutant, while predominantly single spores where observed for *ssgE* mutant.

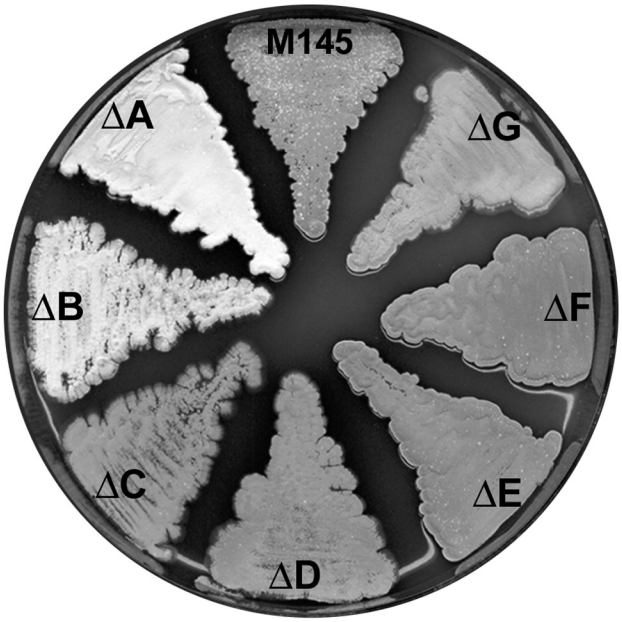

Figure 3: Phenotypes of the *ssgC-G* mutants and their congenic parent *S. coelicolor* M145 on solid media. Strains were grown on SFM at 30°C for 6 days. ΔA, ΔB, ΔC, ΔD, ΔE, ΔF and ΔG are the *ssgA, ssgB, ssgC, ssgD, ssgE, ssgF* and *ssgG* mutants of M145, respectively.

Light microscopy indicated that significant differences in the degree of sporulation also occurred between the *ssgC-ssgF* mutants, verified by repeated spore analyses. Spores were prepared, and diluted to the same spectrophotometric density. Total counts were then done using a haemocytometer and viable counts by plating dilutions (1-10^4 spores/plate) on SFM agar plates. There was a good correlation between microscopic and viable counts, with increased sporulation of GSE1 and GSF1, and reduced sporulation of GSG1. However, spore preparations from the *ssgD* mutant GSD1 consistently contained at least an order of magnitude fewer spores than expected on the basis of its pigmentation, as judged by viable counts and microscopy, suggesting that production of the WhiE spore pigment (Kelemen *et al.*, 1998) was enhanced in this mutant.

Analysis of the mutants by cryo-scanning electron microscopy (cryo-SEM)

Surface-grown colonies of *S. coelicolor ssgC-G* mutants and the parental strain M145 were analysed in detail by cryo-SEM (Fig. 4). *S. coelicolor* M145 produced long spore chains with spore septa at regular intervals, producing 0.8 μm long spores (Fig. 4A-B). Aerial hyphae of the *ssgC* mutant produced extraordinarily long spore chains (Fig. 4C), and contained spores of highly variable lengths (Fig. 4D). In some of the large spores, indentations were visible at the midcell position, suggesting initiated but unfinished septation (Fig. 4D, insert). The *ssgD* mutant produced many straight and undifferentiated aerial hyphae, while spores appeared relatively normal (Fig. 4E-F). Consistent with light microscopy (above), GSE1 and GSF1 sporulated abundantly. The *ssgE* mutant GSE1 showed large areas with only free spores, suggesting premature autolysis-driven spore separation. Perhaps as a result of this spore maturation defect, many of the spores had aberrant sizes in length and occasionally in width (Fig. 4G-H). GSF1 also produced spores of variable sizes (Fig. 4I-J). Cryo SEM failed to visualise the short spore chains typical of the *ssgF* mutant and confirmed by phase contrast microscopy and confocal FM (below); this is most likely a combination of the cryo fixation procedure, where short spore chains are easily lost, and the fact that longer hyphae obscure the shorter ones. *ssgG* mutant GSG1 produced clearly fewer spore chains with normal overall lengths (Fig. 4K), but always containing many irregularly sized spores, most of which were exactly two, three or four times the normal size (detailed in Fig. 4L). As discussed below, septa seem to be occasionally 'skipped' in the *ssgG* mutant.

Confocal Fluorescence Microscopy

Confocal fluorescence microscopy was used to visualise nucleoid distribution and active peptidoglycan synthesis and breakdown during sporulation-specific cell division (Fig. 5, for a full colour version, see p172-173). Nucleic acids were stained with the fluorescent dye propidium iodide (PI), and confirmed using the alternative fluorescent dyes DAPI and 7-aminoactinomycin D (7-AAD). Accumulation of peptidoglycan precursors (as a result of active PG synthesis or breakdown) was visualised by staining with the fluorescein-labelled lectin wheat germ agglutinin (WGA). WGA binds to short oligomers of N-acetylglucosamine (NAG) and N-acetylmuramic acid (NAM), which are alternately coupled to form the peptidoglycan strands (reviewed in (Holtje, 1998)). Fully polymerised peptidoglycan (PG), such as in the mature spore wall, is not recognized by WGA.

The wild type sporulation process on surface-grown cultures is visualised in Fig. 5A, showing fully developed 6 days old *S. coelicolor* M145. Mature spore chains (spo) are not stained with fluo-WGA (right panel), but DNA staining (PI) visualises the completed segregation and condensation of chromosomes (middle panel). In contrast, actively dividing aerial hyphae (aer) are stained very well with fluo-WGA, clearly visualising the build-up of individual septa in a ladder-like fashion, highly similar to FtsZ ladders (Schwedock *et al.*, 1997). Perhaps surprisingly, the DNA still appeared evenly distributed in the aerial hypha, a sign that (completion of) DNA segregation follows septal peptidoglycan synthesis. Earlier stages of sporulation were studied using younger plates (2-4 days old; light image in Fig. 5B, left). WGA binding to the outer side of in particular the spore poles revealed NAM-NAG oligomers, most likely due to peptidoglycan degradation; this shows that these spores undergo the final step of spore maturation, namely the autolytic separation of the cell wall separating the spores (Fig. 5B, right + insert). Expectedly, when wild type spores had fully matured, no WGA staining was observed. DNA had already fully segregated at this stage (Fig. 5B, middle).

The *ssgA* and *ssgB* mutants have a phenotype typical of early sporulation mutants, and fail to produce septa in the aerial hyphae, while vegetative septation was not significantly affected (Keijser *et al.*, 2003; van Wezel *et al.*, 2000). In contrast, the *ssgC* mutant showed extensive *de novo* septum formation in younger aerial hyphae (WGA staining). Surprisingly, coordination of septum formation and DNA segregation was lost in over half of all aerial hyphae seen in this mutant; many empty prespore compartments were observed (Fig. 5D, small arrows), while the intense PI-stained foci indicated the presence of multiple copies of

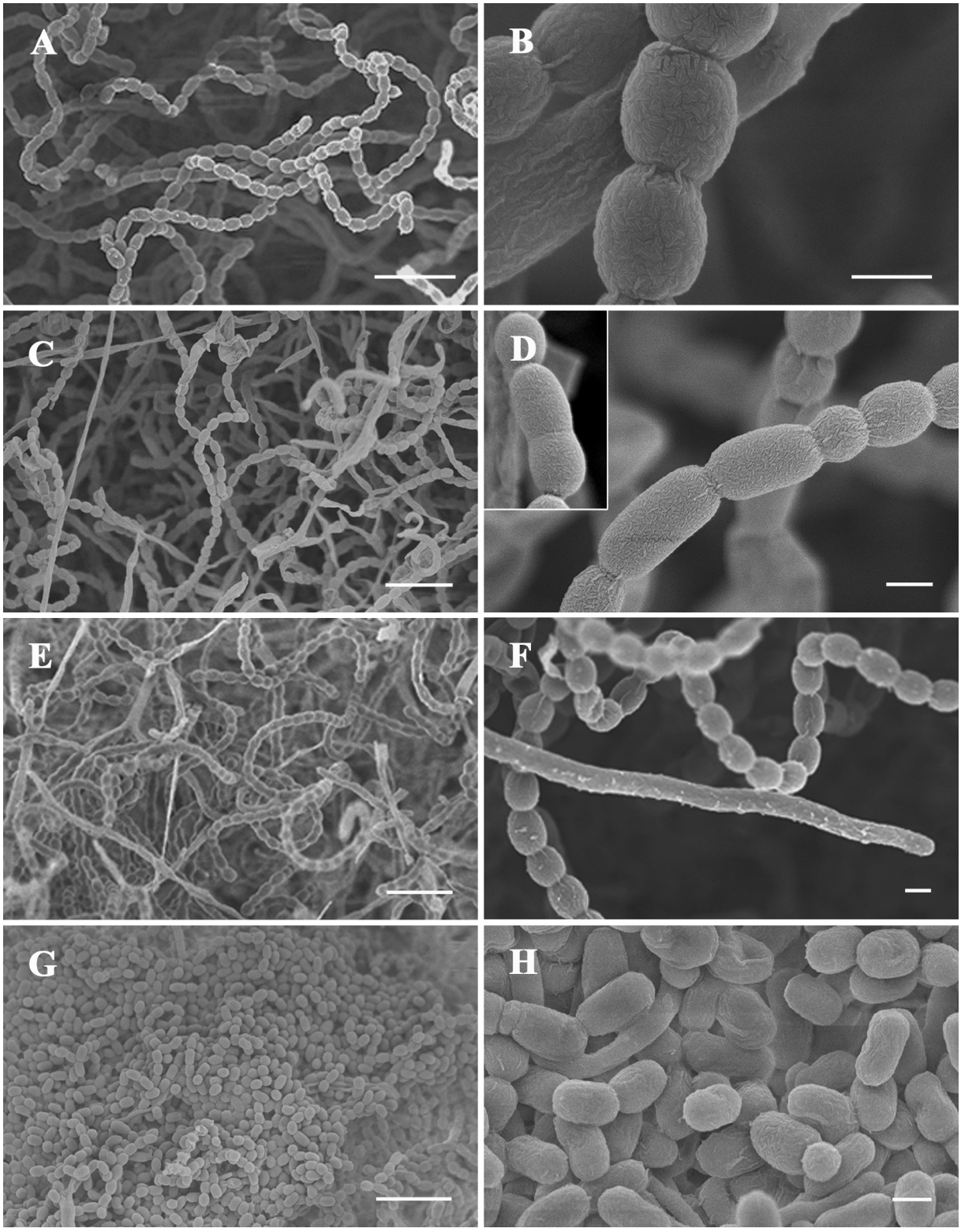
A
B
C
D
E
F
G
H

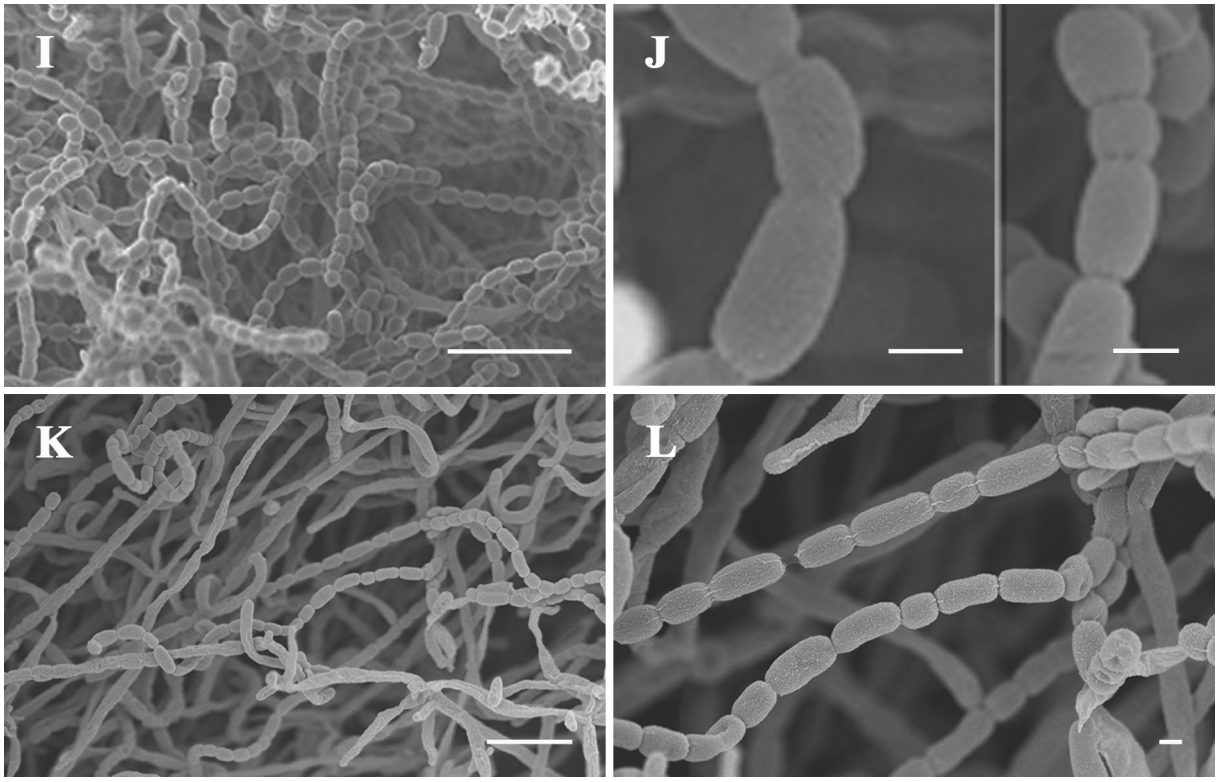

Figure 4: Phenotypic characterisation by cryo-scanning electron microscopy. Samples were taken from 6-day old cultures grown on SFM at 30°C. The left panel shows low magnification (Bar = 5 µm), and the right panel high magnification scanning electron micrographs (Bar = 0.5 µm). **(A-B)** Wild type spore chains of the parental strain M145; **(C-D)** The *ssgC* mutant produces long spore chains **(C)** with spores of irregular sizes **(D)**; **(E-F)** The *ssgD* mutant produced many non-sporulating aerial hyphae and spore chains with irregular spores; **(G-H)** deletion of *ssgE* resulted in the formation of predominantly single spores; **(I-J)** Abundant sporulation of the *ssgF* mutant consisting of spore chains with aberrant spore sizes **(J, insert)**; **(K-L)** *ssgG* mutant with normal- and double-sized spores.

the genome in others (Fig 5D, arrowheads). This is clearly visualised in the DNA/fluo-WGA overlay (Fig. 5D, right panel). Occasionally, spore chains with normal DNA distribution were observed, but these invariably contained mature spores with aberrant sizes (and typically double-sized; Fig. 5C). Spores of the *ssgD* mutant occasionally showed irregular sizes, although DNA distribution appeared normal (Fig. 5E). As described above, mutation of *ssgE* or *ssgF* resulted in strains that sporulated very well, but produced predominantly single spores (*ssgE*; Fig. 5F) or short spore chains (*ssgF*; Fig. 5G). DNA had segregated normally, as shown by the regular pattern of PI staining (middle panels). In contrast to M145, after 7 days of incubation both late sporulation mutants still had many immature spores, and NAG-NAM oligomers were readily identified by WGA staining. In the case of the *ssgE* mutant, only chains of spores were visualised by WGA, and at intersections between adjacent spores. Intriguingly, a large proportion of the *ssgF* spores contained WGA-stained foci exclusively at

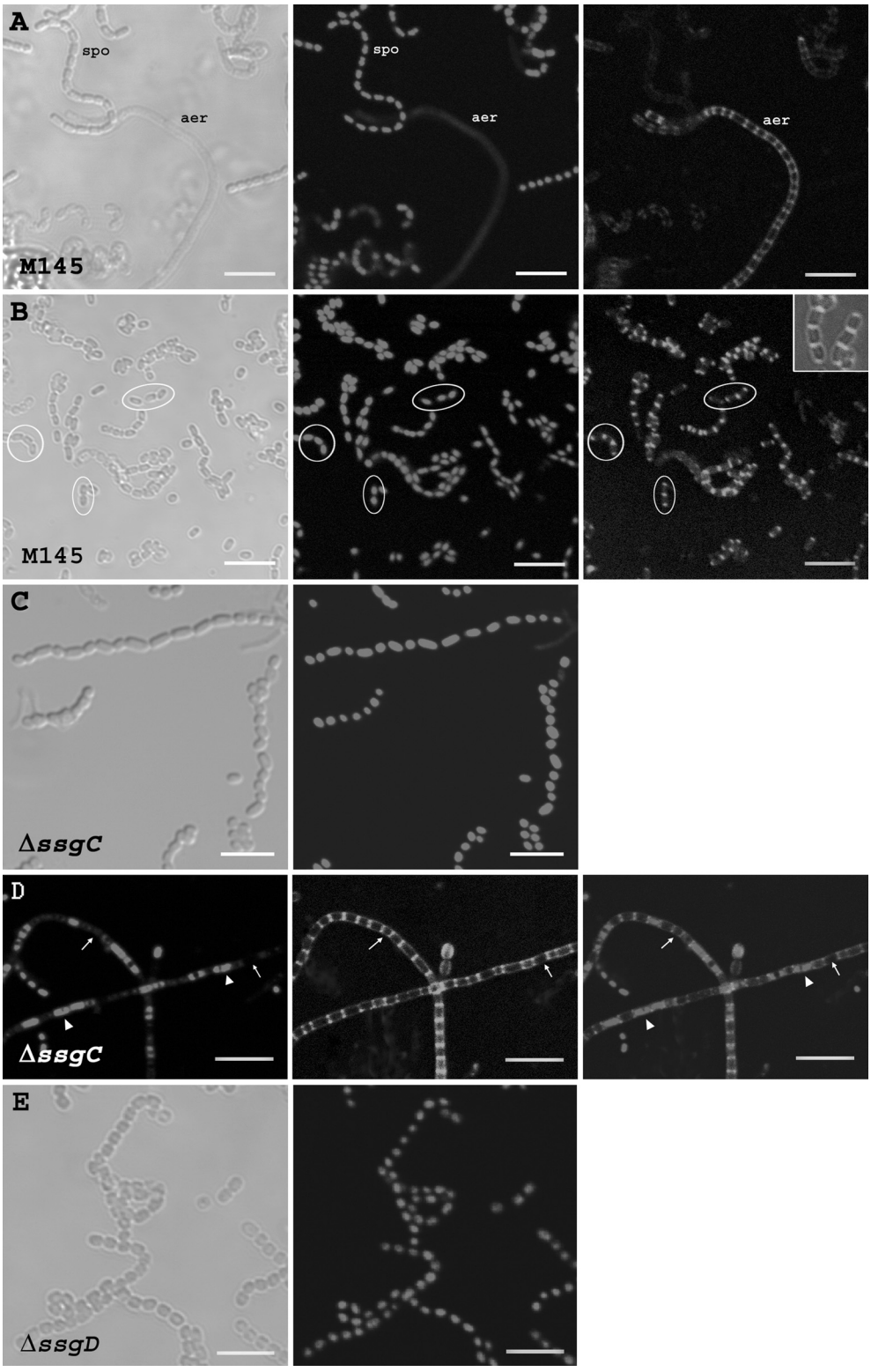
A
spo
aer
M145
spo
aer
aer
B
M145
C
ΔssgC
D
ΔssgC
E
ΔssgD

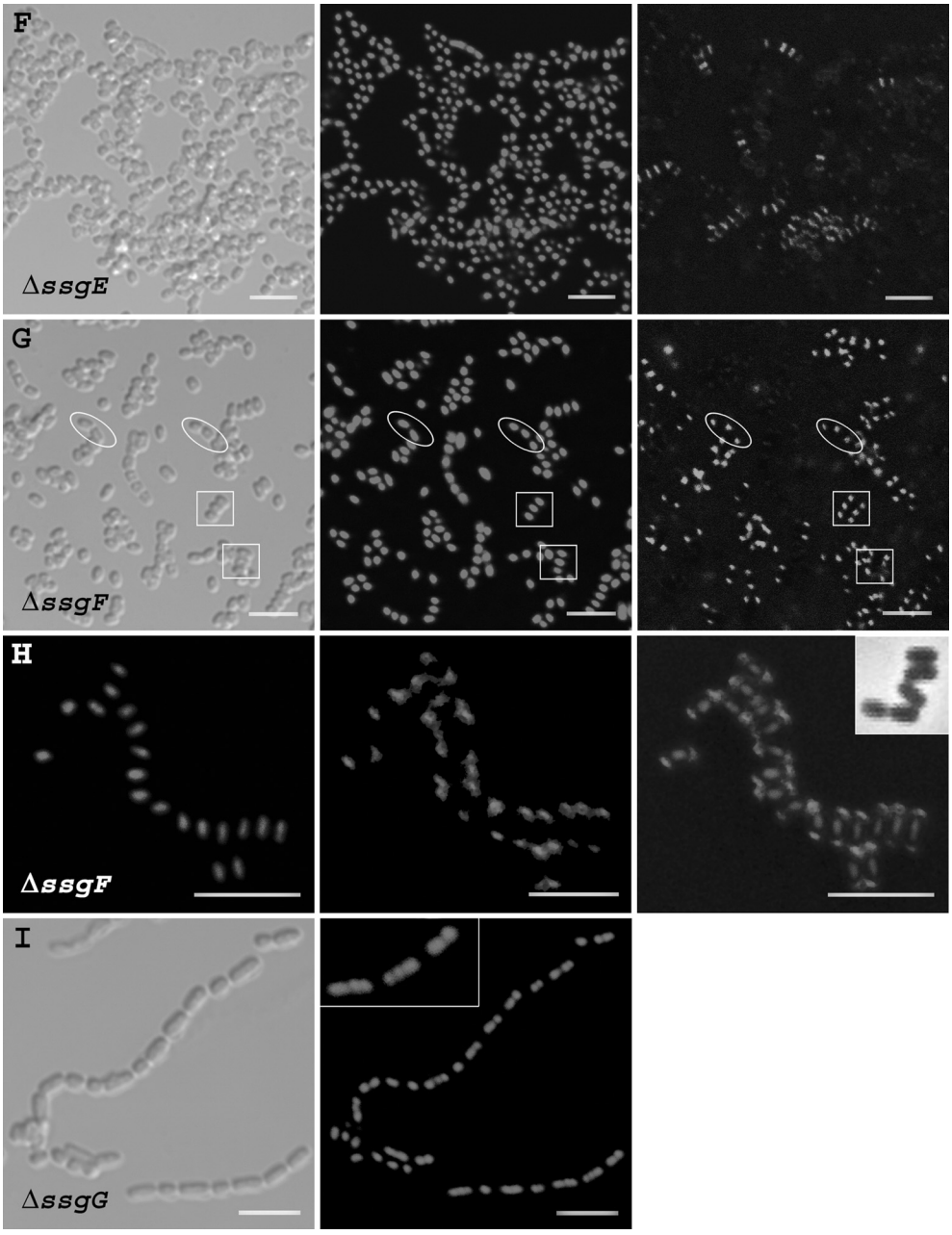

Figure 5: Analysis of the *ssgC-G* mutants by confocal fluorescence microscopy.
Samples were prepared from surface-grown cultures of the parental strain *S. coelicolor* M145 **(A)** and its mutant derivatives Δ*ssgC* **(C-D)**, Δ*ssgD* **(E)**, Δ*ssgE* **(F)**, Δ*ssgF* **(G-H)**, and Δ*ssgG* **(I)** all grown on SFM plates for 6 days at 30°C. *S. coelicolor* M145 **(B)** was grown on SFM plates for 2-4 days at 30°C. DNA and peptidoglycan subunits were visualised with PI (red) and fluorescein-WGA (green), respectively. The first column shows light microscopy micrographs, the middle column shows DNA, and the third column shows peptidoglycan subunits **(A-C, E-G, I)** or the first column shows DNA, the second shows peptidoglycan subunits and the third shows an overlay of PI and WGA **(D-H)**. **(B, insert)** overlay of fluo-WGA and light microscopy of spores of M145 after 2-4 days of growth, clearly showing staining of spore poles by WGA. **(H, insert)** shows a light microscopy micrograph of Δ*ssgF* spores. **(I, insert)** shows a higher magnification of Δ*ssgG* spores with four and respectively three copies of the chromosome. For mature *ssgD* and *ssgG* mutants no WGA stained septa were detected, and images were therefore omitted. Arrowheads show compartments with multiple chromosomes, small arrows show compartments without DNA, white circles highlight WGA-stained spore poles and squares highlight 'rotated' spores. Bar = 5 μm. (Full colour version, see p172-173).

the poles, and always at the outside of the spore walls, similar to M145 in an early stage of the sporulation process (around 4 days old; Fig. 5G). In contrast to the parental M145, where such polar staining disappeared when spores matured, the spores of the *ssgF* mutant always showed this typical polar WGA staining, suggesting a distinct defect in the final stages of autolytic spores separation. Furthermore, many spore chains contained spores that were rotated by 90^0 (Fig. 5G, squares). While such 'rotated' spores were never observed in M145, they constituted approximately 14% (28 out of 201) of all *ssgF* mutant spores. In fact, many spore chains showed a clear transition from normally oriented to rotated spores (Fig. 5H + insert).

As was already apparent from the SEM micrographs, mutation of *ssgG* resulted in many larger compartments with twice, three times or sometimes four times the regular spore size (Fig. 5I + insert). DNA staining clearly identified multiple copies of well-segregated chromosomes in these larger compartments (Fig. 5I), with the DNA content proportional to the increase in spore size (two genomes in a double-sized spore *etcetera*). Thus, DNA segregation could be completed in the absence of septum synthesis (see Discussion).

Transmission electron microscopy (TEM)

TEM was used to closely examine hyphae, septa and spores (Fig. 6). *S. coelicolor* M145 showed typical vegetative cross-walls (Fig. 6A); aerial hyphae produced typical chains of immature (6B) and fully developed mature spores (6C). The spore chains were surrounded by a sheath (small arrow in Fig. 6B-C) that most likely represents the remnants of the parental hyphal wall containing the rodlet layer (David Hopwood, pers. comm.).

The *ssgA* and *ssgB* mutants were studied previously; on mannitol-containing media, the *ssgA* mutant produced occasional regular spore chains (van Wezel *et al.*, 2000), while the *ssgB* mutant was completely devoid of any septa in the sporulation stage (Keijser *et al.*, 2003). Both strains had normal vegetative septa. Interestingly, the *ssgC* mutant strongly resembled the *ssgA*-overexpressing strain GSA3. Around 60% of all cross-walls were irregular (insert in Fig. 6D), as counted from many TEM micrographs of biologically independent samples. In often occurring aberrant vegetative hyphae of the *ssgC* mutant, unfinished cross-walls were observed, which appear like spots of PG in these TEM cross-sections, but are most likely small septal rings in 4D. The distance between them was on average 2 μm (Fig. 6D). The spores of GSC1 were also heteromorphous, with varying lengths and spore walls (Fig. 6E). Interestingly, the *ssgC* mutant strongly fragments in submerged

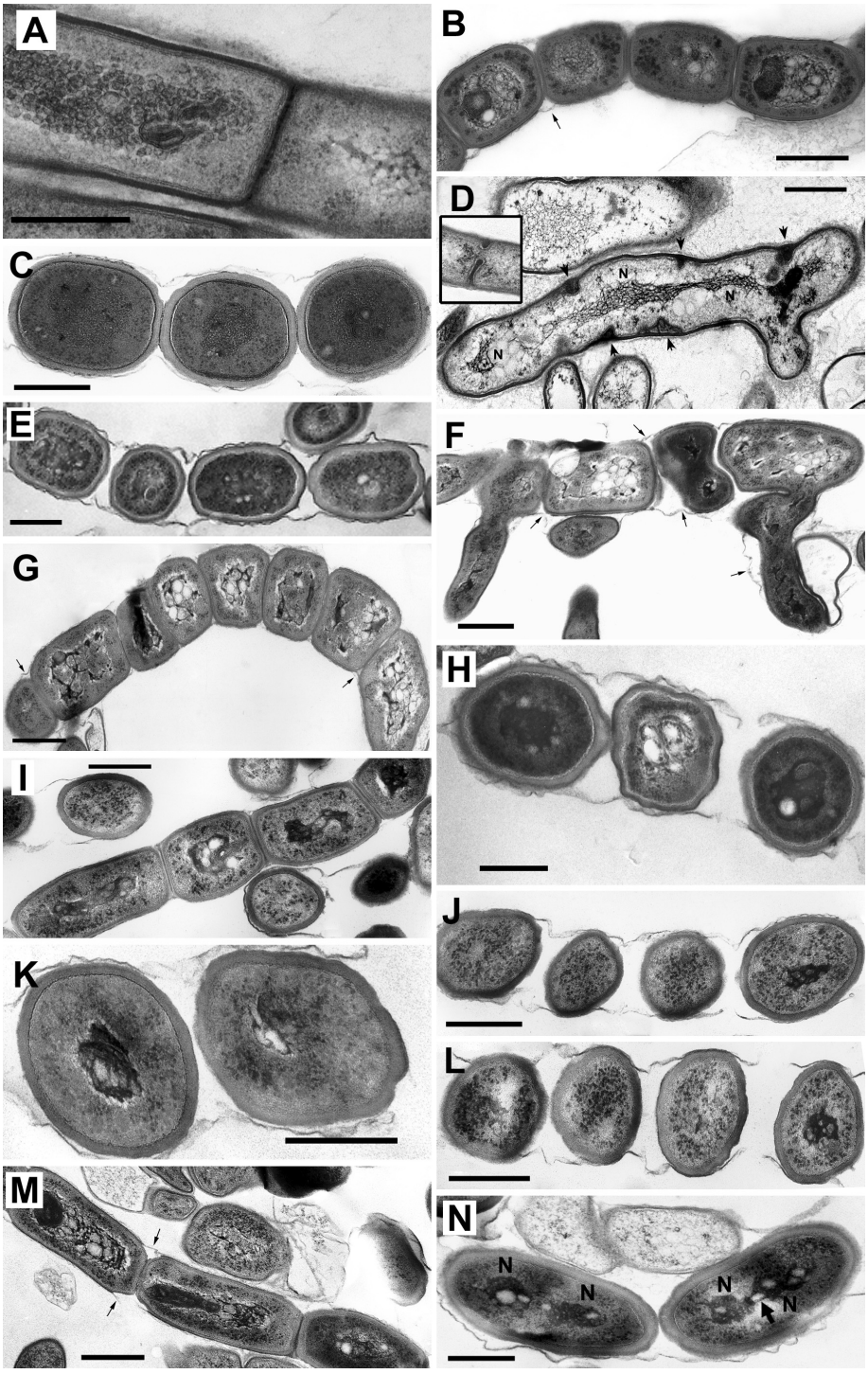

Figure 6: Transmission electron micrographs of hyphae and spores of *S. coelicolor* and its SALP mutant derivatives.
Samples were taken after growth for 6 days on SFM at 30°C. The parental strain M145 produced normal vegetative hypha with cross-walls **(A)**, immature spores **(B)** and mature spore chains **(C)**; In contrast, *ssgC* mutant GSC1 formed irregular vegetative cross-walls **(D+insert)** and heteromorphous spore chains **(E)**. The *ssgD* mutant regularly produced spores with walls with the same width as the aerial hyphae **(F)**, as well as irregular immature **(G)** and mature spore chains **(H)**. Deletion of the late sporulation gene *ssgE* resulted in almost completely normal prespore chains **(I)** and mature spores **(J)**. A large proportion of the mature spore chains of the *ssgF* mutant had spores rotated by 90° **(K-L)**. Around 50% of all spores produced by the *ssgG* mutant were twice, three times or even four times the length of normal spores **(M-N)**, and contained multiple genomes; clearly visible is that the chromosomes had almost completely segregated, but were still linked by a filamentous structure (arrow). The nuclear region is represented by N. Small arrows highlight the sheath surrounding the spore chains. Bar = 0.5 µm.

cultures, and over-expression of *ssgC* inhibits sporulation, again in line with an opposite role of *ssgC* as compared to *ssgA* (not shown).

The *ssgD* mutant showed pleiotropic defects in the integrity of hyphae and spores, perhaps reflecting its high and life-cycle-independent expression ((Traag *et al.*, 2004) and microarray data). Many of the spores had a cell wall similar to that of the lateral wall of non-sporulating aerial hyphae, lacking the typical thick peptidoglycan layer (Fig. 6F). Furthermore, immature spore chains (Fig. 6G) had a highly irregular appearance, with a squashed appearance and with variable spore sizes. Mature spore chains often showed a mix of relatively normal and aberrant spores (Fig. 6H). Analysis of spore preps of GSD1 revealed no difference in heat or lysozyme tolerance to spores from the parental M145 (not shown).

Like most SALP mutants, the *ssgE* mutant produced spores with variable spore sizes (Fig. 6I; see also Fig. 4H). Occasionally, mature spore chains (surrounded by a sheath) were observed but there consistently was a large void between the individual spores.

The *ssgF* mutant produces chains consisting of regular looking spores containing a typical thick spore wall. However, TEM also identified spore chains with spores rotated by 90 degrees, such as also seen by confocal FM (see Fig. 5G-H); here, the individual spores were not attached to each other in the normal head-to-tail fashion, *i.e.* with their spore poles adjacent to each other, but rather in a parallel fashion, resulting in a wider spore chain (800 nm instead of the regular 600 nm; Fig 6K-L).

As SEM and FM analysis of the *ssgG* mutant, also TEM revealed many large spores, with exactly twice, three times or even four time the normal length (Fig. 6M). TEM clearly confirms the presence of multiple genomes in the larger spores, while there is no evidence of any cell wall material between the almost completely segregated chromosomes. This shows that septal peptidoglycan synthesis and DNA segregation are uncoupled in this mutant. Interestingly, while the chromosomes are almost completely separated, they are still attached to each other through a thin filamentous structure (Fig. 6N, arrow).

DNA microarray analysis of cell division and developmental genes

The data above established that the SALPs play a role in the control of peptidoglycan synthesis and autolysis. To judge which PBPs and autolysins present on the *S. coelicolor* genome are most obvious candidates for peptidoglycan synthesis during development, and relate functionally to SALPs, we performed microarray analyses on *S. coelicolor* (Fig. 7, p176). Transcription of SALP genes was compared to that of genes involved in the

maintenance of the peptidoglycan (PBPs and autolysins). As for the SALP genes, microarray analysis of *ssgA* and *ssgC* produced data below the confidence threshold. Detailed analysis performed previously showed that transcription of *ssgA* and its activator *ssgR* is induced towards the onset of sporulation, and *ssgD* is strongly transcribed throughout development (Traag *et al.*, 2004). Microarray data (Fig. 7B, p176) support this for *ssgD* and *ssgR*, and show that *ssgB* is strongly activated towards sporulation. Of the two spore maturation genes, *ssgE* is expressed at a low level, while *ssgF* is strongly expressed, both with a life-cycle independent expression profile. Finally, *ssgG* is expressed relatively strongly during vegetative growth and again towards sporulation, suggesting a possible role in both developmental stages. The expression profiles were confirmed by promoter probing using the *redD* promoter-probe system (van Wezel *et al.,* 2000c). Particularly *ssgB*, *ssgD,* and *ssgF* were expressed in the aerial hyphae (not shown). The transcription profiles were all confirmed by RT PCR analysis and by promoter probing, except for *ssgF*; while microarrays predicted high and almost growth-phase independent expression, detailed analysis showed that *ssgF* is in fact expressed during sporulation, and at a low level.

Several *pbp* genes are developmentally controlled (Fig. 7B, p176). SCO3847 and SCO4013, both encoding homologues of *Bacillus* PBP3, were upregulated during both the onset of both vegetative and aerial growth; SCO5487 and SCO5039 were switched on primarily during early vegetative growth, while the *ftsI*-like genes SCO3156 and SCO3771 were induced at a time related to aerial growth, although transcription of SCO3156 was switched off again during sporulation.

Autolysins are responsible for the breakdown of peptidoglycan, *e.g.* during spore separation. Several autolysins are developmentally controlled; these are either switched on during both vegetative and aerial growth (SCO2116, for one of several AmpD-type autolysins), or relate to a specific developmental stage, namely at a time related to aerial growth (SCO5466, encoding a lysozyme-like autolysin) or to sporulation (SCO4132, encoding the SLT autolysin, the only lytic transglycosylase in *S. coelicolor*). Interestingly, in collaboration with Dr. Rigali (Liege, Belgium) we recently discovered that SCO5466 is strongly downregulated in a *crp* mutant, which fails to produce the cAMP receptor protein CRP (Piette *et al.*, submitted for publication). This mutant is strongly disturbed in autolysis of the prespore chain, confirming the likely involvement of SCO5466 in spore maturation.

DISCUSSION

This paper discusses the role of the SsgA-like proteins in the control of specific aspects of the sporulation process, from initiation of septal peptidoglycan synthesis to the separation of spores from the maturing prespore chain. To better discuss their individual functions, we discriminate between the following landmark events during the sporulation process in aerial hyphae of *Streptomyces* (Fig. 8); (I) Prespore formation, consisting of (IA) septum site selection; (IB) septum initiation; (IC) septum growth; (ID) DNA segregation and condensation; (IE) septum closure; and (II) spore maturation, consisting of (IIA) growth (thickening) of the spore wall peptidoglycan; (IIB) Spore separation by PG autolysis; (IIC) Spore release. Our data show that each of the individual SALP genes affects one of these landmark events, and relate to the control of peptidoglycan synthesis or breakdown. This includes the first examples of proteins that control the exact sites where septa are initiated (stage IA, by SsgG) and autolytic spore separation (stage IIBC, by SsgE and SsgF). The phenotypes of the mutants and the suggested function of the genes during sporulation are summarised in Table 3.

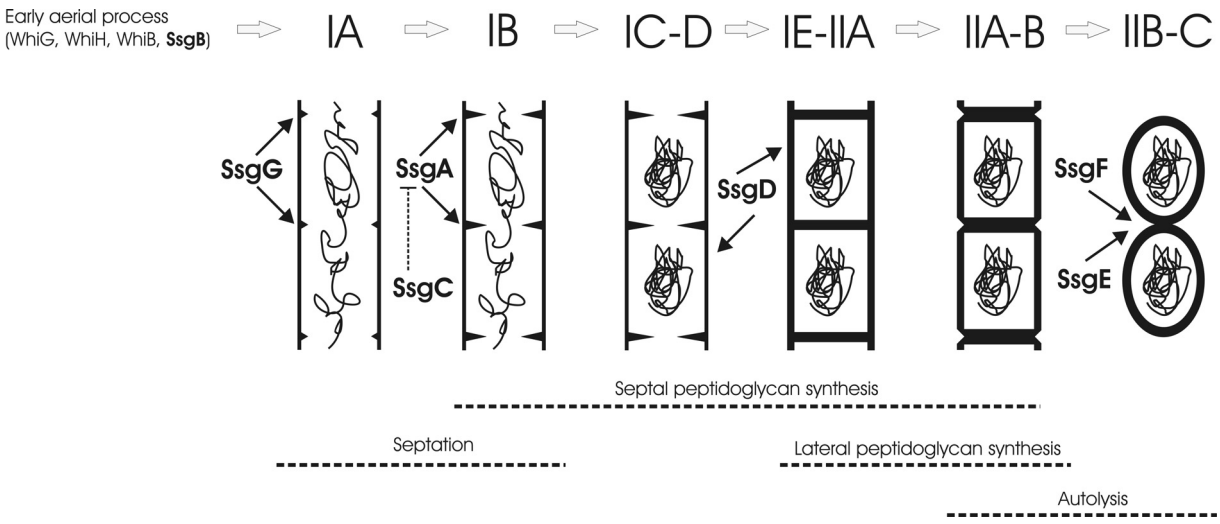

Figure 8: Model of the development of sporulation-committed aerial hyphae and suggested function of SALPs.
Several events observed during the sporulation process in aerial hyphae of *Streptomyces* are shown; (I) Prespore formation, consisting of (IA) septum site selection; (IB) septum initiation; (IC) septum growth; (ID) DNA segregation and condensation; (IE) septum closure; and (II) spore maturation, consisting of (IIA) growth (thickening) of the spore wall peptidoglycan; (IIB) Spore separation by PG autolysis; (IIC) Spore release. The dotted lines represent specific events that occur in the sporulation process. A suggested role for the SALPs is indicated in the figure. SsgB is most likely involved in the signalization for growth cessation. SsgG controles septum site localisation. SsgA is involved in the initiation of septum formation, and is antagonised by SsgC. The function of SsgD is related to the synthesis of peptidoglycan along the lateral cell wall. SsgE and SsgF are involved in the autolysis of the mature spore chain with SsgE controlling correct timing of spore dissociation, and SsgF ensuring correct final stages of autolytic detachment. See Discussion.

Table 3: Phenotype of the SALP mutants and the timing of activity during development.

Gene	Phenotype of SALP mutants	Timing of activity[a]
ssgA	Conditional non-sporulating phenotype; enhanced expression stimulates sporulation-specific cell division	Septum initiation (IB).
ssgB	Strictly non-sporulating phenotype, very large ("immortal") colonies.	Correlates temporally to growth cessation of aerial hyphae prior to onset of sporulation
ssgC	Irregular spores, imperfect segregation of DNA, very long ladders of spore septa.	Controls septum site initiation and DNA segregation (IB)
ssgD	Aberrant spore wall.	Lateral cell wall synthesis (IIA).
ssgE	Predominantly single spores due to accelerated autolysis.	Correct timing of spore dissociation (IIB-C).
ssgF	Short spore chains; old spores were stained with WGA at the outside of the spore poles; rotated spores.	Final stages of spore separation (IIB-C).
ssgG	Septa are regularly skipped, without affecting DNA segregation. Many spores exactly two, three or four times the normal size.	Controls septum site localisation (IA).

a. Numbers (IB-IIC) correspond to developmental phases illustrated in Figure 6.

Control of peptidoglycan synthesis during prespore formation

Microarray data (Fig. 7, p176) and previously published transcriptional analyses revealed that *ssgA* and *ssgB* and to a lesser extent *ssgG* are induced during late aerial growth and early sporulation. Deletion of these genes results in complete (*ssgA*, *ssgB*) or partial (*ssgG*) loss of the ability to sporulate. The aerial hyphae of the *ssgA* and *ssgB* mutants are essentially aseptate. Over-expression of *ssgA* resulted in hyper-septation of both vegetative and aerial hyphae, and TEM micrographs revealed many extremely thick and unfinished cross-walls in the vegetative hyphae, leaving a distinct gap in the middle (van Wezel *et al.*, 2000). This strongly suggests that SsgA activates the initial steps in the polymerisation of septal peptidoglycan. *ssgB* is the most highly conserved cell division-related gene in actinomycetes, and a rare example of a *whi* gene that is not a transcriptional regulator. *ssgB* mutants produce very long aseptate aerial hyphae, forming 'immortal' colonies (Keijser *et al.*, 2003). The sporulation process is initiated as soon as aerial growth ceases (Chater, 2001), requiring a block of PBP2 enzyme activity, and this signal most likely depends on SsgB. Interestingly, many granules accumulate in the hyphae of the *ssgB* mutant (Fig. S3, Noens *et al.*, 2005), which due to their electron-dense nature are likely to contain unincorporated cell wall precursor material. The same granules were also observed in the PBP2 mutant (a kind gift from Dr. G. Hobbs), providing evidence of a functional relationship between SsgB and PBP2.

The function of SsgC is the reverse of that of SsgA. *ssgC* mutants produce the spiral-like distribution of peptidoglycan along the wall of vegetative hyphae, typical of SsgA-overexpressing strains. Also, extraordinary long ladders of septa are often observed in this mutant, with disturbed DNA segregation, similar to strains over-expressing SsgA. *ssgC* is one of the two strain-specific SALPs of *S. coelicolor*. So far, we have only found homologues of

ssgC in strains with low expression of *ssgA* (such as *S. coelicolor* and *S. lividans*; unpublished data). On the basis of our observations, we propose that SsgC functions as an antagonist of SsgA.

The *ssgG* gene is a rare cell division mutant, and an opportunity to improve our understanding of how multiple septum sites are selected and chromosomes are segregated in streptomycetes. Typically, highly regular ladders of septa are produced in sporulation-committed aerial hyphae (Grantcharova *et al.*, 2005; Schwedock *et al.*, 1997). In the *ssgG* mutant, at irregular intervals septa were simply 'missing', resulting in spores exactly twice, three times or even four times the size of normal spores. Excitingly, the chromosomes were well segregated in these multiple-sized spores, resulting in long spores with up to four chromosomes joined only by a thread-like filamentous structure. TEM showed the complete absence of any cell wall material (peptidoglycan) between the segregated chromosomes. So while in wild type cells septal peptidoglycan synthesis is always initated prior to DNA segregation (*e.g.* Fig. 5A), the *ssgG* mutant reveals that in fact the initiation of septal peptidoglycan synthesis is not a requirement *sine qua non* for correct DNA segregation. This sheds new light on this intriguing process.

ssgD mutants produce many prespores and spores with aberrant hyphal walls, including spores with a wall the width of regular hyphae, and irregular prespore chains, suggestive of weakened lateral peptidoglycan. The synthesis of lateral PG is carried out by PBP2 (SCO2605) (Den Blaauwen *et al.*, 2003; Errington *et al.*, 2003) and the highly similar protein encoded by SCO2897. Interestingly, mutational analysis showed that both PBP2 and SCO2897 – revealed by microarray analysis to be strongly expressed throughout the *S. coelicolor* life cycle - are indeed important for lateral wall PG synthesis (G. Hobbs, proceedings of ISBA XIII, Melbourne 2003), suggesting that SsgD allows the correct functioning of at least one of these two PBPs.

Spore maturation: SsgEF control autolytic spore separation

While the insight in the sporulation process in streptomycetes is rapidly improving, little is known of the final stage, the autolytic cleavage of the peptidoglycan connecting the prespores, resulting in mature and separated spores. Our data show that SsgE and SsgF play a specific role in the control of this process. Strains lacking *ssgE* sporulated very well, with normal septation and DNA segregation, but produced predominantly single spores. Since prespores were invariably organised in spore chains, the high frequency of single mature spores must

have arisen from an accelerated maturation process followed by a non-coordinated separation into single spores. This implicates SsgE as a checkpoint for the correct timing of spore dissociation. Interestingly, all streptomycetes whose genome has been sequenced have one SALP that is predicted by the TMPred algorithm to have a transmembrane helix, namely SsgF (aa 14-32) in *S. coelicolor*, SsgW (aa 51-75) in *S. scabies* and SAV580 (aa 85-103) in *S. avermitilis*, with a strong preference for the N-terminus facing the cytoplasm. *ssgF* plays a distinct role during the final stage of spore separation. Deletion of the gene resulted in short spore chains, with spores that were readily stained by WGA, invariably at the poles and at the outside of the spore wall. Since *de novo* synthesis occurs from inside to outside, these peptidoglycan subunits accumulated at the spore poles must have resulted from autolysis of the spore-linking peptidoglycan. Hence, in the absence of SsgF spores fail to complete autolytic detachment due to incomplete breakdown of PG subunits, resulting in more loosely attached prespores and allowing almost free rotation. This is substantiated by our observation of a "flip movement" in several spore chains, with a visible transition from normally oriented spores (poles connected head-to-tail) to 90 degrees rotated spores (poles parallel), with an intermediate spore (45 degrees rotated) in between (Fig. 5H + insert). The likely driving force is the stronger hydrophobic interaction between the long sides of the spores as compared to the poles. Thus, SsgF ensures the final step in autolysis of prespores.

SALPs and the fate of peptidoglycan

Scientists have been searching for an answer to the important question as to how streptomycetes coordinate the synchronous formation of multiple septa and the concomitant segregation of the same number of chromosomes. The cell division machinery is generally very similar to that of other eubacteria, although especially aspects of regulation and localisation are different. Which then are the proteins that make sure that septa are layed down simultaneously, and with such striking regularity? It is likely that this involves *Streptomyces*-specific proteins. The SALPs are obvious candidates; they occur exclusively in actinomycetes that undergo extensive morphological differentiation. Four of the SALPs are present in all streptomycetes, namely *ssgA, ssgB, ssgD,* and *ssgE*, while *ssgG*-type genes are also relatively common. Sequence conservation of the predicted gene products varies from 55% (SsgE) to 100% (SsgB), SsgB being the most highly conserved cell division protein in *Streptomyces* (Flärdh and van Wezel, 2003). Our data now show that all SALPs relate specifically to sporulation-specific cell division, as *ssgX* mutants have various defects in the

build-up or degradation of peptidoglycan during sporulation, but show normal vegetative growth and regular cross-walls. The only exception is the *ssgC* mutant; as discussed, its phenotype is highly similar to a strain over-producing SsgA, showing not only developmental defects, but also the typical enhanced and irregular septation in vegetative hyphae.
The main question that is not so easily answered is what exactly is the mechanism by which the SALPs control the different steps of the sporulation process? At this point, it is important to note that while the classical early *whi* genes such as *whiA,whiB, whiG, whiH, and whiN* (*bldN*) encode (predicted) DNA binding proteins such as σ factors and GntR-family regulators, and hence most likely function at the level of transcriptional control (and are therefore less obvious candidates for an interaction with PBPs and autolysins), ssgA and ssgB are *whi* genes that likely encode structural proteins. Interestingly, we recently obtained convincing evidence that at least SsgA and SsgF form multimers with itself *in vitro* even under denaturing conditions - with up to 5-membered multimers confirmed by mass spectrometry of purified SsgF (GVW, unpublished data). This indicates that SALP multimerisation probably is an essential part of their function. SALPs have no known protein motif, and lack DNA binding activity, which suggests that SALP multimers function by recruiting other proteins to their relevant sites, so as to manage enzymes responsible for the synthesis and autolysis of peptidoglycan.

On the basis of our data we predict the following functional relationships. SsgA - antagonised by SsgC - directly stimulates cell division and the build up of septal PG, and hence it functionally relates to the developmental PBPs involved in septal PG synthesis, *ie.* FtsI, SCO3171 and/or SCO3156. On the basis of the highly similar phenotypes of the respective mutants, PBP2 relates functionally to SsgB, and SCO2897 and/or PBP2 - which are both important for lateral wall PG synthesis - to SsgD. SsgE and SsgF control autolytic spore cleavage, with SsgE preventing premature spore release, a function most likely carried out by SCO5466, and SsgF promoting the cleavage of peptidoglycan strands between the spores in almost mature prespore chains, in prokaryotes carried out by SLT. In accordance with this, SCO5466 and SLT are transcribed in a highly developmental way, suggesting their involvement primarily in spore separation. Finally, SsgG is the first example of a protein specifically involved in the coordination of multiple septation, a unique feature of *Streptomyces* cell division. Solving the question as to how SsgG determines the exact sites

where cell division is initiated will greatly improve our understanding of this intriguing phenomenon.

To further characterise the nature of all functional interactions, we are currently conducting extensive expression analyses in all SALP mutants using genomics approaches, and concentrate on the identification of the exact interaction partners for the SALPs.

ACKNOWLEDGMENTS

We are very grateful to Dr. Glyn Hobbs (Liverpool, UK) for the PBP2 mutant and for discussions, to Hans van der Meulen for excellent technical assistance with TEM, and to Dr. Erik Vijgenboom and Dr. Barend Kraal (Leiden, the Netherlands) and Prof. Sir David Hopwood for discussions. This work was supported by grants from the Netherlands Academy for Arts and Sciences (KNAW) to GPVW and from the BBSRC (UK) to CPS.

3

Analysis of cell division in the *ssg* mutants highlights SsgB and SsgG as important control proteins for the initiation of septum formation

Elke E. E. Noens, Quirinus J. M. Voorham,
Henk K. Koerten and Gilles P. van Wezel

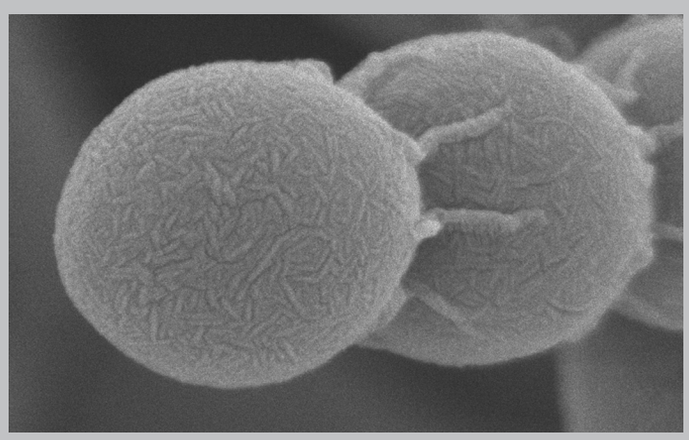

ABSTRACT

During sporulation-specific cell division in aerial hyphae of *S. coelicolor*, a large amount of septa is simultaneously produced, in concert with the segregation and condensation of chromosomes. Members of the family of SsgA-like proteins (SALPs), exclusively occurring in sporulating actinomycetes, play a crucial role in the control of the sporulation process, from septum site selection to spore separation. The first event in sporulation-specific cell division is the localisation of FtsZ to many regularly spaced sites along the wall of the aerial hyphae. Here we show that FtsZ-rings are only infrequently produced in an *ssgB* mutant, while SsgB itself was specifically localised at sporulation septa. In an *ssgG* mutant, the typical FtsZ ladders were observed but rings were regularly missing. SsgG localised in an irregular pattern in vegetative hyphae and in two distinct patterns in aerial hyphae, but was never observed in spores. SsgG most frequently localised as well-separated foci at regular intervals, which resemble the sites for septum synthesis. Non-specific localisation of SsgE and SsgF was observed in aerial hyphae and spores. The combined deletion of *ssgA* and the suspected antagonist *ssgC* resulted in an unconditional non-sporulating, white phenotype, suggesting a functional linkage between SsgA and SsgC.

INTRODUCTION

Streptomycetes undergo two apparently different cell division events (Flärdh and van Wezel, 2003). Vegetative hyphae grow by tip extension in a DivIVA-dependent manner (Flärdh, 2003a). At this stage the hyphae are divided into multi-nucleoid compartments by vegetative septa or cross-walls. After the onset of morphological differentiation, initially aseptate aerial hyphae are erected from the lysing substrate mycelium and form a template for spore production (Chater and Losick, 1997; Chater, 2001). As development progresses, the aerial hyphae are divided into prespores by sporulation septa, which are co-synthesised to form ladders with approximately 1 μm spacing (McCormick *et al.*, 1994; Schwedock *et al.*, 1997). Control of Z-ring localisation and timing is the crucial step in the sporulation process, as this is the first step in sporulation-specific cell division (Grantcharova *et al.*, 2005; McCormick *et al.*, 1994; Schwedock *et al.*, 1997). After septum initiation, proteins responsible for the formation of the divisome are recruited sequentially to the Z-ring and septa are synthesised. At this stage, single chromosomes are segregated into the prespore compartments, the septum is closed, and the spore wall thickens. After completion of the maturation process the uninucleoid spores are separated by autolytic cleavage.

Hence, while most bacteria divide the mother cell into the daughter cells by binary fission with a single septum, up to 100 septa are produced simultaneously during sporulation of *Streptomyces*. Other important differences between cell division in sporulating actinomycetes, like *Streptomyces*, and that of other bacteria, are that cell division is not essential for growth (McCormick *et al.*, 1994; McCormick and Losick, 1996) and the apparent absence of both a *minCDE* control system for septum-site localisation (Autret and Errington, 2001; Marston *et al.*, 1998) and of Z-ring anchoring proteins such as FtsA and ZipA (Errington *et al.*, 2003f; Lowe *et al.*, 2004). This suggests that streptomycetes have species-specific proteins that play a role in the control of its complex cell division. One such family is that of the SsgA-like proteins (SALPs), a family of developmental control proteins exclusively occurring in sporulating actinomycetes (reviewed in (van Wezel and Vijgenboom, 2004)). *S. coelicolor* harbours seven SsgA-like homologues, all playing a role in certain steps of the sporulation process, from initiation of sporulation to the autolytic cleavage of mature spores (Chapter 2). The best studied example is SsgA itself, which was first identified as an effector of cell division in *Streptomyces griseus* (Kawamoto and Ensign, 1995) and specifically stimulates sporulation-specific cell division in *Streptomyces coelicolor* (van

Wezel *et al.*, 2000). Considering that FtsI is the only penicillin-binding protein (PBP) known to be part of the divisome and essential for septal peptidoglycan synthesis, we hypothesised a functional link between SsgA and the activity of FtsI (Chapter 2-4). We previously showed that in fact all SALPs are involved in specific stages of the sporulation process. SsgB is 99-100% conserved in streptomycetes and the only SALP protein present in other sporulating actinomycetes (Keijser *et al.*, 2003). Since *ssgB* mutants produce very long aseptate aerial hyphae (a strictly *whi* phenotype) it is most likely involved in a phase related to growth cessation and onset of Z-ring formation (Keijser *et al.*, 2003; Chapter 2). Similar to SsgA and SsgB, SsgG plays an important role in septum formation, and *ssgG* mutants have a distinctive light grey phenotype (indicative of less efficient sporulation). In fact, SsgG is involved in correct septum-site localisation, evidenced by the fact that during sporulation-specific cell division septa are simply 'skipped' in *ssgG* mutants, but without affecting DNA segregation (Chapter 2). Interestingly, this shows that septation is not a condition *sine qua non* for DNA segregation. The function of SsgC and SsgD is less well-defined. The similarity between *S. coelicolor* lacking *ssgC* and *S. coelicolor* over-producing SsgA (and *vice versa*) suggests that SsgC somehow antagonises the function of SsgA. SsgD is the only SALP that is abundantly produced during both vegetative and aerial growth. The thin cell wall of aerial hyphae and spores suggests that SsgD controls lateral cell wall synthesis at least during development. Finally, mutants lacking either SsgE or SsgF have well-defined spore maturation defects, and the proteins are essential for the correct timing of spore dissociation and the last steps of autolysis, respectively.

In this chapter, we provide a further functional analysis of the SsgA-like proteins, studying the effects of deletion of either of the *ssg* genes in an *ssgA* mutant background. We also investigated the localisation of the Z-ring in all *ssg* mutants and of SsgB, SsgE, SsgF and SsgG, providing novel information on the timing of their expression and their function relative to well-known developmental checkpoint events.

MATERIALS AND METHODS

Bacterial strains and media

The bacterial strains described in this work are listed in Table 1. *E. coli* K-12 strains JM109 (Sambrook *et al.*, 1989) and ET12567 (MacNeil *et al.*, 1992) were used for routine cloning and plasmid propagation and were grown and transformed by standard procedures (Sambrook

et al., 1989). *E. coli* BW25311 (Datsenko and Wanner, 2000) was used to create and propagate the *S. coelicolor* cosmids used for the creation of the fusion of SsgG with EGFP in *S. coelicolor* M145. *E. coli* ET12567 containing pUZ8002 was used for conjugation to *S. coelicolor* (Kieser *et al.*, 2000). *E. coli* transformants were selected in L-broth containing the appropriate antibiotics. *Streptomyces coelicolor* A3(2) M145 was obtained from the John Innes Centre strain collection, and was the parent for the previously created *ssgA* (GSA3) (van Wezel *et al.*, 2000), *ssgB* (GSB1) (Keijser *et al.*, 2003), *ssgC* (GSC1), *ssgD* (GSD1), *ssgE* (GSE1), *ssgF* (GSF1) and *ssgG* (GSG1) mutants (Chapter 2).

All media and routine *Streptomyces* techniques are described in the *Streptomyces* manual (Kieser *et al.*, 2000). Soy flour mannitol (SFM) agar plates were used for making spore suspensions and for microscopical analysis and R2YE agar plates for regeneration of protoplasts and, after the addition of the appropriate antibiotic, for selecting recombinants. For standard cultivation and for plasmid isolation, YEME or TSBS (tryptone soy broth (Difco) containing 10% (w/v) sucrose) were used.

Plasmids, constructs and oligonucleotides

All plasmids and constructs are summarised in Table 2. pIJ2925 (Janssen and Bibb, 1993) is a pUC19-derived plasmid used for routine subcloning. The shuttle vectors pHJL401 (Larson and Hershberger, 1986) and pSET152 (Bierman *et al.*, 1992) were used for cloning in *Streptomyces*, which both have the pUC *ori* for high-copy number replication in *E. coli* and the SCP2* *ori* on pHJL401 (around five copies per chromosome) and the *attp* sequence, allowing integration at the attachment site of bacteriophage φC31, on pSET152 for maintenance in *S. coelicolor*. pIJ487 was used for direct cloning into *S. coelicolor*, which maintains in *S. coelicolor* via the pIJ101 *ori* (50-100 copies per chromosome) (Ward *et al.*, 1986). KF41 is a pSET152-derived integrative vector expressing FtsZ-EGFP (Grantcharova *et al.*, 2005).

PCRs were done with *Pfu* polymerase (Stratagene), in the presence of 10% (v/v) DMSO, with an annealing temperature of 58°C. The oligonucleotides are listed in Table 3.

A 1048 bp fragment harbouring the putative promoter region of *ssgF* (-1048/-1 relative to the translational start codon) was amplified from *Streptomyces coelicolor* M145 genomic DNA using oligonucleotides ssgFpr-F and ssgFpr-R. This section was inserted as an *Eco*RI-*Kpn*I fragment into pIJ2925. Subsequently, *ecfp* was amplified from pECFP (BD Biosciences Clonetech) using primers CFP/YFP-F2 and CFP/YFP-R2, replacing the stop

codon of *ecfp* with a *Bam*HI site. *ecfp* was inserted as a *Kpn*I-*Bam*HI fragment behind the putative promoter region of *ssgF* in pIJ2925. A 492 bp fragment containing *ssgF* was amplified from M145 genomic DNA using oligonucleotides ssgF-F and ssgF-R, replacing the start codon with a *Bam*HI site. This fragment was inserted in frame with the *ecfp* as a *Bam*HI-*Hin*dIII fragment in pIJ2925, resulting in pGWS157. The complete insert of pGWS157 was digested with *Eco*RI-*Bgl*II and the resulting fragment was ligated into the *Eco*RI-*Bam*HI sites of pSET152, giving the integrative vector pGWS158. The same fragment was inserted as an *Eco*RI-*Hin*dIII fragment into pHJL401 and into the multi-copy vector pIJ487, generating pGWS159 and pGWS163, respectively. In this way several plasmids were created that expressed *ecfp-ssgF* fusion from the natural *ssgF* promoter.

Table 1: Bacterial strains.

Bacterial strain	Genotype	Reference
S. coelicolor A3(2) M145	SCP1$^-$ SCP2$^-$	(Kieser *et al.*, 2000)
GSA3	M145 Δ*ssgA* (::*aadA*)	(van Wezel *et al.*, 2000)
GSB1	M145 Δ*ssgB* (::*aac(3)IV*)	(Keijser *et al.*, 2003)
GSC1	M145 Δ*ssgC* (::*aac(3)IV*)	(Noens *et al.*, 2005)
GSD1	M145 Δ*ssgD* (::*aac(3)IV*)	(Noens *et al.*, 2005)
GSE1	M145 Δ*ssgE* (::*aac(3)IV*)	(Noens *et al.*, 2005)
GSF1	M145 Δ*ssgF* (::*aac(3)IV*)	(Noens *et al.*, 2005)
GSG1	M145 Δ*ssgG* (::*aac(3)IV*)	(Noens *et al.*, 2005)
GSAB	M145 Δ*ssgA* (::*aadA*) Δ*ssgB* (::*aac(3)IV*)	This chapter
GSAC	M145 Δ*ssgA* (::*aadA*) Δ*ssgC* (::*aac(3)IV*)	This chapter
GSAD	M145 Δ*ssgA* (::*aadA*) Δ*ssgD* (::*aac(3)IV*)	This chapter
GSAE	M145 Δ*ssgA* (::*aadA*) Δ*ssgE* (::*aac(3)IV*)	This chapter
GSAF	M145 Δ*ssgA* (::*aadA*) Δ*ssgF* (::*aac(3)IV*)	This chapter
GSAG	M145 Δ*ssgA* (::*aadA*) Δ*ssgG*(::*aac(3)IV*)	This chapter
K202	M145 + KF41	(Grantcharova *et al.*, 2005)
GSA5	GSA3 + KF41	This chapter
GSB2	GSB1 + KF41	This chapter
GSC2	GSC1 + KF41	This chapter
GSD2	GSD1 + KF41	This chapter
GSE2	GSE1 + KF41	This chapter
GSF2	GSF1 + KF41	This chapter
GSG2	GSG1 + KF41	This chapter
GSG3	M145 *ssgG-egfp*	This chapter
J3310	M145 *parB-egfp*	(Jakimowicz *et al.,* 2005)
E. coli JM109	See reference	(Sambrook *et al.*, 1989)
E. coli ET12567	See reference	(MacNeil *et al.*, 1992)
E. coli BW25311	See reference	(Gust *et al.*, 2003)
E. coli ET 12567/pUZ8002	See reference	(Gust *et al.*, 2003)

To obtain a translational fusion of SsgE with ECFP, a 1111 bp fragment was amplified from M145 genomic DNA using primers ssgE-F and ssgE-R, harbouring *ssgE* and 790 bp of the upstream region. The stop codon of *ssgE* was replaced with a *Kpn*I site. This section was inserted as an *Eco*RI-*Kpn*I fragment into pIJ2925. Subsequently, *ecfp* was amplified from pECFP (BD Biosciences-Clonetech) with CFP/YFP-F and CFP/YFP-R, replacing the start codon with a *Kpn*I site*,* and inserted as a *Kpn*I-*Hin*dIII fragment behind *ssgE* in pIJ2925, so as

to create pGWS160 that contained an in frame fusion of *ssgE* and *ecfp*. *ssgE-ecfp* of pGWS160 was then inserted as an *Eco*RI-*Bgl*II fragment into an *Eco*RI/*Bam*HI-digested pSET152, giving pGWS161 and as an *Eco*RI-*Hin*dIII fragment into the low-copy shuttle vector pHLJ401 or in the multi-copy vector pIJ487, generating pGWS162 and pGWS164, respectively. Thus, an in frame *ssgE-ecfp* fusion was created, expressed from the natural promoter of *ssgE*.

Table 2: Plasmids and constructs.

Plasmid/ Cosmid	Description	Reference
pHJL401	*Streptomyces/E. coli* shuttle vector (5-10 and around 100 copies per genome, respectively)	(Larson and Hershberger, 1986)
pIJ2925	Derivative of pUC19 (high copy number) with *Bgl*II sites flanking its multiple cloning site	(Janssen and Bibb, 1993)
pSET152	*Streptomyces/ E. coli* shuttle vector (integrative in *Streptomyces*, high copy number in *E. coli*)	(Bierman *et al.*, 1992)
pIJ487	Derivative of pIJ101 *Streptomyces* high copy vector (up to 300 copies per chromosome)	(Ward *et al.*, 1986)
pGWS157	pIJ2925 with 2.3 kb fragment harbouring upstream region of *ssgF* (-1048/-1) *ecfp* (+1/+716) and *ssgF* (+3/+495, relative to *ssgF*)	This chapter
pGWS158	pSET152 with 2.3 kb fragment harbouring upstream region of *ssgF* (-1048/-1) *ecfp* (+1/+716) and *ssgF* (+3/+495, relative to *ssgF*)	This chapter
PGWS159	pHJL401 with 2.3 kb fragment harbouring upstream region of *ssgF* (-1048/-1) *ecfp* (+1/+716) and *ssgF* (+3/+495, relative to *ssgF*)	This chapter
pGWS160	pIJ2925 with 1.9 kb fragment harbouring *ssgE* (-740/+378, relative to *ssgE*) and *ecfp* (+3/+719)	This chapter
pGWS161	pSET152 with 1.9 kb fragment harbouring *ssgE* (-740/+378, relative to *ssgE*) and *ecfp* (+3/+719)	This chapter
pGWS162	pHJL401 with 1.9 kb fragment harbouring *ssgE* (-740/+378, relative to *ssgE*) and *ecfp* (+3/+719)	This chapter
pGWS163	pIJ487 with 2.3 kb fragment harbouring upstream region of *ssgF* (-1048/-1) *ecfp* (+1/+716) and *ssgF* (+3/+495, relative to *ssgF*)	This chapter
pGWS164	pIJ487 with 1.9 kb fragment harbouring *ssgE* (-740/+378, relative to *ssgE*) and *ecfp* (+3/+719)	This chapter
KF41	pSET152-derived integrative vector expressing FtsZ-EGFP	(Grantcharova *et al.*, 2005)

For the creation of an *ssgG-egfp* fusion, the Redirect method was used as described earlier (Gust *et al.*, 2003). For this, primer pairs ssgGred-F and ssgGred-R were designed to amplify an *egfp-aac3(IV)-oriT* cassette from genomic DNA isolated from J3310 (Jakimowicz *et al.*, 2005) including a 10 amino acid flexible, glycine- and proline-rich linker to maximise the likelihood of a functional fusion protein. On either side of the cassette, 40bp extensions were added that are identical to the regions immediately upstream and downstream of the stop codon of *ssgG*. This fragment was introduced into *E. coli* BW25311, containing the cosmid E19A (with *ssgG*) as well as pIJ790 allowing extremely efficient recombination. The subsequent steps were described previously (Noens *et al.*, 2005). As a result, an in frame

fusion of *ssgG* with *egfp* was created in the genome of *S. coelicolor* M145 with an *aacC4* resistance cassette as a selectable marker. The correct insertion was confirmed with PCR and sequencing (not shown).

Table 3: Oligonucleotides.

Primer	DNA sequence	Location 5'end	Relative to
CFP/YFP-F	gact**ggtacc**gtgagcaagggcgaggagctgttc	+3	*cfp/yfp*
CFP/YFP-R	gctg**aagctt**ttacttgtacagctcgtccatgccgag	+719	*cfp/yfp*
CFP/YFP-F2	gact**ggtacc**atggtgagcaagggcgaggagctg	+1	*cfp/yfp*
CFP/YFP-R2	gact**ggatcc**cttgtacagctcgtccatgccgag	+471	*cfp/yfp*
ssgF-F	gctg**gaattc**tcggaaatgatgatcgtcgcccgca	+3	*ssgF*
ssgF-R	gact**ggtacc**gacggccattccttccagttgagc	+494	*ssgF*
ssgFpr-F	gact**ggatcc**agtggtgaccaccacggtgtgcag	-1048	*ssgF*
ssgFpr-R	gctg**aagctt**catctccggtcacgtgtcccgtgg	-1	*ssgF*
ssgE-F	catg**gaattc**agcaggtgcacgccgatcatc	-790	*ssgE*
ssgE-R	gctg**ggtacc**gtgggccaccggctgcgcggtcgccgc	+378	*ssgE*
ssgGred-F	gctcgggatcgacgacgggctggccgagctgctcgccaggctgccgggcccggagctg	+376	*ssgG*
ssgGred-R	ctcaacccgggcaagctcttctgaccgctgccgctcctcacatatgtcggctggagctgcttc	+436	*ssgG*

Restriction sites used for cloning are presented in bold face.

Construction of the ssgA-ssgX double mutants

To obtain double mutants of *ssgA* in combination with a deletion of either of the other *ssg* genes, protoplast fusions were performed between the *ssgA* mutant GSA3 (resistant to spectinomycin and streptomycin) and either GSB1 (Δ*ssgB*), GSC1 (Δ*ssgC*), GSD1 (Δ*ssgD*), GSE1 (Δ*ssgE*), GSF1 (Δ*ssgF*) or GSG1 (Δ*ssgG*) (all resistant to apramycin) as described elsewhere (Kieser *et al.*, 2000). Protoplasts of GSA3 were mixed with a 50-fold excess of protoplasts of GSB1, GSC1, GSD1, GSE1, GSF1 or GSG1. First, $Spc^{R}Str^{R}$ was used for the selection of GSA3. Subsequently, the desired double recombinants were selected by growth on apramycin. The double mutants were designated GSAB (Δ*ssgA*-Δ*ssgB*), GSAC (Δ*ssgA*-Δ*ssgC*), GSAD (Δ*ssgA*-Δ*ssgD*), GSAE (Δ*ssgA*-Δ*ssgE*), GSAF (Δ*ssgA*-Δ*ssgF*) and GSAG (Δ*ssgA*-Δ*ssgG*).

Protein isolation and Western hybridisation

For preparation of protein extracts, *S. coelicolor* M145 was grown on cellophane disks on SFM agar and mycelium was harvested at time points corresponding to vegetative growth (veg), aerial growth (aer) and sporulation (spo), as described earlier (van Wezel *et al.*, 2000). After subjecting the samples to SDS-gel electrophoresis, the gels were blotted onto Hybond-C

super nylon membranes (Amersham), and subsequently immunostained with antibodies directed against SsgE. Anti-SsgE antibodies were used in a 1:5000 dilution.

Microscopy

Confocal fluorescence microscopy

For fluorescence microscopy of strains expressing cell division proteins translationally fused with EGFP or ECFP, sterile coverslips were inserted at a 45° angle into SFM plates and spores were inoculated in the acute angle. After 2 days (for FtsZ-EGFP) and 5 days (for SsgE-ECFP, SsgF-CFP) and 1 to 4 days (for SsgG-EGFP) of incubation at 30°C, coverslips were removed and samples positioned in a drop of 1% agarose or water on a microscope slide. Immuno-fluorescence microscopy of SsgB was carried out as described previously (Schwedock *et al.*, 1997). For this, *S. coelicolor* M145 was grown on SFM for 3 days. Antibodies against SsgB were used in a 1:1000 dilution.

Electron microscopy

Morphological studies of surface-grown aerial hyphae and spores of *S. coelicolor* M145 and mutant derivatives by cryo-scanning electron microscopy (cryo-SEM) was performed as described previously, using a JEOL JSM6700F scanning electron microscope (Keijser *et al.*, 2003). The analysis of cross-sections of hyphae and spores with transmission electron microscopy (TEM) was performed with a Philips EM410 transmission electron microscope as described previously (van Wezel *et al.*, 2000).

RESULTS

Localisation of FtsZ in *ssg* mutants

Previously, we showed that the SsgA-like proteins (SALPs) are involved in specific steps of the sporulation process, from septum-site selection to spore maturation (Chapter 2). The first step in septation is the polymerisation of FtsZ into a Z-ring at the position where the septum will be synthesised. To verify if any of the SALPs affects Z-ring formation or if they are functional at a time prior to Z-ring formation, we expressed FtsZ-EGFP in the various SALP mutants (Fig. 1). For this, mutants were transformed with KF41, a derivative of pSET152, expressing FtsZ-EGFP from its natural promoters. We occasionally observed the fluorescence

indicative for correct FtsZ localisation in the *ssgA* mutant on mannitol-containing media (Fig. 1B), under which conditions the *ssgA* mutant is able to sporulate to some extent, while no FtsZ-EGFP foci were detected in the *ssgA* mutant on glucose-containing media. Occasionally, Z-rings were observed in aerial hyphae of an *ssgB* mutant, which fails to produce aerial septa but sporadically shows constriction in the aerial hyphae (Keijser *et al.*, 2003). The distance of the Z-rings observed in an *ssgB* mutant appeared to be similar as in a *whiH* mutant (Grantcharova *et al.*, 2005) (Fig. 1C). Vegetative cell division was not affected in *ssgB* mutants. As expected, in the light of their ability to sporulate, normal Z-ladders were produced by mutants deficient in ssgC, ssgD, ssgE or ssgF (Fig. 1D-F). Normally spaced FtsZ rings were also visualised in the *ssgG* mutant (Fig. 1H), although 15% of the rings were missing (Fig. 1I-K; arrows) or considerably less intense (Fig. 1I-J; stars) in this mutant. This may account for the lack of septa observed in an *ssgG* mutant, therefore creating prespore compartments twice as long as normal (Fig. 1G).

Creation of ECFP and EGFP fusions

To analyse the localisation of SsgG and of the spore maturation proteins SsgE and SsgF, constructs were made allowing the in frame fusion with *egfp* or *ecfp* (for details see Materials and Methods section). In brief, *ssgE* (preceded by 790 bp of upstream region) was fused in frame with *ecfp*, and the *ssgE-ecfp* fusion was inserted into pSET152, pHJL401 and pIJ487, creating pGWS161, pGWS162 and pGWS164, respectively. Since SsgF is predicted to have a single transmembrane helix, oriented with its N-terminus located in the cytoplasm (Chapter 2), we created an N-terminal fusion between *ssgF* and *ecfp*, expressed from the putative *ssgF* promoter region. Like for *ssgE-ecfp*, the *ecfp-ssgF* fusion gene was inserted into pSET152, pHJL401 and pIJ487 for expression in *S. coelicolor*, creating pGWS158, pGWS159 and pGWS163, respectively. Finally, an SsgG-EGFP fusion was constructed to localise SsgG in *S. coelicolor*. For this purpose, the REDIRECT method was used to express chromosomally encoded EGFP-tagged SsgG as a replacement for the wild type protein (Gust *et al.*, 2003). The resulting strain was designated GSG3**.**

Localisation of SsgB, SsgE, SsgF and SsgG

To visualise the subcellular localisation of SsgB in *S. coelicolor* M145, immuno-fluorescence microscopy using peptide-based anti-SsgB antibodies (G.P. van Wezel, unpublished) was

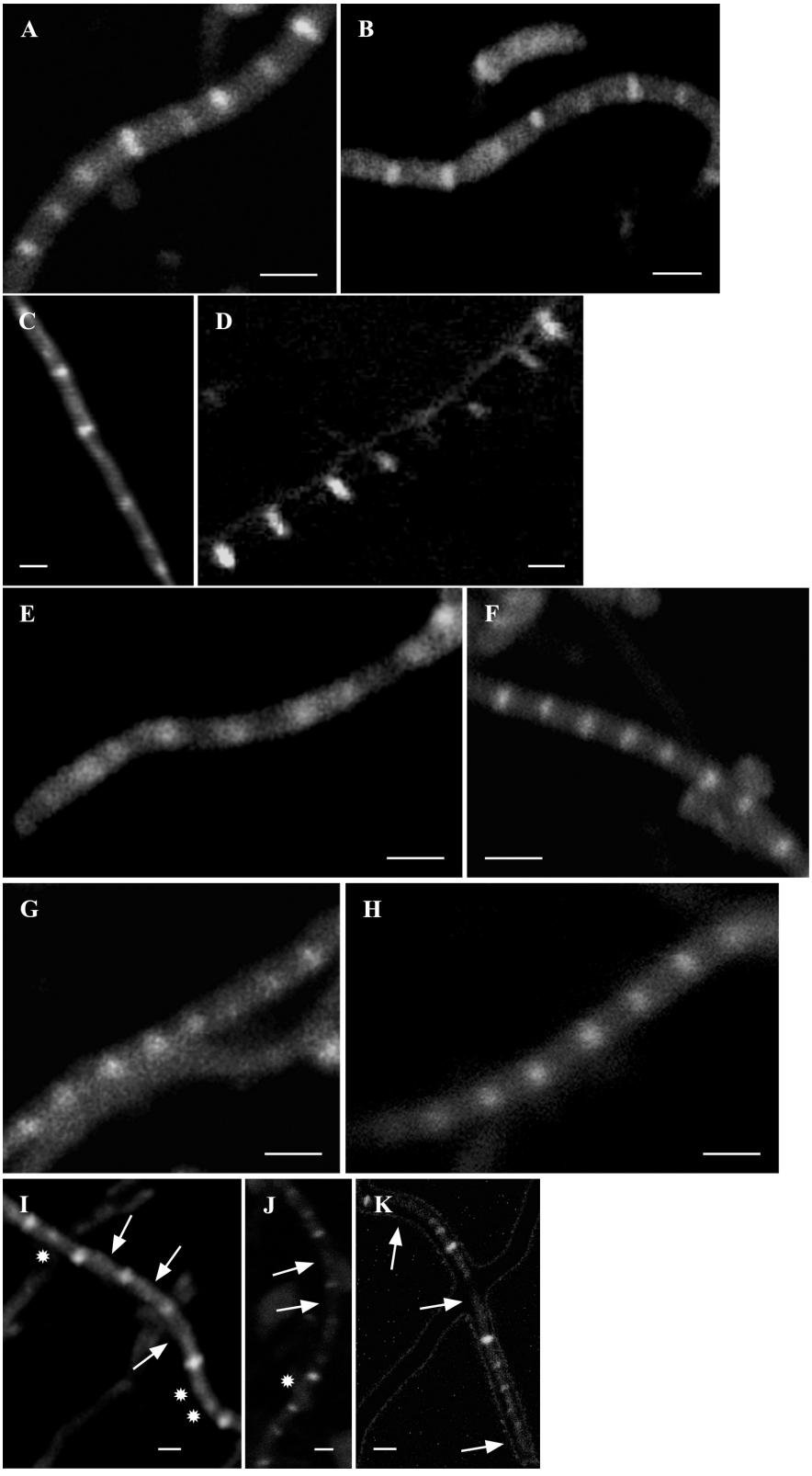

Figure 1: Localisation of FtsZ in the SALP mutants. KF41, a pSET152-derived integrative vector expressing FtsZ-EGFP, was used to localise FtsZ in *S. coelicolor* M145 (**A**), or its *ssgA* (**B**), *ssgB* (**C**), *ssgC* (**D**), *ssgD* (**E**), *ssgE* (**F**), *ssgF* (**G**) and *ssgG* (**H-I-J-K**) mutants. In the *ssgG* mutant, Z-rings are missing (arrows) or considerably less intense (stars). Strains were grown for 2 days on SFM at 30ºC. Bar = 1 μm.

performed on mycelium harvested after 5 days of growth on SFM agar plates, and fixed in paraformaldehyde (see Materials & Methods). Cells were treated with lysozyme and DNA was stained with propidium iodide. Excitingly, SsgB was localised only at sporulation septa, often with the brightest fluorescence closer to the hyphal wall, leaving a distinct gap in the middle of the division ring (Fig. 2A, for a full colour version of Fig. 2, see p177-178). At this moment, the chromosomes were segregated into the prespore compartments. The timing of localisation suggests that SsgB is part of the divisome during sporulation-specific cell division. In a control experiment, we did not detect SsgB in the *ssgB* mutant (not shown).

No specific SsgE-ECFP foci were observed by confocal fluorescence microscopy in *S. coelicolor* M145 harbouring pGWS161 and pGWS164, or in GSE1 containing pGWS162. Rather, aerial hyphae and spores showed diffuse and non-specific fluorescence, with more intense fluorescence in the spores than in the aerial hyphae (Fig. 2B). GSE1 harbouring pGWS162 did not produce the free spores typical of *ssgE* mutants (Chapter 2). Therefore, the construct fully complemented the autolytic defect of *ssgE* mutants, suggesting that the fusion protein was functional and replaced the wild type SsgE (not shown). To further corroborate that the fusion protein was expressed we performed Western analysis on total protein extracts of M145 containing pGWS161 or pGWS164 and of *ssgE* mutant GSE1 harbouring pGWS162, using antibodies directed against a synthetic SsgE peptide (Fig. 3A). All three strains showed a band with a size corresponding to that of the SsgE-ECFP fusion product, indicating that the fusion protein was correctly expressed. Extracts of M145 showed a single band, corresponding to approximately three times the predicted molecular weight of SsgE (13,7kDa), while no such band was observed in extracts of the *ssgE* mutant GSE1 (Fig. 3A-B).

Figure 2: Localisation of SsgB, SsgE, SsgF and SsgG. Strains were grown on SFM for 5 days (SsgB, SsgE-ECFP and SsgF-ECFP) or 1-4 days (SsgG-EGFP) at 30ºC. DNA was visualised with PI (red) **A.** Localisation of SsgB. The first column shows immuno-fluorescence micographs using fluorescein-conjugated anti-SsgB antibodies, the middle column shows light micrographs (top) and DNA (middle, bottom) and the third column shows overlay images from the left and the middle images. Bar = 2 μm. **B-C.** Non-specific localisation of SsgE-ECFP (**B**) and ECFP-SsgF (**C**). ECFP-SsgF shows occasionally brighter foci at the tip of the spores (arrow). Bar = 5 μm. **D.** Localisation of SsgG-EGFP in vegetative hyphae (α-β) and in aerial hyphae (γ-η). α-γ show overlays from light microscopy images and SsgG-EGFP. δ shows light microscopy (left), DNA (middle) and SsgG-EGFP (right) while ε, ζ, η show only SsgG-EGFP. In aerial hyphae, class 1 (γ) shows a staggered pattern while in class 2 (δ-η), foci are laid down in regular pattern, with distances resembling the size between sporulation septa. SsgG was not localised in the spores (δ). Stars show the place where the distance between the foci is double the normal distance and subsequently, spores two times the normal size are created (arrowheads). SsgG-EGFP appeared in the hyphal tips of both vegetative and aerial hyphae (arrows). Bar = 2 μm. (Full colour version, see p177-178).

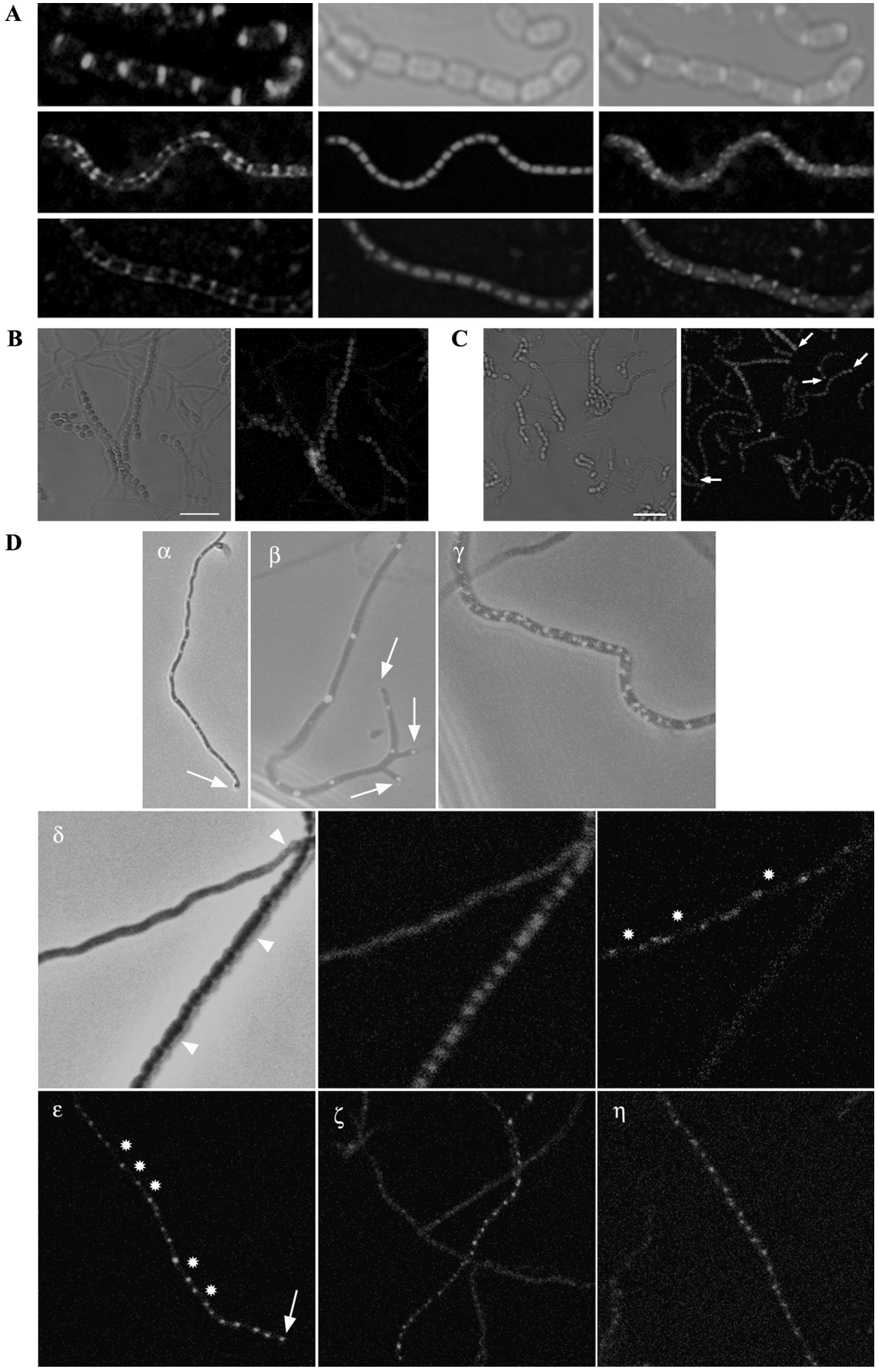
A
B
C
D
α
β
γ
δ
ε
ζ
η

When *S. coelicolor* M145 transformants harbouring either pGWS158, pGWS159 or pGWS163 were analysed by fluorescence microscopy, low levels of ECFP-SsgF were detected in pGWS163 transformants, and not in pGWS158 or in pGWS159 transformants. No specific foci were detected for ECFP-SsgF (Fig. 2C). Rather, like for SsgE-ECFP, we observed diffuse (unfocused) fluorescence in aerial hyphae and spores. Occasionally, brighter foci were seen at the tip of the spores (see arrow Fig. 2C). While significantly fewer spores with a 90° rotation typical of the *ssgF* mutant (Chapter 2) were observed, pGWS159 failed to fully complement the phenotype of the *ssgF* mutant, suggesting that the fusion protein was only partly functional.

When *S. coelicolor* GSG3 - which expresses SsgG-EGFP - was studied by fluorescence microscopy, fluorescent foci corresponding to SsgG were observed already after one day of growth, in an irregular pattern in the vegetative hyphae, invariably with a single spot at the hyphal tips (Fig. 2D; α-β), a localisation similar to that of DivIVA (Flärdh, 2003b). In young aseptate aerial hyphae with non-segregated genomes, we observed specific foci of SsgG-EGFP with two different localisation patterns. The first pattern (Class 1) showed SsgG localised at regular intervals at either side of the aerial hyphae, in a staggered pattern (Fig. 2D; γ), while the second (Class 2) showed SsgG-EGFP as single foci at regular intervals of around 1 μm in the middle of the hyphae (Fig. 2D; δ-ε-ζ-η). The class 2 localisation became more abundant as growth progressed with class 1: class 2 ratios of 40:60 after two days of growth and of 20:80 after four days of growth. Significantly more foci were detected in aerial hyphae than in vegetative hyphae, which is consistent with the strong upregulation of *ssgG* during development (Chapter 2). SsgG-EGFP foci were also found in the tips of the aerial hyphae (Fig. 2D, arrows). While the regularity of SsgG localisation was highly similar to that of Z-rings and septa, around 10% of the foci in class 2 were missing from the expected pattern, such that the distance between the foci was about two or more times the regular septal distance of around 1 μm (Fig. 2D, stars). SsgG was not present in aerial hyphae with visible septa, suggesting that SsgG is only functional during the earliest stages of septum formation. In line with the occasional absence of SsgG-EGFP foci in GSG3, the strain also lacked around 10% of the spore septa (Fig. 2D; arrowheads), sometimes creating spores two or three times the normal size, with normal DNA segregation.

Hence, SsgG-EGFP could not completely revert the phenotype of *ssgG* mutants, which lack approximately 25% of the spore septa, resulting in a partial mutant phenotype.

Multimerisation of SsgE and SsgF

Recently obtained data showed that SsgA and SsgF are able to form homo-multimers *in vitro*, even under denaturing conditions, with up to five-membered multimers as confirmed by mass spectrometry of purified SsgF (Rob van der Heijden and G.P. van Wezel, unpublished data). Western analysis of total protein extracts of *S. coelicolor* M145 revealed a single band around 42 kDa, corresponding to a protein of approximately three times the predicted molecular mass of SsgE (13,7 kDa), while such a band was not observed in extracts of GSE1 (Fig. 3B). This suggests that also SsgE forms multimers, even under denaturing conditions. These preliminary experiments show that SALP proteins may function by multimerisation *in vivo*.

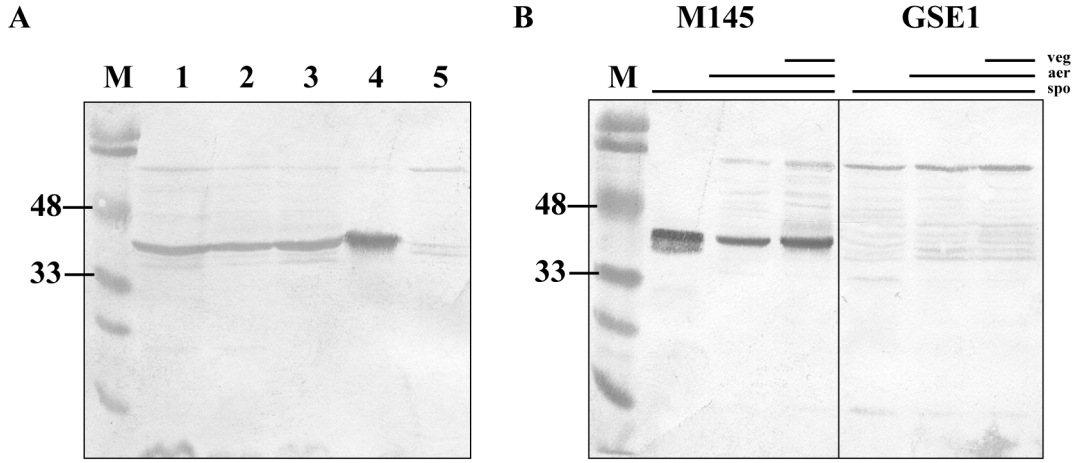

Figure 3A: Analysis of *S. coelicolor* strains expressing SsgE-ECFP. Western blot of protein extracts using antibodies against SsgE (1:5000 dilution). M: Marker; Lane 1, pGWS164 (pIJ487/*ssgE-ecfp*) in M145; Lane 2 pGWS161 (pSET152/*ssgE-ecfp*) in M145; Lane 3, pGWS162 (pHJL401/*ssgE-ecfp*) in GSE1; Lane 4, M145; Lane 5, *ssgE* mutant GSE1. The band around 42 kDa in lane 1, 2, 3 corresponds to SsgE-ECFP. The band around 42 kDa in Lane 4 corresponds to a possible SsgE trimer, which is absent from *ssgE* mutants (lane 5). **3B: Expression of SsgE.** Total protein extracts were prepared from samples of *S. coelicolor* M145 and GSE1, at time points corresponding to vegetative growth (veg), aerial growth (aer) and sporulation (spo). The band, appearing in all wild type samples, corresponding to a molecular weight of around 42 kDa is likely an SsgE trimer. This band is absent in all samples of GSE1.

Construction of double mutants

The *ssgA* mutant is able to produce spores on mannitol-containing media. Z-ring formation appeared to be normal in these sporogenic hyphae (Chapter 4) and the produced spores perform similarly as wild type spores. To investigate the effects of deletion of the other *ssg* genes in an *ssgA* mutant background and, therefore, to consider a possible redundancy between SsgA and one of the other SALPs, double mutants of *ssgA,* in combination with either *ssgB, ssgC, ssgD, ssgE, ssgF* or *ssgG* were created. For this, protoplast fusion was performed between Δ*ssgA* (Spc^RStr^R) and either Δ*ssgB,* Δ*ssgC,* Δ*ssgD,* Δ*ssgE,* Δ*ssgF* or

Δ*ssgG* (all Apra^R). Selection with the appropriate antibiotics gave the desired double mutants, designated GSAB, GSAC, GSAD, GSAE, GSAF and GSAG. The inactivation of the respective *ssg* genes in the double mutants was verified by Southern hybridisation.

***ssgA-ssgX* double mutants**

To visualise the difference in the ability to sporulate, the double mutants GSAB, GSAC, GSAD, GSAE, GSAF and GSAG were plated out on SFM together with the previously made *ssgA* mutant and the wild type M145 (Fig. 4). The *ssgA* mutant GSA3 has a conditionally non-sporulating phenotype. Such a carbon-source dependence of development is found regularly in *bld* mutants (Nodwell and Losick, 1998) but is as far as we know unique for *whi* mutants: GSA3 fails to sporulate on glucose-containing media, but produces some spores on mannitol-containing media (van Wezel *et al.*, 2000). The *ssgB* mutant GSB1 displays a typical white, non-sporulating phenotype on all media (Keijser *et al.*, 2003). The other SALP mutants GSC1, GSD1, GSE1, GSF1 and GSG1 all produce grey-pigmented spores on all media, although the *ssgG* mutant GSG1 produces significantly fewer spores and thus has a lighter appearance on solid media (Chapter 2). Two double mutants GSAB and GSAC had a true carbon source-independent *whi* phenotype. The other double mutants GSAD, GSAE, GSAF and GSAG had a similar phenotype as the single *ssgA* mutant.

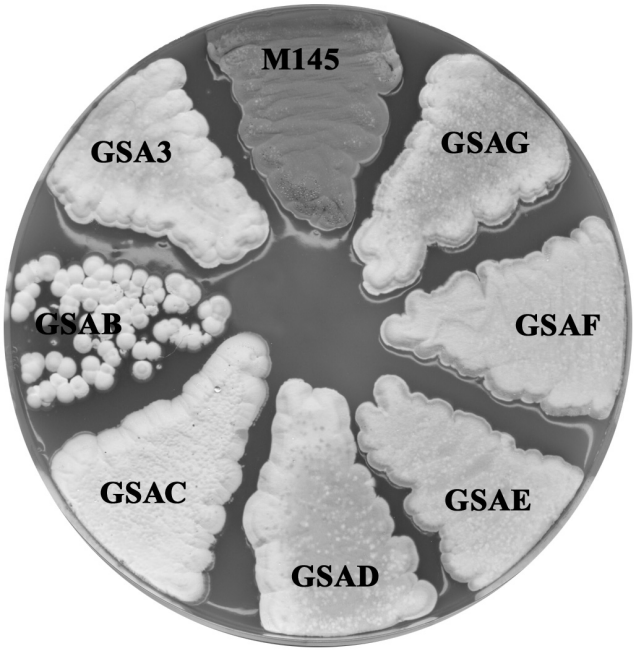

Figure 4: Phenotypes of *ssgAB, ssgAC, ssgAD, ssgAE, ssgAF* and *ssgAG* double mutants. GSAB, GSAC, GSAD, GSAE, GSAF and GSAG were grown together with M145 and GSA3 on SFM for 5 days at 30°C.

Analysis of the double mutants with electron microscopy

Surface-grown colonies of *S. coelicolor* GSAB, GSAC, GSAD, GSAE, GSAF and GSAG were analysed in detail by cryo-SEM together with the parental strain M145 and the *ssgA* mutant GSA3 (Fig. 5). *S. coelicolor* M145 produced long spore chains with spore septa at regular intervals. When we studied GSA3 with cryo-SEM, spore chains were occasionally seen and aerial hyphae were frequently lysed. Regularly, branching of aerial hyphae was observed, a phenomenon never observed in wild type aerial hyphae, possible due to a higher expression of *divIVA* in the *ssgA* single mutant (Chapter 4). All double mutants showed branching in aerial hyphae. Expectedly, the *ssgAB* double mutant GSAB produced no spores. Surprisingly, the combined deletion of *ssgA* and its suspected antagonist *ssgC* also resulted in a strictly *whi* phenotype on all media. Furthermore, branching was seen most frequently in this mutant (approximately 56% of the aerial hyphae), with sometimes up to five branches at one point in the aerial hyphae. The *ssgA* mutant phenotype was dominant over the less severe phenotypes of the single *ssgD, ssgE, ssgF* and *ssgG* mutants, which sporulate much more proficiently than the *ssgA* mutant. Except for the presence of spores, which were exactly twice the normal length in GSAG (Fig. 5; arrows), the phenotypes of GSAD, GSAE, GSAF and GSAG were very similar to that of the *ssgA* mutant.

Transmission electron microscopy was used to study the double mutants in more detail. For GSAB, TEM showed no additional features other than those reported with cryo-SEM. Strikingly, in contrast to *ssgC* mutants or strains overexpressing SsgA, no irregular or unfinished cross walls were observed in the vegetative hyphae of GSAC double mutants. GSAD and GSAG showed the particular phenotypes of the *ssgD* and *ssgG* mutants; spores with a cell wall similar to the lateral hyphal wall for GSAD (Fig. 5, GSAD; insert) and spores exactly twice the normal length for GSAG (Fig. 5, GSAG; insert), suggesting they function in an SsgA-independent manner. The spore maturation defects typical of the *ssgE* and *ssgF* mutants (free and rotated spores, respectively), were not seen in GSAE1 and GSAF1.

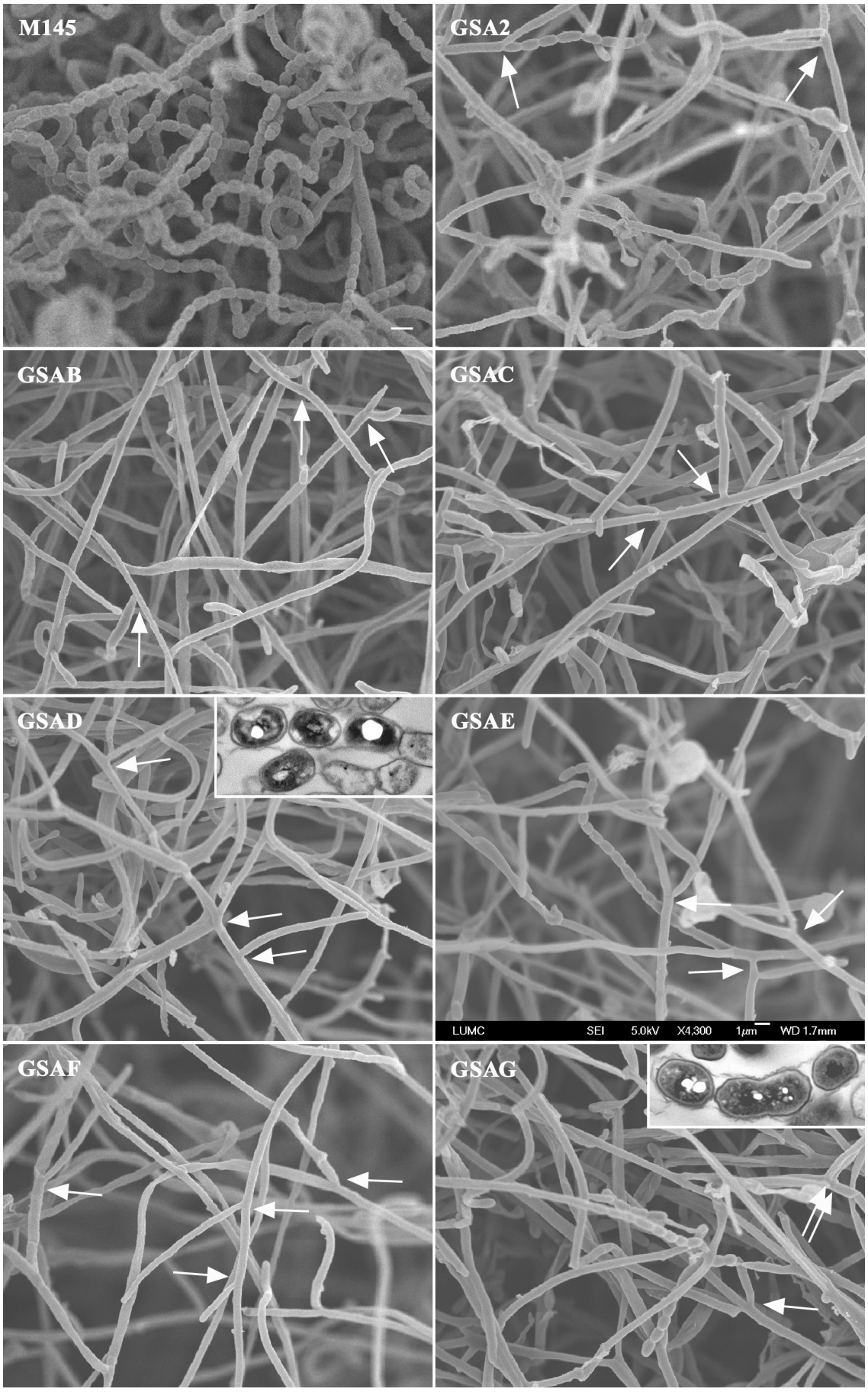
M145
GSA2
GSAB
GSAC
GSAD
GSAE
LUMC SEI 5.0kV X4,300 1μm WD 1.7mm
GSAF
GSAG

Figure 5: Cryo-scanning electron micrographs of the double mutants. Strains were grown on SFM for 5 days at 30°C. Aerial hyphae of GSA3 and all double mutants show frequently branching (arrows). Inserts of GSAD and GSAG show TEM images of typical spores for an *ssgD* and *ssgG* mutant, respectively. Bar = 1 μm.

DISCUSSION

The SALPs belong to a family of sporulation control proteins that occur exclusively in sporulating actinomycetes and are functionally linked to sporulation-specific peptidoglycan synthesis and degradation. In this chapter, we substantiate the previously published model on the function of the SALPs (Chapter 2) by dealing with three topics. These are (1) thelocalisation of FtsZ in sporogenic hyphae of the *ssg* mutants, (2) the localisation of SsgB, SsgE, SsgF and SsgG in hyphae and spores to provide insight into the expression of these proteins in time and space, and (3) the phenotypes of mutants with combined deletion of *ssgA* and either *ssgB, ssgC, ssgD, ssgE, ssgF* or *ssgG*, to work out if these proteins function independently of SsgA or if there is a possible functional redundancy between SsgA and one or more of the other SALPs. For example, this could perhaps explain the unique phenotype of *ssgA* mutants, which are the only conditional *whi* mutants and are able to sporulate on mannitol-containing media.

Analysis of the localisation of SsgB in *S. coelicolor* with SsgB-specific antibodies revealed specific localisation at sporulation septa in spores where DNA segregation was completed. The brightest fluorescence was mainly seen closest to the hyphal wall, with dark sections in the centre, suggesting the formation of an open ring structure. Importantly, Z-rings were only occasionally observed in aerial hyphae of *ssgB* mutants, suggesting that SsgB aids in the initial steps of Z-ring formation, and at the same time follows the growing septum. Recent data suggest that like the developmental *ftsZ* promoter (p2), transcription of *ssgB* depends on WhiH, as transcription from both promoters is almost completely absent in *whiH* mutants ((Flardh *et al.*, 2000); B. Traag and G.P. van Wezel, unpublished results). Conversely, *whiH* transcripts were detected in *ssgB* mutants. The localisation of *ssgB* itself during sporulation is in line with transcriptional analysis, showing that *ssgB* transcription is developmentally regulated, and very strongly upregulated during aerial growth, similar to the transcripiton of *bldN* (Chapter 2). What we know about SsgB is the following: (1) *ssgB* mutants produce normal vegetative cross walls and (2) only infrequent Z-rings in aerial

hyphae, with (3) complete failure to produce sporulation septa, (4) transcription of *ssgB* is strongly reduced in the absence of WhiH, at least in part explaining the non-sporulating phenotype of *whiH* mutants; and (5) SsgB specifically localises to the spore septa. Taken together, this strongly suggests that SsgB is part of the divisome and that the protein is essential for the growth of septal peptidoglycan, a function that is carried out by FtsI. Not unexpectedly, the additional deletion of *ssgA* had no additional effect on development, except that the double mutant had branching aerial hyphae typical of *ssgA* mutants. This suggests that SsgA and SsgB work, at least in part, independently.

Detailed phenotypic analysis suggests that SsgD is involved in correct synthesis of the lateral hyphal and spore walls and SsgE and SsgF control spore maturation (Chapter 2). As expected, the phenotype of the double mutants GSAD, GSAE and GSAF resembled that of *ssgA* mutants, which is in line with the timing of action of SsgA in the sporulation process, *i.e.* most likely prior to that of SsgD, SsgE or SsgF (Chapter 2). If SsgD, SsgE and/or SsgF function independently of SsgA, the few spores produced in the respective double mutants on mannitol-containing media should show at least some of the defects typical of *ssgD*, *ssgE* or *ssgF* single mutants. Indeed, spores of the *ssgAD* double mutant GSAD had a wall thickness similar to that of the lateral hyphal wall of aerial hyphae, a typical consequence of the deletion of *ssgD*, suggesting that SsgD functions in the absence of SsgA. In contrast, the premature spore autolysis giving rise to single spore formation in the *ssgE* mutant, or the 'rotated' spores typical of *ssgF* mutants, were not observed in the *ssgAE* or *ssgAF* double mutants. However, even though some spores were produced in the double mutants, it is almost impossible to study spore maturation defects in an *ssgA* mutant background. To learn more about the role of SsgEF in the spore maturation process and about their localisation, we studied the fate of the two proteins fused to ECFP by fluorescence microscopy. We observed non-specific localisation in the spores and aerial hyphae, with brighter fluorescence in the spores. Considering the fact that either fusion protein could restore correct spore maturation to the respective mutants, it is likely that the proteins were functional, and hence that the diffuse fluorescence truly reflects a more ‘random’ localisation of the protein rather than an experimental artefact such as background fluorescence. Expected, deletion of ssgE or ssgF had no effect on Z-ring formation, in line with their role in spore maturation. Further analysis is required to pinpoint the exact localisation of the two spore maturation proteins, such as immuno-electron microscopy or the use of fluorophores with stronger fluorescence.

Interestingly, the phenotype of *ssgAC* double mutants was the only one that did not simply reflect the combined defects of the single mutants, but rather displayed an almost completely non-sporulating *whi* phenotype under all conditions. Indeed, it was almost impossible to find any spores at all, and eventually no more than three spore chains could be identified with cryo-SEM. This indicates that SsgA and SsgC are functionally linked. Previously, we suggested that SsgC may have an antagonistic function towards SsgA, as the phenotype of an *ssgC* mutant is similar to that of GSA2, a strain over-expressing SsgA (Chapter 2; van Wezel *et al.*, 2000), while *vice versa*, overexpression of SsgC strongly inhibits development. Furthermore, sporulation of *ssgA* mutants can be restored by the introduction of additional copies of *ssgC* (G.P.van Wezel, unpublished results). A possible hypothesis is that SsgA and SsgC both carry out similar functions and are functionally redundant, but hetero-complexes of SsgA and SsgC are inactive. Thus SsgC negatively controls the activity of SsgA, as part of the SsgA pool is titrated out (SsgA is expressed at a higher level than SsgC in *S. coelicolor* M145). Without SsgC, more functional SsgA is available disturbing the finely tuned balance of functional and non-functional SsgA and resulting in hyperseptation of both vegetative and aerial hyphae and irregular spores. A strain with enhanced expression of SsgC would thus effectively resemble *ssgA* mutants, while in the absence of SsgA, the SsgC protein would (partly) take over its function (G.P. van Wezel, pers. comm.). Again in support of the hypothesis postulated above, in the absence of both SsgA and SsgC (in double mutant GSAC), no irregular septa were observed in vegetative hyphae. Until now, we did not succeed in localising SsgC in hyphae and spores of *S. coelicolor*, which may be due to the low expression of *ssgC* from its own promoter.

Transcriptional analysis revealed that SsgG is upregulated slightly during vegetative growth and strongly from early aerial growth (Chapter 2). This is the likely explanation why we observed foci of SsgG-EGFP in both vegetative and aerial hyphae. SsgG-EGFP was observed in aerial hyphae in two localisation patterns; class 1 with a staggered pattern and class 2 showing a ladder-like pattern. It is suggestive that the two classes of patterns observed in aerial hyphae are sequential, as the amount of class 1 decreased over time and was always observed at a lower level than class 2, indicative of its shorter lifespan. In contrast, the amount of the class 2 increased over time. This ladder-like localisation pattern strongly suggests that SsgG localises to the early septum site, corresponding to our earlier evidence that SsgG is involved in septum-site localisation (Chapter 2). The regular ‘gaps’ in the

otherwise regular distribution of SsgG-EGFP correspond very well to the frequency at which septa are lacking and result in double- or triple-sized spores, and are probably due to the fact that SsgG-EGFP fails to fully complement the *ssgG* mutant. Thus, these experiments provide further evidence that SsgG is involved in septum site selection. Excitingly, FtsZ-EGFP localisation was different in *ssgG* mutants as compared with the regularly spaced Z-rings in the wild type strain, with several 'sports' missing in the typical FtsZ ladders. Also, less intense rings were observed, probably reflecting unfinished and non-functional Z-rings. It was suggested previously that streptomycetes need a specific cell division protein for the reorganisation of the pattern of Z-ring formation from the spiral-shaped intermediate to the ladder-pattern (Grantcharova *et al.*, 2005). We suggest that SsgG is involved in this process and this may explain the localisation as a staggered pattern (class 1) as an intermediate to restructure the Z-ring into rings. SsgG is certainly not the only protein involved in the reorganisation of the Z-ring, as normal ladders are still produced in an *ssgG* mutant. In this light, it is important to note that in *ssgB* mutants only very infrequent Z-rings were observed, a phenotype similar to that of *whiH* mutants (Grantcharova *et al.*, 2005; Schwedock *et al.*, 1997) Conversely, in *ssgG* mutants septa are 'missing' around once per 5 μm. We hypothesise that SsgB and SsgG are essential for septum site localisation and have complementary functions in septum site selection, with around 80% of the septa dependent on SsgB and around 20% dependent on SsgG. Besides its function in septum-site localisation, we provide evidence that SsgB also acts as a molecular chaperone for the PBPs responsible for septal PG synthesis (FtsI and/or the developmentally controlled FtsI-like proteins SCO3156 and SCO3771; see Chapter 2). The co-localisation of ssgB and SsgG in the same background and the analysis of a double mutant of *ssgB* in combination with *ssgG* would help us to develop this concept further.

ACKNOWLEDGEMENTS

We thank Klas Flärdh for plasmid pKF41 and for discussions.

4

Loss of the controlled localisation of growth stage-specific cell wall synthesis pleiotropically affects developmental gene expression in an *ssgA* mutant of *Streptomyces coelicolor*

Elke E. E. Noens, Vassilis Mersinias, Joost Willemse, Bjørn A. Traag, Emma Laing, Keith F. Chater, Colin P. Smith, Henk K. Koerten and Gilles P. van Wezel

Mol Microbiol (2007) 64: 1244-1259

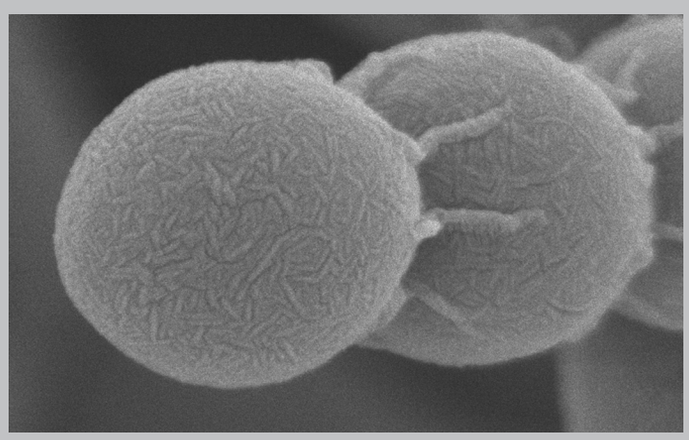

ABSTRACT

Members of the family of SsgA-like proteins (SALPs) are found exclusively in sporulating actinomycetes, and SsgA itself activates sporulation-specific cell division. We previously showed that SALPs play a chaperonin-like role in supporting the function of enzymes involved in peptidoglycan maintenance (PBPs and autolysins). Here we show that SsgA localises dynamically during development, and most likely marks the sites where changes in local cell wall morphogenesis are required, in particular septum formation and germination. In sporogenic aerial hyphae, SsgA initially localises as strong foci to the growing tips, followed by distribution as closely spaced foci in a pattern similar to an early stage of FtsZ assembly. Spore septa formed in these hyphae co-localise with single SsgA-GFP foci, and when the maturing spores are separated, these foci are distributed symmetrically, resulting in two foci per mature spore. Evidence is provided that SsgA also controls the correct localisation of germination sites. Transcriptome analysis revealed that expression of around 300 genes was significantly altered in mutants in *ssgA* and its regulatory gene *ssgR*. The list includes surprisingly many known developmental genes, most of which were upregulated, highlighting SsgA as a key player in the control of *Streptomyces* development.

INTRODUCTION

The correct timing and localisation of cell division, which involves dynamic reorganisation of cell wall synthesis and breakdown, are among the most studied topics in modern microbial cell biology. In most bacteria a single septum forms the cleavage furrow dividing the mother cell into daughter cells, but during growth of the Gram-positive mycelial bacterium *Streptomyces,* vegetative hyphae are divided only occasionally by vegetative septa or cross walls, giving multigenomic compartments, while reproduction involves the simultaneous production of many specialised septa to form long chains of unigenomic spores from multigenomic aerial hyphal compartments (Flärdh *et al.*, 2000; McCormick *et al.*, 1994; Wildermuth and Hopwood, 1970). Correctly organised apical growth and branching of vegetative hyphae depend on the activity of DivIVA (Flärdh, 2003). In contrast to vegetative cross-walls, multiple sporulation septa are produced simultaneously and in a highly coordinated way within a sporogenic aerial hypha. A first step in sporulation-specific cell division is the localisation of FtsZ to many regularly spaced sites along the aerial hyphal wall (Grantcharova *et al.*, 2005). Multiple septa are then simultaneously synthesised in a process in which proteins required for the formation of bacterial divisomes are presumably sequentially directed to the Z ring (Bramhill, 1997; Errington *et al.*, 2003). The segregation of DNA into the prespore compartments is partially dependent on ParA and ParB (Jakimowicz *et al.*, 2002a; Jakimowicz *et al.*, 2005), is accompanied by DNA condensation, and appears to be completed by a process involving septum-located FtsK (Wang et al., 2007). After septum closure, the wall of the prespore compartments thickens and becomes pigmented, and eventually the mature spores are separated by a poorly understood process of autolytic cleavage. Much remains to be learned about the coordinated production of up to 100 sporulation septa in aerial hyphae.

Cell division in mycelial actinomycetes differs from that in other bacteria in lacking *minC* and *minE* homologues for septum-site localisation (Autret and Errington, 2001; Marston *et al.*, 1998), the nucleoid occlusion system Noc, and Z-ring anchoring proteins such as FtsA and ZipA (Errington *et al.*, 2003; Lowe *et al.*, 2004). Instead, several unique protein families have been identified that play a role in the control of cell division (Chater and Chandra, 2006; Flärdh and van Wezel, 2003). One such family is that of the SsgA-like proteins (SALPs), developmental agents that occur exclusively in mycelial actinomycetes, and are unrelated to other known proteins. The model strain *Streptomyces coelicolor* A3(2) harbours seven

paralogues, all involved in specific chaperone-like tasks during development, controlling processes from initiation of sporulation to the autolytic cleavage of spore wall peptidoglycan (PG) (Chapter 2; van Wezel and Vijgenboom, 2004). The most-studied SALP, SsgA itself, was first identified as an effecter of septation in *S. griseus* (Kawamoto and Ensign, 1995). In *S. coelicolor, ssgA* null mutants have an unusual conditional non-sporulating phenotype, the aerial hyphae nearly all being devoid of sporulation septa except on mannitol-containing media, on which some spores are produced (van Wezel *et al.*, 2000a). Overexpression of SsgA results in hyperseptation of both vegetative and aerial hyphae, thus interfering with the control systems that determine the morphological differences between the two cell types. Such overexpression effected the production of extremely thick and irregular septa, often with a gap in the middle, demonstrating disturbance of the concluding stages of the cell division process (van Wezel *et al.*, 2000a). Therefore, SsgA somehow activates the initiation and control of septal peptidoglycan synthesis, probably by influencing the function of Penicillin-Binding Proteins (PBPs) involved in the biogenesis of septal peptidoglycan, which in bacteria is typically carried out by FtsI (Bramhill, 1997).

In this work, we provide an in-depth analysis of *ssgA* using a knockout mutant and an *ssgA-egfp* fusion strain, and employ microarrays to analyse the global changes in gene expression in strains defective in *ssgA*. Clear links between distinct phenotypic anomalies and altered gene expression profiles are provided.

MATERIALS AND METHODS

Bacterial strains and media

The bacterial strains described in this work are listed in Table 1. *E. coli* K-12 strains JM109 (Sambrook *et al.*, 1989) and ET12567 (MacNeil *et al.*, 1992) were used for routine cloning and plasmid propagation, and were grown and transformed by standard procedures (Sambrook *et al.*, 1989). *E. coli* ET12567 containing pUZ8002 was used for conjugation to *S. coelicolor* (Kieser *et al.*, 2000). *E. coli* transformants were selected in L-broth containing the appropriate antibiotics. *Streptomyces coelicolor* A3(2) M145 was obtained from the John Innes Centre strain collection, and was the parent for the previously created *ssgA* mutant GSA3 (van Wezel *et al.*, 2000a). All media and routine *Streptomyces* techniques are described in the *Streptomyces* manual (Kieser *et al.*, 2000). SFM agar plates were used for making spore

suspensions and R2YE agar plates for regeneration of protoplasts and, after the addition of the appropriate antibiotic, for selecting recombinants. Pregermination was performed by heat shock at 50^0C for 10 minutes, followed by shaking at 30^0C for at least 10 hours. For microscopic analysis, streptomycetes were grown on SFM agar plates. For standard cultivation and plasmid isolation, YEME or TSBS [tryptone soy broth (Difco) containing 10% (w/v) sucrose] were used.

Table 1: Bacterial strains, Plasmids and constructs.

Bacterial strain	**Genotype**	**Reference**
S. coelicolor A3(2) M145	$SCP1^-$ $SCP2^-$	(Kieser *et al.*, 2000)
GSA2	M145 + pGWS4-SD	(van Wezel *et al.*, 2000a)
GSA3	M145 Δ*ssgA* (::*aadA*)	(van Wezel *et al.*, 2000a)
GSR1	M145 Δ*ssgR*	(Traag *et al.*, 2004)
K202	M145 + KF41	(Grantcharova *et al.*, 2005)
E. coli JM109	See reference	(Sambrook *et al.*, 1989)
E. coli ET12567	See reference	(MacNeil *et al.*, 1992)
E. coli ET12567/pUZ8002	See reference	(Gust *et al.*, 2003)

Plasmids and constructs	**Description**	**Reference**
pHJL401	*Streptomyces/E. coli* shuttle vector (5-10 copies per genome in *Streptomyces*)	(Larson and Hershberger, 1986)
pIJ2925	Derivative of pUC19 (high copy number) with *Bgl*II sites flanking its multiple cloning site.	(Janssen and Bibb, 1993)
pGWS116	pHJL401 with 1.2 kb fragment harbouring a translational fusion of *ssgA* and *egfp*	This chapter
pGWS4-SD	Integrative construct over-expressing *ssgA*.	(van Wezel *et al.*, 2000a)
KF41	pSET152-derived integrative vector expressing FtsZ-GFP	(Grantcharova *et al.*, 2005)
pFT73	*mycgfp2*$^+$ cloned into *Bam*HI-*Pst*I of pUWL-SK+	(Nothaft *et al.,* 2003)

Plasmids and constructs

All plasmids and constructs described in this paper are summarised in Table 1. pIJ2925 (Janssen and Bibb, 1993) is a pUC19-derived plasmid used for routine subcloning. The shuttle vector pHJL401 has the pUC19 *ori* for high-copy number replication in *E. coli* and the SCP2* *ori* (around five copies per chromosome) for maintenance in *S. coelicolor* (Larson and Hershberger, 1986). An 1860 bp DNA fragment harbouring *ssgR* and *ssgA* was amplified by PCR from M145 genomic DNA using oligonucleotides Q1 and SsgA-GFP3 (Table 2). In this way, a *Kpn*I restriction site was created replacing the *ssgA* stop codon. The fragment was inserted as an *Eco*RI-*Kpn*I fragment into pIJ2925, creating pGWS113. Subsequently, *egfp* was amplified from pFT73 (Nothaft *et al.*, 2003) using oligonucleotides Har_GFP_For and Har_GFP_Rev (Table 2), replacing the start codon of *egfp* by a *Kpn*I restriction site. This

facilitated in frame fusion of *ssgA* and *egfp*. This 716 bp fragment was inserted as an *Kpn*I-*Hin*dIII fragment into pGWS113, resulting in pGWS114. The complete insert was cloned as an *Eco*RI-*Hin*dIII fragment in pHJL401, resulting in pGWS116. The plasmid expresses *ssgA-egfp* from the natural *ssgA* promoter.

Preparation of total RNA

Mycelium used for total RNA isolation was grown on cellophane disks on MM containing 1.5% Hispan agar and 0.5% mannitol as the carbon source. On this medium the strains sporulated well (M145) or poorly (GSA3, GSR1). Mycelium was harvested at times corresponding to vegetative growth (24h), aerial growth (36h, 48h) and sporulation (60h, 72h). RNA was purified using the Kirby-mix protocol (Kieser *et al.*, 2000). RNA purification columns (RNeasy, Qiagen) and DNaseI treatment were used as well as salt precipitation (final concentration 3M sodium acetate pH 4.8) to purify the RNA and fully remove any traces of DNA, respectively. Before use, the RNA preparations were checked for their quality and integrity on the Agilent 2100 Bioanalyzer (Agilent Technologies).

DNA Microarray analysis

For microarray hybridization each RNA sample was reverse-transcribed into Cy3-dCTP-labelled cDNA and co-hybridised with Cy5-dCTP-labelled genomic DNA from *S. coelicolor* M145, as common reference (Bucca *et al.*, 2003). The samples were hybridised to in-house (University of Surrey) fabricated oligonucleotide (50mer) microarrays covering essentially all ORFs of the *S. coelicolor* genome (for array coverage and detailed protocols: www.surrey.ac.uk/SBMS/Fgenomics/Microarrays). The hybridised microarrays were scanned with an Affymetrix 428 laser scanner for fluorescent signal acquisition. The 16-bit TIFF microarray images were analysed with BlueFuse (BlueGnome) spot quantification software and further processed using the statistical computing environment R (Version 2.1.1) and the package Limma (R Development Core Team). An ad-hoc R function was written to normalise all $\log_2$ cDNA/gDNA ratios on all arrays via the block-median (dividing the ratio of each of the 48 blocks by its respective median ratio). The $\log_2$ ratios were then scaled to have the same median-absolute-deviation (MAD) across arrays (Smyth and Speed, 2003; Smyth, 2005). Duplicate good spots (with confidence value >0.1 and spot quality of 1 (two parameters calculated by the BlueFuse software)) were averaged. Technical replicates for the M145 wild type strain were averaged. Data were then filtered such that there was at

least one biological replicate with one good spot in each time point/strain, resulting in a gene list of 7,345 genes for differential expression analysis. Data was then imported into GeneSpring (Version GX) and transformed to linear scale. Significantly differentially expressed genes between each of the deletion mutants and the M145 wild type strain were identified by applying one-way ANOVA ($p<0.05$; Benjamini & Hochberg False Discovery Rate) using GeneSpring. Some additional genes were also identified that demonstrated more than a two-fold change in expression level between wild type and mutant strains in at least two time points. The expression of selected genes was independently assessed with RT-PCR analysis (see below).

Table 2: Oligonucleotides used in PCR and RT-PCR.

Primer	**Sequence (5' -> 3')**	**Location 5' end**	**Relative to**
PCR oligo's			
Q1	ctg**gaattc**tagcatcgagggcaggacatcaga	-1450	*ssgA*
ssgA-GFP3	ctga**ggtacc**cgcgctctgttcctccgccaggatg	+410	*ssgA*
Har_GFP_For	gact**ggtacc**tcgaagggcgaggagctgttcacc	+3	*egfp*
Har_GFP_Rev	gctg**aagctt**ctacttgtacagctcgtccatgccgtg	716	*egfp*
RT-PCR oligo's			
rRNA-For	tcacggagagtttgatcctggctc	+20	16 rRNA
rRNA-Rev	cccgaaggccgtcatccctcacgc	+436	16 rRNA
adpA-F	ctcttcgtggacgacggcgacg	+499	*adpa*
adpA-R	gaaggtgcggcggctcatgtagg	+795	*adpA*
bldN-F	ctacgaccagtacagcgacaccg	+53	*bldN*
bldN-R	gctgtgggttgagccgtcgtacg	+385	*bldN*
divIVA-F	ctatgacgaggacgaggtcgatgc	+86	*divIVA*
divIVA-R	ccatggggccacccatctgctgc	+370	*divIVA*
ftsI-F	gaccatcgaccgcgacatccagtgg	+881	*ftsI*
ftsI-R	gtggcgacgttctcctccagcacg	+1136	*ftsI*
ftsZ-F	catcaccgacctcatcaccacc	+579	*ftsZ*
ftsZ-R	gccgaagatgatgttggcctcg	+876	*ftsZ*
gyrA-F	gttcaggacgaccttggcgaccg	+703	*gyrA*
gyrA-R	gttcaggacgaccttggcgaccg	+978	*gyrA*
parB-F	gtgaaaccgaagagctgacggcacc	+77	*parB*
parB-R	gatggcgtccagctccagctctcg	+345	*parB*
tatA-F	cgtcgtcatcatcctgctgttcgg	+41	*tatA*
tatA-R	cttggtcgtgtccgtcggctcg	+261	*tatA*
SCO0204-F	acgaaccggacatcaccgtggtc	+104	SCO0204
SCO0204-R	agccgtgccatcagcttggtcg	+446	SCO0204

Restriction sites used for cloning are presented in bold face.

PCR and RT-PCR analysis

PCRs were performed with *Pfu* polymerase (Stratagene) in the presence of 10% (v/v) DMSO. The programme used was as follows: 2 min at 95°C followed by 35 cycles of 1 min at 95°C (denaturation), 1 min at 58°C (annealing) and 2-3 min elongation at 72°C (time according to the length of the fragment). RT-PCR analysis was carried out using the Superscript III one

step RT-PCR System with Platinum® *Taq* DNA polymerase (Invitrogen) for the verification of gene expression changes observed in microarray experiments. RNA samples (time points 24h, 48h and 72h matching vegetative growth, aerial growth and sporulation, respectively) were the same as those used for microarray analysis. For each RT-PCR reaction 100 ng of RNA was used together with 1μM (final concentration) of each primer. The program used was as follows: 45 min cDNA synthesis at 48°C, followed by 2 min at 95°C and 25, 29, 31 or 35 cycles of: 45 s at 94°C (denaturation), 30 s at 68°C (annealing) and 30 s at 68°C (elongation). The reaction was completed by 5 min incubation at 68°C. 5μl of each sample was visualised by ethidium bromide staining after electrophoresis on a 2% agarose gel in 1xTAE buffer. The oligonucleotides are listed in Table 2. Quantification of the RT-PCRs was done by scanning the gels using the GS-800 imaging densitometer followed by analysis using Quantity One software (Biorad).

Microscopy

Confocal fluorescence microscopy

The visualisation of DNA (with propidium iodide, Sigma) and cell wall material (FITC-WGA, Biomedica) by confocal fluorescence microscopy was performed as described previously (Chapter 2). For the visualisation of strains containing proteins translationally fused with EGFP, sterile cover slips were inserted at a 45° angle into SFM plates and spores were inoculated in the acute angle. After incubation at 30°C for 2-5 days, coverslips were removed and samples positioned in a drop of water on a microscope slide.

Electron microscopy

Morphological studies of surface-grown aerial hyphae and spores of *S. coelicolor* M145 and mutant derivatives by cryo-scanning electron microscopy (cryo-SEM) were performed as described previously, using a JEOL JSM6700F scanning electron microscope (Keijser *et al.*, 2003).

RESULTS

The *ssgA* mutant has branching aerial hyphae

We showed previously that *ssgA* mutants produce aerial mycelium but have a conditional non-sporulating phenotype, failing to sporulate on glucose-containing solid media, while some spores are produced on mannitol-containing media (van Wezel *et al.*, 2000a). To get a more detailed view of the developing aerial hyphae, we subjected the *ssgA* mutant to detailed cryo- SEM. Interestingly, a significant number (approximately 40%) of the *ssgA* mutant aerial hyphae branched, and some showed multiple branches, with an average branch spacing of 5-10 μm. Despite extensive searches we never observed this phenomenon for aerial hyphae of the parental strain M145 (Fig. 1). Branching was also apparent in double mutants where besides *ssgA* also *ssgB, ssgC, ssgD, ssgE* or *ssgF* and *ssgG* was disrupted, and the branching was significantly enhanced in *ssgAC* double mutants, which had up to five branches at one single point of the aerial hyphae (Noens *et al.,* 2007, Fig. S1; Chapter 3, Fig. 5).

SsgA localises in a development-dependent and dynamic manner

To analyse the localisation of SsgA, we constructed plasmid pGWS116 expressing an *ssgA-egfp* in frame fusion from the natural *ssgA* promoter and introduced it into *S. coelicolor* M145 (see Materials and Methods for details). This plasmid fully complemented *ssgA* mutant GSA3, both in terms of sporulation and of mycelial morphology, indicating that the SsgA-EGFP fusion product was indeed functional and could replace the wild type SsgA.

Confocal fluorescence microscopy revealed a highly dynamic localisation for SsgA-GFP during development (Fig. 2). Discriminating the various stages of aerial development, the following observations were made. Initially, foci were relatively distantly spaced, namely 0.84 ± 0.19 foci per μm (average of 386 foci, measured along the hyphal wall) in the younger aerial hyphae (Fig. 2A, stage 1), which probably correspond to the recently designated and developmentally distinct sub-apical stem compartments (Dalton *et al.*, 2007). At this stage, the aerial hyphae still have the width of vegetative hyphae (approximately 400-500 nm). The hyphae later widen to about 800 nm, which is the width of spores (see *e.g.* Fig. 2D, which demonstrates both types of aerial hyphae). Early stage sporogenic hyphae carried a large amount of SsgA-GFP in the tips, sometimes showing very bright foci (Fig. 2A,C; stage 2). As growth progressed, the foci became less intense and were replaced by foci at alternating sides of the hyphae and around twice as frequent as in young aerial hyphae, namely 1.59 ± 0.34 foci

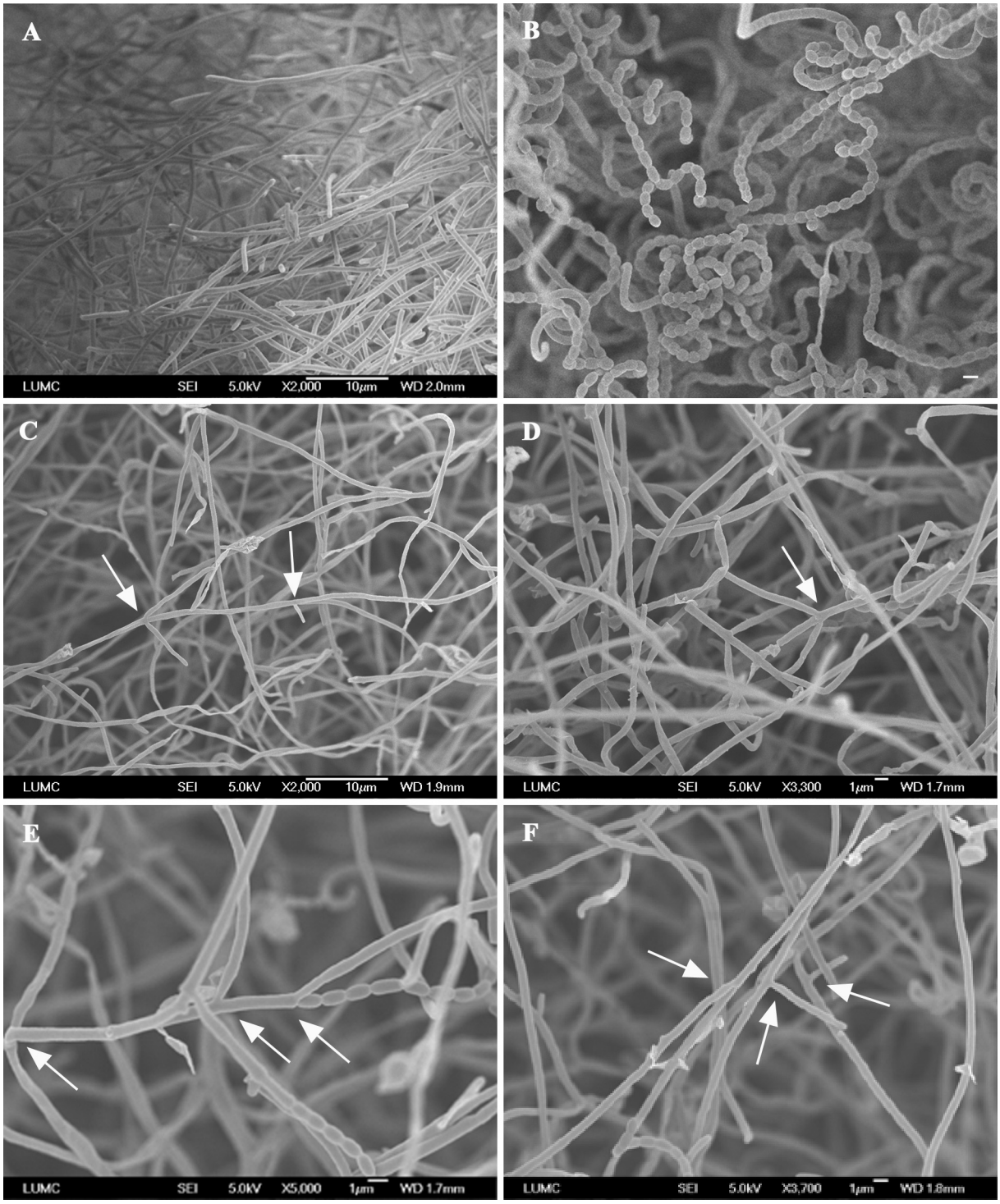

Figure 1: Cryo-scanning electron micrographs of *S. coelicolor* M145 and its *ssgA* mutant GSA3. Cultures were grown on SFM for 2 days (**A-C**) and 5 days h (**B-D-E-F**) at 30°C. **A.** Young aerial hyphae of M145. **B.** Wild type spore chains. **C.** Young, unseptated, aerial hyphae of the *ssgA* mutant that often branched (white arrows). **D-E-F.** Late aerial hyphae of the *ssgA* mutant that often branched and occasionally produced spore chains. A higher proportion of the aerial hyphae in the *ssgA* mutant was lysed, compared with the wild type. Bar = 10 μm.

per μm (average of 870 foci and measured along the hyphal wall) (Fig. 2A, stage 3). Eventually, at sporulation septa we found one spot per septum (Fig. 2A and Fig. 3 (stage 4)). The position of the foci relative to the septa, namely a single spot and immediately adjacent to the hyphal wall, strongly suggests that SsgA is not a part of the divisome, as this is by definition localised in a ring-like fashion. Most of the mature spores (97 out of 127; Table 2) had two foci (average 2.0 ± 0.1 foci per spore: stage 5 in Fig. 3). This suggests splitting and segregation of the initial focus, or alternatively its disassembly and reassembly as two foci. To our knowledge this is the first subcellular localisation of a protein in *Streptomyces* spores.

During vegetative growth, SsgA-GFP foci were observed primarily in (very) young hyphae, including the tips of germinating spores (see below), but no foci were observed in older vegetative mycelium, until differentiation occurred from vegetative to aerial growth (not shown). The previous observation that vegetative cross-wall formation is normal in *ssgA* mutants (van Wezel et al., 2000a) suggests that SsgA does not play a major role in septum synthesis during early growth, so in what follows we focus on the role of SsgA during aerial development.

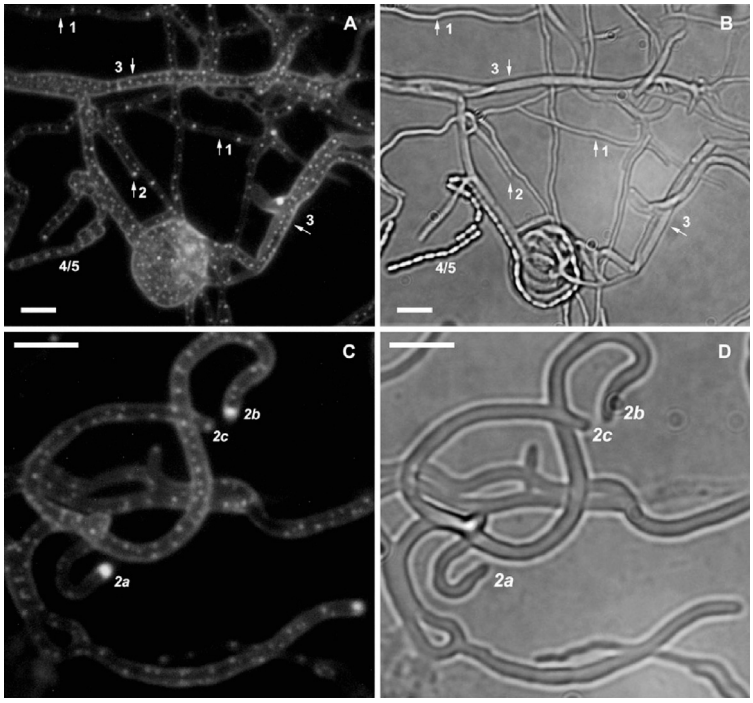

Figure 2: Fluorescence micrographs showing localisation of SsgA-GFP in *S. coelicolor*. Fluorescence microscopy (**A-C**) and phase contrast microscopy (**B-D**) of aerial hyphae expressing SsgA-GFP. Cultures were grown on SFM for 5 days at 30°C. **A-B.** Overview of aerial hyphae showing all stages of development except mature spores. SsgA was localised in several distinguishable patterns in aerial hyphae. Stages (indicated by arrows with a number; see also Fig. 3 and the scheme in Fig. 7): (1) early aerial hyphae; (2) tips of early sporogenic hyphae; (3) sporogenic hyphae; (4) septum site-initiation; (5) septa. The last stages - namely (6) spore separation and (G) germination - are not visible in this image, but are highlighted in Fig. 3, p97. **C-D.** Images showing close up of aerial hyphae with SsgA-GFP foci in the tips. Arrows indicate foci in the tips (stages 2a, 2b and 2c refer to Fig. 7). Bar = 2 μm.

SsgA and the selection of germination sites

The presence of the SsgA-GFP foci in the spores suggested a possible link with the selection of germination sites. To test this, we allowed spores from *S. coelicolor* M145, its *ssgA* mutant and a strain overproducing SsgA (GSA2; (van Wezel *et al.*, 2000a)) to germinate, and counted the number of germ tubes. There was a clear correlation between the average number of germ tubes per spore and the copy number of *ssgA*, with on average 1.7 (± 0.1) germ tubes per spores for the *ssgA* mutant, 2.0 (± 0.1) germ tubes per spore in M145 and 2.5 (± 0.1) germ tubes per spore in GSA2 (Table 2). The number of on average two germ tubes per spore in *S. coelicolor* M145 or in GSA3 complemented with SsgA-GFP corresponded very well to the average number of SsgA-GFP foci per spore (also 2.0 per spore, see above). Furthermore, more of the SsgA-overproducing spores carried four germ tubes (8 out of 115) than the parent M145 (2 out of 99) or the *ssgA* mutant (3 out of 89). In GSA2 we occasionally even identified spores with five emerging germ tubes (one among those that were counted), which was never seen in the parental strain. Generally, in older spores fluorescence was lost, suggesting that SsgA-GFP does not physically support the initiation of germ tube formation, but rather marks the future sites. However, in fresh spores the SsgA-GFP foci co-localised with the emerging germ tubes (labelled 'G' in Fig. 3). Thus, besides its role in the localisation of septa, these data suggest that SsgA is also involved in germination site-localisation. Interestingly, as mentioned above, SsgA-GFP was produced soon after the emergence of vegetative hyphae, and in particular at the tips, suggesting a possible role in (the control of) aerial apical growth (Fig. 3).

Table 3: Statistical analysis of germination frequencies.

Germ tubes per spore	M145	GSA3	GSA3 + *ssgA*-GFP	GSA2	**Foci per spore**	GSA3 + *ssgA*-GFP
1	20	42	14	8	1	14
2	61	34	56	56	2	97
3	16	8	16	42	3	12
4	2	3	1	8	4	4
5	0	0	0	1	5	0
6	0	0	0	0	6	0
Total	**99**	**87**	**87**	**115**	**Total**	**127**
Average	**2.0 ± 0.1**	**1.7 ± 0.1**	**2.0 ± 0.1**	**2.5 ± 0.1**	**Average**	**2.0 ± 0.1**

The table shows the number of spores observed with a certain number of germ tubes (one to six, see left column). Strains analysed were wild type *S. coelicolor* M145, its *ssgA* mutant GSA3, the same GSA3 but complemented with SsgA-GFP, or an SsgA over-expressing strain (GSA2). *Foci per spore* refers to the number of SsgA-GFP foci observed in spores of the *ssgA* mutant GSA3 complemented with a construct expressing SsgA-GFP.

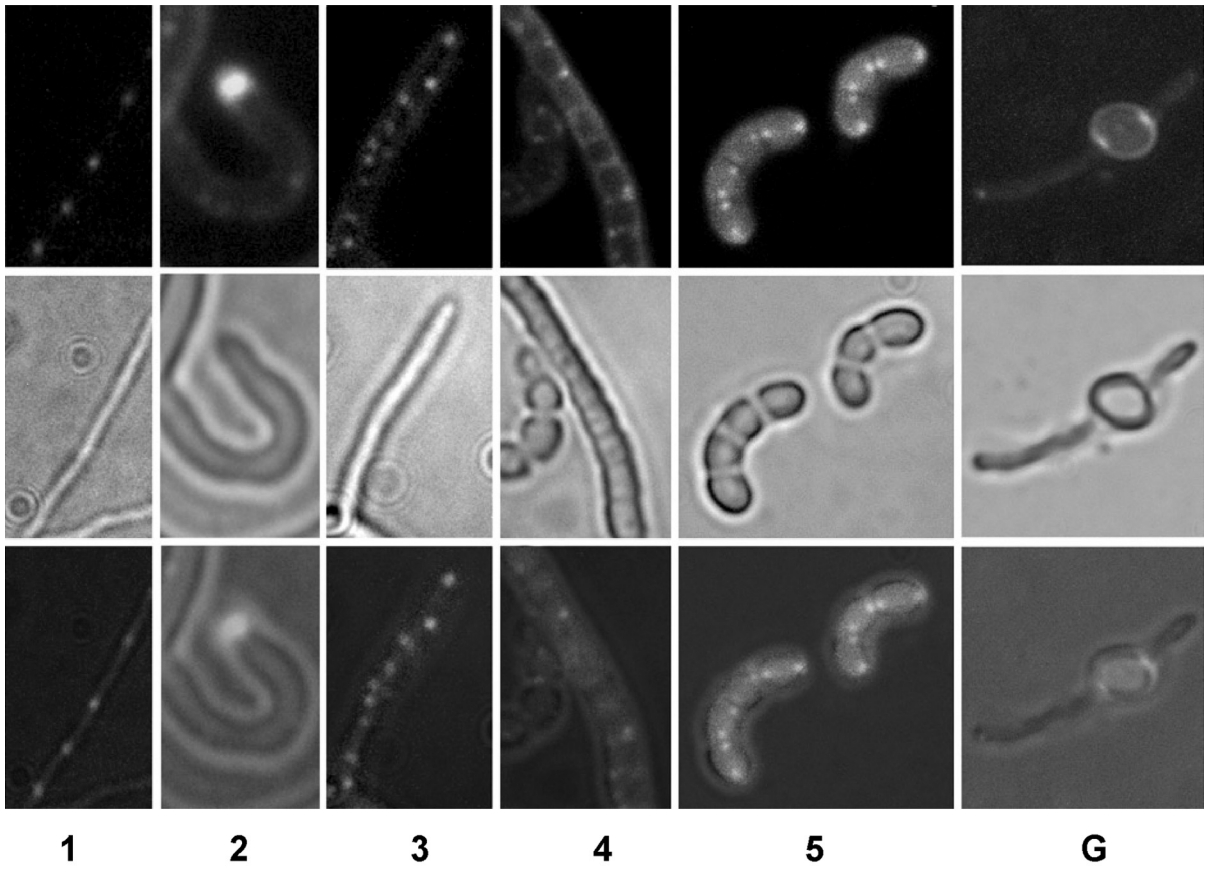

Figure 3: Fluorescence micrographs showing representative localisation of SsgA-GFP in all stages of aerial development. Developmental stages are sequentially labelled **1-5** and **G**, to facilitate comparison to the scheme in Fig. 7. The putative 'sub-apical stem' was postulated recently (Dalton *et al.*, 2007). For strains and growth conditions see Fig. 2, p95.

Global gene expression profiles in M145 and its *ssgA* and *ssgR* deletion mutants

To study the cellular response to the absence of either *ssgA* or *ssgR* and in this way discover more about the function of the respective gene products, we compared the development-dependent gene expression profiles of *S. coelicolor* M145 and its mutants GSA3 (M145 Δ*ssgA*) and GSR1 (M145 Δ*ssgR*) by DNA microarray analysis. Strains were cultivated on MM agar plates with mannitol as the sole carbon source and RNA was isolated from mycelium harvested at five time points, corresponding to vegetative growth (24h), aerial growth (36h, 48h) and sporulation (60h, 72h). Under these conditions, which have been employed for a variety of microarray experiments with *S. coelicolor*, the mutants showed a similar timing of development as its parent, although only a limited number of spores was produced. We used oligonucleotide-based microarrays of *S. coelicolor* (see Materials and Methods for details). The microarray experiments were carried out as independent duplicates. After data normalisation, genes were selected that were differentially expressed between *ssgA*

and *ssgR* deletion mutants compared to M145. We were surprised to find over 300 differentially expressed genes (Noens *et al*., 2007, Table S2).

We previously demonstrated that the readily observable *ssgR* mutant phenotype is primarily caused by the absence of *ssgA* (Traag *et al.*, 2004). However this does not completely rule out that SsgR may regulate other genes. To investigate this, we compared the global expression patterns of both mutants. Strikingly, after normalisation, the overall gene expression profiles in GSA3 and GSR1 were almost identical (Fig. 4, p180), again providing strong evidence that SsgR is the specific activator of *ssgA*.

Effect on transcription of developmental genes

Surprisingly, the genes that were up- or downregulated in the *ssgA* (and *ssgR*) mutant as compared to the parental strain M145 included no less than 35 well-known developmental genes (*e.g. bld, whi, chp, rdl, ssg, par*; see Fig. 5A-B, p180; Noens *et al.,* 2007, Table S2). Both the total number of genes affected by *ssgA* and the proportion that have recognizable developmental relevance were markedly higher than we have found in similar studies of other developmental mutants (*bldA*: A. Hesketh, G.B., E.L., F.F., G.H., C.P.S. and K.F.C., manuscript submitted; *whiI* (Tian *et al.*, 2007); *ssgC*, E.E.N., V.M., K.F.C., C.P.S. and G.P.v.W., unpublished). Thus, SsgA had a stronger impact on the control of the sporulation process than was expected on the basis of data obtained for other developmental mutants. Transcripts of *ftsI,* involved in septum synthesis and encoding the transpeptidase specifically required for septal PG synthesis (Errington, 2001; Holtje, 1998) were among the most over-represented mRNA species in the *ssgA* and *ssgR* mutants (more than three-fold during early aerial growth). Of the SALPs, mRNA of *ssgD* (whose function is still unclear) was more abundant in the mutants from the onset of aerial growth onwards, while the spore maturation *ssgE* and *ssgF* mRNAs were less abundant in the *ssgA* mutant, although the difference for *ssgE* was below the set threshold (two-fold). The mRNA for the major developmental regulatory gene *adpA* (*bldH*) was more than three-fold more abundant at all time points. AdpA is required for *ssgA* transcription in *S. griseus* and affects its expression in *S. coelicolor* (Traag *et al.*, 2004; Yamazaki *et al.*, 2003). *bldN* mRNA, encoding an ECF σ-factor whose transcription is dependent on AdpA, was more abundant in the *ssgA* mutant from early aerial phase onwards (Bibb *et al.*, 2000). Supportive evidence for the increased *adpA* and *bldN* mRNA levels is the increased representation of mRNAs for several components of the BldN regulatory cascade (*bldM, chpA-H;* (Bibb *et al.*, 2000; Elliot *et al.*, 2003)) in the *ssgA* mutant.

The mRNAs for all the chaplin genes *chpACDEFGH* (*chpB* was filtered from the analysis as it failed to pass the quality control) and rodlin (*rdlAB*) genes were very strongly increased. Many *bld* gene transcripts were affected as well, particularly those known to be active throughout the life cycle, which are therefore likely to play an important role during sporulation as well as during earlier stages of the *Streptomyces* life cycle. The mRNAs of the sporulation genes *whiA* and *whiH* were increased in the *ssgA* mutant from early aerial phase onwards, while mRNAs of the late sporulation gene *whiD* and the poorly defined sporulation gene *whiJ* were decreased; *whiB* and *whiG* were not significantly affected in the *ssgA* mutant (Noens *et al.,* 2007, Table S2). Finally, *divIVA* transcript was more than three-fold over-represented in the *ssgA* mutant at a time corresponding to late aerial growth and sporulation, an observation that is possibly linked to the branching of aerial hyphae observed in GSA3 (see Discussion). Despite the strongly enhanced septum formation that follows the over-expression of SsgA, the only differentially abundant cell division-related transcripts were those of of *ftsL* (which is co-transcribed with *ftsI*) and *ftsQ,* both of which were over-represented in the *ssgA* mutant.

Effect of *ssgA* deletion on transcription of secretion genes

The transcripts of five out of thirteen known secretion genes were more abundant in the *ssgA* mutant (Fig. 5C, p180; Noens *et al.,* 2007, Table S2), most of them, namely *tatA*, *tatC, secD, yidC1* (SCO3883)*,* and a homologue of *tatA* (SCO3768 or *tatA2*), by more than two-fold. In contrast, mRNA of *secDF* (SCO6160), encoding the SecDF protein, which is a natural fusion gene of *secD* and *secF* and is required to maintain a high capacity of protein secretion (Bolhuis *et al.*, 1998), was less abundant in all samples of the *ssgA* mutant.

Genes involved in DNA segregation and topology

The transcript abundance for several genes involved in DNA replication and segregation was also disturbed in the *ssgA* mutant (Fig. 5D, p180; Noens *et al.,* 2007, Table S2). More abundant transcripts included those of *parA* and *parB*, encoding chromosome partitioning proteins (Jakimowicz *et al.*, 2002b) and of *gyrA* and *gyrB*, for the two subunits of DNA gyrase (Calcutt, 1994) The *parAB* operon was upregulated during sporulation, while the *gyrAB* operon was upregulated throughout development. Conversely, transcripts of the DNA translocase gene *ftsK* (SCO5750: *spoIIIE* in *Bacillus*)*,* which is recruited to the FtsZ-ring in *E. coli* and *Bacillus subtilis* (Bath *et al.*, 2000; Liu *et al.*, 1998); reviewed in (Errington *et al.*,

2001)), and to developing sporulation septa in *S. coelicolor* (Wang et al., 2007) was less abundant in GSA3 at all time points. Besides the changed abundance of these five mRNAs, transcript abundance was also affected for genes close to the chromosomal origin of replication, *oriC*: from SCO3826 until SCO3923, mRNAs for 30% of the genes in this segment are differentially abundant, perhaps as a result of the enhanced expression of parB and/or DNA gyrase in the mutants (see Discussion).

Verification of microarray data by RT PCR

To independently verify the expression patterns of the microarray experiment, semi-quantitative RT-PCR was performed on RNA from the parental strain M145 and the *ssgA* mutant, using oligonucleotide pairs for a selection of targets (*ftsZ, divIVA, ftsI, parB, adpA, bldN*, *tatA,* and the *luxR*-like SCO0204) with 16S rRNA as the control (Fig. 6A). We used RNA samples corresponding to 24h (vegetative growth), 48h (aerial growth) and 72h (spores). The relative transcript abundance of *divIVA, ftsI, parB, ftsZ, adpA, bldN* and *tatA* (all up in GSA3 in comparison to in M145) and SCO0204 (strongly down in GSA3) corresponded well to the results obtained from the microarray analysis. We could not reproduce the microarray patterns for *ssgF* and *ftsK* (not shown). The RT-PCR data were quantified and presented after correction for 16S rRNA (Fig. 6B).

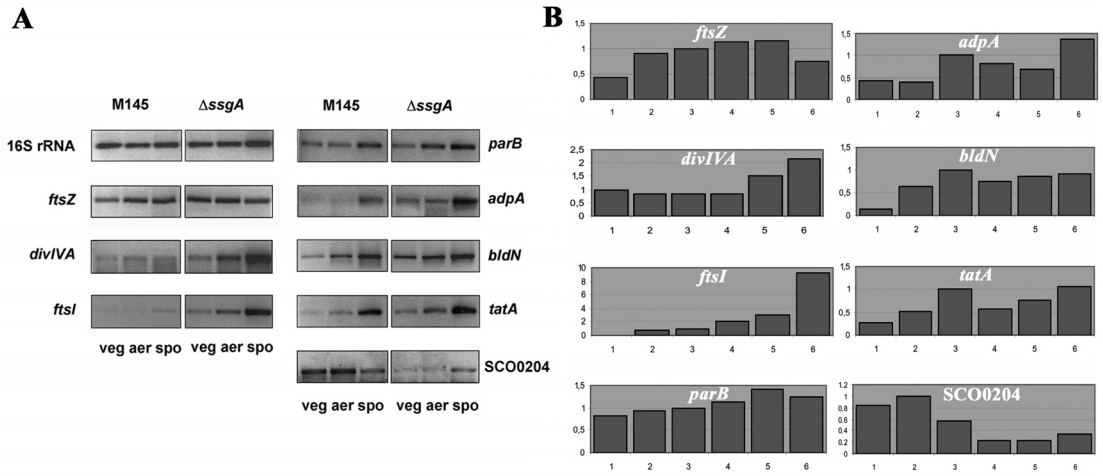

Figure 6: A. Transcriptional analysis of important SsgA-responsive genes by RT-PCR. Transcriptional analysis of *ftsZ, divIVA, ftsI, parB, adpA, bldN*, *tatA,* SCO0204 and 16S rRNA by semi-quantitative RT-PCR in M145 and the *ssgA* mutant. RNA samples at time points 24h, 48h and 72h were chosen corresponding to vegetative growth (veg), aerial growth (aer) and sporulation (spo) respectively. 16S rRNA and *ftsZ* were used as a control. These expression patterns conform well to the data obtained by transcriptomic analysis. **B. Quantification of RT-PCR results.** After the intensity of the bands was measured, the background value was subtracted from the total value, which was than corrected for 16S rRNA. For each gene, the highest value of the wild type was set to one. The RNA samples of M145 (1-3 on the X-axis) and of GSA3 (4-6) correspond to 24h (1, 4), 48h (2, 5) and 72h (3, 6). To allow easy comparison the highest value obtained for any of the three time points for the parental strain M145 was set to the arbitrary value of 1. The data were quantified and analysed using a GS-800 imaging densitometer and Quantity One software (BioRad).

The *ssgA* mutant shows disturbed DNA segregation and/or condensation

Considering the unexpectedly strong effect of the absence of *ssgA* on the expression of genes involved in DNA topology and segregation/condensation, we analysed the DNA distribution in aerial hyphae and (pre)spores by confocal fluorescence microscopy of samples stained with propidium iodide (PI). When aerial hyphae are actively growing, the DNA is distributed evenly in the hyphae (*i.e.* DNA segregation follows septation); while in mature spores the DNA is completely segregated, with one chromosome per spore (Jakimowicz *et al.*, 2005; Chapter 2). Interestingly, distribution of chromosomes was rather irregular in the *ssgA* mutant spore compartments (Fig. 7A, for a full colour version of Fig. 7, see p181), with many spores showing either very strong staining of nucleoids or no staining at all, while the wild type strain showed normal DNA segregation. This suggests disturbed segregation and/or condensation of chromosomes. In an *S. coelicolor* transformant with enhanced expression of SsgA, DNA segregation was normal.

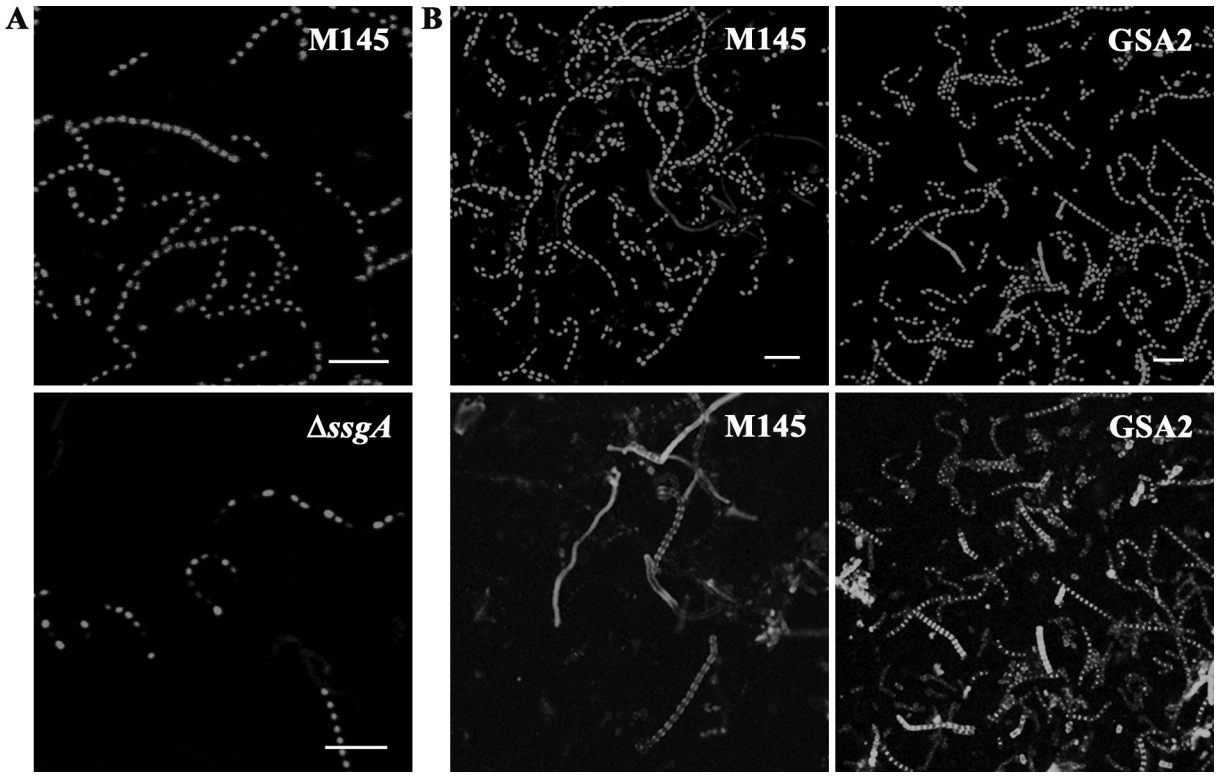

Figure 7: Visualisation of DNA and peptidoglycan subunits by fluorescence microscopy. Cultures were grown on SFM for 5 days at 30 °C**. A.** DNA content of *S. coelicolor* and the *ssgA* mutant revealed by propidium iodide (PI). The *ssgA* mutant is disturbed in DNA segregation. **B.** *S. coelicolor* M145 and its SsgA-overexpressing derivative GSA2. Left column shows DNA visualised with PI; right column shows peptidoglycan subunits visualised with f-WGA. GSA2 shows strongly enhanced septation in young aerial hyphae. f-WGA-stained foci also were observed between spores in the mature spore chains, most likely indicative of autolysis. Bar = 5 μm. (Full colour version, see p181).

To visualise *de novo* septal peptidoglycan synthesis, samples were also stained with fluorescein-conjugated wheat germ agglutinin (f-WGA), which stains unincorporated peptidoglycan subunits. Young aerial hyphae of surface-grown cultures of a strain with enhanced expression of SssA showed strongly enhanced production of septal peptidoglycan with many ladders typical of sporulation-specific cell division (Fig. 7B), in line with our earlier observation that SsgA activates the synthesis of septa (van Wezel *et al.*, 2000b). This phenotype is similar to the phenotype of a mutant in *ssgC*, which may antagonise SsgA function (Chapter 2). Additionally, f-WGA-stained foci were observed between spores in the mature spore chains, most likely indicative of the autolytic activity needed for spores to separate.

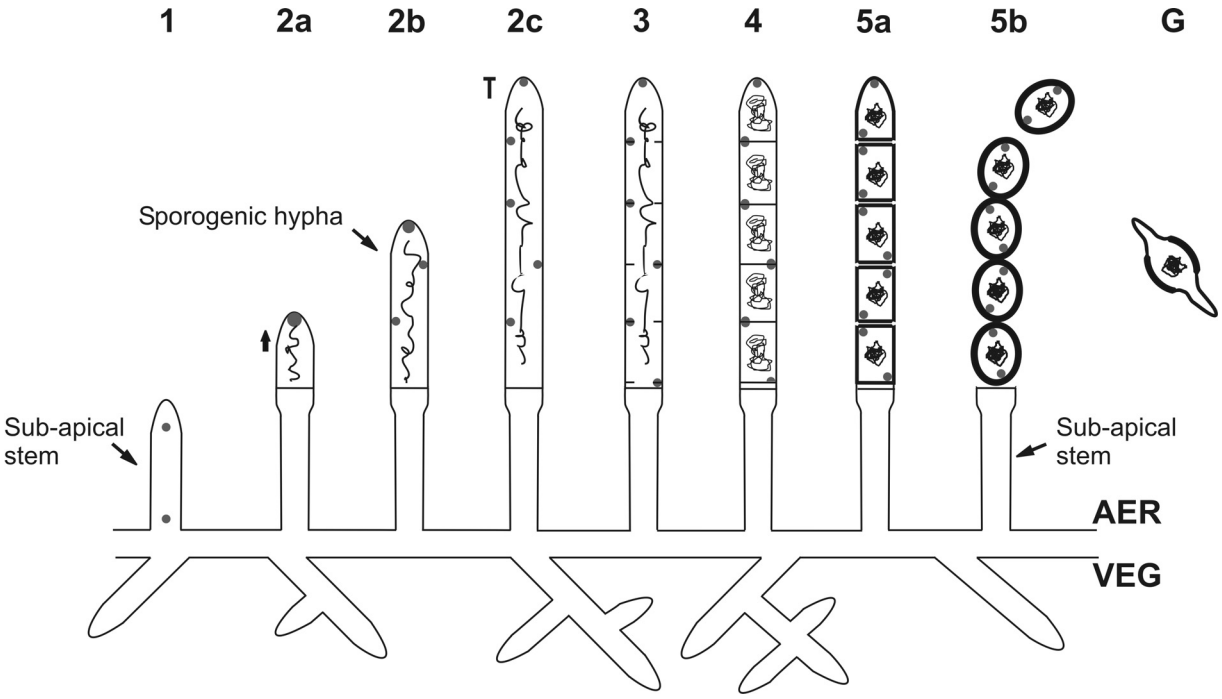

Figure 8: Scheme showing the localisation of SsgA-GFP during development of *S. coelicolor* M145. Grey spots refer to the observed localisation of SsgA-GFP foci. **Developmental stages:** (**1**) early aerial growth; (**2**) growth of aerial hyphae destined to be converted into spores ('sporogenic hyphae'); (**3**) in-growth of septa and DNA segregation/condensation; (**4**) completion of septa; (**5**) spore maturation (**5a**, completion of spore-wall synthesis; **5b**, autolytic spore separation); (**G**) germination of spores. Note that DNA is segregated after the initation of septum synthesis (between stages 3 and 4). For close-up images of SsgA-GFP localisations see Fig. 2, p95 and Fig. 3, p97.

DISCUSSION

SsgA is an activator of sporulation-specific cell division: *ssgA* mutants have almost no sporulation septa, while over-expression of the protein results in hyperseptation, which has been exploited to reduce mycelial clump size in industrial fermentations (van Wezel *et al.*, 2006). As shown previously, overexpression of SsgA alone can change morphology such that not only massive septa (up to 10 times the thickness of regular vegetative cross-walls) are produced, but the width of vegetative hyphae is approximately doubled to match that of sporogenic aerial hyphae (around 800 nm (van Wezel *et al.*, 2000a)). Hence, SsgA directly activates the synthesis of septal PG. Since SALPs lack a DNA binding motif, their effects may well be mediated via a direct interplay with components of the cell-division apparatus, and in particular with PBPs (in the cases of SsgA, SsgB and SsgG) and autolysins (in the cases of SsgE and SsgF) (Chapter 2). Two major issues concerning SsgA have been addressed here: its cellular localisation and likely function at different developmental stages; and the global transcriptional response to its absence.

SsgA controls events that require major changes in local cell wall morphogenesis at several developmental stages

Confocal fluorescence microscopy showed that most relatively fresh spores have two well-separated SsgA foci that co-localise with emerging germ tubes, implicating SsgA in determining where germination is initiated. SsgA is not essential for germination, but in its absence the average number of germ tubes per spore is reduced (<1.7 germ tubes per spore). Overproduction of SsgA enhances the number of germ tubes (2.5 per spore, against 2.0 in the parent M145).

Although SsgA is not important for vegetative cross-wall formation, we did observe SsgA foci at the tips of emerging germ tubes and young vegetative hyphae. Over-expression results in submerged sporulation, suggesting that ectopic SsgA expression disturbs the mechanisms that discriminate vegetative hyphae from aerial hyphae (van Wezel *et al.*, 2000a). Thus, SsgA-mediated submerged sporulation can now be reinterpreted as a response of the sporulation regulatory cascade to an ectopically realised checkpoint, the initiation of multiple septation. During sporulation of aerial hyphae, SsgA occurs at several distinct localisations (Fig. 2 and 3). The data are summarised in Fig. 8. Initially, SsgA-GFP formed relatively widely-spaced foci in the centre of young aerial hyphae; this may either represent an early

stage of SsgA assembly, or a yet unresolved compartment-specific function of SsgA in the so-called sub-apical stem (Dalton *et al.*, 2007). At the next stage, sporogenic hyphae emerged. These were distinguished by their increased diameter to around 600 nm, from around 400 nm for vegetative and young aerial hyphae. As sporogenic hyphae extended, bright foci were visible in the tips at first. These then faded while an increasing number of closely spaced foci formed behind the tip, resulting in a spacing similar to the foci of FtsZ-GFP (Grantcharova *et al.*, 2005) and the localisation of ParB complexes before septation (Jakimowicz *et al.*, 2005), and in line with the earlier observed upregulation of *ssgA* from the onset of sporulation (Traag *et al.*, 2004). This suggests that SsgA carried by the growing aerial tip may be distributed at regular intervals in aerial hyphae to mark future sites of septum formation. One speculative possibility is that the initial function of such SsgA foci is to establish new sites for peptidoglycan synthesis, associated with the accelerating elongation of aerial hyphal apical compartments, as the numbers of chromosomes increase exponentially (see (Chater and Losick, 1997), for a discussion). In turn, this could underpin much of the spatial regularity associated with sporulation. When hyphal elongation stops, the SsgA-associated peptidoglycan biosynthetic capacity could then instead be used for the formation of septum-associated wall material, via the acquisition of FtsI. Transcripts of *ftsI* were over-represented in the *ssgA* mutant, and FtsI is the only PBP known to be recruited by the divisome (after Z-ring formation has completed) and in other bacteria is responsible for the production of septal peptidoglycan (Botta and Park, 1981). The enhanced expression of *ftsI* may be a compensatory response to the absence of SsgA and hence of septal PG synthesis.

As sporulation septation progresses, SsgA localises on one peripheral edge of the sporulation septa, and finally appears as two foci, one at each end of each spore, which, by marking the sites of future germ tube emergence, complete the sequence of functions that SsgA mediates during the life cycle. The surprisingly regular pattern of septation presumably requires proteins that help mark the wall of aerial hyphae where in the future the (up to 100) septa must be localised (Flärdh and van Wezel, 2003; Schwedock *et al.*, 1997). Otherwise it is difficult to see how the highly regular spacing of around 1 μm can be achieved (almost) simultaneously. Interestingly, such cell wall marking occurs in filamentous fungi by septins, such as SepA in *Aspergillus nidulans* (Harris *et al.*, 1999). Like SsgA, SepA belongs to an entirely new family of cell division-related proteins with little similarity to other protein families (Longtine *et al.*, 1996; Longtine and Bi, 2003).

Comparison of the SsgA-GFP localisation data with the observed morphological changes due to either deletion or over-expression of *ssgA* shows an obvious relationship of SsgA with the processes that require major changes to the cell wall, and in particualr with germination, tip growth and septum synthesis. The enhanced expression of *divIVA* in the *ssgA* mutant, together with the localisation of SsgA in tips of germ tubes and growing (aerial) hyphae suggested a possible functional relationship with DivIVA, which determines the polarity of mycelial growth and is located at the tips of germ tubes and hyphae. SsgA disappeared as vegetative growth progressed, suggesting a role for SsgA during the initial stages of vegetative growth. The upregulation of *divIVA* in *ssgA* mutants was particularly apparent at later time points correlating to aerial growth and when branching of mutant aerial hyphae was observed by cryo-SEM. Hyphae grow by tip extension controlled among others by DivIVA, and enhanced expression of DivIVA gave rise to several new sites of cell wall synthesis, with hyperbranching as a result (Flärdh, 2003). A role of SsgA in the control of branching frequency and/or branch-site selection is supported by the large number of small branches produced when SsgA is overproduced. However, many of these small branches fail to extend beyond 1-2 μm, suggesting that the machinery required to extend apical growth is not sufficiently abundant to support growth of most of the branches. Although SsgA-GFP was abundant in the tips of all aerial hyphae, the localisation of DivIVA in aerial hyphae is unknown, but perhaps similar during hyphal extension (K. Flärdh, personal communication). Upregulation of *divIVA* during later development in the *ssgA* mutant may well be responsible for the branching observed in the *ssgA* mutant aerial hyphae, which is in line with recent experiments that established a function for DivIVA in aerial growth (K. Flärdh, personal communication).

What model can we distill from these seemingly diverse data to explain the function of SsgA? As argued above, in each case (septation, branching and germination) a significant change in the local cell wall morphogenesis is effected, requiring opening of the cell wall (and peptidoglycan), followed by *de novo* peptidoglycan and membrane synthesis and - certainly in the case of sporulation-specific cell division – coordination along the hypha and probably previously determined site selection. Taking into account the observed relationship between SALPs and peptidoglycan-related enzymes (PBPs and autolysins; (Chapter 2)) we propose that SsgA is a chaperonin-like protein that plays an important role in marking the cell wall for major changes at a later moment in time, and in particular in determining the sites for

septation and germination. Such a function is comparable to that of SepA in the morphologically very similar filamentous fungi.

Disturbance of SsgA-mediated changes in cell wall biosynthesis causes many changes in the expression of developmentally relevant genes, suggesting that SsgA contributes to an important developmental checkpoint.

Changes in apparent gene expression in the *ssgA* mutant are likely to be the combined result of two major factors: feedback to the genome of information from specific changes in the cellular state caused by *ssgA* mutation; and changes in the relative abundance of cell types. Remarkably, the transcripts of around 300 genes were increased or decreased in relative abundance by at least two-fold in the mutant, at two or more time points. This is much more than observed for other developmental mutants: the highest number previously reported is the 125 transcripts affected in a *whiI* mutant (Tian et al, 2007), and only 17 transcripts were reported to be affected by a *bldN* mutation (Elliott et al., 2003). Overall, these considerations make it likely that the changes in the transcriptome caused by mutation of *ssgA* are largely specific effects on gene expression, rather than simply reflecting changes in the proportions of different cell types.

Strikingly, the products of genes affected by *ssgA* included close to 40 well-known cell-cycle control proteins (see below). These do not include genes that encode the components of the divisome scaffold (*i.e.* the Z-ring and supporting proteins), with *ftsQ* and the *ftsI-ftsL* operon as exceptions. This, and the fact that the *ssgA* mutant produces occasional spore chains on mannitol-containing media, and that FtsZ-GFP rings were formed under these conditions, indicates that indeed SsgA is not essential *per se* for Z-ring formation in aerial hyphae (Fig. 1, Chapter 3).

The mRNA profiles in the *ssgA* and *ssgR* mutants were very similar, in line with our earlier experiments showing that SsgR is the specific transcriptional activator of *ssgA* (Traag *et al.*, 2004). It is therefore highly likely that SsgR regulates only the downstream-located *ssgA*. In fact, the observed (high) similarity in the mRNA profiles provides strong support for the validity of the microarray data obtained for the *ssgA* mutant (Fig. 5, p180).

Effects on chromosome segregation and secretion

We observed a highly irregular distribution of chromosomes in the spore compartments when *ssgA* mutants were grown under conditions that allow full development. Our microarray

analysis suggests that this disturbed DNA distribution is at least partially due to the altered expression of *parAB* and *gyrAB*. The development-specific expression of *gyrA* and *gyrB* and of *parA* and *parB* in the wild type was further enhanced in the *ssgA* mutant. *gyrA* and *gyrB* are the two genes for DNA gyrase, a type II DNA topoisomerase responsible for the catalysis of the negative supercoiling of the DNA in replication, while ParA and ParB contribute to correct partitioning of the chromosomes into the unigenomic spore compartments ((Kim *et al.*, 2000); Jakimowicz et al., manuscript submitted). Changes in the expression of *gyrAB, parAB* and also *ftsK* (although the latter could not be corroborated by RT-PCR analysis) might well have effects on the correct segregation, condensation and topology of the chromosomes. Surprisingly, besides the *gyr* and *par* genes, many other *ori*-proximal genes showed deregulated expression in the *ssgA* mutant. Genome-wide, the expression of >4 % of the genes is affected significantly in the *ssgA* mutant, while 30 out of 98 *ori*-proximal genes, namely ORFs SCO3826 – SCO3923, are affected. Suggestively, *ssgRA* (SCO3925-3926) lie immediately next to this cluster of genes. Many of these genes are essential genes involved in DNA synthesis and maintenance.

Finally, the expression of genes that encode proteins involved in the Sec and Tat secretion pathways is also significantly affected by *ssgA* mutation. Most of these genes show increased transcription in the mutant relative to its parent M145, except for the *secDF* gene (decreased). We recently showed that enhanced *ssgA* expression has a strongly positive effect on secretion (and production) of enzymes in *Streptomyces lividans* (van Wezel *et al.*, 2006). Thus, the secretion genes respond similarly as *ftsI*: SsgA is known to enhance the associated processes (septum formation, secretion), but the relevant genes are upregulated in an *ssgA* mutant, perhaps as a compensatory effect. Comparison of microarray data on the *ssgA* mutant with those of a strain over-expressing *ssgA* (not yet available) could shed more light on this puzzling phenomenon.

The position of *ssgA* in the developmental hierarchy

What is the position of SsgA in the developmental control hierarchy? Our experiments and previous observations strongly suggest a function for SsgA in the coordination of septal peptidoglycan synthesis. The prime candidate for the latter is *ftsI*, one of the more strongly over-expressed genes in the *ssgA* mutant (see below). The timing for SsgA function is also highlighted by the response of the *whi* genes: the earlier-acting aerial hyphal developmental genes *whiA*, *whiH, whiI* and *whiJ* were over-expressed in the *ssgA* mutant, while spore

maturation genes, including *ssgE* and *ssgF* (both important for correct autolytic spore separation), *sigF, whiD,* and the spore pigment cluster *whiE* (Kelemen *et al.*, 1998; Molle *et al.*, 2000; Chapter 2)), were under-expressed. This remarkable tendency suggests that the irregularities of the *ssgA* mutant in developmental gene expression are most likely a checkpoint effect, *i.e.* the septum formation/DNA partitioning checkpoints have not been passed. We also observed significant over-expression of several *bld* genes, including *bldB, bldC, bldD, bldG* and the *adpA* (*bldH*) responsive genes, including *bldN*, in the *ssgA* mutant. While *bld* genes are by definition essential for early developmental events, their mRNA levels remain high and in some cases strongly increase late on (*e.g. bldN* (Bibb *et al.*, 2000)) and they were particularly abundant in the *ssgA* mutant at late time points. The *chp* genes for the chaplin proteins, which are part of the spore coat (Claessen *et al.*, 2003; Elliot *et al.*, 2003), as well as the functionally related *rdl* genes, were all markedly over-expressed in the *ssgA* mutant (Fig. 5B, p180; Noens *et al.,* 2007, Table S2). Thus, the phenotypic and transcriptional analyses together suggest that SsgA plays a crucial role in the control of morphogenetic processes leading to the formation of septal peptidoglycan in aerial hyphae, at a time relating to the activities of WhiA and WhiB, and prior to or at the onset of Z-ring formation, and that the failure of the septation checkpoint prevents the expression of genes for post-septation functions. A similar effect was implied in a previous report (Flardh *et al.*, 2000) showing that at least some late functions were not carried out when sporulation septum formation was prevented by a developmental stage-specific deficiency of FtsZ.

Conclusion

SsgA is an important cell-cycle control protein that most likely functions by (facilitating the) marking of the cell wall for future major changes in cell wall morphogenesis, with a clear involvement in and stimulatory effect on coordinated sporulation-specific cell division and spore germination, and perhaps also on branching. This, together with the localisation data, supports the idea that SsgA fulfils a chaperone-like function, aiding the cell wall synthesising machineries to find the exact positions for future peptidoglycan synthesis. In this way, SsgA may be one of the proteins that compensate for the absence of septum-localising proteins such as FtsA, ZipA, Noc and MinCE in unicellular bacteria. The search for direct interaction partners for SsgA should better our understanding as to how SsgA functions at the molecular level.

ACKNOWLEDGEMENTS

We thank Gerda Lamers for help with fluorescence microscopy, Marie Elliot and Sebastien Rigali for discussions and Klas Flärdh for plasmid KF41 and for sharing unpublished data. The work was supported by EU Marie Curie training grant HPMF-CT-2002-01676 to KFC and Jay Hinton (Institute of Food Research, Norwich), by BBSRC grants G18886 to CPS and G18887 to KFC, and by grants of the Royal Dutch Academy for Arts and Sciences (KNAW) and the Netherlands Organisation for Scientific Research (NWO) to GPvW.

5

MreBCD and Mbl of *Streptomyces coelicolor* are required for the integrity of aerial hyphae and spores

Elke E. E. Noens, Paola Mazza, Kathrin Shirner,
Nina Grantcharova, Mieke Mommaas, Henk K. Koerten,
Gunther Muth, Klas Flärdh, Wolfgang Wohlleben
and Gilles P. van Wezel

Parts of this chapter have been published in
Mol Microbiol (2006) 60: 838-852

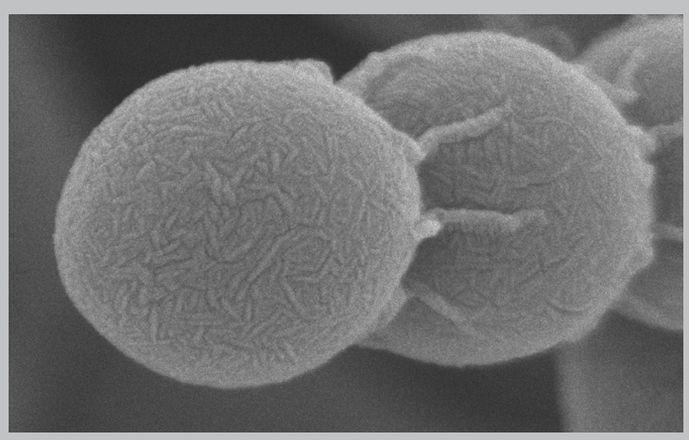

ABSTRACT

The cytoskeletal protein MreB is involved in cell shape determination and chromosome segregation in many rod-shaped bacteria. PCR-based and Southern analysis of various actinomycetes, supported by analysis of genome sequences, revealed *mreB* orthologues only in genera that form an aerial mycelium and spores, although a distant relative was found in *Rhodococcus*. We analysed MreBCD and Mbl in *Streptomyces coelicolor*. Ectopic overexpression of *mreB* impaired growth, and caused swellings and lysis of hyphae. *mreB* and *mbl* null mutants were created, which showed normal vegetative growth but aberrant development. Analysis of null mutants deleted for either *mreB, mreC, mreD, mreBCD*, *mbl* or *pbp2* were subjected to an intensive study using electron microsocpy. All mutants had similar anomalies, with swelling and lysing aerial hyphae and spores of aberrant dimensions, indicative of disruption of the cell wall integrity. An MreB-EGFP fusion protein localised at the septa of sporulating aerial hyphae, as bipolar foci in young spores, and as ring- or shell-like pattern inside mature spores. No specific localisation was observed in vegetative hyphae, although transcription of *mreB* was at least as high as in aerial hyphae. Immunogold electron microscopy using MreB-specific antibodies revealed that MreB is located immediately underneath the spore wall. Thus, MreBCD and Mbl are not essential for vegetative growth of *S. coelicolor*, but exert their function in the formation of environmentally stable spores, thereby primarily influencing the assembly of the spore cell wall.

INTRODUCTION

Bacterial morphologies range from spherical and rod-shaped to curved, helical and filamentous. A major determinant of cell shape is the bacterial cell wall, which consists of glycan strands cross-linked by short peptides. Isolated peptidoglycan sacculi can retain the shape of the bacterial cell, and mutants defective in peptidoglycan synthesis typically show an altered morphology (Cabeen and Jacobs-Wagner, 2005; Young, 2003). However, not only the enzymes that are directly involved in the synthesis and assembly of peptidoglycan affect the morphology. It is becoming increasingly clear that cytoskeletal elements exist in the bacterial cytoplasm (Lowe *et al.*, 2004) and that these determine the architecture of the cell wall, with a strong impact on cell shape. These include homologues of all three major types of eukaryotic cytoskeletons. MreB-proteins are actin homologues that produce microfilament-like fibers and determine rod-shape in many bacteria (Jones *et al.*, 2001; van den Ent *et al.*, 2001); crescentin (CreS) produces intermediate filament-like elements in *Caulobacter crescentus* that give rise to a curved cell shape (Ausmees *et al.*, 2003); FtsZ is a tubulin-homologue that assembles into a cytokinetic ring at the site of cell division and directs cell division and formation of the septal peptidoglycan (Margolin, 2005).

MreB is a member of the HSP70-actin-sugar kinase (ASHKA) superfamily of proteins (Bork *et al.*, 1992), and its crystal structure is strikingly similar to the structure of actin (van den Ent *et al.*, 2001). Purified MreB of *Thermotoga maritima* polymerises *in vitro* to form filaments with a spacing between the MreB monomers of 51 Å, which is reminiscent of the spacing between the subunits (55 Å) in actin filaments (van den Ent *et al.*, 2001). MreB-like proteins have been studied primarily in *E. coli* (MreB), *B. subtilis* (MreB, Mbl, MreBH) and *C. crescentus* (MreB), and immuno-fluorescence microscopy and GFP-tagging showed that they form helical-like structures underneath the cell envelope (Jones *et al.*, 2001; Shih *et al.*, 2003; Soufo and Graumann, 2003). MreB is essential in *E. coli* and *B. subtilis*, and its depletion resulted in increased cell width, loss of cell shape and eventually lysis (Formstone and Errington, 2005; Jones *et al.*, 2001; Kruse *et al.*, 2005; Lee and Cohen, 2003). The MreB-like Mbl protein is required for determination of the rod-shape of *B. subtilis*, and forms helical cytoskeletal structures that are needed for incorporation of new peptidoglycan along the lateral wall during cell elongation (Daniel and Errington, 2003). While these observations suggest that MreB-like proteins form actin-like fibers defining the bacterial cell shape, the precise cellular function of MreB proteins remains unclear. Recent studies link MreB to

peptidoglycan synthesis (Daniel and Errington, 2003), correct chromosome segregation (Gitai *et al.*, 2005; Kruse *et al.*, 2003; Soufo and Graumann, 2003), and cell polarity (Gitai *et al.*, 2004). Interestingly, the MreB homologue of the rod- and coccoid-shaped *Rhodobacter sphaeroides* failed to produce helical structures and rather formed a ring at the mid-cell position of elongating cells, suggesting it also plays a role in septal peptidoglycan synthesis in this organism (Slovak *et al.*, 2005). Thus, MreB may well have different functions in different organisms.

mreB is almost invariably part of an operon with *mreC* and *mreD*, and typically followed by *pbp2*, which is transcribed from its own promoter. Like *mreB*, the *mreC* and *mreD* genes are essential in *E. coli* and *B. subtilis,* and their depletion results in lost control of cell shape, spheroid morphology and lysis (Kruse and Gerdes, 2005; Leaver and Errington, 2005; Lee and Stewart, 2003). A link between the actin-like cytoskeleton formed by the MreB family and the lateral cell wall synthesis machinery is suggested (Daniel and Errington, 2003; Errington, 2003; Kruse and Gerdes, 2005). *pbp2* from *S. coelicolor*, encoding a penicillin-binding protein (PBP) has high similarity with *E. coli* PBP2, which is involved in elongation of the lateral cell wall (Vinella *et al.*, 1993) and with SpoVD, a PBP important for sporulation in *B. subtilis* (Daniel *et al.*, 1994). Absence of the elongation system in *E. coli* and *B. subtilis* leads to the formation of rounded cells (Wei *et al.*, 2003).

The absence of an *mre* gene cluster in coccoid species such as *Streptococcus*, *Staphylococcus* and *Lactococcus* suggests that a spherical shape may relate to the absence of an *mre*-dependent system and that MreB is particularly important in rod-shaped cells (Jones *et al.*, 2001). However, the rod-shaped actinomycete *Corynebacterium glutamicum* also lacks *mreB*-like genes in its genome and establishes its rod-shape in an MreB-independent way, through growth of the cell wall only at the cell poles (Daniel and Errington, 2003). Most other actinomycetes also lack *mreB*, but streptomycetes are a notable exception as their genomes contain well-conserved *mreB*-homologues (see below). The genome of *S. coelicolor* contains an *mreBCD-pbp2* gene cluster and a separately located *mbl* gene. In this chapter, we describe the creation and study of cytoskeletal mutants, which are studied by advanced electron microscopy, confocal fluorescence microscopy and transcriptional analysis. We provide evidence that all components play an important role in the control of the shape of aerial hyphae and spores.

MATERIALS AND METHODS

Bacterial strains and culturing conditions

The *E. coli* and *S. coelicolor* A3(2) strains are listed in Table 1. *S. coelicolor* strains were cultivated on SFM or R2YE agar plates or in TSB medium, with or without the appropriate antibiotics as indicated (Kieser *et al.*, 2000). Cultivation of strains and procedure for DNA manipulation was performed as previously described for *E. coli* (Sambrook *et al.*, 1989) and *S. coelicolor* (Kieser *et al.*, 2000). Protoplasts of *S. coelicolor* M145 were transformed with the plasmids pPM1 or pGM190 as described previously (Kieser *et al.*, 2000).

Table 1: Strains of *E. coli* and *S. coelicolor*.

Strain	Characteristics	Reference
E. coli BL21(DE3)pLysS	See reference	Invitrogen
E. coli ET 12567	See reference	(MacNeil *et al.*, 1992)
E. coli DH5α	See reference	(Woodcock *et al.*, 1989)
E. coli BW 25311/pIJ790	See reference	(Gust *et al.*, 2003)
S. coelicolor M145	SCP1$^-$ SCP2$^-$	(Kieser *et al.*, 2000)
mreB-IM	M145 *ΔmreB::aac(3)IV*	This chapter
mreB-IFD	M145 *ΔmreB*	This chapter
mreB-IFDc	M145 *ΔmreB attB$_{\Phi C31}$::mreB*	This chapter
Δ*mreC*	M145 Δ*mreC::aac(3)IV*	(Burger *et al.*, 2000)
Δ*mreD*	M145 Δ*mreD::aac(3)IV*	W. Wollheben
Δ*mreBCD*	M145 Δ*mreBCD::aac(3)IV*	W. Wollheben
Δ*mbl*	M145 *Δmbl::aac(3)IV*	This chapter
Δ*pbp2*	M145 Δ*pbp2::aac(3)IV*	G. Hobbs
SCPM6	M145 *attB$_{\Phi C31}$:: mreB-egfp*	This chapter

Plasmids

All plasmids and constructs are listed in table 2. The oligonucleotides are listed in table 3.

To obtain a construct for the expression of MreB in *S. coelicolor*, the *mreB* gene was amplified from *S. coelicolor* M145 genomic DNA by PCR using primers PM1 and PM2, the PCR product was digested with *Nde*I-*Hin*dIII and cloned behind the thiostrepton-inducible promoter *PtipA* by inserting it in the *Streptomyces* multi-copy plasmid pGM190 (G. Muth, unpublished data) digested with the same enzymes. The resulting plasmid was designated pPM1. To construct a C-terminal fusion with the EGFP protein, *mreB* was amplified from *S. coelicolor* M145 genomic DNA using primers PM5 and PM6, and cloned as an *Nde*I-*Bgl*II fragment in front of the *egfp* gene in plasmid pTST101 (J. Altenbuchner, personal communication). The resulting *mreB-egfp* fusion was removed from pTST101 with *Nde*I and *Bam*HI and cloned in the integrative *Streptomyces* vector pSET152 (Bierman *et al.*, 1992)

digested with the same enzymes, generating pPM4. Plasmid pPM6 was constructed to complement the *mreB* deletion mutant by amplifying the *mreB* gene with its promoter region from *S. coelicolor* M145 genomic DNA with primers PM11 and PM12 and cloning the PCR product as a *Bgl*II-*Eco*RI fragment in pSET152 (Bierman *et al.*, 1992). Finally, to allow high-level production of MreB in *E. coli* to use for preparation of antibodies, *mreB* was amplified by PCR from *S. coelicolor* genomic DNA using primers PM7 and PM2, and the resulting DNA fragment was digested with *Bam*HI and *Hin*dIII and cloned in pRSETB (Invitrogen), so as to form an in frame fusion with the His-tag (pPM5).

Table 2: Plasmids and constructs.

Plasmid/ Cosmid	Description	Reference
pGM190	*Streptomyces* multi-copy plasmid with thiostrepton-inducible promoter *PtipA*	G. Muth; unpublished data
pTST101	*E. coli* plasmid containing *malE-egfp*	J. Altenburgher
pSET152	*Streptomyces/ E. coli* shuttle vector (integrative in *Streptomyces*, high copy number in *E. coli*)	(Bierman *et al.*, 1992)
pRSETB	*E. coli* plasmid with high level expression from the bacteriophage T7 promoter and N-terminal polyhistidine (6xHis) tag	Invitrogen
C88	Cosmid clone containing *mreB*	(Bentley *et al.*, 2002)
C24	Cosmid clone containing *mbl*	(Bentley *et al.*, 2002)
PM1	pGM190 with a DNA fragment harbouring *mreB*	This chapter
PM4	pSET152 with a DNA fragment harbouring *mreB* and *egfp*	This chapter
PM5	pRSETB with a DNA fragment harbouring *mreB*	This chapter
PM6	pSET152 with a DNA fragment harbouring *mreB* with its promoter region	This chapter
PM11	Mutant cosmid C88 with coding region of *S. coelicolor mreB* replaced by *aacC4*	This chapter
PM12	Mutant cosmid C88 with an in frame deletion of *S. coelicolor mreB*	This chapter
C24/Δ*mbl*	As PM11, but for *S. coelicolor mbl*	This chapter

Protein purification and Western analysis

His_6-tagged MreB was expressed in *E. coli* BL21 containing pPM5 and purified with Ni-NTA spin columns (Qiagen) under denaturing conditions, as described in the supplier's manual. Rabbit polyclonal antibodies were raised against the purified protein (Eurogentec). For expression of MreB in *S. coelicolor*, transformants were inoculated in TSB containing kanamycin (50 μg ml^{-1}), and thiostrepton was added to 10 μg ml^{-1} (final concentration) for induction of expression. After 18h of growth, mycelium was collected and lysed with a French Press. Crude extracts were mixed with an equal volume of 2X sample buffer (125 mM Tris-HCl pH 6.8; 4% SDS; 20% glycerol; 2.0 mM EDTA; 0.02% bromophenol blue; 3% dithiothreitol), heated at 100°C for 5 min and loaded on SDS-polyacrylamide gels (12.5%).

Proteins were capillary transferred to a nitrocellulose membrane (Pall Corporation). MreB was detected using a 1:250 dilution of polyclonal anti-MreB serum.

Table 3: Oligonucleotides.

Primer	Sequence (5'→3')
PM1	cg**catatg**gggaactcaatgtcgttc
PM2	ga**aagctt**acgtcatctacggggcg
PM5	cg**catatg**tgatccttcttcgggac
PM6	gg**agatct**gatgaacgacattga
PM7	aa**ggatcc**ggggaactcaatgtcg
PM9	ccctcaaaagctcctgggaaggccagtcgaatcctgatggatatcattccgg**ggatcc**gtcgacc
PM10	ggagatcgtctcgtacggcggaaccgaagtgttacgtcagatatctgtaggctggagctgcttc
PM11	g**cagatc**tgacgccatgtcagtcga
PM12	gc**gaattc**ggcggaaccgaagtgtta
PM13	gccgtgcgcccgctgaaggacgg
PM14	agcagcgcgcgccgccgcggt
mbl-F	ggccccgcacggtccgcgctctcgggaggattcgccatgattccggggatccgtcgacc
mbl-R	tgcgtcaggcttccccggtcgccgcccggcggcggatcatgtaggctggagctgcttc
mreB-Fli	cgtccgtcgtcgcgatcaacacc
mreB-Rli	gtgatctcgaagtcggcgatgacg
mreC-Fli	cctcaaggcgaagctcggcagc
mreC-Rli	cgctcctatggcgatgacctgg
mreD-Fli	ctggtgatccaggtgagcgtcc
mreD-Rli	ccgacgtggccgtagaccagg

Restriction sites are written in bold.

Cell Fractionation

S. coelicolor M145 and its derivative SCPM6 (containing *mreB-egfp*) were grown for 2-3 days in 150 ml TSB with appropriate antibiotics at 30°C and harvested by centrifugation. Mycelium was resuspended in 6 ml 25 mM Tris-HCl (pH 7.5), 100 mM NaCl and 1 mM protease inhibitor (Complete EDTA-free tablets, Roche), and the cells were lysed using the French Press. The cell extract was centrifuged at 90,000 x g for 30 min at 4°C; the cytosolic fraction was stored, while the pellet fraction was resuspended in a buffer of 25 mM Tris-HCl (pH 7.5), 1 M NaCl and 20% glycerol, stirred for 2h at 4°C and centrifuged at 90,000 x g for 30 min at 4°C. The supernatant containing membrane-associated proteins was stored at –20°C, and the membrane-containing pellet fraction was solubilised in 25 mM Tris-HCl (pH 7.5), 1 M NaCl, 20% glycerol and 2% Triton X-100, stirred overnight at 4°C and again centrifuged for 30 min at 90,000 xg.

Creation of *mreB* and *mbl* null mutants

To create *mreB* and *mbl* mutants, the PCR-targeting procedure described by (Gust *et al.*, 2003) was used. The *ΩaacC4* cassette (which confers apramycin resistance) was PCR-

amplified from pIJ773 with oligonucleotides PM9 and PM10 for *mreB* and mbl-F and mbl-R for *mbl*. Cosmids C88 and C24 were used for *mreB* (C88.22c, SCO2611) and *mbl* (C24.22, SCO2451), respectively. The subsequent steps were described in detail in (Noens *et al.*, 2005). DNA of mutant candidates was isolated and tested with PCRs and Southern hybridisations to confirm the absence of the chromosomal *mreB* or *mbl*, respectively. The resulting mutants were designated *mreB*-IM (for the *mreB* insertional mutant) and Δ*mbl* (for the *mbl* insertional mutant).

In order to remove the disruption cassette still present in *mreB*-IM, the knock-out cosmid pPM11 was introduced in *E. coli* DH5α/pCP20 that expresses the FLP recombinase for removal of the *aacC4* cassette (Gust *et al.*, 2003). The resulting cosmid pPM12 carrying the in frame deletion of *mreB* was transformed to *S. coelicolor mreB*-IM (Kieser *et al.*, 2000). Transformants were first selected for insertion of the cosmid by single cross over (Km^R) and then screened for the double-cross over event (loss of both kanamycin and apramycin resistance). The loss of the disruption cassette was confirmed with PCR and Southern blot analysis. This mutant was designated *mreB*-IFD.

RNA isolation and RT-PCR

mreB-IFD and its parent *S. coelicolor* M145 were grown on cellophane disks on MM containing 1.5% Hispan agar and 0.5% mannitol as the carbon source. Mycelium was harvested at times corresponding to vegetative growth (20h-24h), aerial growth (36h-40h-48h) or sporulation (48h-60h-72h-96h). *mreB*-IM and M145 were grown in TSBS medium and mycelium was collected during exponential growth at a OD of around 0.4. RNA was purified using a modified version of the Kirby protocol (Kieser *et al.*, 2000). RNA purification columns (RNeasy, Qiagen) and DNaseI treatment were used as well as salt precipitation (final concentration 3M NaAc pH 4.8) to purify the RNA and remove any traces of DNA. RT-PCR analysis was carried out using the Superscript III one step RT-PCR System with Platinum® *Taq* DNA polymerase (Invitrogen). For each RT-PCR reaction 100 ng of RNA was used together with 1μM (final concentration) of each primer. Reactions without reversed transcription were used as a control for the absence of genomic DNA in the samples. The program was as follows: 45 min cDNA synthesis (reversed transcription) at 48°C, followed by 2 min at 95°C and 25, 29, 31 or 35 cycles of: 45 s at 94°C (denaturation), 30 s at 68°C (annealing) and 30 s at 68°C (elongation). The reaction was completed by 5 min incubation at 68°C. 5μl of each sample was tested by electrophoresis on a 2% agarose gel in

1xTAE buffer and EtBr-stained DNA visualised on a UV transilluminator. The oligonucleotides are listed in Table 2.

Microscopy

Phase contrast microscopy.

For light microscopy, sterile coverslips were inserted at a 45° angle into SFM agar and spores were inoculated in the acute angle along the glass surface. Coverslips were removed after 3-4 days of incubation at 30°C and mounted in PBS containing 50% glycerol on poly L-lysine-coated slides. Alternatively, 10 µl of liquid-grown culture was spotted directly on microscope slides covered with 1% agarose under a coverslip. Samples were analysed with an Olympus System Microscope BX60 with F-view II camera.

Electron Microscopy.

Morphological studies of surface-grown aerial hyphae and spores of *S. coelicolor* M145 and its mutants by cryo-scanning electron microscopy (cryo-SEM) was performed as described previously, using a JEOL JSM6700 SEM (Keijser *et al.*, 2003). Strains were grown for 5 days at 30°C on SFM agar plates. Transmission electron microscopy (TEM) for the analysis of ultra thin cross-sections of hyphae and spores was performed as described previously (van Wezel *et al.*, 2000). Samples were taken after 5 days of growth at 30°C on SFM. For immuno-electron microscopy spores were fixed in 2% paraformaldehyde with 0.2% glutaraldehyde in PHEM buffer for 2 hours at room temperature. After washing in PBS the spores were pelleted and embedded in 12% gelatine. The pellet was cut into 1 mm^3 cubes, cryo-protected in 2.3 M sucrose and snap frozen in liquid nitrogen. Ultra thin cryo-sections were labelled with rabbit anti-MreB (1:2000) and 15 nm protein A-gold particles. The labelled sections were embedded and contrasted in methylcellulose with uranyl acetate. All samples were viewed with a Philips EM 410 electron microscope (Eindhoven, The Netherlands).

RESULTS

The *mre* genes are highly conserved among streptomycetes and analysis of the sequenced genomes of *S. coelicolor* (Bentley *et al.*, 2002) and *S. avermitilis* (Ikeda *et al.*, 2003) and of the partial sequence of *S. scabies* (http://www.sanger.ac.uk/Projects/S_scabies) revealed

almost complete conservation of the predicted gene products MreB (SCO2611; 343 aa) and between 85-90% amino acid identity for MreC (SCO2610; 341 aa) and for MreD (SCO2609; 223 aa). In addition, a gene encoding the mreB-like protein Mbl (SCO2451; 360 aa) was detected in all sequenced streptomycetes, which shares 43% amino acid identity with MreB. The genomic organisation around *mreBCD* and *mbl* is presented in Fig. 1.

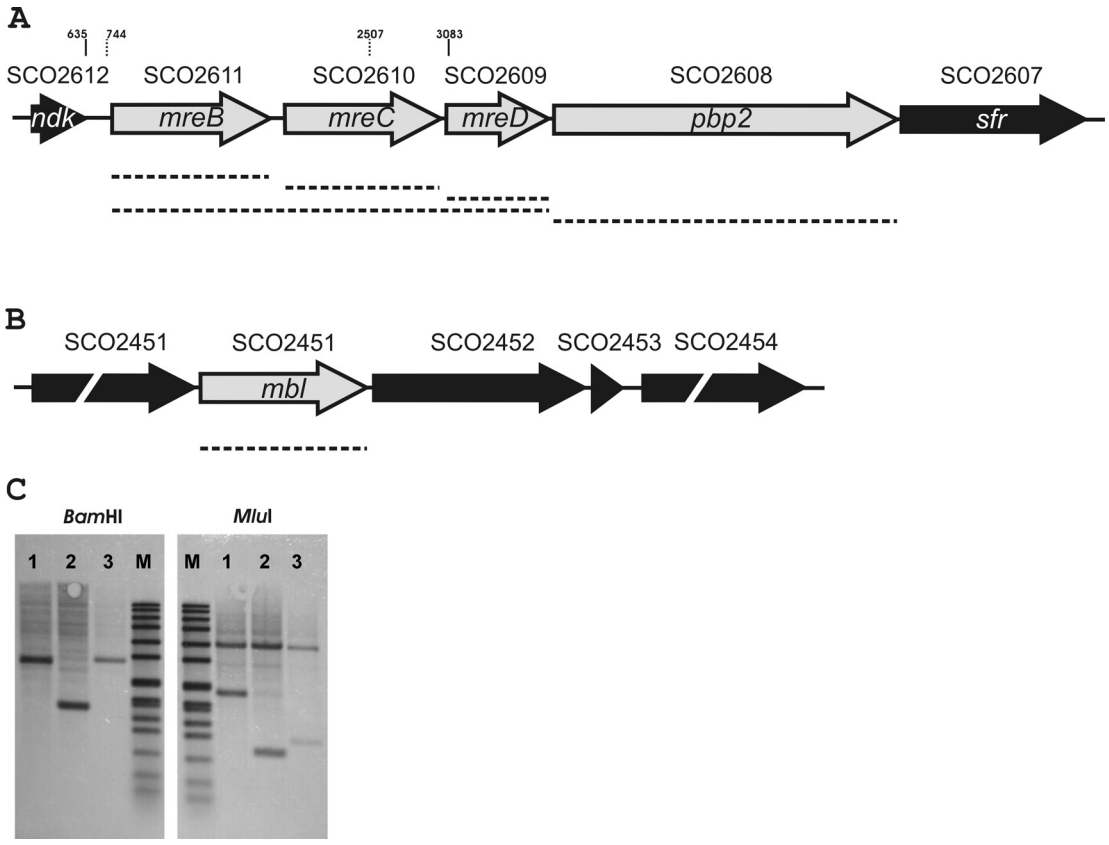

Figure 1: Genomic organisation of *mreBCD, pbp2* (A) and *mbl* (B) in *S. coelicolor.* *mreBCD, pbp2* and *mbl* are shown as grey arrows, while adjacent genes are shown as black arrows. Above the arrows are the corresponding SCO numbers. The dotted line under the genes represents the codon sequence, which is replaced by the apramycin cassette *aac*C4 in *mreB*-IM, Δ*mreC*, Δ*mreD*, Δ*mreBCD* and Δ*pbp2*, respectively (**A**) and in Δ*mbl* (**B**). For *mreB*-IFD, the same frame is deleted as *mreB*-IM. *Bam*HI and *Mlu*I restriction sites are presented as a full and dotted vertical line in A, respectively. **C.** Southern blot analysis performed with genomic DNA of M145 (1), *mreB*-IFD (2) and *mreB*-IM (3). The genomic DNA was digested with *Bam*HI or *Mlu*I and the *mreC* gene was used as probe. (M) DNA marker VII, DIG labelled (Roche).

In the sequenced genomes of *S. coelicolor*, *S. avermitilis* and *S. scabies,* the *mreBCD* operon is preceded by *ndk* (SCO2612), encoding a nucleoside diphosphate kinase, and followed by *pbp2* (SCO2608), encoding a penicillin-binding protein (Burger *et al.*, 1998) and *sfr* (SCO2607), coding for an FtsW/SpoVE/RodA family protein. MreC, MreD, PBP2 and Sfr are all predicted membrane proteins, with MreC and PBP2 (769 aa) harbouring a single N-terminal transmembrane (TM) domain at the immediate N-terminus (TM corresponding to aa

9-29 for MreC and to aa 14-32 for PBP2), so that the bulk of each protein faces the exterior, while MreD is a highly hydrophobic protein with five predicted TM domains, probably with the N-terminus facing the cytoplasm and the C-terminal part outside the cell. Sfr (372 aa) contains 10 predicted TM domains.

Table 4: Presence of *mreB* in different actinomycetes and the relationship of the ability to form aerial mycelium and spores.

Strain	Reference	Aerial mycelium[1]	Production of spores [2]	Amplified product [3]	Southern blot detection[4]
Microbacterium testaceum	DSM 20166	-	-	-	-
Nocardioides simplex	DSM 20130	-	-	-	-
*Corynebacterium glutamicum**	DSM 20300	-	-	-	-
Rhodococcus rhodochrous	DSM 43241	-	-	-	-
Tsukamurella paurometabola	DSM 20262	-	-	-	-
Gordonia sp. ACTA 2262	lab collection	-	-	-	-
Actinoplanes friuliensis	Aretz *et al*., 2000	-	+	-	-
Actinoplanes sp.	ATCC 31042	-	+	-	n.t
Micromonospora sp. Tü53	lab collection	-	+	-	-
Streptomyces olivaceus Tü8	lab collection	+	+	+	+
Streptomyces reticuli Tü45	lab collection	+	+	+	+
Streptomyces rimosus Tü58	lab collection	+	+	+	+
Streptosporangium roseum Tü74	lab collection	+	+	+	+
Streptoverticillum mobaraense Tü1063	lab collection	+	+	+	+

*: *mreB* not found after BLAST search in the sequenced genome (www.expasy.org/tools/blast/?CORGL.)

-: absence of an amplified product of the expected size ([3]), absence of aerial mycelium formation ([1]), absence of spores ([2]), absence of a band hybridysing to a *S. coelicolor mreB* probe.

+: presence of an amplified product of the expected size ([3]) a band hybridysing to a *S. coelicolor mreB* probe ([4]), formation of aerial mycelium ([1]), formation of spores ([2]).

[3] The presence of an *mreB* homologue in the tested strains deduced by the amplified PCR product obtained using primers designed in highly conserved regions of *mreB*.

n.t.: not tested

mreB is found only in actinomycetes that produce an aerial mycelium and spores

In order to assess how widespread the *mreB* genes are among actinomycetes, genomic DNA was isolated from various actinomycetes and PCR was performed using primers PM13 and PM14 (Table 3) designed to match two highly conserved regions of *mreB* and, therefore, did not distinguish between the two *mreB*-like genes on the *Streptomyces* genomes, and the PCR reactions should amplify both *mreB* and *mbl*, producing products of the same size. We obtained a band of the expected size in all tested *Streptomyces* strains, as well as in *Streptoverticillum mobaraense* and in *Streptosporangium roseum*. In contrast, we failed to detect such a band with actinomycetes that do not produce aerial hyphae, including *Actinoplanes* (*A. friuliensis* and *Actinoplanes sp*.), *Micromonospora sp*., *Corynebacterium glutamicum*, *Microbacterium testaceum*, *Nocardioides simplex, Gordonia sp.* and *Rhodococcus rhodochrous*, suggesting the lack of an *mreB* homologue in these organisms.

These findings were confirmed by Southern blot analyses using *mreB* of *S. coelicolor* as a probe (Table 4). MreB proteins therefore seem to be present only in strains that produce both aerial mycelium and spores (see Discussion). Interestingly, a single *mreB* homologue was identified in the genome sequence of the non-sporulating actinomycete *Rhodococcus* sp. RHA1 (www.Rhodococcus.ca). While a blastP search with the predicted gene product showed only significant homology to MreB, the overall similarity was significantly lower than expected for a true MreB homologue (around 40% amino acid identity to many proven or expected MreB proteins). The function of this interesting protein awaits further analysis.

Expression of MreB in S. coelicolor leads to growth impairment and lysis

Overexpression of *E. coli* MreB in *E. coli* leads to inhibition of cell division (filamentous phenotype), probably due to a reduction of FtsI activity, which is enhanced in *mreB* mutants (Wachi and Matsuhashi, 1989). To analyse the effects of overexpression of *S. coelicolor* MreB in *S. coelicolor*, the gene was cloned under the control of the thiostrepton-inducible *tipA* promoter in the *E. coli-Streptomyces* shuttle vector pGM190; the construct was designated pPM1. When *S. coelicolor* M145 transformed with pPM1 was plated on SFM plates containing 10 μg/ml thiostrepton, the strain failed to grow (Fig. 2B), while the same strain harbouring the control plasmid pGM190 (without insert) showed normal growth (Fig. 2D); this indicated that overexpression of MreB on solid medium is lethal.

To study the effect of *S. coelicolor* MreB overexpression on the growth of substrate mycelium, spores of *S. coelicolor* carrying either pPM1 or the control plasmid were inoculated in TSB medium and grown at 30°C. After 8-12 hours of growth, MreB expression was induced by the addition of 10 μg/ml thiostrepton. Interestingly, it was possible to overexpress MreB in liquid-grown cultures, although these cultures grew significantly slower than those of the parental strain harbouring the empty vector pGM190 (Fig. 3). Swelling of the extremities of the hyphae and extensive lysis of the mycelium of pPM1 transformants was observed already two hours after induction (Fig. 3C), while the pGM190 transformants remained unaffected. Overexpression of MreB in *S. coelicolor* containing pPM1 was confirmed by Western blot analysis with anti-MreB antibodies (data not shown). To analyse whether MreB overexpression affects spore germination, spores of pPM1 transformants were inoculated in liquid culture containing thiostrepton (Fig. 3D-E-F). The spores were able to germinate, but the elongation of germ tubes was inhibited (Fig. 3F) and the hyphae failed to elongate properly.

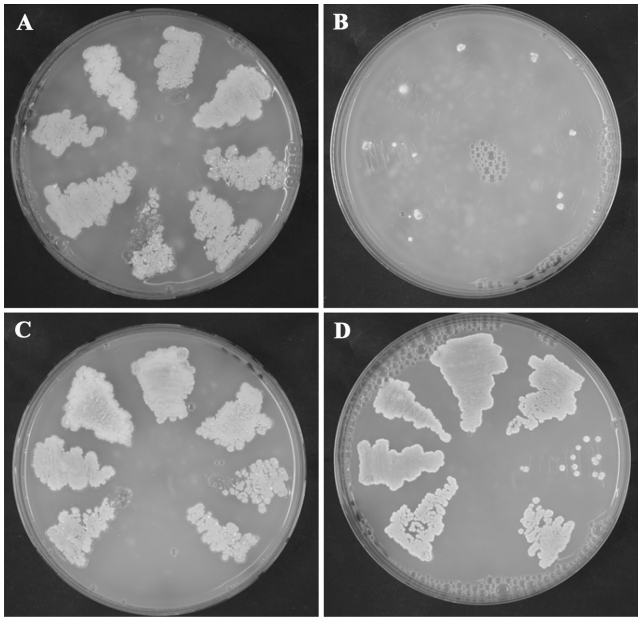

Figure 2: Lethal effect of MreB overexpression on solid growth. *S. coelicolor* M145 strains were plated in absence (**A-C**) and presence (**B-D**) of 10 μg ml^{-1} of the inducer thiostrepton. *S. coelicolor* M145 carrying pPM1 [*tipAp-mreB*] (**A-B**) and the vector pGM190 (**C-D**) were streaked onto the plates indicated. Each patch is an independent isolate of the strains.

Mutational analysis of *mreB* and *mbl*

Previous attempts to inactivate *mreB* by gene disruption using the temperature-sensitive *Streptomyces* vector pGM9 were unsuccessful (Burger *et al.*, 2000). Despite this failure, a renewed attempt using the Redirect technology allowed us to construct an insertion mutant of *mreB* (*mreB*-IM) in which *mreB* was replaced by the apramycin resistance cassette *aac(3)IV* (1384 bp) (Fig. 1A). The gene replacement was verified with PCR and Southern analysis (Fig. 1C), and the lack of MreB was confirmed with Western blot analysis using anti-MreB antiserum (data not shown) (Mazza *et al.*, 2006). The *mreB*-IM mutation is expected to have polar effects to *mreC* and *mreD*, as these genes appear to be transcribed as an operon (Burger *et al.*, 2000). In order to avoid such polar effects, an *mreB* in frame deletion mutant (*mreB*-IFD) was constructed removing the apramycin cassette from the chromosome of the *mreB*-IM mutant (see Materials and Methods section). The loss of the resistance marker and the exact location of the deletion were confirmed by PCR and Southern analysis (Fig. 1C). To confirm that the absence of an intact *mreB* was responsible for the observed phenotype, pPM6, containing a single copy of the *mreB* gene under its own promoter was introduced in *mreB*-IFD, generating the *mreB*-complemented strain *mreB*-IFDc. We simultaneously analysed the *mreB* mutants with *mreB*-IFDc to verify that the observed mutant phenotype was solely due to the gene replacement and not to a second-site mutation.

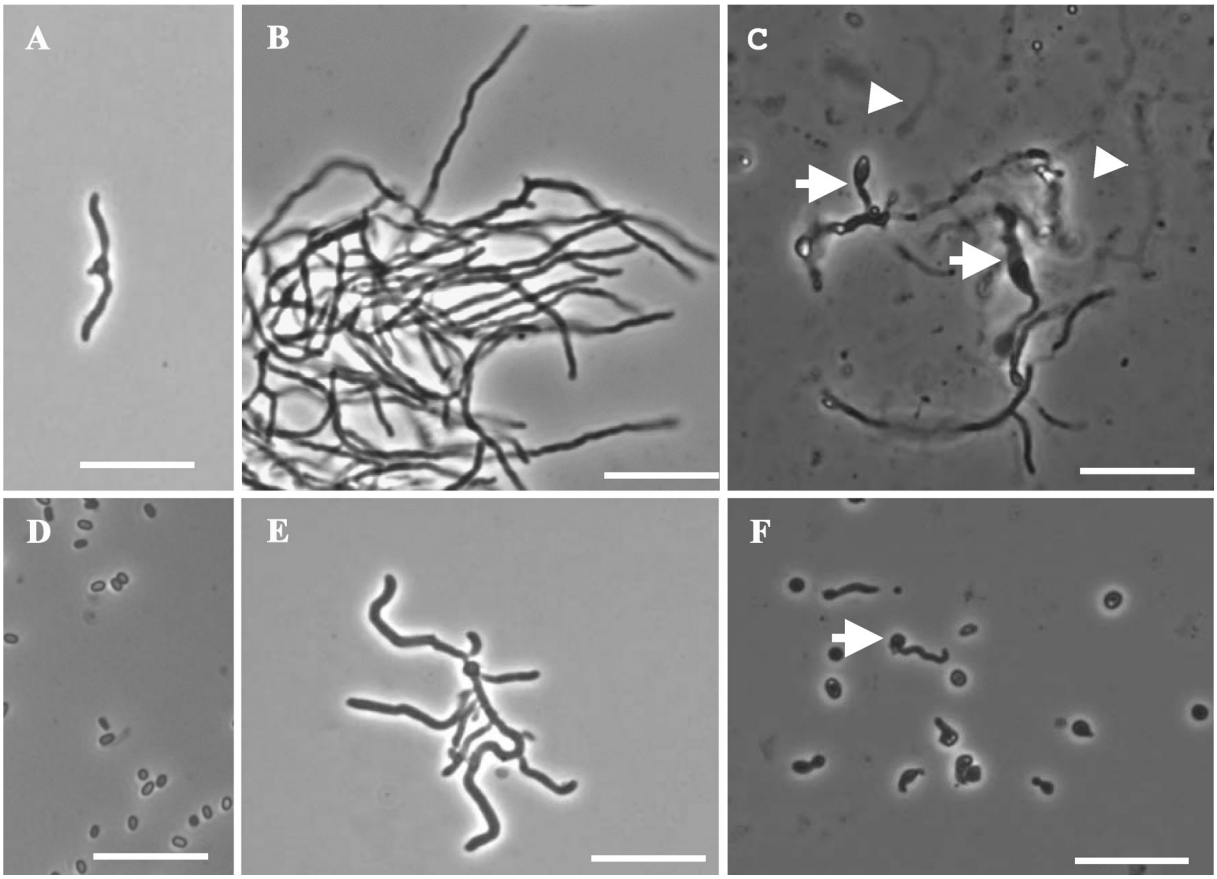

Figure 3: Effect of MreB overexpression on vegetative growth (A-B-C) in liquid culture and on spore germination (D-F-E). Spores of *S. coelicolor* M145 carrying pPM1 [tipAp-*mreB*] were inoculated in TSB medium. After 12 h of growth (**A**) the cultures were supplemented (**C**) or not (**B**) with 10 µg $ml^{-1}$of the inducer thiostrepton. Images were taken 8 hours after induction. **C**: Arrowheads show hyphal lysis and arrows swelling of hyphae induced by MreB overexpression. Bar = 10 µm. Spores of the strain carrying pPM1 [*tipAp-mreB*] were inoculated in TSB medium (**D**) and grown in the absence (**E**) and presence (**F**) of 25 µg $ml^{-1}$of the inducer thiostrepton. Under inducing conditions spores were able to germinate (arrow), but elongation of germ tubes was inhibited. Bar = 10 µm.

Using a similar approach as described for *mreB*-IM, we created an *mbl* mutant (Δ*mbl*; Fig. 1B). In this mutant *mbl* was replaced with the apramycin cassette *aacC4*, which was verified by PCR and Southern blot analysis (data not shown). An in frame deletion mutant has not yet been made for *mbl*. Considering the short distance between the genes, it is not unlikely that *mbl* forms an operon with the downstream-located genes SCO2452 (for a two-component sensor histidine kinase) and SCO2453 (for a protein with unknown function). Therefore, polar effects due to the insertion of the apramycin cassette have to be taken into consideration.

Transcriptional analyis of *mreBCD*

mreBCD appear to be transcribed as an operon. To establish if indeed transcription of *mreCD* was not affected by the deletion of *mreB* in the *mreB-IFD* mutant or by the substitution of *mreB* by *aacC4* in the *mreB*-IM mutant, we analysed the transcription of *mreBCD* using RT-PCR. Total RNA was isolated from M145 and *mreB*-IFD grown on SFM at different time points corresponding to vegetative growth (20h-24h), aerial growth (36h-40h) and sporulation (48h-60h-72h-96h) and from two independently grown liquid cultures of both M145 and *mreB*-IM, exponentially grown until an OD of around 0.4. Analysis of the RNA samples by RT-PCR with oligonucleotide pairs for *mreB*, *mreC* or *mreD* showed that indeed *S. coelicolor mreB*, *mreC* and *mreD* were transcribed throughout the *S. coelicolor* life-cycle and with a similar expression pattern (Fig. 4A). Transcription of *mreC* and *mreD* were similar in M145 and in *mreB*-IFD, underlining that developmental defects observed for *mreB*-IFD would be solely due to the deletion of *mreB* and not to polar effects on *mreCD* (Fig. 4B). Finally, the transcription of *mreC* appeared to be higher in *mreB*-IM than in M145, while *mreD* transcription seemed to be similar or higher in *mreB*-IM than in M145 (Fig. 4C). Therefore, certain anomalies of the *mreB*-IM mutant may be the result of a different expression of mreC*D*.

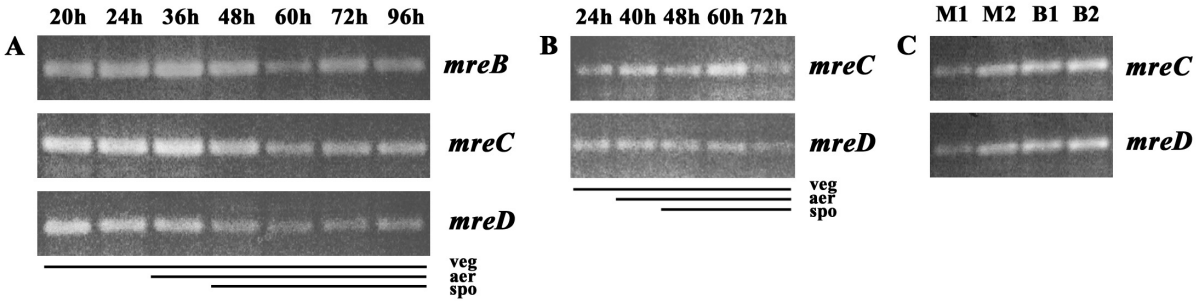

Figure 4: Transcriptional analysis of *mreB, mreC* and *mreD* in the parental strain M145 (A), in *mreB*-IFD (B) and in *mreB*-IM (C). RNA from M145 and *mreB*-IFD was isolated at different time points from cultures grown on cellophane disk on SFM. The corresponding developmental stages are indicated by the bars under the lanes (**A-B**). RNA was isolated from two liquid cultures of both M145 (M1-M2) and mreB-IM (B1-B2), independently grown until an OD of around 0.4 (**C**).

mre, pbp2 and *mbl* mutants are compromised in development

S. coelicolor M145 and its mutant derivatives *mreB*-IM, *mreB*-IFD, Δ*mreC,* Δ*mreD,* Δ*mreBCD,* Δ*mbl* and Δ*pbp2* were plated on R2YE (Fig. 5A) and SFM agar plates (Fig. 5B), and the ability of the strains to produce grey-pigmented spores was first assessed visually. The *mreB*-IM and *pbp2* mutants produced spores after 5 days of growth on R2YE agar plates, although they had a lighter pigmentation than the parent M145. In contrast, *mreB*-IFD, Δ*mreC,* Δ*mreD,* Δ*mreBCD* and Δ*mbl* all failed to produce aerial hyphae or spores (bald phenotype) within 5-6 days. After prolonged incubation (7 days for Δ*mreD* and Δ*mbl*; 10 days for *mreB*-IFD and Δ*mreC*) these five mutants produced a small amount of aerial hyphae as well as some spores on R2YE, except Δ*mreBCD*, which never entered morphological differentiation and thus had a strictly bald phenotype.

On SFM agar plates, all mutants produced significantly fewer spores than the wild type, as indicated by their lighter grey appearance, although this effect was significantly less pronounced in Δ*mreD* and Δ*mreB*-IM (Fig. 5). The ability of Δ*mreBCD* to produce abundant aerial hyphae and spores underlined that like many *bld* mutants, the *mreBCD* mutant had a conditionally non-sporulating phenotype (Nodwell and Losick, 1998; Rigali *et al.*, 2006), with sporulation on mannitol-containing media (such as SFM), but a non-sporulating, bald phenotype on glucose-containing media (such as R2YE).

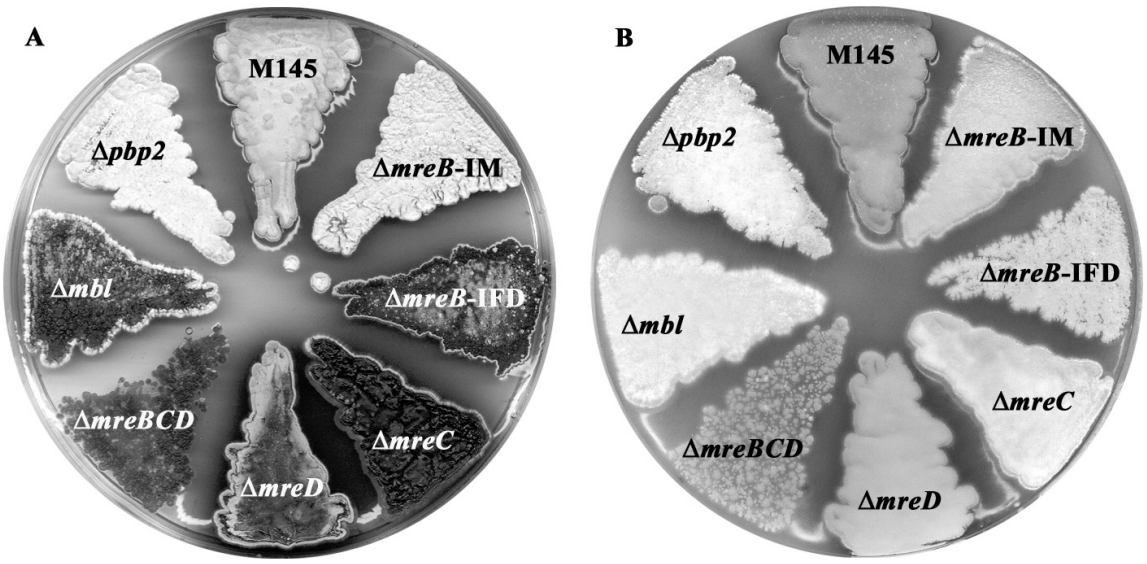

Figure 5: Phenotype of the mutants and their congenic parent *S. coelicolor* M145 on solid media. Strains were grown for 5 days at 30°C on R2YE (**A**) and SFM (**B**).

Analysis of the mutants by electron microscopy

To analyse the phenotypes of the mutants in more detail, all mutants were grown on SFM agar plates for 5 days and analysed in detail by cryo-scanning electron microscopy (Fig. 6) and transmission electron microscopy (Fig. 7). The results are summarised in Table 5. After 5 days of growth on solid medium, M145 showed typical examples of sporogenic aerial hyphae, prespore chains and mature spores (Fig. 6A-7A). The *mreBCD* mutant occasionally produced spores with irregular lengths and/or a swollen appearance (Fig. 6B-7B). The aerial hyphae were regularly swollen and more frequently lysed than in the parental strain. Around 25% of the vegetative cross walls of Δ*mreBCD* were thick and irregular.

All four *mre* single mutants (*mreB*-IM, *mreB*-IFD, Δ*mreC* and Δ*mreD* (Fig. 6C-D-E-F; 7C-D-E-F) produced spores with irregular sizes and swollen spores/hyphae, as did Δ*mreBCD* (Fig. 6B-7B). Many spores were found with a thin spore wall typical of that of vegetative or young aerial hyphae (Fig. 7C-D-E-F; arrowheads). Aerial hyphae were also more frequently lysed in these mutants. This defective phenotype was most prominent in *mreB*-IM, which produced many more misshapen spores than the other *mre* mutants, often with extremely heteromorphous shapes (Fig. 6C-7C). As in Δ*mreBCD*, around 25% of the vegetative cross walls of *mreB*-IM were thick and irregular, around 6% of which were unfinished, suggestive of a thick, asymmetric ring. Mutant *mreB*-IM accumulated electron-dense granules in its hyphae and spores (Fig. 7C), similar to those observed in *ssgB* mutants, which are likely to contain unincorporated cell wall precursor material (Keijser *et al.,* 2003). Spores of both *mreB* single mutants showed premature germination. Additionally, *mreB*-IM harboured completely segregated chromosomes, as visualised by propidium iodide (not shown), while nucleoids of *mreB*-IM were invariably surrounded by electron-lucent (white) material. This was also observed in *mreB*-IFD, Δ*mreC* and Δ*mreD* (Fig. 7D-E-F; arrows). The nature and origin of this material is unknown.

The defects observed in Δ*mbl* corresponded to those previously described for the *mre* mutants, with a high proportion of spores showing aberrant shapes and different sizes, and premature germination occurring regularly (Fig. 6G-7G). However, spore formation appeared to be more severely compromised in this mutant.

pbp2 mutants produced significantly fewer spores than the parental strain. Few spores appeared to be swollen although frequently, spores with irregular shapes were observed (Fig.

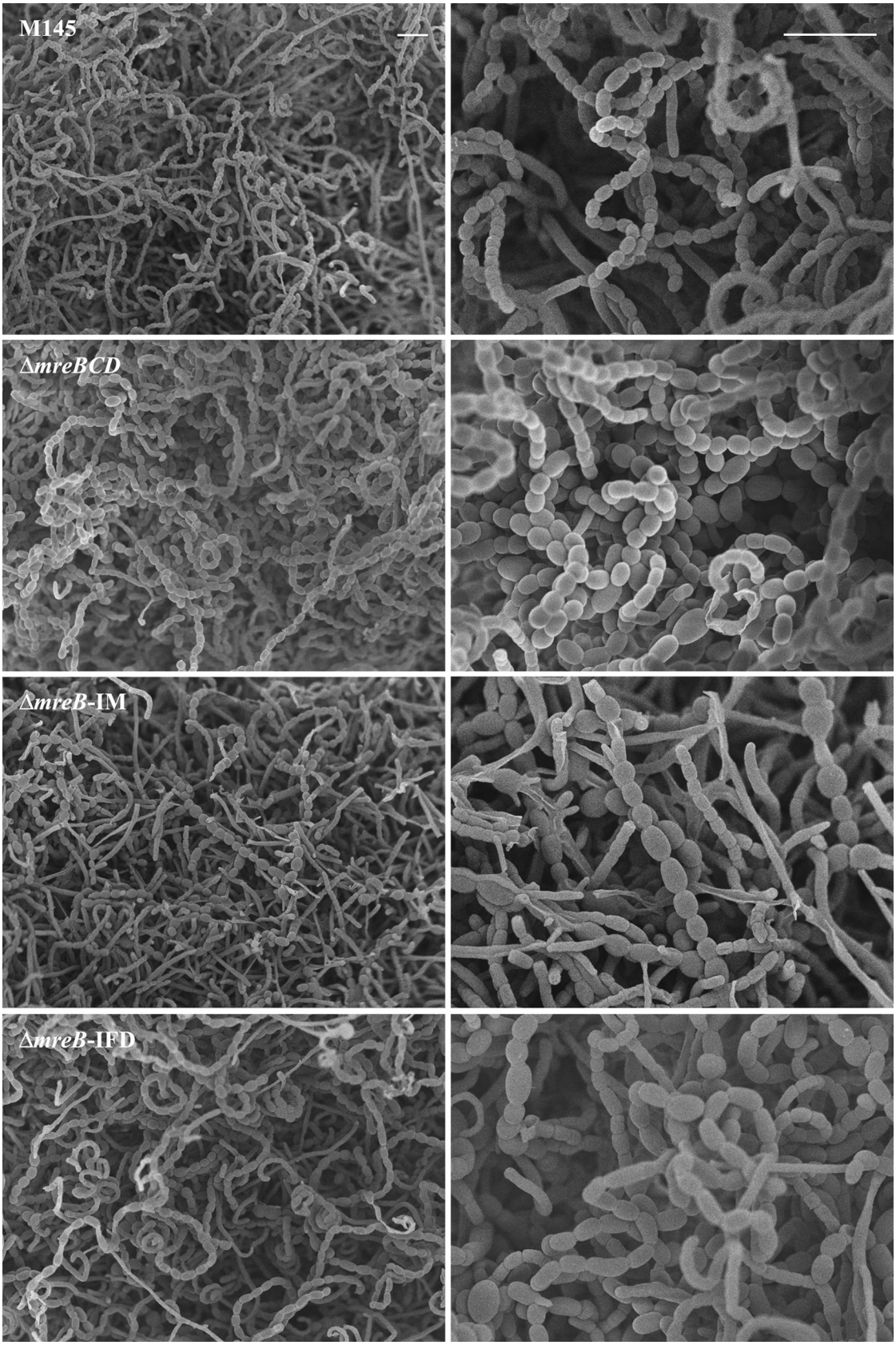
M145
Δ*mreBCD*
Δ*mreB*-IM
Δ*mreB*-IFD

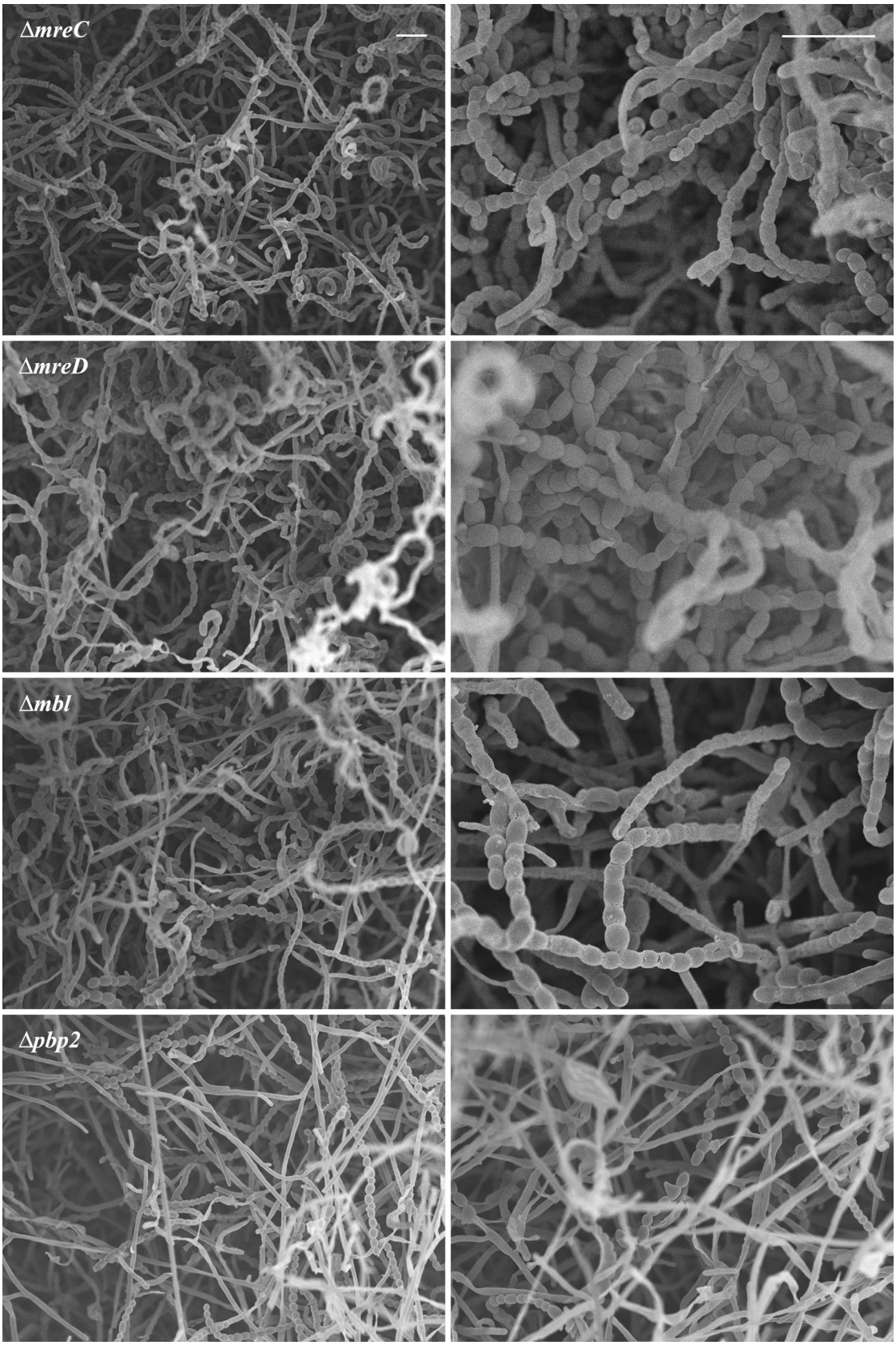

Figure 6: Phenotypic characterisation of the parental strain M145 and the mutants by cryo-scanning electron microscope. Samples were taken after 5 days of growth on SFM. Bar = 5 μm.

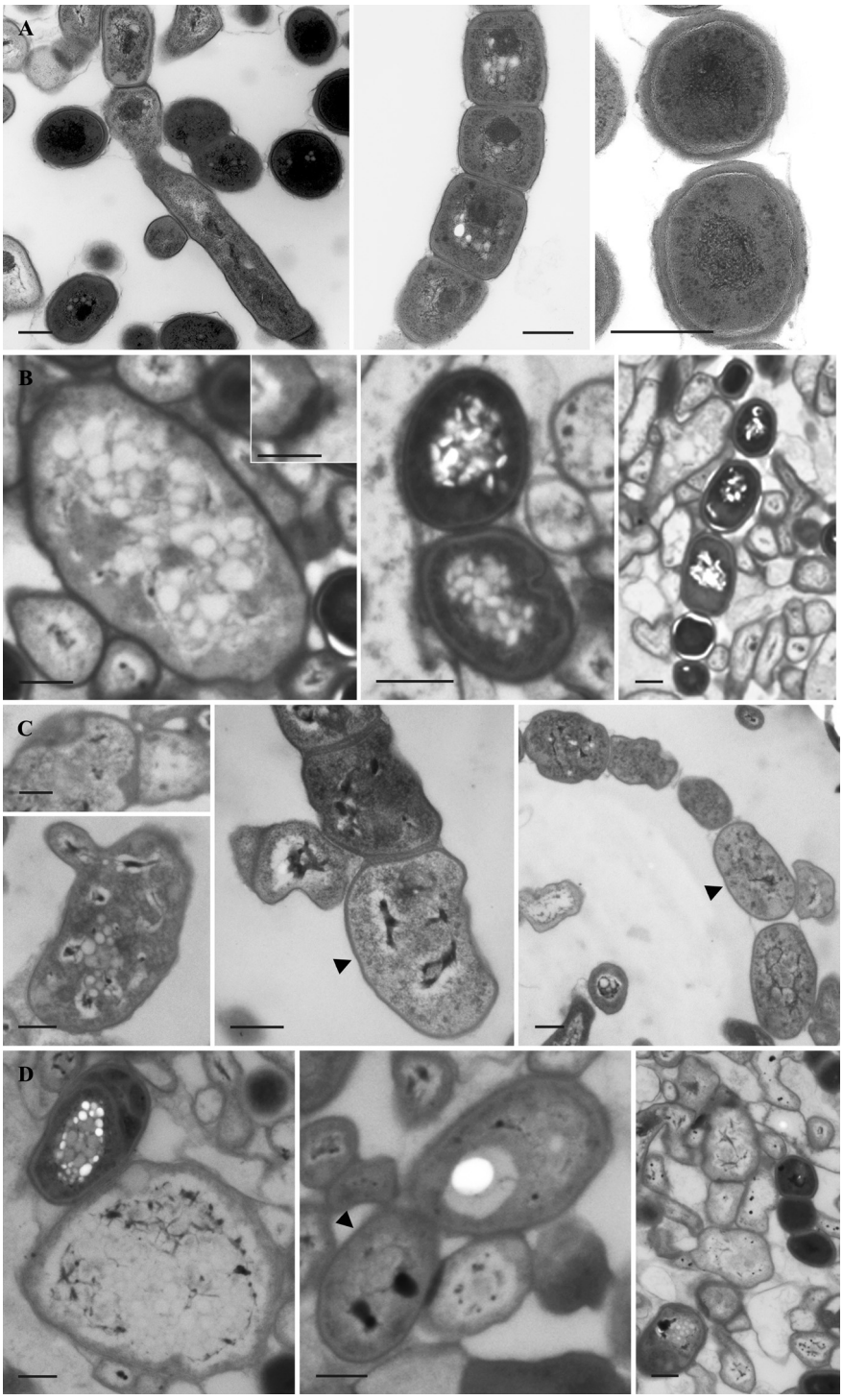

Figure 7: Transmission electron microscope images of hyphae and spores of the parental strain M145 and the mutants. A-H: Samples were taken after 5 days of growth on SFM. **A**: M145; **B**: Δ*mreBCD*; **C**: *mreB*-IM; **D**: *mreB*-IFD; **E**: Δ*mreC*; **F**: Δ*mreD*; **G**: Δ*mbl* and **H**: Δ*pbp2*. **A**: aerial hyphae (left), immature spores (middle) and mature spore chains (right). **B-G**: bloated hyphae (left), swollen spores (middle) and spores with irregular dimensions (right). **H**: Electrodense granules accumulated in hyphae (left), swollen hyphae (middle) and irregular spores (right). Aberrant cross walls are observed in B and C (insert). Arrowheads point to the cell wall of spores, lacking the thick peptidoglycan layer, typical for mature spores. **I-L**: Images of vegetative hyphae were taken after 2 days of liquid growth. **I**: M145; **J**: *mreB*-IM; **K-L**: Δ*mbl*. Bar = 0.5 µm.

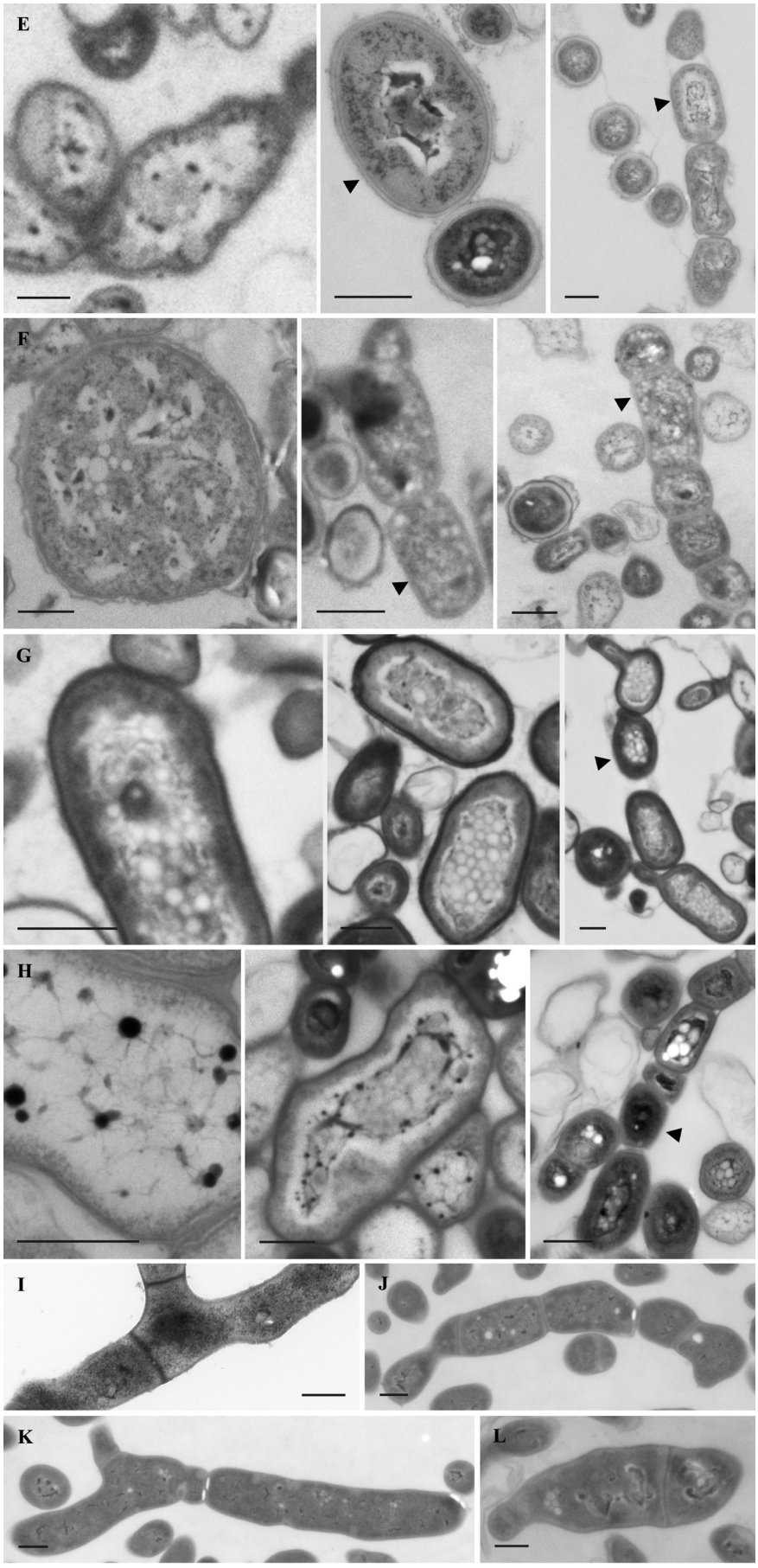
E
F
G
H
I
J
K
L

6H-7H). Aerial hyphae were frequently lysed. As in *mreB*-IM, electron-dense granules accumulated in the hyphae and spores of the *pbp2* mutant.

To investigate if *mreB* and *mbl* play a role during vegetative growth, cross sections of two days old solid-grown cultures of Δ*mbl* and *mreB*-IM were analysed by TEM. The morphology of vegetative hyphae and cross-walls was very similar to that of the wild type strain. However, the distance between cross-walls of liquid-grown hyphae of *mreB*-IM and Δ*mbl* was often less than 2 μm, while the cross-walls of wild type hyphae were laid down with a frequency of approximately one per 8 μm. Analysis of liquid-grown mycelium of both mutants revealed swollen hyphae (Fig. 7I-J-K-L), providing supportive evidence that Mbl and MreB are important for the stability of both vegetative and aerial growth.

Table 5: Characteristics of different mutants.

	Spores	Swollen spores	Premature germina-tion	Irregular spore length	Irregular, thin spore wall	Lysed aerial hyphae	Swollen hyphae
M145	++	-	-	-	-	+/-	-
***mreB*-IM**	+	+++	+	+	+	+	+
***mreB*-IFD**	+	+	+	+	+	+	+
ΔmreC	+	+	-	+	+	+	+
ΔmreD	++	+	-	+	+	+	+
ΔmreBCD	+++	+	-	+	-	+	+
Δmbl	+	++	++	+	+	+	+
Δpbp2	+	+	-	+	+/-	+	+

+++: very high amounts. ++: high amounts. +: average amounts. +/-: rarely but seen. -: absent.

MreB is a membrane-associated protein that localises at the septa of aerial hyphae and at the spore wall

Recent results showed that MreB in *B. subtilis* and *E. coli* forms helical structures located on the inner surface of the cytoplasmic membrane (Formstone and Errington, 2005; Jones *et al.*, 2001; Kruse *et al.*, 2003; Shih *et al.*, 2003) and that it is only weakly associated with the membrane (Slovak *et al.*, 2005), while MreC and MreD are membrane proteins (Kruse *et al.*, 2005). In order to localise MreB in *S. coelicolor* M145, an MreB-EGFP fusion protein was created under the control of the natural *mreB* promoters, and cloned in pSET152, generating pPM4 (see Materials and Methods). This plasmid almost fully complemented *mreB*-IM, indicating that the MreB-EGFP fusion protein was functional.

During vegetative growth, only diffuse fluorescence was observed in the hyphae, although expression of MreB-EGFP was confirmed by Western blot analysis with both anti-

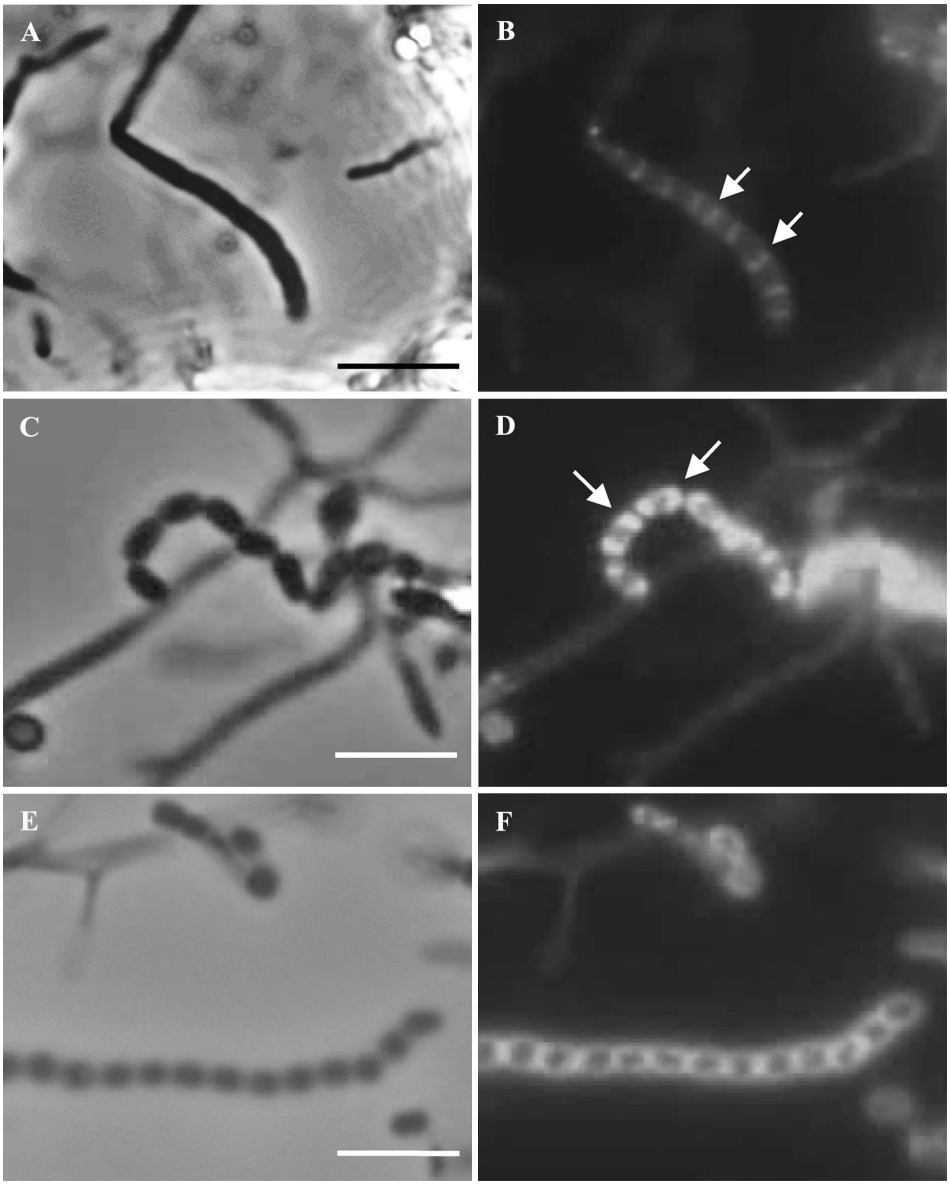

Figure 8: Localisation of the MreB-EGFP fusion protein during morphological differentiation. MreB-EGFP was detected at sporulation septa in aerial hyphae (**B**), at the poles of prespores (**D**) and subsequently covering the whole spore wall in spore chains (**F**). **A-C-E**: phase contrast; **B-D-F**: fluorescence microscopy. Bar = 5 μm.

MreB and anti-GFP antibodies (data not shown). However, very clear fluorescence signals were specifically localised at the septa of sporogenic aerial hyphae (Fig. 8). As shown in Fig. 8B, bands of fluorescence coincided with the constrictions caused by sporulation septation. Simultaneous labeling of septa with fluorescent conjugates of wheat germ agglutinin confirmed that MreB-EGFP overlapped with the septa (data not shown). MreB-GFP was also localised at the tip of the sporogenic aerial hyphae. However, it is not clear whether MreB-EGFP also localised to the basal septa sometimes seen at the bottom of sporogenic hyphal

cells (Kwak *et al.*, 2001). In prespore chains, foci were localised at the cell poles generated by sporulation septation (Fig. 8D; arrows), including the tip of last spore in the chain, which is not preceded by a septum. Successively, in more mature spores, the MreB-EGFP signal completely surrounded the spores, giving rise to ring-like appearance of the fluorescence (Fig. 8F). However, in fully mature spores most of the fluorescence from the MreB-EGFP fusion had disappeared (data not shown). Closer inspection of the localisation of MreB by immunogold electron microscopy revealed abundant and specific labelling, particularly close to the inside of the spore walls of wild type spores (Fig. 9). In the control experiment where hyphae and spores from the *mreB* insertion mutant (*mreB*-IM) were imaged, only background labeling was obtained.

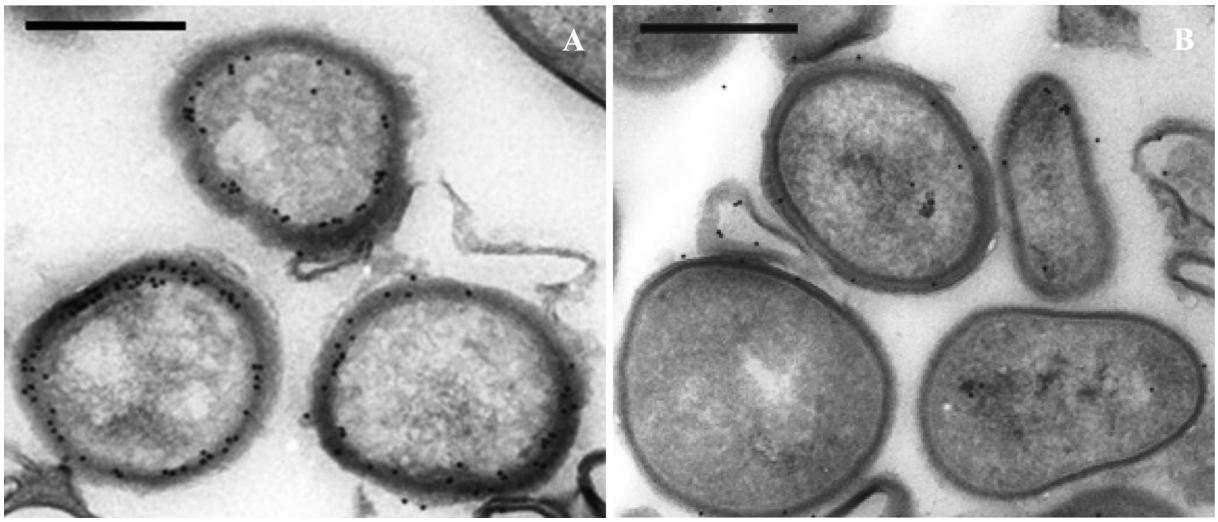

Figure 9: High-resolution localisation of MreB in *S. coelicolor* spores. Specific localisation of MreB in spores by *in situ* hybridisation of thin sections (immuno-electron microscopy) of spore preparations of *S. coelicolor* M145 (**A**), using gold-labelled anti-MreB antibodies. No specific labelling was obtained with any of the independent *mreB* mutants (**B**). Notice the highly variable spore sizes and less dense spore wall of the mreB null mutant. Bar = 500 nm.

The cellular localisation of MreB was further examined by cell fractionation and Western analysis using anti-MreB antibodies. Mycelium and spores grown on SFM agar plates were disrupted in a French-Press and the cytoplasmic, the membrane-associated and the membrane fractions were individually isolated. MreB was detected in the cytoplasmic fraction and in the membrane-associated fraction, while we failed to detect MreB in the membrane fraction (data not shown). The same result was obtained when localisation of the MreB-EGFP fusion protein was examined, indicating that the localisation of MreB-EGFP was the same as for the wild type protein.

DISCUSSION

In this study, we present the mutational and functional characterisation of the *mreBCD* and *mbl* genes, which encode actin-like cytoskeletal proteins, and of *pbp2*. The creation of the deletion of *mreB* is surprising in itself, as earlier failed attempts suggested that in contrast to *mreC* and *mreD*, *mreB* was an essential gene (Burger *et al.*, 2000). The discrepancy may be explained by a higher frequency of allelic exchange in the REDIRECT method, due to the much larger regions flanking the *mreB* locus that were available for recombination. Since several *mreB* mutants were isolated in independent experiments with frequencies that are typical for gene inactivation experiments using the REDIRECT procedure, it appears unlikely that *mreB* is essential in *Streptomyces* and that lethality of the *mreB* mutations was masked by (a) suppressor mutation(s), as has been described for other bacteria (Kruse et al., 2005). This is further supported by the observation that *mreB* is absent from many non-sporulating actinomycetes.

Deletion of either *mreB* or *mbl* gave no obvious phenotype during vegetative growth in early solid samples, but a significantly detrimental effect was observed on liquid-grown mycelia, where hyphae of *mreB* mutants and to lesser extent of *mbl* mutants had a swollen appearance, with a significantly shorter spacing between the cross walls as in the parent. Furthermore, in *mreB*-IM and Δ*mreBCD* approximately 30% of the cross wall in the vegetative hyphae are thick and irregular, which could be due to an enhancement of FtsI, also observed in *mreB* mutants in *E. coli* (Wachi and Matsuhashi, 1989).

Transcriptional analysis by S1 nuclease mapping (Burger *et al.*, 2000) and RT-PCR studies (this work) revealed that *S. coelicolor mreB* and *mbl* are transcribed at similar levels throughout the *S. coelicolor* life-cycle, and expression of MreB was confirmed by Western blot analysis in liquid-grown cultures (data not shown). Thus, MreB and Mbl play an important role in the stability of the young hyphae under certain growth conditions, although the exact function needs further analysis. It cannot be excluded that there could be some degree of redundancy between MreB and Mbl, and only a double mutant can rule this out. However, based on the lack of MreB-EGFP signals at hyphal tips, it seems unlikely that MreB would play a direct role in the elongation of the hyphae, which occurs primarily at the tips. Sequence analysis of genomic DNA of different actinomycetes showed that only strains forming both an aerial mycelium and spores possess an *mreBCD* cluster, supporting the idea that the Mre proteins may not be required for vegetative growth in actinomycetes. One

apparent exception was *Rhodococcus* sp. RHA1, an actinomycete that only grows vegetatively, and has an mreB gene, although the low similarity of its predicted gene product to other MreBs (at best 40% amino acid identity) suggests that it may have a different function. While deletion of *mreB* affected hyphal stability but otherwise allowed normal vegetative growth, enhanced expression of *mreB* was highly toxic. After germination of spores the elongation of germ tubes was inhibited and hyphae lysed. Obviously, the presence of too much MreB severely interferes with normal growth, perhaps by recruiting penicillin-binding proteins, thereby inhibiting their function in cell wall synthesis.

From our data we conclude that MreBCD and Mbl are required for correct sporulation and play an important role in spore wall synthesis. The aerial hyphae and spores of the *mreB, mreC, mreD* and *mreBCD* deletion mutants were swollen, and irregularities in the spore cell walls were observed using TEM and spores of *mreB*-IFD were sensitive to heat and treatment with SDS. This is consistent with the observation that deletion of *mreBCD* in *B. subtilis* causes increased cell width and cell lysis (Formstone and Errington, 2005; Leaver and Errington, 2005). Loss of MreB leads to a change in resistance of the cell wall to osmotic or mechanical stress, due to the absence or incorrect assembly of cell wall components. In analogy, the absence of MreBCD in *S. coelicolor* impairs cell wall assembly, primarily during sporulation. The spore wall composition of streptomycetes is not well studied. However, it is different in thickness from vegetative hyphal walls and has often two layers, although qualitative differences in peptidoglycan components have not been reported (Ensign, 1978; Glauert and Hopwood, 1961). The importance of the spore wall may be indicated by the fact that spores acquire resistance to different physiological and mechanical stresses, which the substrate mycelium does not have. Consistently, the *mreB* mutants failed to mount resistance against two types of stress, namely heat and incubation with SDS.

The fact that deletion of *mreB, mreC* or *mreD* or the entire *mreBCD* gene cluster leads to a similar phenotype, strongly suggests that MreB, MreC and MreD act together and do not have any obvious independent role in the control of *Streptomyces* morphology and development. For example, in *mreBCD* mutants there is no expression of *mreB, mreC* or *mreD* and the phenotype of this mutant is highly similar to that of *mreB*-IFD. However, while *mreB*-IM and *mreB*-IFD have similar phenotypes, *mreB*-IM shows more ‘swollen’ spores, and many aberrant cross-walls, and this may be due to the polar effect of the insertional mutation on *mreC* and *mreD*. It was published previously that the apramycin resistance cassette has strong promoter activity (van Wezel *et al.*, 2005), and it is, therefore, unclear how

the expression of *mreCD* and flanking genes (*ndk, pbp2, sfr*) is affected in *mreB*-IM. Conceivably, deregulated expression of MreC and MreD might lead to recruitment of PBPs and thus prevent them for correct functioning.

Both *mbl* and *mreB* mutants produced spores with heteromorphous shapes that often germinate prematurely, and this even more frequently in the *mbl* mutant. The altered appearance of the nucleoids in *mreB* mutants was not observed in the *mbl* mutant, suggesting that only genes in the *mreBCD* cluster affect DNA segregation. Despite differences in the frequency and the degree of the observed anomalies, most of the defects were of similar nature, suggesting that the functions of Mbl and MreB may be similar, and that functional redundancy may exist between the two actin-like proteins.

To learn more about the function of MreB we studied the localisation of MreB-EGFP. In the rod-shaped bacteria *B. subtilis* and *E. coli* MreB forms helical filaments just underneath the cell surface (Jones *et al.*, 2001; Shih *et al.*, 2003), while in *Caulobacter crescentus* MreB undergoes two distinct localisation patterns, namely during the cell elongation phase as spirals that traverse along the longitudinal axis of the cell, and during cell division as an FtsZ-dependent transverse band at the mid-cell position (Figge *et al.*, 2004). In *S. coelicolor,* we failed to detect the typical helical-like structures described for *E. coli*, *B. subtilis* and *C. crescentus*. MreB-EGFP was observed as diffuse fluorescence in vegetative hyphae, indicating that MreB was randomly distributed in the vegetative mycelium, perhaps suggesting it occurred primarily in its monomeric form. Conversely, during development MreB-EGFP localised at the septa of sporogenic aerial hyphae and subsequently underneath the cytoplasmic membrane of the spores, as shown at high resolution by immunogold electron microscopy. While it is possible that the C-terminal fusion of GFP to MreB interferes to some extent with its function, and hence we cannot ascertain that MreB-EGFP precisely reproduced the localisation patterns for the natural MreB, the fusion protein was able to complement the *mreB* mutant phenotype and MreB-EGFP localised to the same subcellular fractions of *S. coelicolor* as MreB itself.

In *S. coelicolor,* septation occurs both during vegetative growth and sporulation, but MreB localisation was specific for sporulation septa. It is clear that MreB is not required for the formation of sporulation septa *per se*, as *mreB* mutants were still able to septate and produced viable spores. However, it should be tested whether MreB-localisation could be FtsZ-dependent, as seen in *C. crescentus* (Figge *et al.*, 2004), for example by localising MreB in different *S. coelicolor ftsZ* mutants, such as in an *ftsZ* mutant impaired in Z-ring formation

in sporogenic aerial hyphae, but not in vegetative mycelium (Grantcharova *et al.*, 2003). In *Rhodobacter sphaeroides*, MreB localises predominantly at the mid-cell position (Slovak *et al.*, 2005). The authors speculate that this mid-cell localisation for MreB might reflect the fact that this region is the main site of peptidoglycan synthesis rather than that MreB plays a direct role in septation. In an analogous manner, MreB in *S. coelicolor,* which was shown to localise at the sporulation septa, could be needed in subsequent steps for spore formation, rather than playing a crucial role in the sporulation-specific cell division.

Based on the localisation of MreB at the spore wall and the important role of MreB, MreC, MreD and Mbl in maintaining the integrity of the spore wall, we anticipate that these proteins are involved in thickening of the spore wall and may be recruiting PBPs and other peptidoglycan-related proteins during the sporulation process. The *mre* genes of *S. coelicolor* and *S. avermitilis* are linked genetically to *pbp2* and *sfr* (Burger *et al.*, 2000). PBP2 is a penicillin-binding protein with high similarity to *E. coli* PBP2, which is involved in cell elongation (Vinella *et al.*, 1993), and with SpoVD, a PBP important for synthesis of the spore cortex in *B. subtilis* (Daniel *et al.*, 1994). The product of *sfr* shows similarity to RodA, a protein involved in peptidoglycan synthesis during cell elongation in *E. coli*, and SpoVE, a protein required for the synthesis of the spore cortex peptidoglycan in *B. subtilis* (Henriques *et al.*, 1998). Inactivation of *pbp2* leads to a phenotype that resembles that of the *mreB* mutant. In *E. coli,* MreB, MreC and MreD were proposed to function as a membrane-bound complex directing the PBP2-dependent longitudinal cell wall synthesis (Kruse *et al.*, 2005), while in *B. subtilis*, it was suggested that MreC and MreD couple the helical Mbl 'cables' to the extracellular cell wall synthesising machinery (Leaver and Errington, 2005). We suggest that also in *S. coelicolor* these proteins participate in the same process. A complex may be formed including PBPs and the Mre proteins, which acts primarily during spore wall assembly. This leads to the following hypothesis on the mode of action of MreB in *S. coelicolor*: MreB is expressed at similar levels during the life cycle and it is localised rather dispersely in the cytosol of vegetative hyphae. At this stage, it contributes to the stability and stress resistance of the cell wall. When sporulation septation occurs, MreB condenses at the sporulation septa, possibly in an FtsZ-dependent manner. As MreB most likely is a membrane-associated protein, this structure may be anchored to the cell membrane through the two membrane proteins MreC and MreD and used to recruit and localise proteins responsible for spore wall formation, perhaps including PBP2 and the product of *sfr*. Further studies to localise PBP2 and Sfr in *mre* mutants and interaction studies between the Mre

proteins and the products of *pbp2* and *sfr* are necessary to understand the unique role of MreB in *Streptomyces coelicolor* A3(2). It will also be important to clarify the role of Mbl in this organism, and to determine whether there could be some functional redundancy between this protein and MreB. A mutant with combined deletions of *mbl* and *mreB* is the first obvious step to better out understanding of the role of these important morpho-proteins in the life cycle of streptomycetes.

ACKNOWLEDGEMENTS

We thank Wolfgang Wohlleben for Δ*mreC*, Δ*mreD* and Δ*mreBCD* and Glyn Hobbs for Δ*pbp2*.

FtsX and FtsE import autolytically produced peptidoglycan subunits during sporulation-specific cell division in *Streptomyces coelicolor*

Elke E. E. Noens, Henk K. Koerten and Gilles P. van Wezel

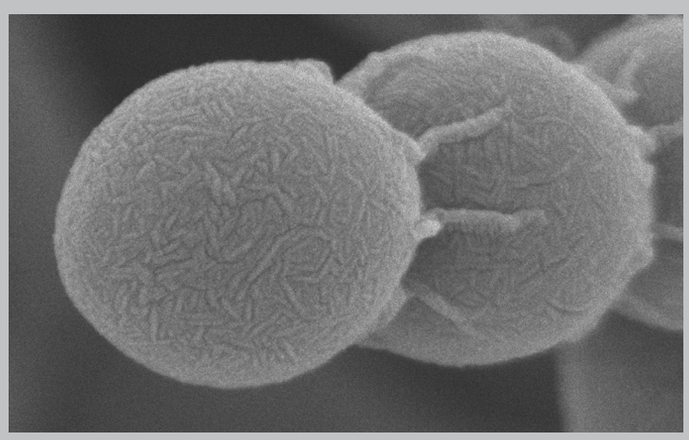

ABSTRACT

Cell division results in the formation of a septum that divides the mother cell into daughter cells. This is initiated by the formation of a ring of the tubulin-like protein FtsZ (the Z-ring), which functions as a scaffold for the construction of the septum. Subsequently, other cell division proteins are recruited to the Z-ring, forming the divisome or septosome. The cell division proteins FtsE and FtsX together form an ABC transporter, with FtsE functioning as the ATP-binding protein and FtsX as the membrane transporter. In *E. coli*, both proteins localise to division sites during the later stages of cell growth. *E. coli ftsE* null mutants are only viable on high salt medium and have a filamentous phenotype. We constructed an *ftsX* null mutant of *S. coelicolor*, but despite many efforts were unable to create an *ftsE* mutant. The fact that *ftsX* mutants are viable but not *ftsE* mutants suggests that FtsE may interact with at least one other ATP-requiring and essential transport protein. The *ftsX* mutant produces branches close to the base of a spore chain and accumulates peptidoglycan subunits between adjacent maturing spores. We show that FtsE localises to sporulation septa, at the same sites where peptidoglycan subunits accumulate and that FtsEX are not required for Z-ring formation. Our experiments demonstrate that FtsEX participate during the last stages of cell division, during autolytic spore separation, and most likely function by re-importing peptidoglycan subunits for recycling.

INTRODUCTION

Cell division involves the formation of a septum at the mid-cell position in most of bacteria. In *E. coli*, a collection of genes is required for septum formation, with two main features: the proteins encoded by these genes localise to the site of septum synthesis and mutants fail to septate at the non-permissive temperature (*fts*, filamentation temperature sensitive) (Errington *et al.*, 2003). The name *fts* has been extended to other cell division genes even if they are not known temperature-sensitive alleles. The first event of septation is the polymerisation of FtsZ, the prokaryotic homologue of tubulin, into a Z-ring functioning as a template for the construction of the septum. The other proteins are recruited to the Z-ring in a hierarchical order, which is almost completely linear in *E. coli* (FtsA, ZipA, (ZapA) → FtsEX → FtsK → FtsQ → FtsL/YgbQ → FtsW → FtsI → FtsN → AmiC) (Schmidt *et al.*, 2004) although recent work suggests that assembly of the divisome in *E. coli* involves the formation of subcomplexes, which are assembled into the divisome in a concerted mode (Vicente and Rico, 2006). Conversely, in *B. subtilis* similar division proteins (DivIB, DiVIC, FtsL, PBP-2B and FtsW) are cooperatively recruited to the division site and the division proteins are all completely interdependent for assembly (Errington *et al.*, 2003). Hence, the mode of division ring assembly appears to be quite similar in these two bacteria.

While in most bacteria a single septum is formed, dividing the mother cell into two daughter cells, two separate and morphologically distinct cell division events occur in the Gram-positive mycelium bacterium *Streptomyces*; cross-walls are laid down in vegetative hyphae to subdivide these into large multinucleoid compartments, while during development aerial hyphae erect from the lysing vegetative mycelium and many septa are simultaneously produced to form long chains of spores (Chater, 2001). There are some major and very interesting differences between cell division in streptomycetes and that in other eubacteria. For example, multiple septa are simultaneously produced in a ladder-like fashion (Schwedock *et al.*, 1997), and cell division is not essential for reproduction. The latter was shown by the viability of an *ftsZ* or *ftsQ* null mutant in *S. coelicolor*, while both proteins are essential in several kinds of bacteria (Bennett and McCormick, 2001; McCormick *et al.*, 1994; McCormick and Losick, 1996). Furthermore, assembly of the Z-ring is probably differently organised, as streptomycetes lack FtsA and ZipA, which anchor the Z-ring to the membrane in *E. coli* and *B. subtilis* (Errington *et al.*, 2003; Lowe *et al.*, 2004), while of the MinCDE control system for septum-site localisation (Autret and Errington, 2001; Marston *et al.*, 1998),

only homologues of MinD are present. These homologues do not seem to play a role in septum-site localisation (J. McCormick and G.P. van Wezel, unpublished data). Hence, a lot of information on septum formation in *S. coelicolor* is still missing, and we focus in particular on the differences between the 'non-physical division' by cross-wall formation in vegetative hyphae and the 'separative division' during sporulation.

In this chapter, we investigate the function of the cell division proteins FtsE and FtsX in *S. coelicolor*. *ftsEX* form an operon and the proteins they encode show similarity to ABC transporters, with FtsE resembling the ATP-binding component interacting with the membrane component FtsX. Typically, ABC transporters are anchored in the membrane by two separate regions, each containing six transmembrane domains. These residues, most likely, form the channel through which the substrates cross the membrane (Higgins, 1992). In bacteria, ABC transporters are mainly involved in nutrient uptake, although they also participate in the export of toxins, antibiotics and other undesired compounds, among others contributing to bacterial multidrug resistance (Locher, 2004). FtsX harbours only four hydrophobic segments, which are potential transmembrane helices (de Leeuw *et al.*, 1999). In most bacteria, *ftsEX* form an operon with *ftsY*, encoding the receptor of the signal recognition particle (SRP), which is essential for the correct insertion of FtsX, FtsE and other proteins into the plasma membrane (de Leeuw *et al.*, 1999; Du and Arvidson, 2003; Gill and Salmond, 1990). In actinomycetes, *ftsY* is located elsewhere in the genome, which does not necessarily mean that its role in the membrane topology of FtsEX – if any - is less important. In *E. coli*, FtsEX participate directly in cell division. An *ftsE* null mutation, with polar effects on *ftsX*, is viable on high salt medium only, where it shows moderate filamentation without being temperature sensitive. A decrease in salt concentration results in extreme filamentation and in cell death. Therefore, *ftsE* is a conditional salt-dependent essential gene in *E. coli*. Both proteins localise to the septal ring during late stages of cell growth and are important for the stability of the septal ring, especially in salt-free media (de Leeuw *et al.*, 1999; Schmidt *et al.*, 2004).

Here we describe the characteristics of an *ftsX* deletion mutant in *S. coelicolor*. By using an FtsZ-EGFP translational fusion in this mutant, we were able to draw conclusions about the order proteins are recruited to the divosome. We also show that FtsE localises at spore septa in maturing spore chains. All these data show that FtsEX are important in the later stages of cell division.

MATERIALS AND METHODS

Bacterial strains and media

The bacterial strains described in this work are listed in Table 1. *E. coli* K-12 strains JM109 (Sambrook *et al.*, 1989) and ET12567 (MacNeil *et al.*, 1992) were used for routine cloning and plasmid propagation and were grown and transformed by standard procedures (Sambrook *et al.*, 1989). *E. coli* ET12567 containing pUZ8002 was used for conjugation to *S. coelicolor* (Kieser *et al.*, 2000). *E. coli* transformants were selected in L-broth containing the appropriate antibiotics. *Streptomyces coelicolor* A3(2) M145 was obtained from the John Innes Centre strain collection and was the parent of the *ftsX* mutant described in this work. All media and routine *Streptomyces* techniques used are described in the *Streptomyces* manual (Kieser *et al.*, 2000). SFM agar plates were used for making spore suspensions and R2YE agar plates for regeneration of protoplasts and, after the addition of the appropriate antibiotic, for selecting recombinants. For standard cultivation and for plasmid isolation, YEME or TSBS (tryptone soy broth (Difco) containing 10% (w/v) sucrose) were used. For microscopical analysis, streptomycetes were grown on SFM agar plates.

Table 1: Bacterial strains.

Bacterial strain	Genotype	Reference
S. coelicolor A3(2) M145	SCP1$^-$ SCP2$^-$	(Kieser *et al.*, 2000)
S. coelicolor A3(2) MT1110	SCP1$^-$ SCP2$^-$	(Kieser *et al.*, 2000)
GSX1	M145 *ftsX*::Tn*5062*	This chapter
E. coli JM109	See reference	(Sambrook *et al.*, 1989)
E. coli ET12567	See reference	(MacNeil *et al.*, 1992)
E. coli ET 12567/pUZ8002	See reference	(Gust *et al.*, 2003)

Plasmids, constructs and oligonucleotides

All plasmids and constructs described in this chapter are summarised in Table 2. PCRs were done with *Pfu* polymerase (Stratagene), in the presence of 10% (v/v) DMSO, with an annealing temperature of 58°C. All used oligonucleotides are listed in Table 3.

General cloning vectors

pIJ2925 is a pUC19-derived plasmid used for routine subcloning (Janssen and Bibb, 1993). The shuttle vectors pHJL401 (Larson and Hershberger, 1986) and pSET152 (Bierman *et al.*, 1992) were used for cloning in *Streptomyces*, which both have the pUC *ori* for high-copy number replication in *E. coli* and the SCP2* *ori* on pHJL401 (around five copies per

chromosome) and the *attP* sequence, allowing integration at the attachment site of bacteriophage φC31, on pSET152 for maintenance in *S. coelicolor*. The suicide vector pSET151 contains the pUC *ori* for replication in *E. coli* and *oriT* RK2 for conjugation from *E. coli* to *Streptomyces* (Bierman *et al.*, 1992) and was used for recombination experiments.

Table 2: Plasmids and constructs.

Plasmid/ Cosmid	Description	Reference
pHJL401	*Streptomyces/E. coli* shuttle vector (5-10 and around 100 copies per genome, respectively)	(Larson and Hershberger, 1986)
pSET151	*Streptomyces* integrating plasmid with *E. coli* ori	(Bierman *et al.*, 1992)
KF41	pSET152-derived integrative vector expressing FtsZ-EGFP	(Grantcharova *et al.*, 2005)
pGWS113	pIJ2925 with 2,5 kb fragment harbouring a translational fusion of *ssgA* and *egfp*	(Noens *et. al.,* 2007)
E59	Cosmid clone containing *ftsX* and *ftsE*	(Bentley *et al.*, 2002)
E59(*ftsX*::Tn*5062*)	Cosmid E59 carrying a Tn*5062* insertion in *ftsX*	(Bishop *et al.,* 2004)
E59(*ftsE*::Tn*5062*)	Cosmid E59 carrying a Tn*5062* insertion in *ftsE*	(Bishop *et al.,* 2004)
pGWS136	pSET152 with 1,6 kb fragment harbouring an in frame fusion of *ftsE* and *gfp*	This chapter
pGWS137	pSET152 with 1,6 kb fragment harbouring an in frame fusion of *ftsX* and *gfp*	This chapter
pGWS144	pSET151 with 2 kb fragment harbouring the putative *ftsEX* promoter region and *ftsX* (-1512/+15 and +677/+2173, relative to *ftsE*)	This chapter
pGWS145	pHJL401 with 2 kb fragment harbouring the putative *ftsEX* promoter region and *ftsX* (-1512/+15 and +677/+2173, relative to *ftsE*)	This chapter
pGWS146	PGWS144 harbouring an apramycin resistance cassette replacing *ftsE*	This chapter

Homologous recombination experiments and construction of the ftsX mutant

Derivatives of cosmid E59 carrying a Tn*5062* insertion in *ftsX* and *ftsE*, respectively, were generated by *in vitro* transposition (Bishop *et al.*, 2004). These recombinant cosmids were transferred to *E. coli* ET12567 containing the conjugative plasmid pUZ8002, allowing direct conjugational transfer of the mutant cosmid to *S. coelicolor*. Simultaneous screening for loss of the cosmid sequences (Kan^S) and presence of the resistance cassette ($Apra^R$) is indicative of the desired mutant.

The *ftsE* disruption constructs were made as follows. Primers were designed in such a way as to allow amplification of the -1512/+15 (using FtsE-F1 + FtsE-R1) and +677/+2173 (using FtsE-F2 and FtsE-R2) sections relative to *ftsE* from the *S. coelicolor* genome. After digestion with *Eco*RI-*Xba*I and *Xba*I-*Hin*dIII, respectively, these fragments were ligated simultaneously into *Eco*RI-*Hin*dIII-digested pSET151, resulting in pGWS144 containing an in frame deletion of *ftsE*. Subsequently, the *aac(3)IV* gene, conferring apramycin resistance was inserted into the *Xba*I site of pGWS144, creating pGWS146, which has the +16/+676 region of *ftsE* replaced by *aac(3)IV*. Thiostrepton resistance was a selectable marker for the vector sequences for both pGWS144 and pGWS146.

Construct for the complementation of the ftsX mutant

For the complementation of the *ftsX* mutant, the insert of pGWS144 was cloned as an *Eco*RI-*Hin*dIII fragment into pHJL401 generating the low-copy vector pGWS145 that contains wild type *ftsX* expressed from its own promoter.

Constructs for FtsX-EGFP and FtsE-EGFP

A 978 bp fragment harbouring the putative *ftsEX* promoter region and *ftsE* and a 1893 bp fragment harbouring the putative *ftsEX* promoter region and *ftsEX* were amplified from genomic DNA from *S. coelicolor* using oligonucleotides E59_27_28_F + E59_27 (-STOP) and E59_27_28_F + E59_28 (-STOP), respectively. In this way, the stop codons of *ftsE* and *ftsX* were replaced by a *Kpn*I site. The two fragments were inserted into *Eco*RI-*Kpn*I-digested pGWS113 (Chapter 4), replacing *ssgA* and thereby creating an in frame fusion of *ftsE* and *ftsX* with *egfp,* respectively. The inserts of the two constructs were inserted as an *Eco*RI-*Bgl*II fragment into an *Eco*RI-*Bam*HI digested pSET152, creating pGWS136 and pGWS137, respectively.

Table 3: Oligonucleotides.

Primer	Sequence (5' → 3')	Location 5' end	Relative to
FtsE-F1	gctg**gaattc**gctttgaacattcggaatggtgagg	-1512	*ftsE*
FtsE-R1	gctg**tctaga**gtcgaatcggatcacggatgc	+15	*ftsE*
FtsE-F2	gctg**tctaga**taccagcactgacgagccacag	+677	*ftsE*
FtsE-R2	gctg**aagctt**cactgcgcagccggtcgccctcc	+2173	*ftsE*
E59_27_28_F	gctg**gaattc**cagttcgcgcacaccaaccggtc	-248	*ftsE*
E59_27 (-STOP)	gctgcg**ggtacc**ggcggcggcatcatcggcggcggccaccttcaggtacttgcgcaacgc	+690	*ftsE*
E59_28 (-STOP)	gctgcg**ggtacc**ggcggcggcatcatcggcggcggcgtgctggtagccgtagacaccgc	+918	*ftsX*

Restriction sites are presented in bold face.

Microscopy

Electron microscopy

Morphological studies of surface-grown aerial hyphae and spores of *S. coelicolor* M145 and GSX1 by cryo-scanning electron microscopy (cryo-SEM) were performed as described previously, using a JEOL JSM6700F scanning electron microscope (Keijser *et al.*, 2003). Transmission electron microscopy (TEM) for the analysis of cross-sections of hyphae and spores was performed with a Philips EM410 transmission electron microscope as described previously (van Wezel *et al.*, 2000).

Fluorescence microscopy

For the visualisation of strains containing proteins translationally fused to EGFP, sterile coverslips were inserted at a 45° angle into SFM plates and spores were inoculated in the acute angle. After 2 days (for FtsZ-EGFP) and 4-5 days (for FtsE-EGFP and FtsX-EGFP) of incubation at 30°C, coverslips were removed and samples positioned in a drop of water/1% agarose on a microscope slide.

Visualisation of DNA (propidium iodide (PI), Sigma) and cell wall material (FITC-WGA, Biomedica) by confocal fluorescence microscopy was performed as described previously (Chapter2). For these experiments, strains were grown on SFM for 5 days at 30°C.

Immuno-fluorescence microscopy of FtsE was carried out as described previously (Schwedock *et al.*, 1997). For this, *S. coelicolor* M145 was grown on SFM for 3 days at 30°C. Antibodies against FtsE were used in a dilution of 1:1000 and visualised using an Alexa Fluor® 488-labelled goat anti-rabbit secondary antibody (Molecular Probes) at a concentration of 7,5 µg/ml. Antibodies against FtsE were a kind gift of Joen Luirink (VU Amsterdam) and were directed against *E. coli* FtsE monomers and dimers.

Computer analysis

The TMHMM2 program (http://www.ch.embnet.org/software/TMPRED_form.html) was used for the prediction of transmembrane domains in proteins and T-Coffee (http://www.ch.embnet.org/software/TCoffee.html) and Boxshade 3.21 (http://www.ch.embnet.org/software/BOX_form.html) for multiple protein alignment.

RESULTS

Alignment of FtsE and FtsX homologues

FtsEX belong to the family of ABC transporters; FtsE resembles the ATP-binding protein and interacts with the membrane component FtsX (de Leeuw *et al.*, 1999; Schmidt *et al.*, 2004; Ukai *et al.*, 1998). Surprisingly, the predicted amino acid sequence of *S. coelicolor* FtsE (ScFtsE) shares only 49% identical and 70% similar amino acid residues with *E. coli* FtsE and 55% and 62% aa identity with FtsE from *B. subtilis* and *M. tuberculosis*, respectively (Fig. 1A).

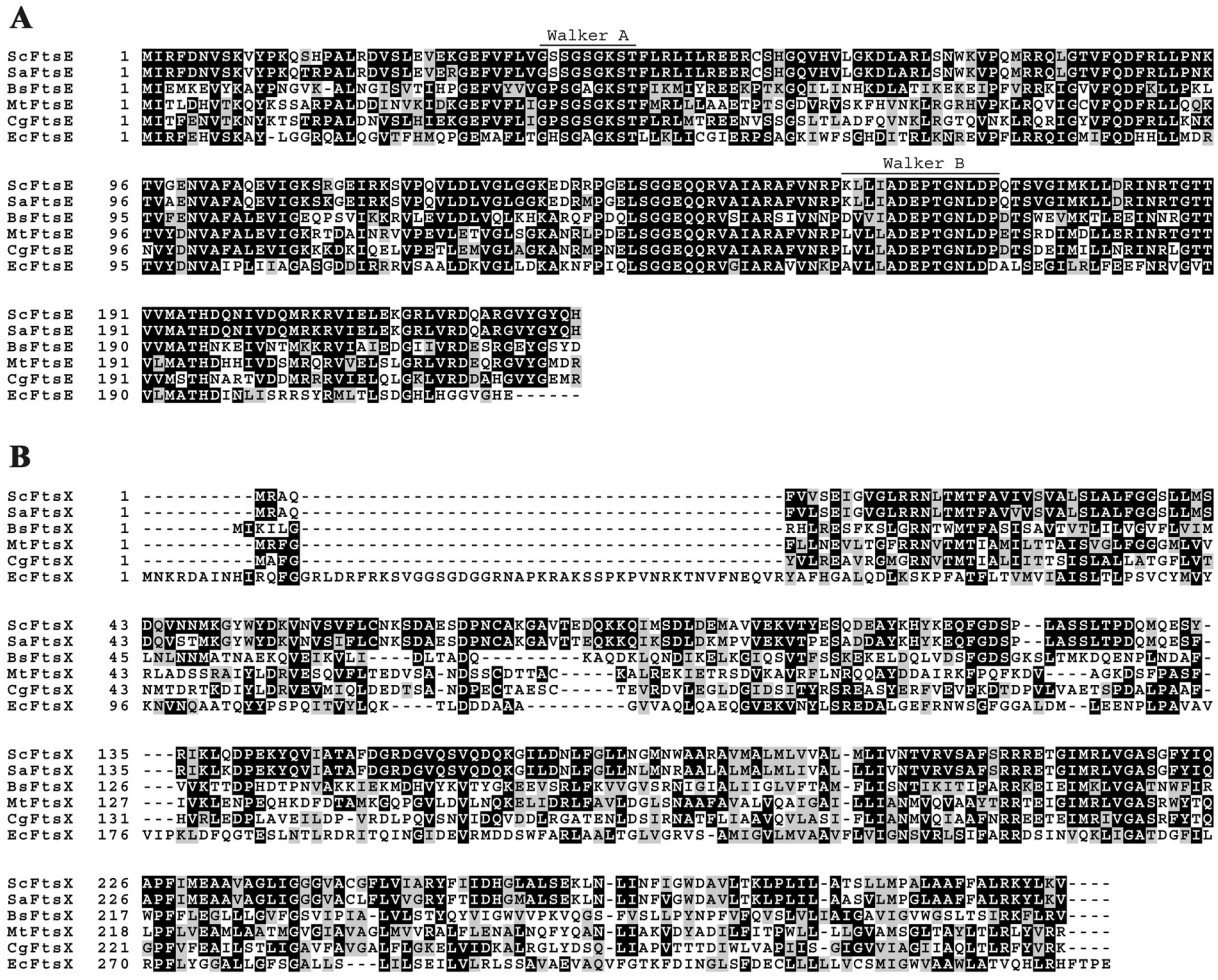

Figure 1: Sequence alignment of FtsE (A) and FtsX (B). Multiple alignments from various bacterial genera were carried out using T-Coffee (http://www.ch.embnet.org/software/TCoffee.html). Amino acids marked with black or grey boxes indicate sequence identity or similarity, respectively. The dashes indicate the gaps introduced to optimise the alignment. This was done using Boxshade 3.21 (http://www.ch.embnet.org/software/BOX_form.html). ScFtsE/X: FtsE and FtsX of *S. coelicolor*, SaFtsE/X: FtsE and FtsX of *S. avermitilis*, BsFtsE/X: FtsE and FtsX of *B. subtilis*, MtFtsE/X: FtsE and FtsX of *Mycobacterium tuberculosis*, CgFtsE/X: FtsE and FtsX of *Corynebacterium glutamicum* and EcFtsE/X: FtsE and FtsX of *E. coli*. Walker A and B consensus sequences in FtsE are marked.

ScFtsE contains the Walker A and B consensus motifs that make up the ATP-binding site in proteins of the ABC family. The Walker A motif (GXXGXGKT/S) of both ATP and GTP-binding proteins is located between aa residues 36-43 of ScFtsE, which also contains the P-loop lysine residue that is in direct contact with the β- and γ-phosphate of the bound NTP (Saraste *et al.*, 1990). Even more surprisingly, the homology between FtsX proteins of different species is lower than that of FtsE proteins (Fig. 1B). For example, *S. coelicolor* FtsX (ScFtsX) shows only very limited similarity to the homologue from *E. coli* (20% identical and 45% similar residues). Similarly to FtsX of *E. coli*, ScFtsX is predicted to have four transmembrane domains, instead of the six typical of membrane components of other ABC transporters.

Construction of an ftsX mutant

ftsE (SCO2969) and *ftsX* (SCO2968) form an operon and lie relatively close to the origin of replication on cosmid E59 of the ordered cosmid library of *S. coelicolor* (Redenbach *et al.*, 1996). Upstream of *ftsE* lies SCO2970, encoding a membrane protein, while downstream of *ftsX* a cluster of genes is found that is the tmRNA-mediated trans-translation (Withey and Friedman, 2002), including ssrA for tmRNA, smpB (SCO2966) for small protein B (Braud *et al.*, 2006) and ctpA (SCO2967) a carboxy-terminal processing protease, most likely involved in proteolytic degradation of proteins tagged by the tmRNA protein tagging system (Fig. 2).

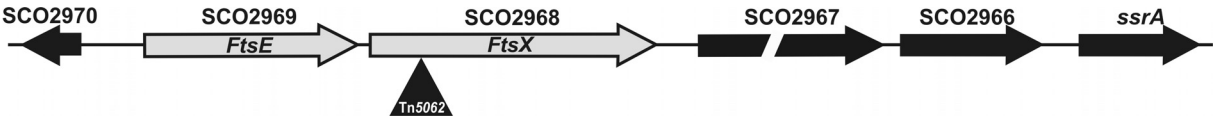

Figure 2: Genomic organisation of *ftsEX*. *ftsEX* are shown as grey arrows while adjacent genes are shown as black arrows. The corresponding SCO-numbers are shown above the arrows. SCO2967 encodes for a carboxy-terminal processing protease, most likely involved in proteolytic degradation of proteins tagged by the tmRNA tagging system. SCO2970 encodes for a membrane protein. The triangle indicates the position of TN*5062* insertion inactivating *ftsX*.

E59(*ftsX*::Tn*5062*) and E59(*ftsE*::Tn*5062*) were introduced into *S. coelicolor* M145 by conjugation from *E. coli* ET12567/pUZ8002. For E59(*ftsX*::Tn*5062*), simultaneous screening for loss of the cosmid sequences (Kan^S) and presence of the resistance cassette ($Apra^R$) gave several independent mutants. Southern hybridisation confirmed that the correct recombination event had occurred (not shown). This mutant was designated GSX1 (*ftsX*::Tn*5062*). Surprisingly, despite many attempts we were unable to obtain mutant double recombinants for

E59(*ftsE*::Tn*5062*). Using the plasmids pGWS144, harbouring an in frame deletion of *ftsE*, and pGWS146, where the +16/+676 region of *ftsE* was replaced by an apramycin cassette, we tried to create an *ftsE* deletion strain, in a different manner. Since *ftsE* is preceding the co-transcribed *ftsX*, introduction of pGWS146 into the genome of *S. coelicolor* will have a polar effect on the transcription of *ftsX*. Both plasmids were introduced into *S. coelicolor* M145. Double recombination was checked for both constructs, giving loss of thiostrepton resistance for pGWS144 and additional apramycin resistance for pGWS146. After introduction of pGWS146 and during screening for double recombination, only 10% of the cells were single cross-overs and apramycin resistant. In other words, 90% of the cells had lost the plasmid and recombination invariably led to the wild type genotype. Also after introduction of pGWS144, all double recombinants checked harboured the wild type *ftsE*. Since in *E. coli* an *ftsE* null mutant is only viable in the presence of more than 0.5% NaCl (de Leeuw *et al.*, 1999), the knock-out experiments were repeated with and without the addition of different concentrations of NaCl, but in either case double recombinants were never obtained. Our inability to create an *ftsE* deletion mutant using three different techniques may be an indication that (in contrast to *ftsX*) *ftsE* is an essential gene in *S. coelicolor*.

Characterisation of the *ftsX* mutant

When plated on SFM agar plates for 5 days, the *ftsX* mutant GSX1, had a lighter grey appearance than the parental strain M145, suggesting it produced significantly fewer spores (Fig. 3). To characterise the *ftsX* mutant in more detail, the mutant was grown together with the parental strain on SFM for 5 days at 30°C and analysed by electron and fluorescence microscopy. Cryo-scanning electron microscopy revealed relatively regular spore chains.

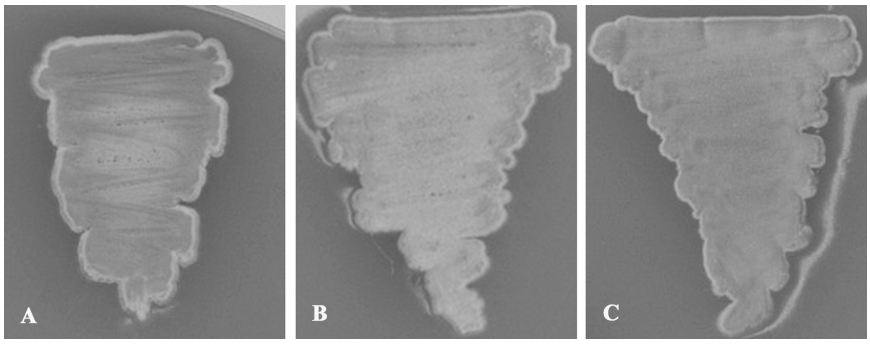

Figure 3: Phenotypes of the *ftsX* mutant (B), its genetically complemented derivative (C) and its congenic parent *S. coelicolor* M145 (A) on solid media. Strains were grown on SFM at 30°C for 5 days.

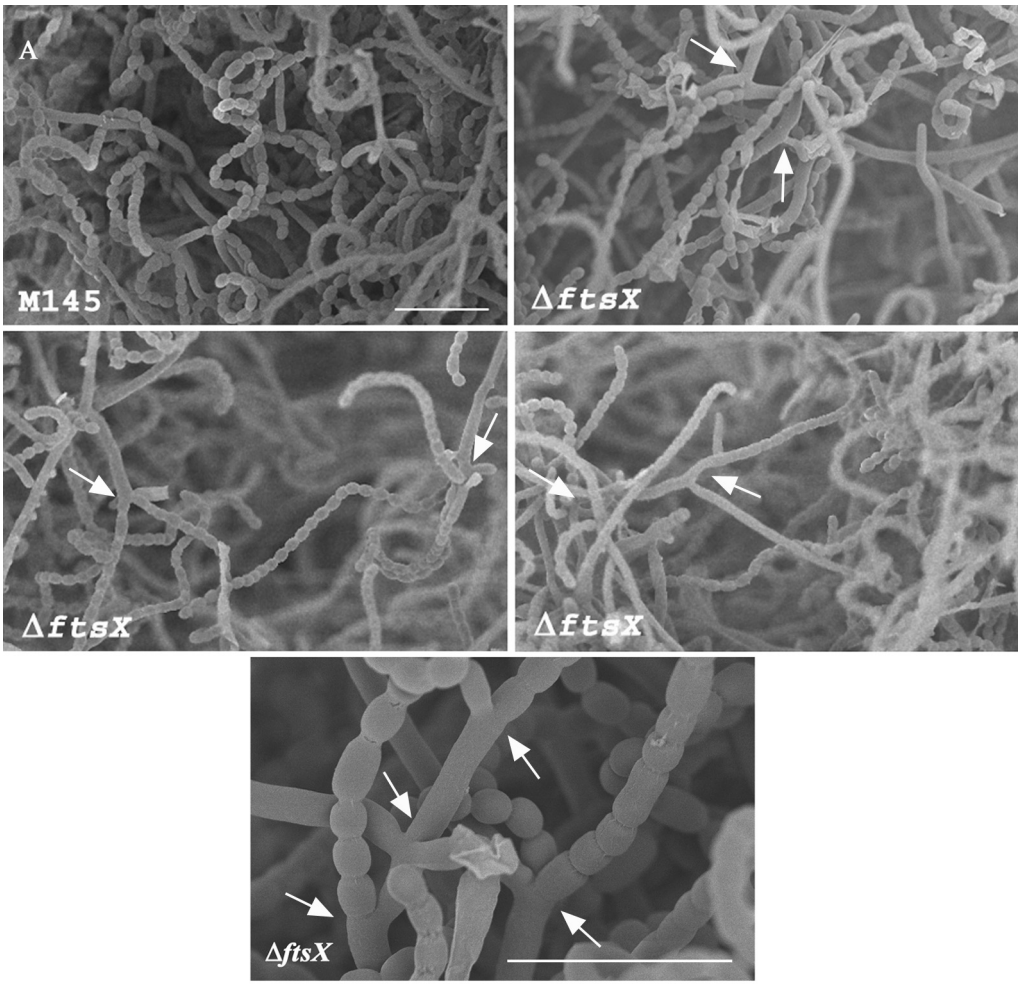
A
M145
ΔftsX
ΔftsX
ΔftsX
ΔftsX

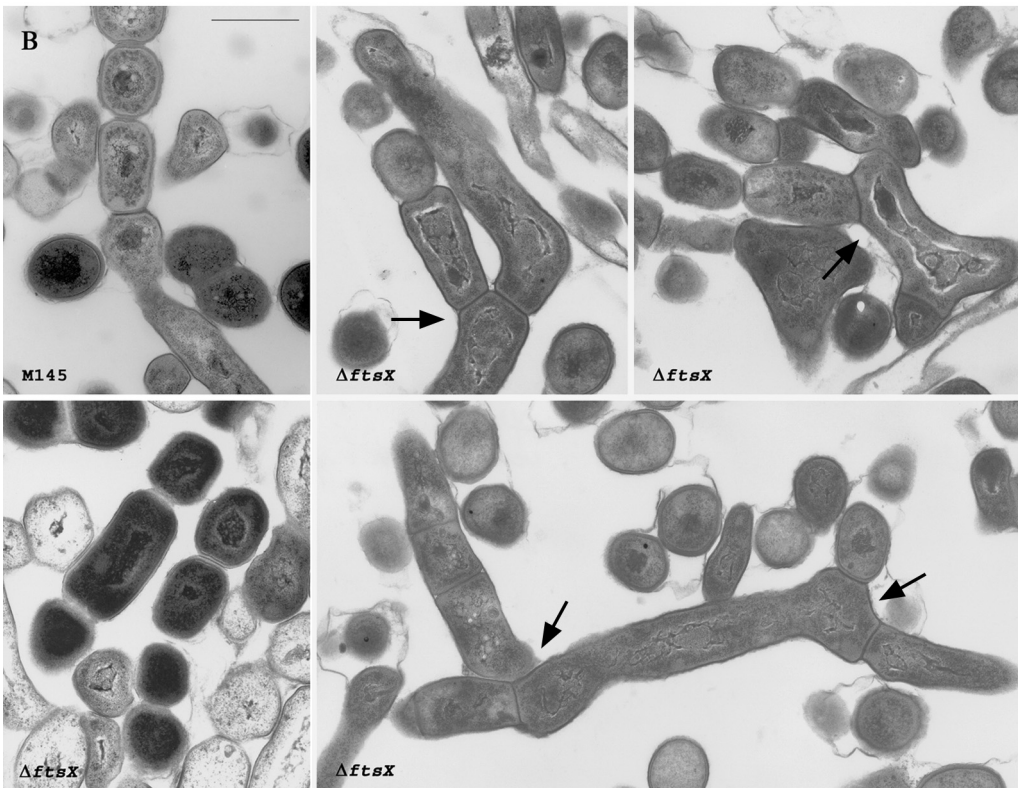
B
M145
ΔftsX
ΔftsX
ΔftsX
ΔftsX

Figure 4: Phenotypic characterisation of an *ftsX* mutant by cryo-scanning electron microscopy and transmission electron microscopy. Samples were taken from 5-day old cultures grown on SFM at 30°C. **A.** Cryo-SEM of spores and aerial hyphae of M145 and the *ftsX* mutant. Bar = 5 μm. **B.** TEM of aerial hyphae and spore chains of M145 and the *ftsX* mutant. Bar = 1 μm. **A-B:** Branches of aerial hyphae close to the base of the spore chain were detected in the *ftsX* mutant (arrows).

Surprisingly however, the mutant aerial hyphae frequently showed branching close to the base of the spore chain, which was never observed in the wild type strain (Fig. 4A). The same branches were also identified by high-resolution transmission electron microscopy, which also revealed irregular spore sizes (Fig. 4B).

Nucleic acid distribution in the *ftsX* mutant appeared to be very similar as in the wild type. However, around 70% of the Δ*ftsX* spores showed WGA-stained foci at the spore poles in comparison with the staining at the spore poles in the wild type (Fig. 5, for a full colour version, see p184).

GSX1 was restored to the phenotype of the parental strain by the introduction of a low copy-number vector harbouring the relevant *ftsX* gene and its promoter sequence (pGWS145). This complemented Δ*ftsX* strain was included in the microscopical analysis, verifying its re-established phenotype (not shown).

Localisation of FtsZ-EGFP in the *ftsX* mutant

In *E. coli*, studies were performed to reveal an order of assembly for Fts proteins into a multiprotein complex, called the divisome. Localisation of FtsX in *E. coli* appears to require FtsZ, FtsA and ZipA, but not the downstream division proteins FtsK, FtsQ, FtsL and FtsI (Schmidt *et al.*, 2004). To determine if FtsZ is dependent on FtsX for localisation at the septum site, we constructed an *ftsX* mutant harbouring FtsZ fused to EGFP. Regularly spaced FtsZ rings were detected in sporogenic aerial hyphae (Fig. 6A, for a full colour version of Fig. 6, see p185). This suggests that the correct localisation of FtsZ is not dependent on FtsX.

Localisation of FtsX and FtsE

In *E. coli*, FtsE and FtsX were localised at the division site in cells, which were on average longer, indicating that these proteins are functional during later stages of cell growth and remain at the division site until division is complete. Therefore, it has been suggested that FtsEX might be involved in the constriction of the septal ring or alternatively, may assist in the insertion of one or more division proteins into the cytoplasmic membrane (Schmidt *et al.*, 2004).

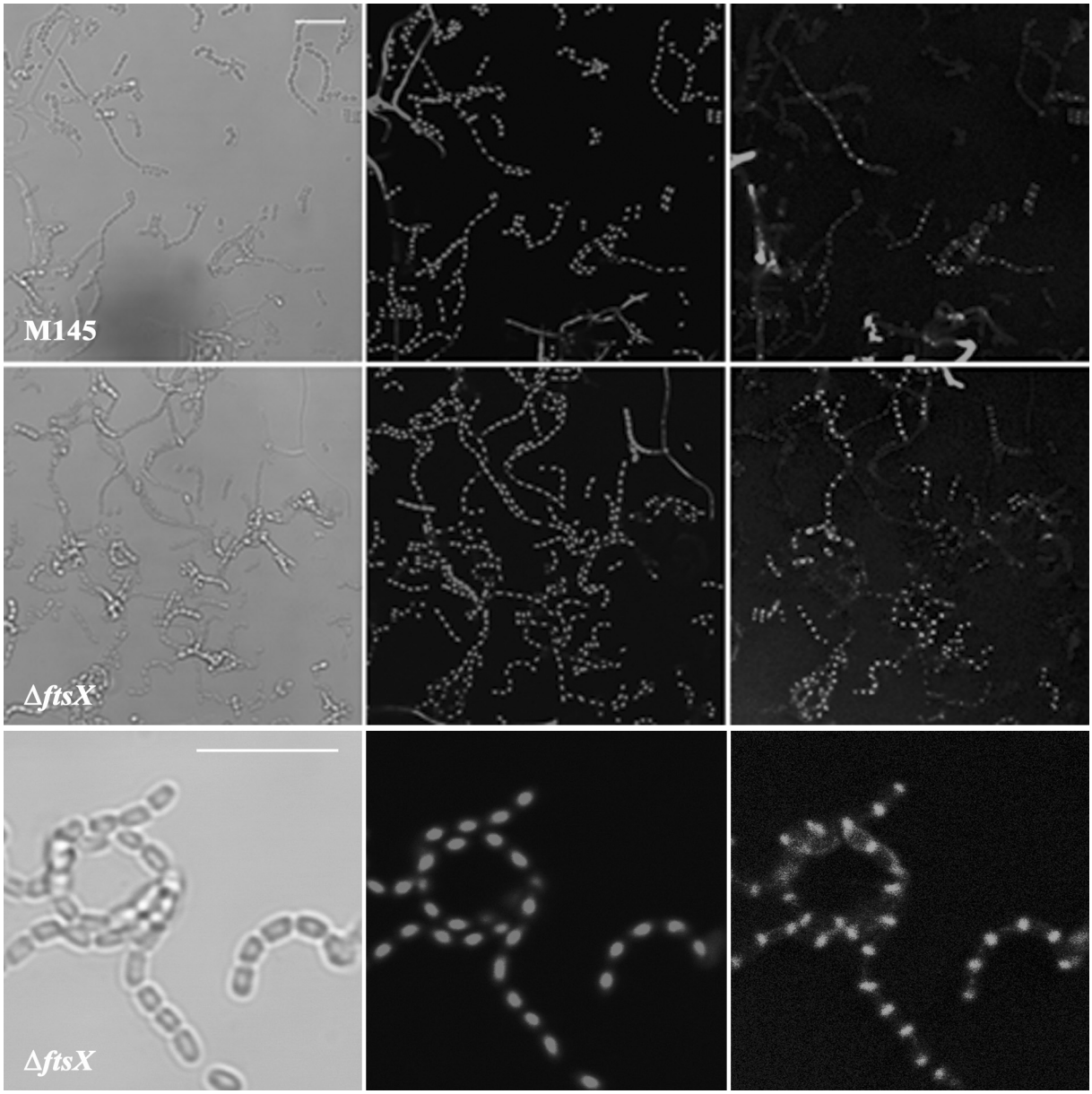

Figure 5: Analysis of an *ftsX* mutant by confocal fluorescence microscopy. Samples were prepared from 5-day old surface-grown cultures at 30°C of the parental strain M145 and the *ftsX* mutant. DNA and peptidoglycan subunits were visualised with PI (middle column) and fluorescein-WGA (right column). The left column shows light microscopy images. Bar = 5 µm. (Full colour version, see p184).

In order to localise FtsE and FtsX, we constructed pGWS136 and pGWS137, expressing in frame fusions of *ftsE-egfp* and *ftsX-egfp*, respectively, from their natural promoters (See Materials and Methods section). However, we could not detect any specific localisation of the GFP-tagged proteins in *S. coelicolor* transformants harbouring either pGWS136 or pGWS137, which could mean that the fusion with EGFP interferes with the

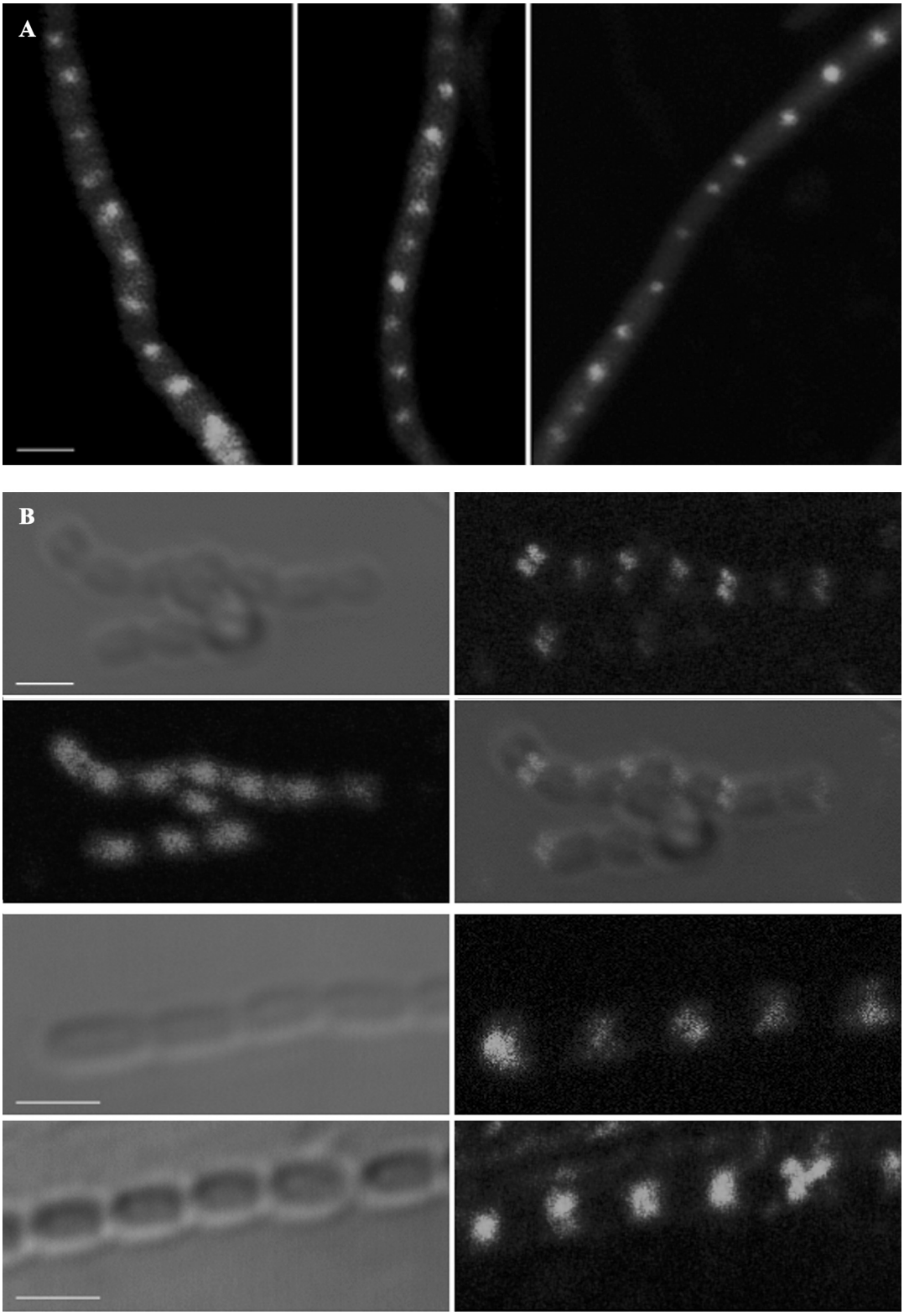

Figure 6: A. FtsZ-rings in an *ftsX* mutant. Strains were grown on SFM for 2 days at 30°C. **B. Cellular localisation of FtsE using anti-FtsE antibodies.** Strains were grown on SFM for 5 days at 30°C. Propidium iodide was used to visualise DNA. The left column shows light microscopy images and the right column represents FtsE localisation (Row 1-3-4) or the left column shows DNA and the right column shows an overlay of the images of row 1 (Row 2). Bar = 1 μm. (Full colour version, see p185).

proper function of the protein. In *E. coli*, researchers also could not identify specific foci for FtsE-EGFP (Schmidt *et al.*, 2004). Considering our failure to identify the GFP-tagged proteins, we attempted localisation of the proteins with immuno-fluorescence microscopy using *E. coli* antibodies. Cells were stained after treatment with lysozyme. Propidium iodide was used to visualise the DNA. FtsE localised at a time after the completion of DNA segregation, at the spore septa of maturing spore chains, which was visualised as a ladder. The fluorescent signal was brighter at either side of the septum (close to the hyphal walls) with less bright fluorescence in the middle of the septum (Fig. 6B). The localisation pattern of FtsE in the *ftsX* mutant was similar as in the parental strain (not shown). This localisation pattern of FtsE is similar to that of SsgB (Chapter 3), which may indicate that these proteins are recruited to the divisome at the same time, and may interact directly (see also Chapter 3).

DISCUSSION

In this chapter, we have investigated the function of FtsE and FtsX in *S. coelicolor*. These two proteins are homologous to an ABC transporter complex in *E. coli* that is since long known to play a role in cell division, although its precise function is still unknown. Sequence comparison indicates that FtsEX can be placed with importers rather than exporters (Schmidt *et al.*, 2004). An *ftsX* mutant of *S. coelicolor* was not obviously defective in cell division. The strain produced regular spore chains and normal vegetative septa. However, frequent branching was observed in the aerial hyphae, at the base of the spore chain. In comparison to the wild type, a significantly larger proportion of *ftsX* mutant mature spores showed accumulation of peptidoglycan (PG) precursors during autolytic separation. PG subunits released during septal constriction might be transported back into the spores, perhaps mediated by FtsEX, to enter a recycling pathway. Recycling of PG was already reported to happen during PG biosynthesis, while a significant proportion of the turnover is related to cell division (Goodell, 1985; Park, 1993). Subsequently, these recycled subunits could participate in spore wall synthesis and/or cell wall synthesis during spore germination and hyphal growth. Cells lacking FtsX may be disturbed in this PG import and the remaining subunits are then stained with Fluo-WGA. This staining of PG subunits at the spore poles was also seen in spores lacking SsgF (Chapter 2), although the typical 90° rotation of loosely attached spores, due to incomplete breakdown of PG subunits, was not seen in the *ftsX* mutant. This could be another indication that the stained subunits accumulate because of a disturbance in transport

rather than a deficiency in breakdown. FtsEX could also function in recruiting cell division proteins functional in this process. The phenotype of an *ftsX* mutant could be the result of the lack of *ftsX* and/or of free FtsE, which might interact with another protein and exerts its function as an ATP-binding protein in another process. Attempts to create an *ftsE* knock out strain failed, even with the addition of extra salt in the medium, suggesting that FtsE might be an essential protein interacting with at least one other ATP-requiring and essential transport protein. There is at least one other example reported of an ATP-binding protein assisting more than one ABC transport system. For example, MsiK was originally identified as the ATPase for the maltose transport system but apparently provides energy to no less than 30 other processes (Schlosser *et al.*, 1997) and S. Rigali, personal communication). ScFtsE has a homology of about 50% with EcFtsE, and working with constructs containing the full sequence of *ScftsEX* in *E. coli*, was difficult and appeared to be toxic for the *E. coli* cells.

Localisation studies of FtsE and FtsX, using a fusion with EGFP failed to work, possibly because these proteins are not able to function properly as GFP fusions. The cellular localisation of FtsE was discovered using peptide antibodies directed against FtsE. As in *E. coli*, where both FtsX and FtsE localise at the septum in a later stage of cell growth, *S. coelicolor* FtsE was localised to the septum and this was after DNA segregation in maturing spores.

Fluorescence was brighter at the sides of the septum, indicating that FtsE might be forming an open ring-like structure. Assuming that, as in *E. coli*, FtsX and FtsE form a complex together, it is very tempting to speculate that FtsX localises, with FtsE, at septum sites. The localisation of FtsE at the periphery of the septum in maturing spores is again suggesting that FtsEX have a function during autolytic spore separation. This observation supports the hypothesis that FtsEX are active during later stages of sporulation. It was also suggested that in *E. coli* FtsEX are involved in constriction of the septal ring or in insertion of a division protein into the membrane (Schmidt *et al.*, 2004). Our data strongly suggest that the latter is not the case, but rather that FtsX allows transport of autolytically produced PG subunits back into the cells.

FtsZ is capable of producing the normal Z-ring in an *ftsX* mutant. Therefore, FtsZ does not need FtsX for its function. During FtsE localisation, DNA segregation was finished and septa appeared to be closed in the maturing spores, leading us to speculate that FtsK, involved in DNA segregation during sporulation, and FtsI, taking part in septum synthesis, will have the ability to localise and function without FtsX. It appears that in *S. coelicolor* the order of

recruiting proteins to the septal ring is different from that in *E. coli*. This could be the result of the different order of events taking place in cell division in *S. coelicolor*, where DNA segregation happens after septum initiation and constriction occurs after septum closure, while in *E. coli* segregation of the chromosome happens before the start of septum synthesis and constriction happens during septum synthesis.

We anticipate that *S. coelicolor* FtsE and FtsX, interact with each other and constitute an ABC transporter. From the localisation at septum sites in maturing spores and the accumulation of PG subunits during constriction, we hypothesise that FtsEX function during spore separation by autolysis, most likely as a recycling component. Still, the exact function of these proteins needs further investigation. Two crucial question that remain include are they really transporters and if so, what do they import.

ACKNOWLEDGEMENTS

We are thankful to P. Herron and P. Dyson for providing us with cosmid E59 carrying transposon mutations in *ftsE* or *ftsX* and to J. Luirink for peptide antibodies directed against *E. coli* FtsE and FtsX.

7

Summary and Discussion
&
Nederlandse samenvatting

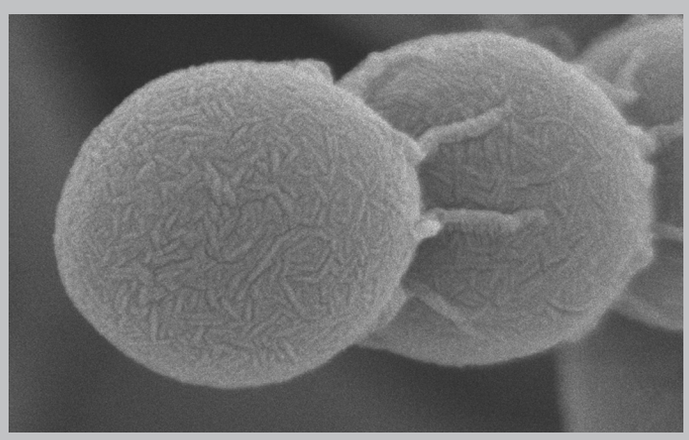

SUMMARY AND DISCUSSION

Streptomycetes differ from most bacteria because of their unusual, complex life cycle. While most bacteria divide the mother cell into two daughter cells by the formation of a single septum at the mid-cell position, *Streptomyces* has two types of cell division. During vegetative growth, the hyphae are divided into connected multinucleoid compartments separated by cross-walls. During development, which starts after an environmental trigger, ladders of regularly spaced septa are produced in the aerial hyphae, which later differentiate into spore chains, resulting in many single cellular spores (Chater, 2001). This complex life cycle harbours some features that are unique to streptomycetes, such as that cell division is dispensable for vegetative growth (McCormick *et al.*, 1994; McCormick and Losick, 1996), making them very interesting organisms for the study of bacterial cell division. Generally, the cell division machineries of streptomycetes and other bacteria are highly similar. A major exception are the proteins that are responsible for the stability (FtsA, ZipA) and bundling of FtsZ protofilaments (ZapA, EzrA) and for the spatial control of the placement of FtsZ (MinC, MinE, SulA and Noc) (Michie and Lowe, 2006), which are apparently absent in *S. coelicolor* and *S. avermitilis*, raising the important question as to how the localisation of multiple Z-rings is coordinated and how these rings attach to the cell wall. This suggests that several division proteins that replace these important proteins in streptomycetes still need to be identified (Flärdh and van Wezel, 2003).

Since vegetative hyphae do not physically separate while spores do detach, proteins that are absolutely required for the separation process will be only active during the sporulation process. In this way, we are able to distinguish between proteins that play a role in the general cell division process and proteins that are required specifically for autolytic cell separation (during cytokinesis).

This is exemplified by the FtsEX membrane transport system (Chapter 6). *ftsE* and *ftsX* lie in one operon and the proteins they encode resemble an ABC transporter. FtsX forms a pore in the membrane for the transport of a specific component, while FtsE is an ATPase that delivers the energy for this transport. While this transporter was identified decades ago as essential for cell division, its precise function is still unknown. This is quite exceptional, and in fact the *ftsEX* operon is one of the last (sets of) *fts* genes whose function is still largely unknown. Interestingly, it could be established that cross-walls are apparently normal in *ftsX* mutants, but during the process of spore separation, peptidoglycan subunits accumulating at

the spore poles. This strongly suggests that FtsE and FtsX facilitate the transport (import) of subunits arising from peptidoglycan autolysis back into the cells where they could be reused. This is a very good example of how Streptomycetes can be used as a tool to analyse general cell division proteins.

How then does the divisome dock to the cell wall and how is the synchronous synthesis of multiple septa coordinated? In this thesis, evidence is provided that members of the SALP family of proteins, a novel family of small (130-140 aa) proteins with no similarity to any other protein (Keijser *et al.*, 2003), are candidates for such a function. SsgA, SsgB and SsgG are all involved in septum-site localisation and may compensate for the absence of proteins involved in these processes in unicellular bacteria. Six or seven SsgA-like proteins have been identified in the *Streptomyces* genomes that have been sequenced so far, namely from *S. avermitilis*, *S. coelicolor* and *S. scabies*. In this thesis, it is shown that all the SALPs have defined functions during sporulation-specific cell division of *S. coelicolor* (Chapter 2-3-4). SsgA activates sporulating-specific cell division. Enhanced expression of SsgA results in a strong increase of septum formation and in thick, irregular septa and the formation of spore-like bodies in liquid cultures. Deletion of *ssgA* blocks septum formation on glucose-containing media, although some viable spores are produced on mannitol-containing media (van Wezel *et al.*, 2000). The transcription profiles of many developmental genes were changed in the *ssgA* mutant, most likely as a result of a feedback to the genome because of changes in cellular state. Some of these changes could be directly linked to observed functions of SsgA. SsgA activates septal peptidoglycan synthesis and the expression of *ftsI* is highly upregulated in an *ssgA* mutant. *ssgA* mutants form branches in their aerial hyphae and they overexpress *divIVA*. Localisation studies showed that SsgA was localised at the tip of growing aerial hyphae and ends up at future septum sites. Eventually, when the spores are separated SsgA is equally divided over the two spores and the number of foci of SsgA-GFP in the spores could be correlated statistically to the number of germ tubes emerging from germinating spores. This suggests that SsgA may mark the cell wall for future major alterations during development, especially the localisation of septa and of germ tubes, but perhaps also of branches.

SsgG is involved in septum site selection, perhaps by helping the reorganisation of the FtsZ spiral into the Z-ring. Eventually, this Z-ring forms the scaffold for septum synthesis. The dynamic localisation of SsgG is relatively similar to the reorganisation of FtsZ from a spiral into a ladder of rings. According to the distance between the foci of SsgG (around 1

μm), it is likely that SsgG ends up at future septum sites. These data support its possible function in the reorganisation of FtsZ into rings. Interestingly, on average one out of five of the septa were 'missing' in *ssgG* mutants, suggesting that SsgG does not exert this function of reorganising FtsZ on its own. It is unclear if SsgG affects all septa, or only a specific fraction of them, for example marking yet unidentified subcompartments.

In contrast to SsgG, SsgB is essential for sporulation, and in its absence development is blocked at an early stage of aerial growth. While occasional Z rings were observed, no septa were produced in *ssgB* mutants. Excitingly, SsgB was localised at sporulation septa of maturing spores, suggesting that SsgB may be part of the divisome, perhaps acting as a molecular chaperone for PBPs responsible for septal peptidoglycan synthesis, such as FtsI and/or the developmentally controlled FtsI-like proteins SCO3156 and SCO3771. The high amino acid identity seen between SsgB and SsgG (57%, the highest homology between any of the SALPs) may reflect their similar function.

The ability of *ssgA* mutants to produce some viable spores on mannitol-containing media may be explained by the presence of *ssgC*, which can complement *ssgA* mutants at higher copy number, which suggests that SsgA and SsgC carry out similar functions. Indeed, *ssgAC* double mutants have a strictly white phenotype under all conditions. However, mutants of *ssgC* mutants have a phenotype very similar to that of SsgA overproducing strains (very large and unfinished septa at high frequency in vegetative hyphae) and *vice versa*. This, together with the unpublished observation that SALP proteins form multimers at least in vitro, suggests that SsgA and SsgC may interact, forming an inactive complex. This hypothesis needs further testing, for example using a two-hybrid screen,

Our data showed that SsgE and SsgF play a specific role in spore maturation. As *ssgE* mutants produced predominantly single spores, SsgE is presumably a checkpoint for the correct timing of spore dissociation. In the absence of SsgF, spores could not complete autolytic detachment, due to incomplete breakdown of peptidoglycan subunits. This resulted in loosely attached prespores, which could freely rotate and resulted in a visible transition from normally oriented spores to 90º rotated spores. Thus, SsgF controls the cleavage of the peptidoglycan strands between the spores in almost mature chains. In prokaryotes, this function is carried out primarily by the lytic transglycosylase (SLT, SCO4132). A functional relation between the two proteins is therefore anticipated.

Finally, SsgD is the only SALP that is expressed strongly during vegetative growth, although its function is still largely unknown. The only clear defect in *ssgD* mutants was

found during sporulation, where many (pre)spores with aberrant hyphal walls were observed, including spores with a wall, which was the width of aerial hyphae. Presumably, SsgD assists in the correct functioning of cell wall-related proteins involved in lateral peptidoglycan synthesis, such as PBP2 or SCO2897.

Summarising the observations discussed above, the data imply that the SALPs function, possibly as multimers, by recruiting other proteins to their relevant sites, in order to control enzymes responsible for the synthesis and autolysis of peptidoglycan. The question still remains how the chaperone-like SALPs are themselves localised. We have evidence that the localisation of SsgA depends on MreBCD, as the SsgA-GFP localisation pattern is disturbed in mreB mutants. The role of the actin-like cytoskeletal proteins MreB and Mbl in *S. coelicolor* is the subject of Chapter 5. *mreB* is located in the highly conserved *mre* cluster, together with *mreC* and *mreD,* encoding two membrane proteins. These genes are often followed by *pbp2*, which encodes a penicillin-binding protein (PBP). *mreB* orthologues are only present in actinomycetes that produce an aerial mycelium and spores, except from the non-sporulating actinomycete *Rhodococcus* sp. RHA1 that harbours a single *mreB* homologue. Considering the low homology (around 40%) to other MreB proteins, MreB of *Rhodococcus* may have another, yet unidentified function. While MreB, MreC and MreD are essential proteins in *E. coli* and *B. subtilis*, mutants of *S. coelicolor* lacking these proteins are viable. All mutants had similar defects, which were indicative for the disruption of the cell wall integrity. Additionally, MreB was localised at the septa of sporulating aerial hyphae, subsequently as bipolar foci in young spores and eventually in a ring- or shell-like pattern inside the mature spores. Therefore, MreB is present at the places of cell wall synthesis at that particular moment of development. Based on these data, a complex may be formed including the Mre proteins and PBPs, which is most likely active during spore wall assembly, presumably by recruiting PBPs, such as PBP2, and other peptidoglycan-related proteins during the sporulation process. In *E. coli,* MreB, MreC and MreD were proposed to function as a membrane-bound complex directing the PBP2-dependent longitudinal cell wall synthesis (Kruse *et al.*, 2005), while in *B. subtilis*, it was suggested that MreC and MreD couple the helical Mbl 'cables' to the extracellular cell-wall synthesising machinery (Leaver and Errington, 2005). In *S. coelicolor*, further investigation is needed into the exact role of the two MreB homologues. Although the defects in the two mutants were rather similar, differences in the frequency and the degree of the observed anomalies were observed.

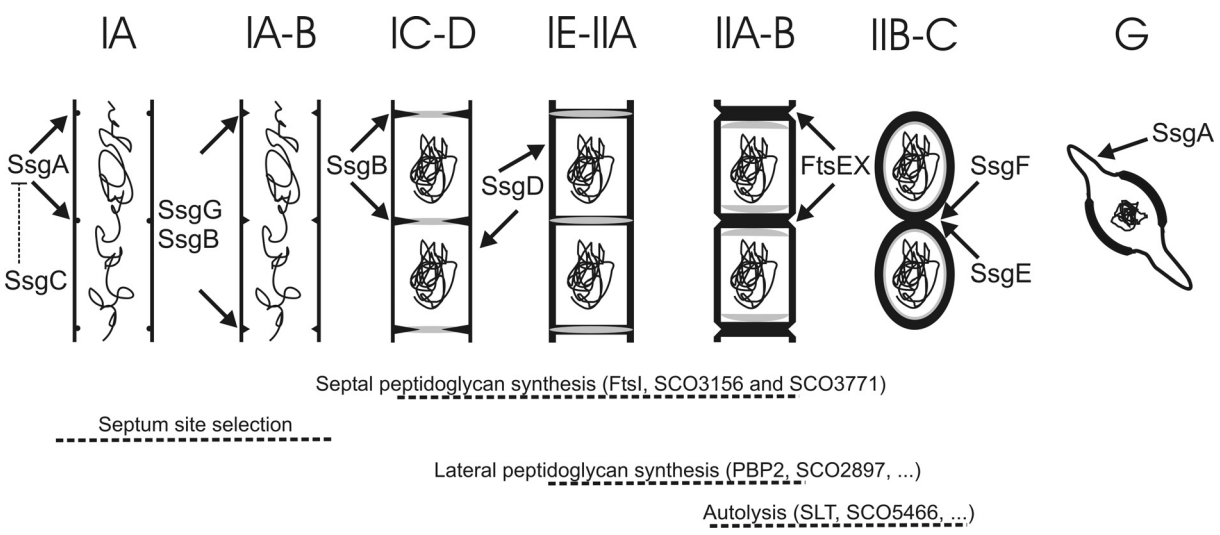

Figure 1: Model of the development of sporogenic aerial hyphae including the suggested function of the SALPs, MreB and FtsEX. MreB is depicted as grey structures. Several events observed during sporulation of aerial hyphae of *Streptomyces* are shown: (I) prespore formation, consisting of (IA) septum site selection; (IB) septum initiation; (IC) septum growth; (ID) DNA segregation and condensation; (IE) septum closure; and (II) spore maturation, consisting of (IIA) growth (thickening) of the spore wall peptidoglycan; (IIB) spore separation by PG autolysis; (IIC) spore release. The dotted lines represent specific events that occur in the sporulation process, including the proteins involved in these events. (G) Germination.

Figure 1 shows a model of the development of sporogenic aerial hyphae including the timing of action and suggested function of all proteins discussed above.

Future research

Where to go from here? To address the exact function of the different SALPs, life cell imaging techniques (FRET, FRAP) and immunoprecipitation studies should provide more insight into the mobility of the SALPs and their interaction partners. Creating deletion mutants of these interaction partners should then give more insight into the process they are involved in but would also show if the SALPs have multiple functions and partners. Knowing the tertiary structure of the proteins is a prerequisite to obtain insight into the structure and function of possible relatives. Another important question that remains to be addressed is how the SALPs themselves are recruited. New evidence showed that this recruitment may be carried out directly or indirectly by cytoskeletal proteins. Further research is required to address this interesting possibility. Characterisation of a double mutant lacking both *mreB* and *mbl* is important to provide more insight into the function of the cytoskeleton in streptomycetes. Localisation studies of Mbl are necessary in order to find out if this protein is involved in a different process than its homologue MreB. Finally, to understand the true

function of FtsE and FtsX, a conditional *ftsE* mutant needs to be created and the peptidoglycan subunits that accumulate in the *ftsX* mutant (and that are the putative transported molecules) need to be identified. The FtsEX story is a good example of how streptomycetes can serve as very good tools to address longstanding issues in cell division and developmental microbiology.

NEDERLANDSE SAMENVATTING

Het onderzoek verricht tijdens dit promotieonderzoek behandelt hoofdzakelijk de groei en de celdeling van de Gram-positieve grondbacterie *Streptomyces coelicolor*. Deze bacterie volgt een andere groeiwijze vergeleken met de meeste, andere bacteriën, en vertoont twee verschillende vormen van celdeling waardoor er een vergelijking bestaat met sommige eukaryote schimmels. Omdat de celdeling in dit interessante organisme anders is dan het bacterieel prototype, bevat deze bacterie bepaalde families van eiwitten die in geen enkel ander organisme voorkomen.

De levenscyclus van *S. coelicolor*

Groei begint bij de ontkieming van één enkele spore die uiteindelijk een heel netwerk van lange, vertakkende draden of hyfen vormt, ook wel vegetatief of substraat mycelium genoemd. Deze hyfen worden onderverdeeld in compartimenten, die een variërend aantal chromosomen bevatten. De verdeling gebeurt door een muur van instulpend celwand materiaal, de zogenaamde cross-walls of vegetatieve septa. Deze specifieke septa leiden niet tot een fysische scheiding van de cellen. Het compartiment dat door dit septum is afgesloten van het topje van de hyfe krijgt zo de mogelijkheid om zijn dimensies uit te breiden door het creëren van een vertakking dicht bij het septum. Op deze manier wordt er een complex, multicellulair netwerk verwezenlijkt. Wanneer de omstandigheden onleefbaar worden (bijvoorbeeld bij het opraken van voedingsstoffen in de bodem), stimuleert het vegetatief mycelium de ontwikkeling van onvertakte luchthyfen. Dit proces gaat gepaard met de afbraak van het vegetatief mycelium dat als voedsel dient voor de groei van het luchtmycelium. Dit is dan ook de reden waarom deze bacteriën antibiotica produceren, om zo andere hongerige micro-organismen op een afstand te houden. De luchthyfen moeten uit de natte bodem de lucht in groeien en worden daarom bedekt met een waterafstotend laagje. Aan de tip van elke hyfe worden op een bepaald moment en tezelfdertijd tientallen sporulatiesepta op regelmatige afstand van elkaar gevormd. Deze septa zullen de hyfen onderverdelen in prespore compartimenten die elk één chromosoom krijgen. De sporen ondergaan een rijpingsproces waarbij hun celwand extreem verdikt, en zullen uiteindelijk door een proces van autolyse (‘zelfontleding’) van elkaar gescheiden worden. De wind, water of insecten dragen de sporen naar plaatsen waar betere levensomstandigheden heersen waar ze zullen ontkiemen.

De SALPs en het lot van het peptidoglycaan

In hoofdstuk 2, 3 en 4 worden de functies bestudeerd van een eiwitfamilie die enkel voorkomt in sporulerende actinomyceten, de klasse waar ook streptomyceten onder vallen. Deze eiwitten worden de SALPs genoemd (**S**sg**A-l**ike **p**roteins), en tellen zeven leden, van SsgA tot SsgG. In dit proefschrift laat ik zien dat deze eiwitten een belangrijke rol spelen tijdens het sporulatieproces in *S. coelicolor*.

Uit deze experimenten kunnen we concluderen dat SsgA, SsgB en SsgG een belangrijke rol spelen in de positionering van het septum tijdens de sporulatie, een taak die in andere meer eenvoudig bacteriën wordt uitgevoerd door andere (niet verwante) eiwitten, zoals FtsA, ZipA en het Min controlesysteem.

De expressie van SsgA kan direct gecorreleerd worden aan de afstand tussen de septa. Stammen waarin SsgA in grote hoeveelheid tot expressie wordt gebracht, zoals *S. netropsis*, tonen scheidingswanden op ongeveer 1 μm van elkaar. Deze stammen produceren dan ook sporen in vloeibaar medium. Daarentegen zijn er ook stammen, zoals *S. coelicolor*, die een veel lagere hoeveelheid SsgA produceren en deze produceren elke 8-10 μm een scheidingswand. Verhoogde expressie van SsgA in *S. coelicolor* resulteert in meer septa, in verdikte, onregelmatige septa en in de vorming van sporen in vloeibaar medium. Stammen zonder SsgA kunnen daarentegen enkel op bepaalde media een beperkte hoeveelheid septa aanmaken. Als reactie op de afwezigheid van SsgA gaat bijvoorbeeld de expressie van *ftsI*, een gen dat codeert voor één van de PBPs betrokken bij septumsynthese, sterk omhoog. SsgA wordt gelokaliseerd in de tip van groeiende luchthyfen en komt uiteindelijk terecht op de plaatsen waar een septum zal worden gebouwd. Dit ingroeiende septum verdeelt SsgA uiteindelijk over de twee sporen. Ook is er een verband aangetoond tussen de hoeveelheid SsgA en het aantal ontkieminsbuizen in een spore. Hoogstwaarschijnlijk is SsgA nodig om een markering achter te laten in gebieden waar celwand materiaal gesynthetiseerd moet worden, zoals aan de tip van groeiende hyfen, op toekomstige sepum plaatsen en op toekomstige ontkiemingsplaatsen.

SsgG is hoogstwaarschijnlijk betrokken bij de reorganisatie van de FtsZ-spiraal in een FtsZ-ring. Deze ringen geven de plaats aan waar het septum zal komen en precies op deze plekken gaat SsgG uiteindelijk lokaliseren. Mutanten die SsgG niet produceren missen soms dan ook een septum waardoor ze sporen produceren die twee, drie of zelfs vier keer zo lang zijn als normale sporen. Ondanks de afwezigheid van de septa wordt de rest van het differentiatieproces gewoon goed voltooid, zoals het segregeren en condenseren van de

chromosomen. Dit toont aan dat DNA segregatie niet afhankelijk is van de synthese van septa.

Stammen zonder SsgB kunnen geen septa meer aanmaken en verliezen dus hun eigenschap om sporen te maken. FtsZ ringen worden in deze *ssgB* mutant sporadisch gevormd. Het eiwit SsgB vormt een open ring op het groeiende septum. Dus SsgB is essentieel voor de positionering en synthese van de septa en stuurt hoogstwaarschijnlijk een eiwit aan dat betrokken is bij de synthese van het peptidoglycaan, het materiaal waaruit de celwand en dus ook het septum zijn opgebouwd. Deze eiwitten worden penicillinebindende proteins (PBPs) genoemd omdat ze interactie kunnen aangaan met op penicilline lijkende antibiotica waardoor ze inactief worden en daardoor de celwandsynthese blokkeren met de dood van het organisme als gevolg.

De reden waarom SsgA nog enkele sporen kan aanmaken ligt wellicht aan de aanwezigheid van SsgC. Een verklaring zou kunnen zijn dat SsgC dezelfde functie heeft als SsgA maar wanneer het interactie aangaat met SsgA, er een inactief complex ontstaat. Zo kunnen stammen zonder SsgA en SsgC helemaal geen sporen aanmaken, terwijl een *ssgC* mutant goed sporuleert maar met zijn extreem hoge septale peptidoglycaansynthese gelijkt op een SsgA-overproducerende stam.

Van SsgD is nog weinig bekend maar er wordt verondersteld dat dit eiwit betrokken is bij de synthese van de sporewand. *ssgD* mutanten produceren namelijk veel, rijpe sporen zonder de typische dikke, beschermende wand.

De twee laatste SALPs, SsgE en SsgF, zijn betrokken bij de laatste stappen in het rijpingsproces van de sporen, namelijk de scheiding ervan. Zo produceren *ssgE* mutanten weinige rijpe sporen in ketens maar wel heel veel losse sporen, hetgeen dus suggereert dat SsgE betrokken is bij de correcte timing van deze scheiding en onder normale omstandigheden voortijdige afsnoering voorkomt. In de afwezigheid van SsgF kunnen de sporen niet volledig worden gescheiden en blijven ze verbonden door een dunne laag peptidoglycaan. Daaruit concluderen we dat SsgF één van de lytische enzymen controleert die verantwoordelijk zijn voor het scheiden van de sporen. Hieruit kunnen we besluiten dat het merendeel van de SALPs een belangrijke functie hebben bij het aansturen van enzymen betrokken bij de synthese en afbraak van peptidoglycaan tijdens het sporulatieproces.

Het cytoskelet van streptomyceten

Recent is ontdekt dat niet alleen de celwand verantwoordelijk is voor de vorm van een bacterie, maar dat prokaryoten tevens in het bezit zijn van structurele elementen die hierbij een belangrijke rol spelen. Deze (infra)structurele elementen vormen tezamen het cytoskelet. In eukaryoten is het sinds lang bekende cytoskelet functioneel in de vormgeving van de cel, de mobiliteit en verdediging van de cel en levert het een belangrijke bijdrage aan het organiseren van intracellulair transport en de celdeling. MreB eiwitten vertegenwoordigen één groep van cytoskeletale elementen in prokaryoten, namelijk de actinehomologen. Men heeft aangetoond dat MreB polymeriseert en zo actine-achtige eiwittenfilamenten vormt die betrokken zijn in de vormgeving en in chromosoomsegregatie van vele staafjesbacteriën. Ook *S. coelicolor* bevat twee van deze MreB-achtige eiwitten, namelijk MreB en Mbl. MreB bevindt zich in de zeer geconserveerde *mre* gencluster, die ook de membraaneiwitgenen *mreC* en *mreD* omvat. Direct achter deze genen ligt *pbp2*, een gen dat codeert voor een PBP. Alhoewel MreB, MreC and MreD essentiële eiwitten zijn in *E. coli* en *B. subtilis*, werden er levensvatbare mutanten gecreëerd in *S. coelicolor*. Mutanten waarin *mreB, mreC, mreD, mreBCD, mbl* of *pbp2* waren uitgeschakeld, zijn in detail bestudeerd met elektronenmicroscopie (Hoofdstuk 5). Al deze mutanten vertoonden gelijkaardige defecten die erop wijzen dat de integriteit van de celwand aangetast is. MreB eiwitten werden gelokaliseerd op de sporensepta, later op de twee polen van jonge sporen en uiteindelijk vormden de eiwitten een schil aan de binnenkant van de sporen. Gebaseerd op deze resultaten nemen we nu aan dat MreB, MreC, MreD and Mbl hoogstwaarschijnlijk zijn betrokken in het verdikkingsproces van de sporewand. Vermoedelijk doen ze dit door PBPs, zoals PBP2, te werven tijdens het sporulatieproces.

FtsEX en hergebruik van peptidoglycaan tijdens de sporulatie

In het laatste hoofdstuk worden twee celdelingseiwitten beschreven die al bekend waren als vaste leden van het septosoom of divisoom, de verzamelnaam voor alle eiwitten die betrokken zijn bij septumvorming. FtsE en FtsX vormen samen een ABC transporter. FtsX vormt een porie in het membraan waardoor een specifieke component wordt getransporteerd en FtsE is het eiwit dat de energie daarvoor levert door ATP te verbranden. In *E. coli* zijn deze eiwitten op het sepum gelokaliseerd van cellen die hun celdeling bijna voltooid hebben. In *S. coelicolor* lokaliseert FtsE en vermoedelijk ook FtsX, op de septa tussen sporen aan het einde van hun rijpingsproces. In een *ftsX* mutant worden afbraakproducten van het peptidoglycaan

die vrijkomen tijdens de scheiding van de sporen opgestapeld tussen de polen van de sporen. Wij vermoeden dat deze componenten normaal terug in de cel worden getransporteerd waar ze hergebruikt worden voor de synthese van nieuwe celwand. Aan de hand van de resultaten concluderen wij dat FtsX een goede kandidaat is om dit transport te verwezenlijken. Aangezien we niet in staat waren om een *ftsE* mutant te maken, veronderstellen we dat FtsE nog in tenminste één ander essentieel transport wordt tewerkgesteld als energieleverancier of dat de conformatie van FtsX in de afwezigheid van FtsE lethaal is. Dit werk wordt momenteel voortgezet, onder meer om de te transporteren moleculen te identificeren en om conditionele mutanten te proberen te creëren en zo inzicht te krijgen in de exacte lokalisatie en functie van FtsEX.

Streptomyceten zijn, door hun andere groeiwijze ideale organismen om diverse aspecten van de bacteriële celdeling te bestuderen die anders slechts met moeite te onderzoeken zijn. In dit proefschrift tonen we aan dat door hun multicellulaire groei, de celdeling doorheen de evolutie is afgeweken van het bacterieel prototype en nieuwe eiwitten die daarvoor compenseren, zoals de SALPs, zijn ontstaan.

Appendices

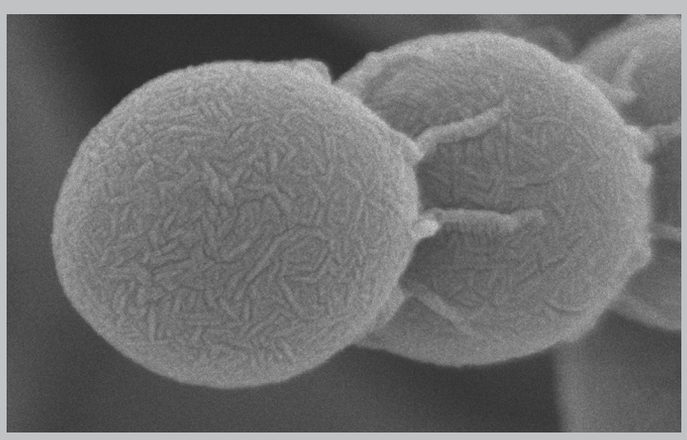

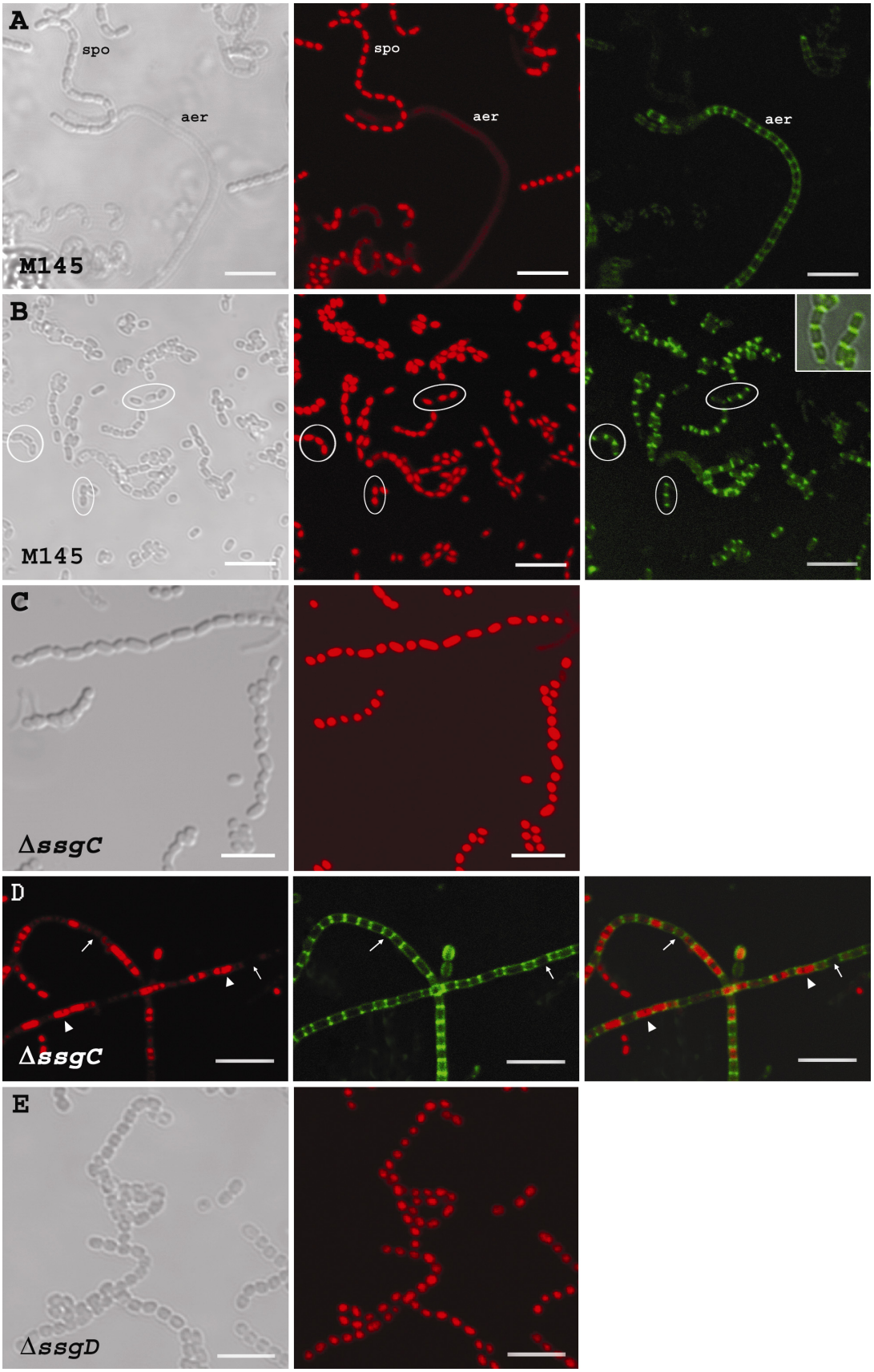
A
spo
aer
M145
spo
aer
aer
B
M145
C
ΔssgC
D
ΔssgC
E
ΔssgD

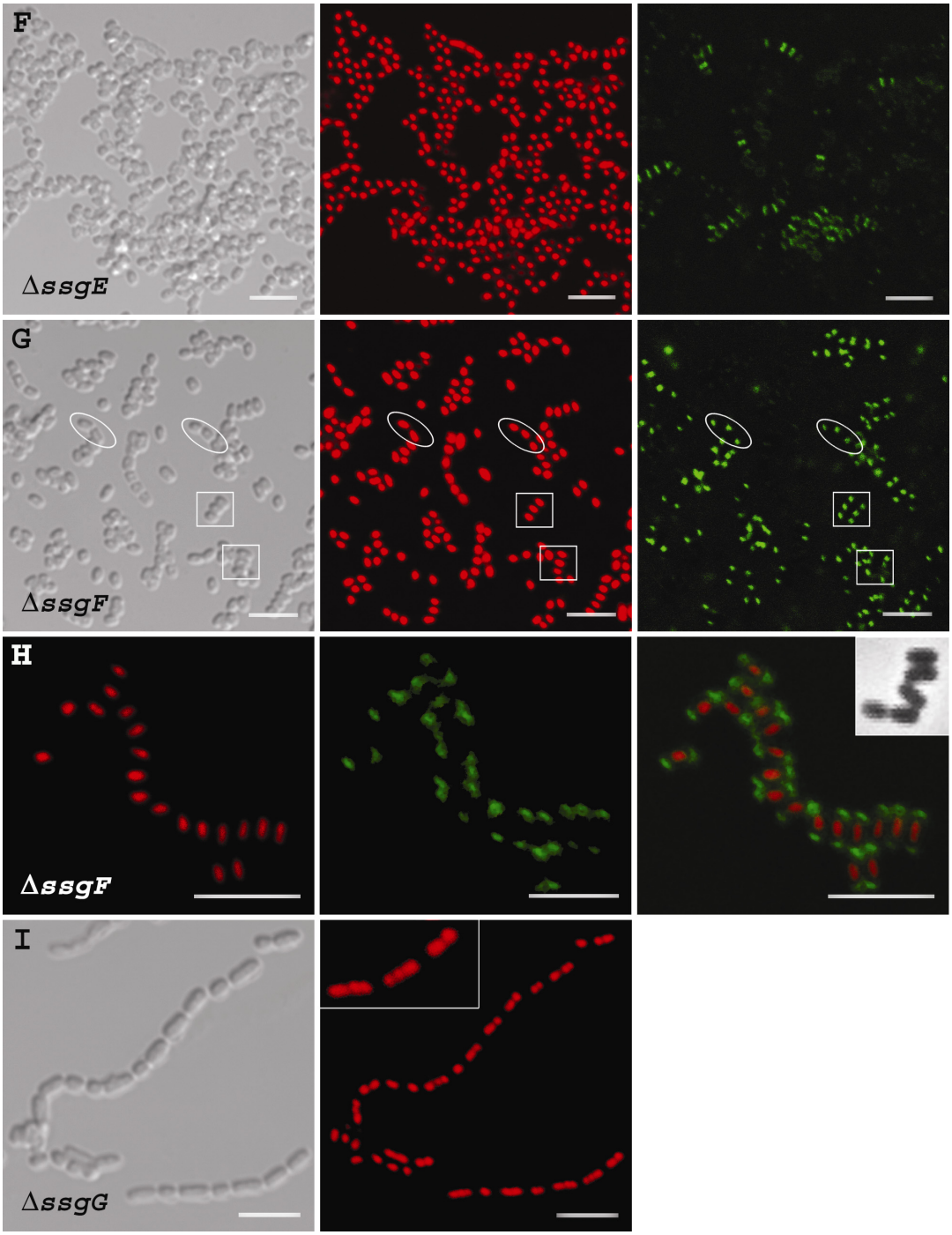

Figure 5, Chapter 2: Analysis of the *ssgC-G* mutants by confocal fluorescence microscopy.
Samples were prepared from surface-grown cultures of the parental strain *S. coelicolor* M145 **(A)** and its mutant derivatives Δ*ssgC* **(C-D)**, Δ*ssgD* **(E)**, Δ*ssgE* **(F)**, Δ*ssgF* **(G-H)**, and Δ*ssgG* **(I)** all grown on SFM plates for 6 days at 30°C. *S. coelicolor* M145 **(B)** was grown on SFM plates for 2-4 days at 30°C. DNA and peptidoglycan subunits were visualised with PI (red) and fluorescein-WGA (green), respectively. The first column shows light microscopy micrographs, the middle column shows DNA, and the third column shows peptidoglycan subunits **(A-C, E-G, I)** or the first column shows DNA, the second shows peptidoglycan subunits and the third shows an overlay of PI and WGA **(D-H)**. **(B, insert)** overlay of fluo-WGA and light microscopy of spores of M145 after 2-4 days of growth, clearly showing staining of spore poles by WGA. **(H, insert)** shows a light microscopy micrograph of Δ*ssgF* spores. **(I, insert)** shows a higher magnification of Δ*ssgG* spores with four and respectively three copies of the chromosome. For mature *ssgD* and *ssgG* mutants no WGA stained septa were detected, and images were therefore omitted. Arrowheads show compartments with multiple chromosomes, small arrows show compartments without DNA, white circles highlight WGA-stained spore poles and squares highlight 'rotated' spores. Bar = 5 μm.

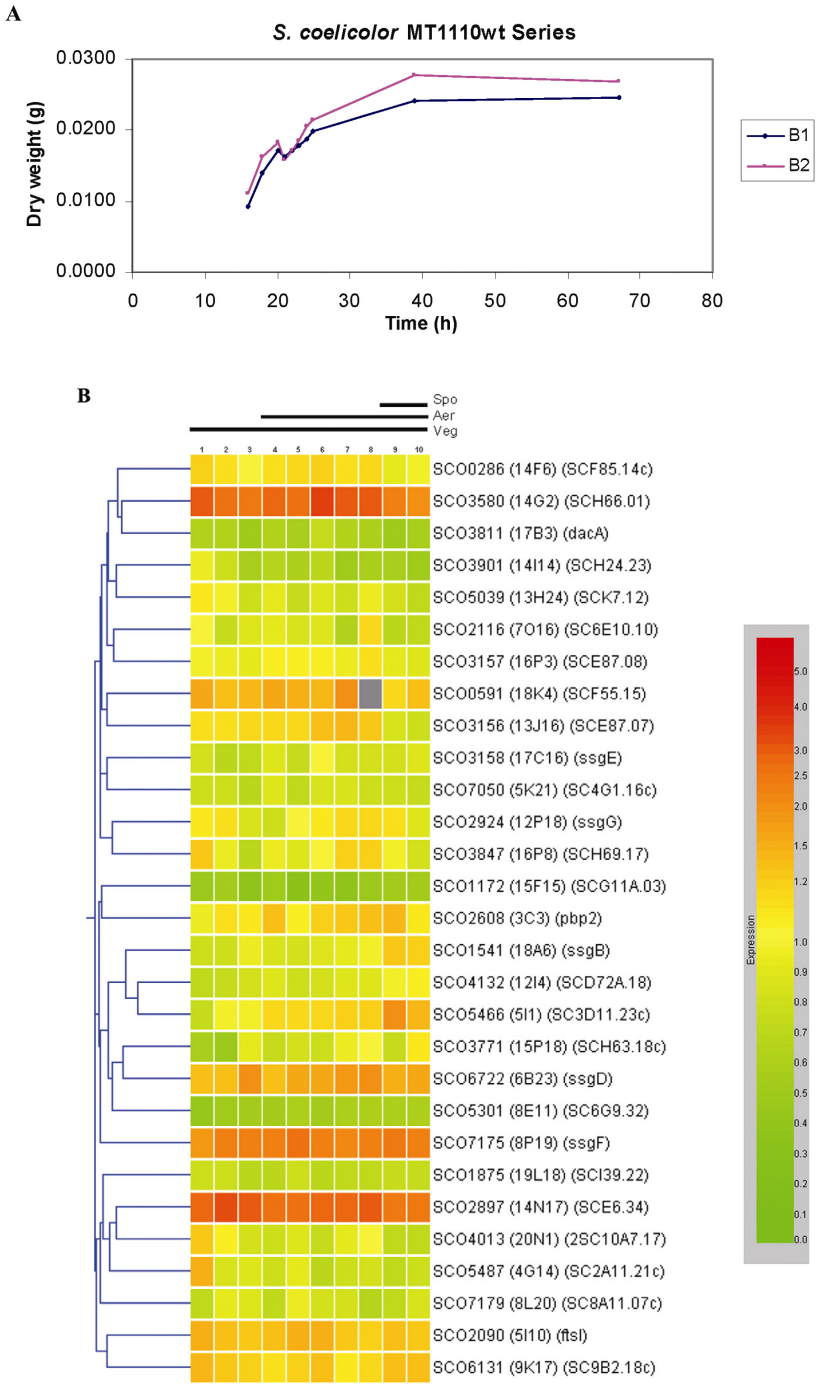

Figure 7, Chapter 2: DNA microarray analysis of developmental and cell wall-related genes in *S. coelicolor* MT1110. cDNA from *S. coelicolor* MT1110 (wild type) labelled with Cy3 d-CTP and gDNA from *S. coelicolor* M145 labelled with Cy5 d-CTP were co-hybridised on microarrays. Colour coding: red indicates a high transcriptional level and green indicates a low transcriptional level. Grey represents a data point below a confidence threshold. The same microarrays were used to analyse RNA isolated from *S. lividans* 1326. This resulted in highly similar data for the SALP genes and the most prominent PBPs and autolysins (not shown). **6A.** Growth curves of two biologically independent experiments. Samples were harvested at ten time points (indicated by a dot). Samples: **1-3,** vegetative growth; **4,** transition from vegetative to aerial; **5-8,** aerial growth; **9-10,** sporulation. **6B.** Gene tree of expression profiles of *ssgA*-like genes and genes encoding penicillin-binding proteins (PBPs) and autolysins. RNA time points: (1) 16 h; (2) 18 h; (3) 20 h; (4) 21 h; (5) 22 h; (6) 23 h; (7) 24 h; (8) 25 h; (9) 39 h; (10) 67 h. Sample 4 corresponded to the onset of aerial mycelium formation and spores were already produced at sample 9. **6C.** Colour scale indicating normalised expression levels.

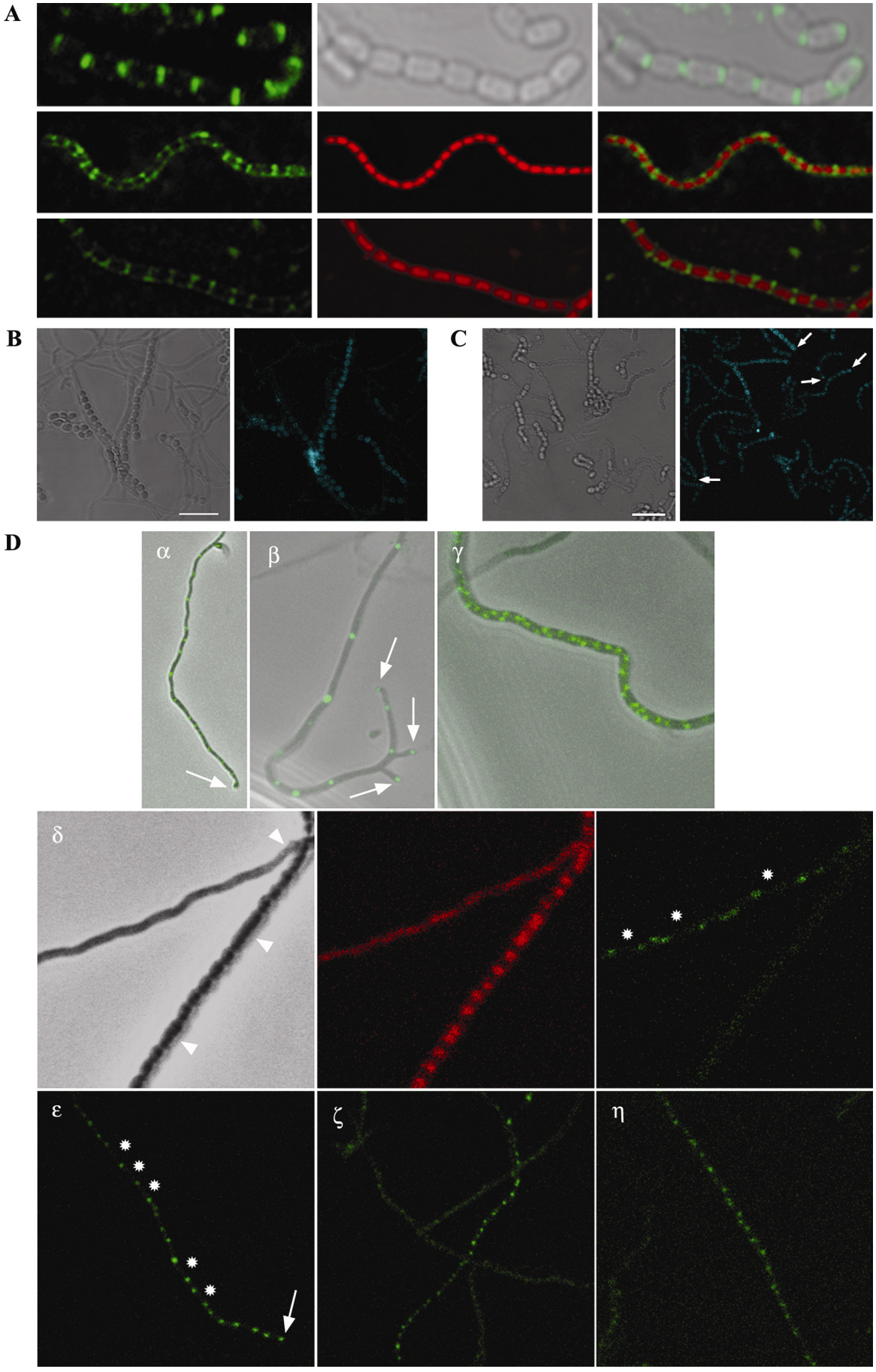
A
B
C
D
α
β
γ
δ
ε
ζ
η

Figure 2, Chapter 3, p177: Localisation of SsgB, ssgE, ssgF and SsgG. Strains were grown on SFM for 5 days (SsgB, SsgE-ECFP and SsgF-ECFP) or 1-4 days (SsgG-EGFP) at 30ºC. DNA was visualised with PI (red) **A.** Localisation of SsgB. The first column shows immuno-fluorescence micographs using fluorescein-conjugated anti-SsgB antibodies, the middle column shows light micrographs (top) and DNA (middle, bottom) and the third column shows overlay images from the left and the middle images. Bar = 2 μm. **B-C.** Non-specific localisation of SsgE-ECFP (B) and ECFP-SsgF (C). ECFP-SsgF shows occasionally brighter foci at the tip of the spores (arrow). Bar = 5 μm. **D.** Localisation of SsgG-EGFP in vegetative hyphae (α-β) and in aerial hyphae (γ-η). α-γ show overlays from light microscopy images and SsgG-EGFP. δ shows light microscopy (left), DNA (middle) and SsgG-EGFP (right) while ε, ζ, η show only SsgG-EGFP. In aerial hyphae, class 1 (γ) shows a staggered pattern while in class 2 (δ-η), foci are laid down in regular pattern, with distances resembling the size between sporulation septa. SsgG was not localised in the spores (δ). Stars show the place where the distance between the foci is double the normal distance and subsequently, spores two times the normal size are created (arrowheads). SsgG-EGFP appeared in the hyphal tips of both vegetative and aerial hyphae (arrows). Bar = 2 μm.

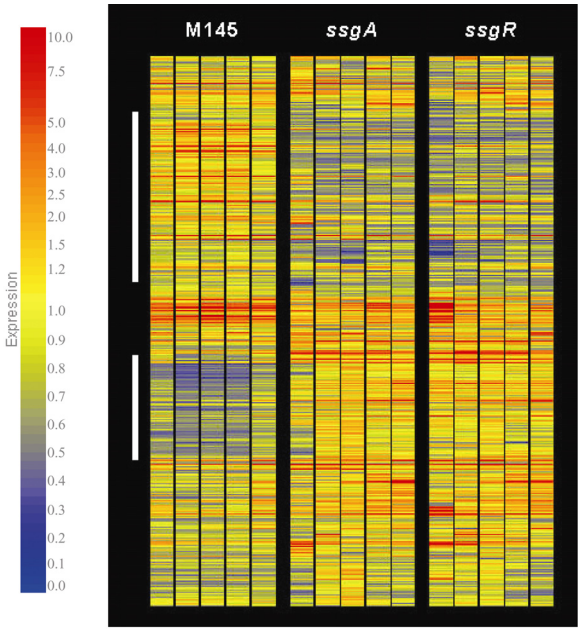

Figure 4, Chapter 4: Comparison of the global expression patterns of genes in *ssgA* and *ssgR* mutant. RNA from GSA3 (M145 Δ*ssgA*) and GSR1 (M145 Δ*ssgR*) was isolated from mycelium grown on MM agar, corresponding to vegetative growth (24h), aerial growth (36h, 48h) and sporulation (60h, 72h). Genes were clustered hierachically according to similarity in expression profile. The lanes represent the time points of RNA isolation for the parental strain M145 (left), the *ssgA* mutant (middle), and the *ssgR* mutant (right).

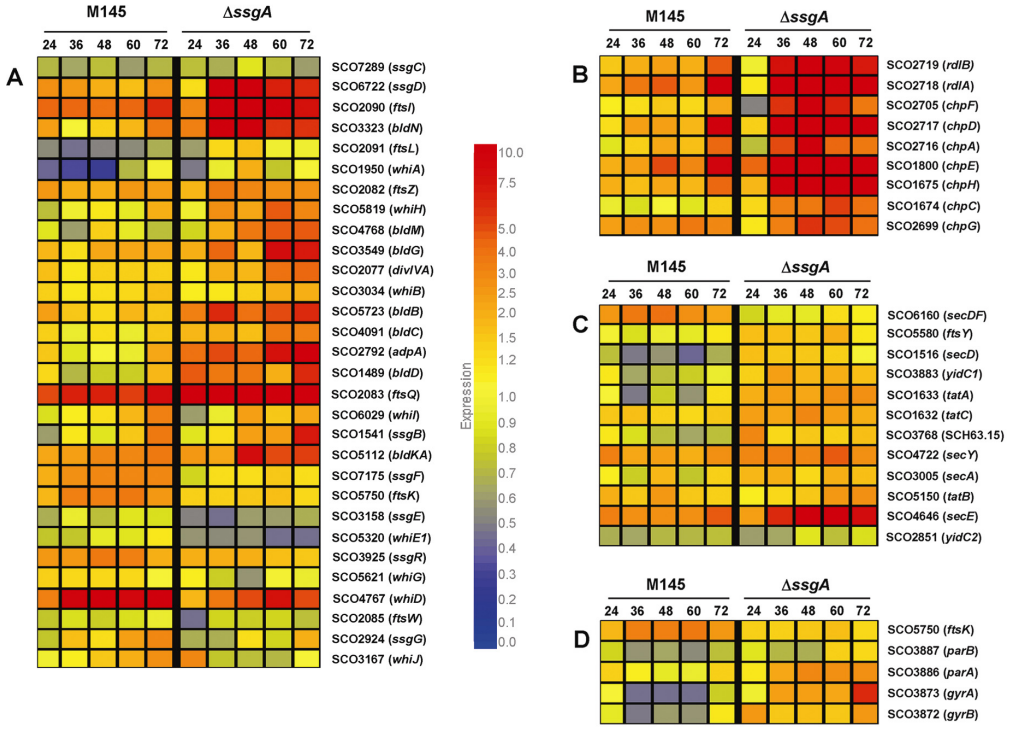

Figure 5, Chapter 4: Comparison of the expression profiles of several classes of genes between M145 and the *ssgA* mutant. RNA from M145 and GSA3 (M145 Δ*ssgA*) was isolated from mycelium grown on MM agar, corresponding to vegetative growth (24h), aerial growth (36h, 48h) and sporulation (60h, 72h). Expression profiles of genes are shown, involved in cell division and development (**A**), chaplins and rodlins (**B**), secretion (**C**) and DNA replication and segregation (**D**). Genes were clustered hierarchically according to similarity in expression profile. The lanes represent the time points of RNA isolation for the parental strain M145 (left) and the *ssgA* mutant (right).

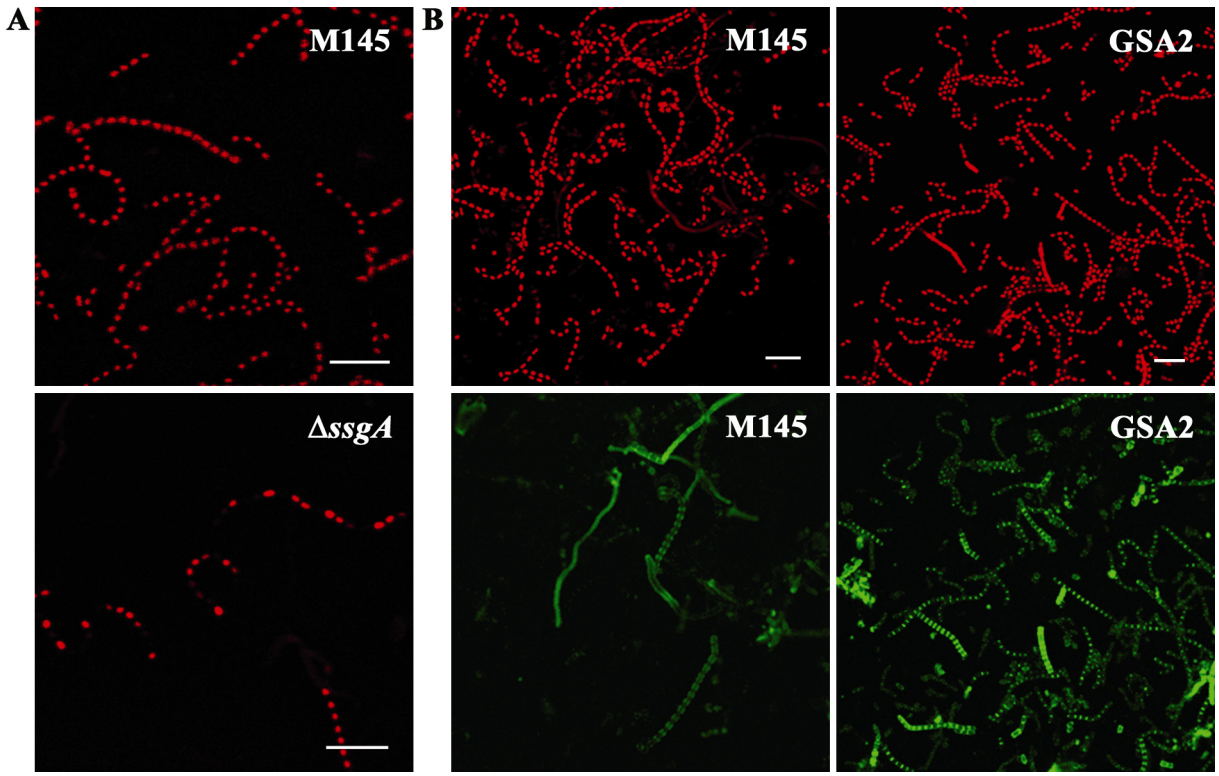

Figure 7, Chapter 4: Visualisation of DNA and peptidoglycan subunits by fluorescence microscopy. Cultures were grown on SFM for 5 days at 30 °C**. A.** DNA content of *S. coelicolor* and the *ssgA* mutant revealed by propidium iodide (PI). The *ssgA* mutant is disturbed in DNA segregation. **B.** *S. coelicolor* M145 and its SsgA-overexpressing derivative GSA2. Left column shows DNA visualised with PI; right column shows peptidoglycan subunits visualised with f-WGA. GSA2 shows strongly enhanced septation in young aerial hyphae. f-WGA-stained foci also were observed between spores in the mature spore chains, most likely indicative of autolysis. Bar = 5 μm.

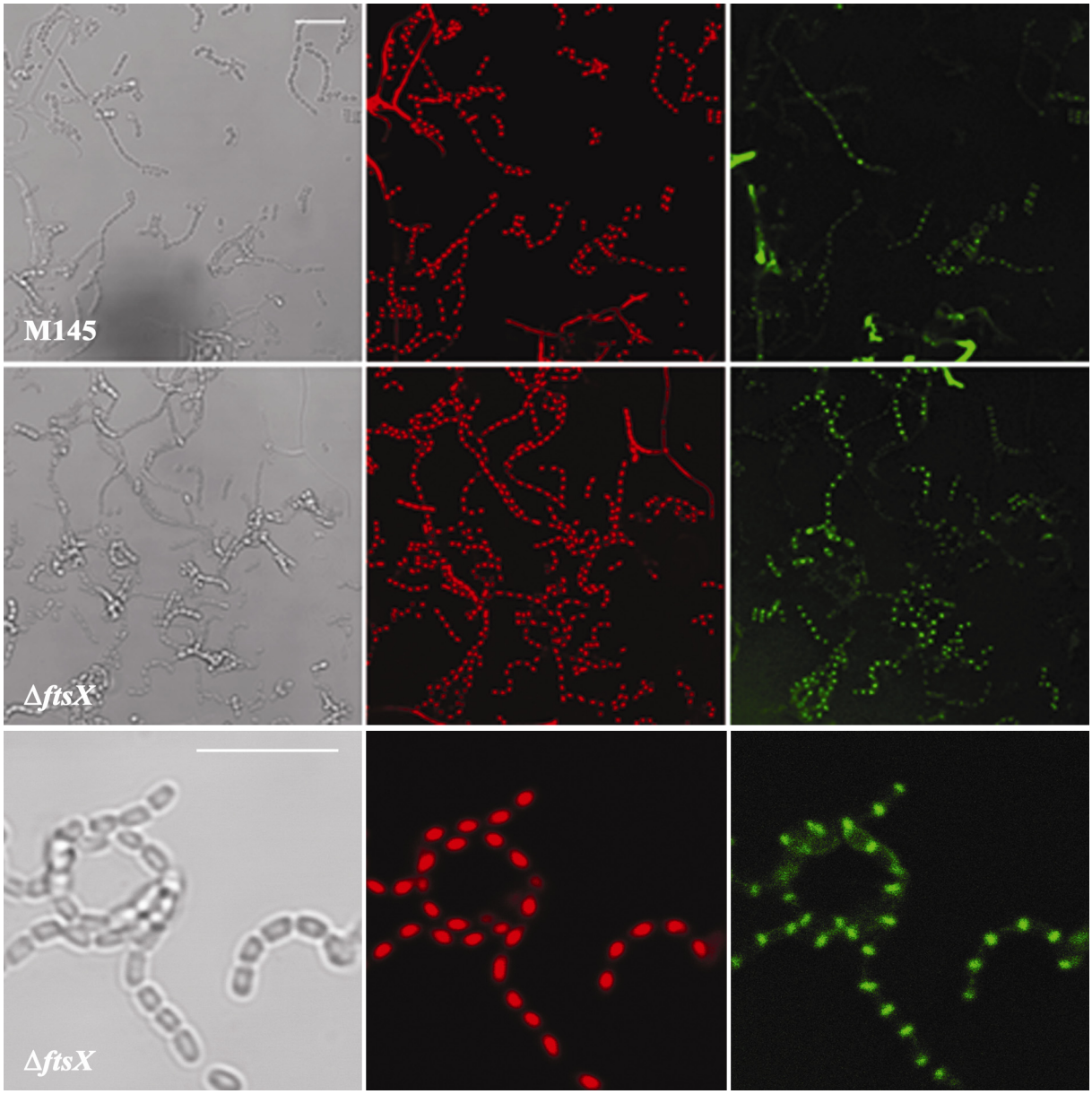

Figure 5, Chapter 6: Analysis of an *ftsX* mutant by confocal fluorescence microscopy. Samples were prepared from 5-day old surface-grown cultures at 30°C of the parental strain M145 and the *ftsX* mutant. DNA and peptidoglycan subunits were visualised with PI (middle column) and f-WGA (right column). The left column shows light microscopy images. Bar = 5 μm.

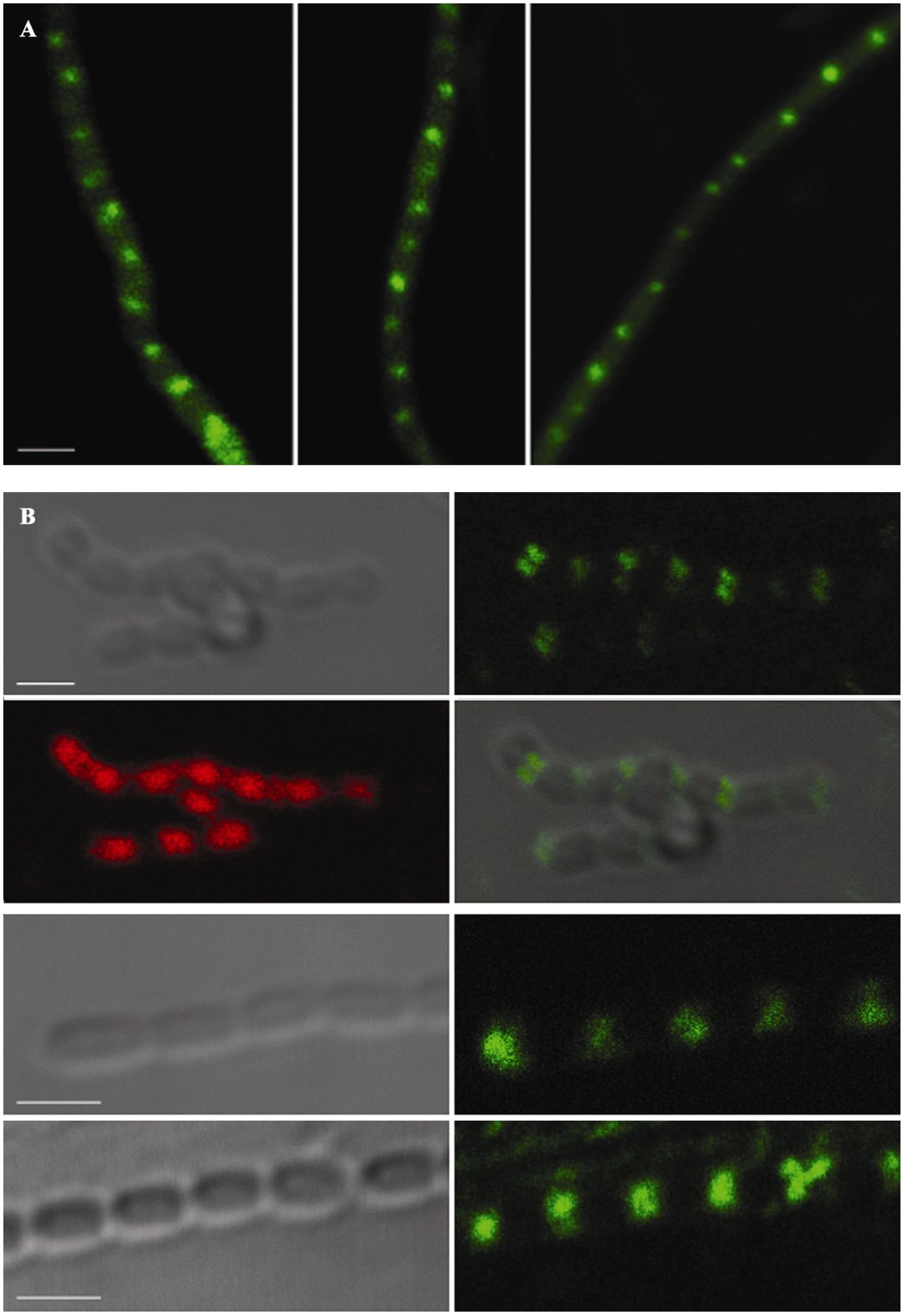

Figure 6, Chapter 6: A. FtsZ-rings in an *ftsX* mutant. Strains were grown on SFM for 2 days at 30°C. **B. Cellular localisation of FtsE using anti-FtsE antibodies.** Strains were grown on SFM for 5 days at 30°C. Propidium iodide was used to visualise DNA. The left column shows light microscopy images and the right column represents FtsE localisation (Row 1-3-4) or the left column shows DNA and the right column shows an overlay of the images of row 1 (Row 2). Bar = 1 μm.

REFERENCES

Addinall, S.G., Cao, C., and Lutkenhaus, J. (1997) FtsN, a late recruit to the septum in *Escherichia coli*. *Mol Microbiol* **25**: 303-309.

Ainsa, J.A., Parry, H.D., and Chater, K.F. (1999) A response regulator-like protein that functions at an intermediate stage of sporulation in *Streptomyces coelicolor* A3(2). *Mol Microbiol* **34**: 607-619.

Ainsa, J.A., Ryding, N.J., Hartley, N., Findlay, K.C., Bruton, C.J., and Chater, K.F. (2000) WhiA, a protein of unknown function conserved among gram-positive bacteria, is essential for sporulation in *Streptomyces coelicolor* A3(2). *J Bacteriol* **182**: 5470-5478.

Aretz W, Meiwes J, Seibert G, Vobis G, Wink J. (2000) Friulimicins: novel lipopeptide antibiotics with peptidoglycan synthesis inhibiting activity from Actinoplanes friuliensis sp. nov. I. Taxonomic studies of the producing microorganism and fermentation. *J Antibiot* (Tokyo) **53**:807-15.

Ausmees, N., Kuhn, J.R., and Jacobs-Wagner, C. (2003) The bacterial cytoskeleton: an intermediate filament-like function in cell shape. *Cell* **115**: 705-713.

Autret, S., and Errington, J. (2001) Dynamic proteins in bacteria. *Dev Cell* **1**: 10-11.

Barilla, D., Rosenberg, M.F., Nobbmann, U., and Hayes, F. (2005) Bacterial DNA segregation dynamics mediated by the polymerizing protein ParF. *Embo J* **24**: 1453-1464.

Bath, J., Wu, L.J., Errington, J., and Wang, J.C. (2000) Role of *Bacillus subtilis* SpoIIIE in DNA transport across the mother cell-prespore division septum. *Science* **290**: 995-997.

Bennett, J.A., and McCormick, J.R. (2001) Two new loci affecting cell division identified as suppressors of an *ftsQ*-null mutation in *Streptomyces coelicolor* A3(2). *FEMS Microbiol Lett* **202**: 251-256.

Bentley, S.D., Chater, K.F., Cerdeno-Tarraga, A.M., Challis, G.L., Thomson, N.R., James, K.D., Harris, D.E., Quail, M.A., Kieser, H., Harper, D., Bateman, A., Brown, S., Chandra, G., Chen, C.W., Collins, M., Cronin, A., Fraser, A., Goble, A., Hidalgo, J., Hornsby, T., Howarth, S., Huang, C.H., Kieser, T., Larke, L., Murphy, L., Oliver, K., O'Neil, S., Rabbinowitsch, E., Rajandream, M.A., Rutherford, K., Rutter, S., Seeger, K., Saunders, D., Sharp, S., Squares, R., Squares, S., Taylor, K., Warren, T., Wietzorrek, A., Woodward, J., Barrell, B.G., Parkhill, J., and Hopwood, D.A. (2002) Complete genome sequence of the model actinomycete *Streptomyces coelicolor* A3(2). *Nature* **417**: 141-147.

Bernhardt, T.G., and de Boer, P.A. (2003) The *Escherichia coli* amidase AmiC is a periplasmic septal ring component exported via the twin-arginine transport pathway. *Mol Microbiol* **48**: 1171-1182.

Bernhardt, T.G., and de Boer, P.A. (2004) Screening for synthetic lethal mutants in *Escherichia coli* and identification of EnvC (YibP) as a periplasmic septal ring factor with murein hydrolase activity. *Mol Microbiol* **52**: 1255-1269.

Bernhardt, T.G., and de Boer, P.A. (2005) SlmA, a nucleoid-associated, FtsZ binding protein required for blocking septal ring assembly over chromosomes in *E. coli*. *Mol Cell* **18**: 555-564.

Bibb, M. (1996) 1995 Colworth Prize Lecture. The regulation of antibiotic production in *Streptomyces coelicolor* A3(2). *Microbiology* **142**: 1335-1344.

Bibb, M.J., Molle, V., and Buttner, M.J. (2000) sigma(BldN), an extracytoplasmic function RNA polymerase sigma factor required for aerial mycelium formation in *Streptomyces coelicolor* A3(2). *J. Bacteriol.* **182**: 4606-4616.

Bierman, M., Logan, R., O'Brien, K., Seno, E.T., Rao, R.N., and Schoner, B.E. (1992) Plasmid cloning vectors for the conjugal transfer of DNA from *Escherichia coli* to *Streptomyces* spp. *Gene* **116**: 43-49.

Bignell, D.R., Warawa, J.L., Strap, J.L., Chater, K.F., and Leskiw, B.K. (2000) Study of the bldG locus suggests that an anti-anti-sigma factor and an anti-sigma factor may be involved in *Streptomyces coelicolor* antibiotic production and sporulation. *Microbiology* **146**: 2161-2173.

Bigot, S., Corre, J., Louarn, J.M., Cornet, F., and Barre, F.X. (2004) FtsK activities in Xer recombination, DNA mobilization and cell division involve overlapping and separate domains of the protein. *Mol Microbiol* **54**: 876-886.

Bishop, A., Fielding, S., Dyson, P., and Herron, P. (2004) Systematic insertional mutagenesis of a streptomycete genome: a link between osmoadaptation and antibiotic production. *Genome Res* **14**: 893-900.

Blondelet-Rouault, M.H., Weiser, J., Lebrihi, A., Branny, P., and Pernodet, J.L. (1997) Antibiotic resistance gene cassettes derived from the omega interposon for use in *E. coli* and *Streptomyces*. *Gene* **190**: 315-317.

Bolhuis, A., Broekhuizen, C.P., Sorokin, A., van Roosmalen, M.L., Venema, G., Bron, S., Quax, W.J., and van Dijl, J.M. (1998) SecDF of *Bacillus subtilis*, a molecular Siamese twin required for the efficient secretion of proteins. *J Biol Chem* **273**: 21217-21224.

Bork, P., Sander, C., and Valencia, A. (1992) An ATPase domain common to prokaryotic cell cycle proteins, sugar kinases, actin, and hsp70 heat shock proteins. *Proc Natl Acad Sci U S A* **89**: 7290-7294.

Botta, G.A., and Park, J.T. (1981) Evidence for involvement of penicillin-binding protein 3 in murein synthesis during septation but not during cell elongation. *J Bacteriol* **145**: 333-340.

Bramhill, D., and Thompson, C.M. (1994) GTP-dependent polymerization of *Escherichia coli* FtsZ protein to form tubules. *Proc Natl Acad Sci U S A* **91**: 5813-5817.

Bramhill, D. (1997) Bacterial cell division. *Annu Rev Cell Dev Biol* **13**: 395-424.

Braud, S., Lavire, C., Bellier, A., and Mazodier, P. (2006) Effect of SsrA (tmRNA) tagging system on translational regulation in *Streptomyces*. *Arch Microbiol* **184**: 343-352.

Bucca, G., Brassington, A.M., Hotchkiss, G., Mersinias, V., and Smith, C.P. (2003) Negative feedback regulation of *dnaK*, *clpB* and lon expression by the DnaK chaperone machine in *Streptomyces coelicolor*, identified by transcriptome and in vivo DnaK-depletion analysis. *Mol Microbiol* **50**: 153-166.

Buddelmeijer, N., and Beckwith, J. (2002) Assembly of cell division proteins at the *E. coli* cell center. *Curr Opin Microbiol* **5**: 553-557.

Buddelmeijer, N., and Beckwith, J. (2004) A complex of the *Escherichia coli* cell division proteins FtsL, FtsB and FtsQ forms independently of its localization to the septal region. *Mol Microbiol* **52**: 1315-1327.

Burger, A., Brandt, B., Susstrunk, U., Thompson, C.J., and Wohlleben, W. (1998) Analysis of a *Streptomyces coelicolor* A3(2) locus containing the nucleoside diphosphate kinase (*ndk*) and folylpolyglutamate synthetase (*folC*) genes. *FEMS Microbiol Lett* **159**: 283-291.

Burger, A., Sichler, K., Kelemen, G., Buttner, M., and Wohlleben, W. (2000) Identification and characterization of the *mre* gene region of *Streptomyces coelicolor* A3(2). *Mol Gen Genet* **263**: 1053-1060.

Bushell, M.E. (1988) Growth, product formation and fermentation technology. In *Actinomycetes in biotechnology*. London, UK: Academic press, pp. 185-217.

Cabeen, M.T., and Jacobs-Wagner, C. (2005) Bacterial cell shape. *Nat Rev Microbiol* **3**: 601-610.

Calcutt, M.J. (1994) Gene organization in the *dnaA-gyrA* region of the *Streptomyces coelicolor* chromosome. *Gene* **151**: 23-28.

Carballido-Lopez, R., Formstone, A., Li, Y., Ehrlich, S.D., Noirot, P., and Errington, J. (2006) Actin homolog MreBH governs cell morphogenesis by localization of the cell wall hydrolase LytE. *Dev Cell* **11**: 399-409.
Chater, K.F. (1972) A morphological and genetic mapping study of white colony mutants of *Streptomyces coelicolor*. *J Gen Microbiol* **72**: 9-28.
Chater, K.F., Bruton, C.J., Plaskitt, K.A., Buttner, M.J., Mendez, C., and Helmann, J.D. (1989) The developmental fate of S. coelicolor hyphae depends upon a gene product homologous with the motility sigma factor of B. subtilis. *Cell* **59**: 133-143.
Chater, K.F., and Losick, R. (1997) Mycelial life style of *Streptomyces coelicolor* A3(2) and its relatives. In *Bacteria as multicellular organisms*. Shapiro, J.A. and Dworkin, M. (eds). New York: Oxford University Press, pp. 149-182.
Chater, K.F. (1998) taking a genetic scalpel to the *Streptomyces* colony. *Microbiology* **144**: 1465-1478.
Chater, K.F. (2001) Regulation of sporulation in *Streptomyces coelicolor* A3(2): a checkpoint multiplex? *Curr Opin Microbiol* **4**: 667-673.
Chater, K.F., and Chandra, G. (2006) The evolution of development in *Streptomyces* analysed by genome comparisons. *FEMS Microbiol Rev* **30**: 651-672.
Claessen, D., Wosten, H.A., van Keulen, G., Faber, O.G., Alves, A.M., Meijer, W.G., and Dijkhuizen, L. (2002) Two novel homologous proteins of *Streptomyces coelicolor* and *Streptomyces lividans* are involved in the formation of the rodlet layer and mediate attachment to a hydrophobic surface. *Mol Microbiol* **44**: 1483-1492.
Claessen, D., Rink, R., de Jong, W., Siebring, J., de Vreugd, P., Boersma, F.G., Dijkhuizen, L., and Wosten, H.A. (2003) A novel class of secreted hydrophobic proteins is involved in aerial hyphae formation in *Streptomyces coelicolor* by forming amyloid-like fibrils. *Genes Dev* **17**: 1714-1726.
Claessen, D., Stokroos, I., Deelstra, H.J., Penninga, N.A., Bormann, C., Salas, J.A., Dijkhuizen, L., and Wosten, H.A. (2004) The formation of the rodlet layer of streptomycetes is the result of the interplay between rodlins and chaplins. *Mol Microbiol* **53**: 433-443.
Corbin, B.D., Geissler, B., Sadasivam, M., and Margolin, W. (2004) Z-ring-independent interaction between a subdomain of FtsA and late septation proteins as revealed by a polar recruitment assay. *J Bacteriol* **186**: 7736-7744.
Covarrubias, L., Cervantes, L., Covarrubias, A., Soberon, X., Vichido, I., Blanco, A., Kupersztoch-Portnoy, Y.M., and Bolivar, F. (1981) Construction and characterization of new cloning vehicles. V. Mobilization and coding properties of pBR322 and several deletion derivatives including pBR327 and pBR328. *Gene* **13**: 25-35.
Dalton, K., Thibessard, A., Hunter, J.I.B., and Kelemen, G.H. (2007) A novel compartment, the "sub-apical stem" of the aerial hyphae, is the location of a SigN dependent, developmentally distinct transcription in *Streptomyces coelicolor*. *Mol Microbiol* **In press**.
Daniel, R.A., Drake, S., Buchanan, C.E., Scholle, R., and Errington, J. (1994) The *Bacillus subtilis spoVD* gene encodes a mother-cell-specific penicillin-binding protein required for spore morphogenesis. *J Mol Biol* **235**: 209-220.
Daniel, R.A., and Errington, J. (2003) Control of cell morphogenesis in bacteria: two distinct ways to make a rod-shaped cell. *Cell* **113**: 767-776.
Daniel, R.A., Noirot-Gros, M.F., Noirot, P., and Errington, J. (2006) Multiple interactions between the transmembrane division proteins of *Bacillus subtilis* and the role of FtsL instability in divisome assembly. *J Bacteriol* **188**: 7396-7404.
Datsenko, K.A., and Wanner, B.L. (2000) One-step inactivation of chromosomal genes in *Escherichia coli* K-12 using PCR products. *Proc Natl Acad Sci U S A* **97**: 6640-6645.
Davis, N.K., and Chater, K.F. (1992) The *Streptomyces coelicolor* whiB gene encodes a small transcription factor-like protein dispensable for growth but essential for sporulation. *Mol Gen Genet* **232**: 351-358.
de Leeuw, E., Graham, B., Phillips, G.J., ten Hagen-Jongman, C.M., Oudega, B., and Luirink, J. (1999) Molecular characterization of *Escherichia coli* FtsE and FtsX. *Mol Microbiol* **31**: 983-993.
Den Blaauwen, T., Aarsman, M.E., Vischer, N.O., and Nanninga, N. (2003) Penicillin-binding protein PBP2 of *Escherichia coli* localizes preferentially in the lateral wall and at mid-cell in comparison with the old cell pole. *Mol Microbiol* **47**: 539-547.
Derouaux, A., Halici, S., Nothaft, H., Neutelings, T., Moutzourelis, G., Dusart, J., Titgemeyer, F., and Rigali, S. (2004) Deletion of a cyclic AMP receptor protein homologue diminishes germination and affects morphological development of *Streptomyces coelicolor*. *J Bacteriol* **186**: 1893-1897.
Du, Y., and Arvidson, C.G. (2003) Identification of ZipA, a Signal Recognition Particle-Dependent Protein from *Neisseria gonorrhoeae*. *J Bacteriol* **185**: 2122-2130.
Dye, N.A., Pincus, Z., Theriot, J.A., Shapiro, L., and Gitai, Z. (2005) Two independent spiral structures control cell shape in *Caulobacter*. *Proc Natl Acad Sci U S A* **102**: 18608-18613.
Eccleston, M., Ali, R.A., Seyler, R., Westpheling, J., and Nodwell, J. (2002) Structural and genetic analysis of the BldB protein of *Streptomyces coelicolor*. *J Bacteriol* **184**: 4270-4276.
Edwards, D.H., and Errington, J. (1997) The *Bacillus subtilis* DivIVA protein targets to the division septum and controls the site specificity of cell division. *Mol Microbiol* **24**: 905-915.
Elliot, M., Damji, F., Passantino, R., Chater, K., and Leskiw, B. (1998) The *bldD* gene of *Streptomyces coelicolor* A3(2): a regulatory gene involved in morphogenesis and antibiotic production. *J Bacteriol* **180**: 1549-1555.
Elliot, M.A., and Leskiw, B.K. (1999) The BldD protein from *Streptomyces coelicolor* is a DNA-binding protein. *J. Bacteriol.* **181**: 6832-6835.
Elliot, M.A., Bibb, M.J., Buttner, M.J., and Leskiw, B.K. (2001) BldD is a direct regulator of key developmental genes in *Streptomyces coelicolor* A3(2). *Mol. Microbiol.* **40**: 257-269.
Elliot, M.A., Karoonuthaisiri, N., Huang, J., Bibb, M.J., Cohen, S.N., Kao, C.M., and Buttner, M.J. (2003) The chaplins: a family of hydrophobic cell-surface proteins involved in aerial mycelium formation in *Streptomyces coelicolor*. *Genes Dev* **17**: 1727-1740.
Ensign, J.C. (1978) Formation, properties, and germination of actinomycete spores. *Annu Rev Microbiol* **32**: 185-219.
Erickson, H.P., Taylor, D.W., Taylor, K.A., and Bramhill, D. (1996) Bacterial cell division protein FtsZ assembles into protofilament sheets and minirings, structural homologs of tubulin polymers. *Proc Natl Acad Sci U S A* **93**: 519-523.
Errington, J. (2001) Septation and chromosome segregation during sporulation in *Bacillus subtilis*. *Curr Opin Microbiol* **4**: 660-666.
Errington, J., Bath, J., and Wu, L.J. (2001) DNA transport in bacteria. *Nature Rev. Mol. Cell Biol.* **2**: 538-544.
Errington, J. (2003) Regulation of endospore formation in *Bacillus subtilis*. *Nat Rev Microbiol* **1**: 117-126.
Errington, J., Daniel, R.A., and Scheffers, D.J. (2003) Cytokinesis in bacteria. *Microbiol Mol Biol Rev* **67**: 52-65.
Fernandez-Moreno, M.A., Caballero, J.L., Hopwood, D.A., and Malpartida, F. (1991) The act cluster contains regulatory and antibiotic export genes, direct targets for translational control by the *bldA* tRNA gene of *Streptomyces*. *Cell* **66**: 769-780.
Figge, R.M., Divakaruni, A.V., and Gober, J.W. (2004) MreB, the cell shape-determining bacterial actin homologue, co-ordinates cell wall morphogenesis in *Caulobacter crescentus*. *Mol Microbiol* **51**: 1321-1332.
Flärdh, K., Findlay, K.C., and Chater, K.F. (1999) Association of early sporulation genes with suggested developmental decision points in *Streptomyces coelicolor* A3(2). *Microbiology* **145**: 2229-2243.

Flärdh, K., Leibovitz, E., Buttner, M.J., and Chater, K.F. (2000) Generation of a non-sporulating strain of *Streptomyces coelicolor* A3(2) by the manipulation of a developmentally controlled *ftsZ* promoter. *Mol. Microbiol.. Nov* **38**: 737-749.
Flärdh, K. (2003a) Growth polarity and cell division in *Streptomyces*. *Curr Opin Microbiol* **6**: 564-571.
Flärdh, K. (2003b) Essential role of DivIVA in polar growth and morphogenesis in *Streptomyces coelicolor* A3(2). *Mol Microbiol* **49**: 1523-1536.
Flärdh, K., and van Wezel, G.P. (2003) Cell division during growth and development of *Streptomyces*. In *Recent developments in bacteriology*. Pandalai, S.G. (ed). Trivandrum, India: Transworld research network.
Formstone, A., and Errington, J. (2005) A magnesium-dependent mreB null mutant: implications for the role of mreB in *Bacillus subtilis*. *Mol Microbiol* **55**: 1646-1657.
Fu, X., Shih, Y.L., Zhang, Y., and Rothfield, L.I. (2001) The MinE ring required for proper placement of the division site is a mobile structure that changes its cellular location during the *Escherichia coli* division cycle. *Proc Natl Acad Sci U S A* **98**: 980-985.
Gill, D.R., and Salmond, G.P. (1990) The identification of the *Escherichia coli ftsY* gene product: an unusual protein. *Mol Microbiol* **4**: 575-583.
Gitai, Z., Dye, N., and Shapiro, L. (2004) An actin-like gene can determine cell polarity in bacteria. *Proc Natl Acad Sci U S A* **101**: 8643-8648.
Gitai, Z., Dye, N.A., Reisenauer, A., Wachi, M., and Shapiro, L. (2005) MreB actin-mediated segregation of a specific region of a bacterial chromosome. *Cell* **120**: 329-341.
Glauert, A.M., and Hopwood, D.A. (1961) The fine structure of *Streptomyces violaceoruber* (*S. coelicolor*). III. The walls of the mycelium and spores. *J Biophys Biochem Cytol* **10**: 505-516.
Goehring, N.W., Gueiros-Filho, F., and Beckwith, J. (2005) Premature targeting of a cell division protein to midcell allows dissection of divisome assembly in *Escherichia coli*. *Genes Dev* **19**: 127-137.
Goehring, N.W., Gonzalez, M.D., and Beckwith, J. (2006) Premature targeting of cell division proteins to midcell reveals hierarchies of protein interactions involved in divisome assembly. *Mol Microbiol* **61**: 33-45.
Goodell, E.W. (1985) Recycling of murein by *Escherichia coli*. *J Bacteriol* **163**: 305-310.
Grantcharova, N., Ubhayasekera, W., Mowbray, S.L., McCormick, J.R., and Flärdh, K. (2003) A missense mutation in *ftsZ* differentially affects vegetative and developmentally controlled cell division in *Streptomyces coelicolor* A3(2). *Mol Microbiol* **47**: 645-656.
Grantcharova, N., Lustig, U., and Flardh, K. (2005) Dynamics of FtsZ assembly during sporulation in *Streptomyces coelicolor* A3(2). *J Bacteriol* **187**: 3227-3237.
Gray, D.I., Gooday, G.W., and Prosser, J.I. (1990) Apical hyphal extension in *Streptomyces coelicolor* A3(2). *J Gen Microbiol* **136**: 1077-1084.
Grossman, A.D. (1995) Genetic networks controlling the initiation of sporulation and the development of genetic competence in *Bacillus subtilis*. *Annu Rev Genet* **29**: 477-508.
Gueiros-Filho, F.J., and Losick, R. (2002) A widely conserved bacterial cell division protein that promotes assembly of the tubulin-like protein FtsZ. *Genes Dev* **16**: 2544-2556.
Gust, B., Challis, G.L., Fowler, K., Kieser, T., and Chater, K.F. (2003) PCR-targeted *Streptomyces* gene replacement identifies a protein domain needed for biosynthesis of the sesquiterpene soil odor geosmin. *Proc Natl Acad Sci U S A* **100**: 1541-1546.
Harris, S.D., Hofmann, A.F., Tedford, H.W., and Lee, M.P. (1999) Identification and characterization of genes required for hyphal morphogenesis in the filamentous fungus *Aspergillus nidulans*. *Genetics* **151**: 1015-1025.
Henriques, A.O., Glaser, P., Piggot, P.J., and Moran, C.P., Jr. (1998) Control of cell shape and elongation by the *rodA* gene in *Bacillus subtilis*. *Mol Microbiol* **28**: 235-247.
Higgins, C.F. (1992) ABC transporters: from microorganisms to man. *Annu Rev Cell Biol* **8**: 67-113.
Higgins, D.G., Thompson, J.D., and Gibson, T.J. (1996) Using CLUSTAL for multiple sequence alignments. *Methods Enzymol* **266**: 383-402.
Holtje, J.V. (1998) Growth of the stress-bearing and shape-maintaining murein sacculus of *Escherichia coli*. *Microbiol Mol Biol Rev* **62**: 181-203.
Hu, Z., and Lutkenhaus, J. (1999) Topological regulation of cell division in *Escherichia coli* involves rapid pole to pole oscillation of the division inhibitor MinC under the control of MinD and MinE. *Mol Microbiol* **34**: 82-90.
Hunt, A.C., Servin-Gonzalez, L., Kelemen, G.H., and Buttner, M.J. (2005) The *bldC* developmental locus of *Streptomyces coelicolor* encodes a member of a family of small DNA-binding proteins related to the DNA-binding domains of the MerR family. *J Bacteriol* **187**: 716-728.
Ikeda, H., Ishikawa, J., Hanamoto, A., Shinose, M., Kikuchi, H., Shiba, T., Sakaki, Y., Hattori, M., and Omura, S. (2003) Complete genome sequence and comparative analysis of the industrial microorganism *Streptomyces avermitilis*. *Nat Biotechnol* **14**: 14.
Jakimowicz, D., Chater, K., and Zakrzewska-Czerwinska, J. (2002) The ParB protein of *Streptomyces coelicolor* A3(2) recognizes a cluster of *parS* sequences within the origin-proximal region of the linear chromosome. *Mol Microbiol* **45**: 1365-1377.
Jakimowicz, D., Gust, B., Zakrzewska-Czerwinska, J., and Chater, K.F. (2005) Developmental-stage-specific assembly of ParB complexes in *Streptomyces coelicolor* hyphae. *J Bacteriol* **187**: 3572-3580.
Jakimowicz, D., Mouz, S., Zakrzewska-Czerwinska, J., and Chater, K.F. (2006) Developmental control of a *parAB* promoter leads to formation of sporulation-associated ParB complexes in *Streptomyces coelicolor*. *J Bacteriol* **188**: 1710-1720.
Janssen, G.R., and Bibb, M.J. (1993) Derivatives of pUC18 that have *Bgl*II sites flanking a modified multiple cloning site and that retain the ability to identify recombinant clones by visual screening of *Escherichia coli* colonies. *Gene* **124**: 133-134.
Jiang, H., and Kendrick, K.E. (2000) Characterization of *ssfR* and *ssgA*, two genes involved in sporulation of *Streptomyces griseus*. *J. Bacteriol.* **182**: 5521-5529.
Jones, L.J., Carballido-Lopez, R., and Errington, J. (2001) Control of cell shape in bacteria: helical, actin-like filaments in *Bacillus subtilis*. *Cell* **104**: 913-922.
Justice, S.S., Garcia-Lara, J., and Rothfield, L.I. (2000) Cell division inhibitors SulA and MinC/MinD block septum formation at different steps in the assembly of the *Escherichia coli* division machinery. *Mol Microbiol* **37**: 410-423.
Kato, J.Y., Suzuki, A., Yamazaki, H., Ohnishi, Y., and Horinouchi, S. (2002) Control by A-factor of a metalloendopeptidase gene involved in aerial mycelium formation in *Streptomyces griseus*. *J Bacteriol* **184**: 6016-6025.
Kawamoto, S., and Ensign, J.C. (1995) Cloning and characterization of a gene involved in regulation of sporulation and cell division in Streptomyces griseus. *Actinomycetologica* **9**: 136-151.
Kawamoto, S., Watanabe, H., Hesketh, A., Ensign, J.C., and Ochi, K. (1997) Expression analysis of the *ssgA* gene product, associated with sporulation and cell division in *Streptomyces griseus*. *Microbiology* **143**: 1077-1086.

Keijser, B.J., van Wezel, G.P., Canters, G.W., and Vijgenboom, E. (2002) Developmental regulation of the *Streptomyces lividans ram* genes: involvement of RamR in regulation of the *ramCSAB* operon. *J Bacteriol* **184**: 4420-4429.
Keijser, B.J., Noens, E.E., Kraal, B., Koerten, H.K., and van Wezel, G.P. (2003) The *Streptomyces coelicolor ssgB* gene is required for early stages of sporulation. *FEMS Microbiol Lett* **225**: 59-67.
Kelemen, G.H., Brown, G.L., Kormanec, J., Potuckova, L., Chater, K.F., and Buttner, M.J. (1996) The positions of the sigma-factor genes, *whiG* and *sigF*, in the hierarchy controlling the development of spore chains in the aerial hyphae of *Streptomyces coelicolor* A3(2). *Mol Microbiol* **21**: 593-603.
Kelemen, G.H., Brian, P., Flärdh, K., Chamberlin, L., Chater, K.F., and Buttner, M.J. (1998) Developmental regulation of transcription of *whiE*, a locus specifying the polyketide spore pigment in *Streptomyces coelicolor* A3 (2). *J Bacteriol* **180**: 2515-2521.
Kelemen, G.H., Viollier, P.H., Tenor, J., Marri, L., Buttner, M.J., and Thompson, C.J. (2001) A connection between stress and development in the multicellular prokaryote *Streptomyces coelicolor* A3(2). *Mol Microbiol* **40**: 804-814.
Kieser, T., Bibb, M.J., Buttner, M.J., Chater, K.F., and Hopwood, D.A. (2000) *Practical Streptomyces genetics.* Norwich, U.K.: John Innes Foundation.
Kim, H.J., Calcutt, M.J., Schmidt, F.J., and Chater, K.F. (2000) Partitioning of the linear chromosome during sporulation of *Streptomyces coelicolor* A3(2) involves an *oriC*-linked *parAB* locus. *J Bacteriol* **182**: 1313-1320.
Koonin, E.V. (1993) A superfamily of ATPases with diverse functions containing either classical or deviant ATP-binding motif. *J Mol Biol* **229**: 1165-1174.
Kormanec, J., and Sevcikova, B. (2002) The stress-response sigma factor sigma(H) controls the expression of *ssgB*, a homologue of the sporulation-specific cell division gene *ssgA*, in *Streptomyces coelicolor* A3(2). *Mol Genet Genomics* **267**: 536-543.
Kruse, T., Moller-Jensen, J., Lobner-Olesen, A., and Gerdes, K. (2003) Dysfunctional MreB inhibits chromosome segregation in *Escherichia coli*. *Embo J* **22**: 5283-5292.
Kruse, T., Bork-Jensen, J., and Gerdes, K. (2005) The morphogenetic MreBCD proteins of *Escherichia coli* form an essential membrane-bound complex. *Mol Microbiol* **55**: 78-89.
Kruse, T., and Gerdes, K. (2005) Bacterial DNA segregation by the actin-like MreB protein. *Trends Cell Biol* **15**: 343-345.
Kwak, J., Dharmatilake, A.J., Jiang, H., and Kendrick, K.E. (2001) Differential regulation of *ftsZ* transcription during septation of *Streptomyces griseus*. *J Bacteriol* **183**: 5092-5101.
Larson, J.L., and Hershberger, C.L. (1986) The minimal replicon of a streptomycete plasmid produces an ultrahigh level of plasmid DNA. *Plasmid* **15**: 199-209.
Lawlor, E.J., Baylis, H.A., and Chater, K.F. (1987) Pleiotropic morphological and antibiotic deficiencies result from mutations in a gene encoding a tRNA-like product in *Streptomyces coelicolor* A3(2). *Genes Dev* **1**: 1305-1310.
Leaver, M., and Errington, J. (2005) Roles for MreC and MreD proteins in helical growth of the cylindrical cell wall in *Bacillus subtilis*. *Mol Microbiol* **57**: 1196-1209.
Lee, J.C., and Stewart, G.C. (2003) Essential nature of the mreC determinant of *Bacillus subtilis*. *J Bacteriol* **185**: 4490-4498.
Lee, K., and Cohen, S.N. (2003) A *Streptomyces coelicolor* functional orthologue of *Escherichia coli* RNase E shows shuffling of catalytic and PNPase-binding domains. *Mol Microbiol* **48**: 349-360.
Leskiw, B.K., Bibb, M.J., and Chater, K.F. (1991a) The use of a rare codon specifically during development? *Mol Microbiol* **5**: 2861-2867.
Leskiw, B.K., Lawlor, E.J., Fernandez-Abalos, J.M., and Chater, K.F. (1991b) TTA codons in some genes prevent their expression in a class of developmental, antibiotic-negative, *Streptomyces* mutants. *Proc Natl Acad Sci U S A* **88**: 2461-2465.
Leskiw, B.K., and Mah, R. (1995) The bldA-encoded tRNA is poorly expressed in the *bldI* mutant of *Streptomyces coelicolor* A3(2). *Microbiology* **141 (Pt 8)**: 1921-1926.
Levin, P.A., Kurtser, I.G., and Grossman, A.D. (1999) Identification and characterization of a negative regulator of FtsZ ring formation in *Bacillus subtilis*. *Proc Natl Acad Sci U S A* **96**: 9642-9647.
Liu, G., Draper, G.C., and Donachie, W.D. (1998) FtsK is a bifunctional protein involved in cell division and chromosome localization in *Escherichia coli*. *Mol Microbiol* **29**: 893-903.
Locci, R. (1980) Response of developing branched bacteria to adverse environments. II. Micromorphological effects of lysozyme on some aerobic actinomycetes. *Zentralbl Bakteriol A* **247**: 374-382.
Locher, K.P. (2004) Structure and mechanism of ABC transporters. *Curr Opin Struct Biol* **14**: 426-431.
Longtine, M.S., DeMarini, D.J., Valencik, M.L., Al-Awar, O.S., Fares, H., De Virgilio, C., and Pringle, J.R. (1996) The septins: roles in cytokinesis and other processes. *Curr Opin Cell Biol* **8**: 106-119.
Lowe, J., van den Ent, F., and Amos, L.A. (2004) Molecules of the bacterial cytoskeleton. *Annu Rev Biophys Biomol Struct* **33**: 177-198.
MacNeil, D.J., Gewain, K.M., Ruby, C.L., Dezeny, G., Gibbons, P.H., and MacNeil, T. (1992) Analysis of *Streptomyces avermitilis* genes required for avermectin biosynthesis utilizing a novel integration vector. *Gene* **111**: 61-68.
Margolin, W. (2005) FtsZ and the division of prokaryotic cells and organelles. *Nat Rev Mol Cell Biol* **6**: 862-871.
Marston, A.L., Thomaides, H.B., Edwards, D.H., Sharpe, M.E., and Errington, J. (1998) Polar localization of the MinD protein of *Bacillus subtilis* and its role in selection of the mid-cell division site. *Genes Dev* **12**: 3419-3430.
Matsuhashi, M., Wachi, M., and Ishino, F. (1990) Machinery for cell growth and division: penicillin-binding proteins and other proteins. *Res Microbiol* **141**: 89-103.
Mazza, P., Noens, E.E., Schirner, K., Grantcharova, N., Mommaas, A.M., Koerten, H.K., Muth, G., Flardh, K., van Wezel, G.P., and Wohlleben, W. (2006) MreB of *Streptomyces coelicolor* is not essential for vegetative growth but is required for the integrity of aerial hyphae and spores. *Mol Microbiol* **60**: 838-852.
McCormick, J.R., Su, E.P., Driks, A., and Losick, R. (1994) Growth and viability of *Streptomyces coelicolor* mutant for the cell division gene *ftsZ*. *Mol Microbiol* **14**: 243-254.
McCormick, J.R., and Losick, R. (1996) Cell division gene *ftsQ* is required for efficient sporulation but not growth and viability in *Streptomyces coelicolor* A3(2). *J Bacteriol* **178**: 5295-5301.
Mendez, C., Brana, A.F., Manzanal, M.B., and Hardisson, C. (1985) Role of substrate mycelium in colony development in *Streptomyces*. *Can J Microbiol* **31**: 446-450.
Merrick, M.J. (1976) A morphological and genetic mapping study of bald colony mutants of *Streptomyces coelicolor*. *J Gen Microbiol* **96**: 299-315.
Michie, K.A., and Lowe, J. (2006) Dynamic filaments of the bacterial cytoskeleton. *Annu Rev Biochem* **75**: 467-492.
Molle, V., and Buttner, M.J. (2000) Different alleles of the response regulator gene *bldM* arrest *Streptomyces coelicolor* development at distinct stages. *Mol Microbiol* **36**: 1265-1278.
Molle, V., Palframan, W.J., Findlay, K.C., and Buttner, M.J. (2000) WhiD and WhiB, homologous proteins required for different stages of sporulation in *Streptomyces coelicolor* A3(2). *J. Bacteriol.. Mar* **182**: 1286-1295.

Nguyen, K.T., Tenor, J., Stettler, H., Nguyen, L.T., Nguyen, L.D., and Thompson, C.J. (2003) Colonial differentiation in *Streptomyces coelicolor* depends on translation of a specific codon within the *adpA* gene. *J Bacteriol* **185**: 7291-7296.
Nodwell, J.R., Mcgovern, K., and Losick, R. (1996) an oligopeptide permease responsible for the import of an extracellular signal governing aerial mycelium formation in *Streptomyces coelicolor*. *Mol. Microbiol.* **22**: 881-893.
Nodwell, J.R., and Losick, R. (1998) Purification of an extracellular signaling molecule involved in production of aerial mycelium by *Streptomyces coelicolor*. *J Bacteriol* **180**: 1334-1337.
Nodwell, J.R., Yang, M., Kuo, D., and Losick, R. (1999) Extracellular complementation and the identification of additional genes involved in aerial mycelium formation in *Streptomyces coelicolor*. *Genetics* **151**: 569-584.
Noens, E.E., Mersinias, V., Traag, B.A., Smith, C.P., Koerten, H.K., and van Wezel, G.P. (2005) SsgA-like proteins determine the fate of peptidoglycan during sporulation of *Streptomyces coelicolor*. *Mol Microbiol* **58**: 929-944.
Noens, E.E., Mersinias, V., Willemse, J., Traag, B.A., Laing, E., Chater, K.F., Smith, C.P., Koerten, H.K., and van Wezel, G.P. (2007) Loss of the controlled localisation of growth stage-specific cell wall synthesis pleiotropically affects developmental gene expression in an ssgA mutant of *Streptomyces coelicolor*. *Mol Microbiol.* **64**:1244-59.
Nothaft, H., Dresel, D., Willimek, A., Mahr, K., Niederweis, M., and Titgemeyer, F. (2003) The phosphotransferase system of *Streptomyces coelicolor* is biased for N-acetylglucosamine metabolism. *J Bacteriol* **185**: 7019-7023.
Ohnishi, Y., and Horinouchi, S. (1999) Regulation of secondary metabolism and morphological differentiation by a microbial hormone in *Streptomyces*. *Tanpakushitsu Kakusan Koso* **44**: 1552-1561.
Ohnishi, Y., Seo, J.W., and Horinouchi, S. (2002) Deprogrammed sporulation in *Streptomyces*. *FEMS Microbiol Lett* **216**: 1-7.
Park, J.T. (1993) Turnover and recycling of the murein sacculus in oligopeptide permease-negative strains of *Escherichia coli*: indirect evidence for an alternative permease system and for a monolayered sacculus. *J Bacteriol* **175**: 7-11.
Pichoff, S., and Lutkenhaus, J. (2002) Unique and overlapping roles for ZipA and FtsA in septal ring assembly in *Escherichia coli*. *Embo J* **21**: 685-693.
Piette, A., Derouaux, A., Gerkens, P., Noens, E.E., Mazzucchelli, G., Vion, S., Koerten, H.K., Titgemeyer, F., De Pauw, E., Leprince, P., van Wezel, G.P., Galleni, M., and Rigali, S. (2005) From dormant to germinating spores of *Streptomyces coelicolor* A3(2): new perspectives from the *crp* null mutant. *J Proteome Res* **4**: 1699-1708.
Pope, M.K., Green, B.D., and Westpheling, J. (1996) The bld mutants of *Streptomyces coelicolor* are defective in the regulation of carbon utilization, morphogenesis and cell--cell signalling. *Mol Microbiol* **19**: 747-756.
Pope, M.K., Green, B., and Westpheling, J.R.W., IV (1998) the *bldb* gene encodes a small protein required for morphogenesis, antibiotic production, and catabolite control in *Streptomyces coelicolor*. *J. Bacteriol.* **180**: 1556-1562.
Potuckova, L., Kelemen, G.H., Findlay, K.C., Lonetto, M.A., Buttner, M.J., and Kormanec, J. (1995) A new RNA polymerase sigma factor, sigma F, is required for the late stages of morphological differentiation in *Streptomyces* spp. *Mol Microbiol* **17**: 37-48.
Prentki, P., and Krisch, H.M. (1984) In vitro insertional mutagenesis with a selectable DNA fragment. *Gene* **29**: 303-313.
Prosser, J.I., and Tough, A.J. (1991) Growth mechanisms and growth kinetics of filamentous microorganisms. *Crit Rev Biotechnol* **10**: 253-274.
Redenbach, M., Kieser, H.M., Denapaite, D., Eichner, A., Cullum, J., Kinashi, H., and Hopwood, D.A. (1996) a set of ordered cosmids and a detailed genetic and physical map for the 8 mb *Streptomyces coelicolor* a3(2) chromosome. *Mol. Microbiol.* **21**: 77-96.
Rigali, S., Schlicht, M., Hoskisson, P., Nothaft, H., Merzbacher, M., Joris, B., and Titgemeyer, F. (2004) Extending the classification of bacterial transcription factors beyond the helix-turn-helix motif as an alternative approach to discover new cis/trans relationships. *Nucleic Acids Res* **32**: 3418-3426.
Rigali, S., Nothaft, H., Noens, E.E., Schlicht, M., Colson, S., Muller, M., Joris, B., Koerten, H.K., Hopwood, D.A., Titgemeyer, F., and van Wezel, G.P. (2006) The sugar phosphotransferase system of *Streptomyces coelicolor* is regulated by the GntR-family regulator DasR and links N-acetylglucosamine metabolism to the control of development. *Mol Microbiol* **61**: 1237-1251.
Rothfield, L., Taghbalout, A., and Shih, Y.L. (2005) Spatial control of bacterial division-site placement. *Nat Rev Microbiol* **3**: 959-968.
Ryding, N.J., Kelemen, G.H., Whatling, C.A., Flärdh, K., Buttner, M.J., and Chater, K.F. (1998) A developmentally regulated gene encoding a repressor-like protein is essential for sporulation in *Streptomyces coelicolor* A3(2). *Mol Microbiol* **29**: 343-357.
Ryding, N.J., Bibb, M.J., Molle, V., Findlay, K.C., Chater, K.F., and Buttner, M.J. (1999) New sporulation loci in *Streptomyces coelicolor* A3(2). *J. Bacteriol.* **181**: 5419-5425.
Sambrook, J., Fritsch, E.F., and Maniatis, T. (1989) *Molecular cloning: a laboratory manual.* Cold Spring harbor, N.Y.: Cold Spring Harbor laboratory press.
Sanchez, M., Valencia, A., Ferrandiz, M.J., Sander, C., and Vicente, M. (1994) Correlation between the structure and biochemical activities of FtsA, an essential cell division protein of the actin family. *Embo J* **13**: 4919-4925.
Saraste, M., Sibbald, P.R., and Wittinghofer, A. (1990) The P-loop--a common motif in ATP- and GTP-binding proteins. *Trends Biochem Sci* **15**: 430-434.
Schlosser, A., Kampers, T., and Schrempf, H. (1997) The *Streptomyces* ATP-binding component MsiK assists in cellobiose and maltose transport. *J Bacteriol* **179**: 2092-2095.
Schmidt, K.L., Peterson, N.D., Kustusch, R.J., Wissel, M.C., Graham, B., Phillips, G.J., and Weiss, D.S. (2004) A predicted ABC transporter, FtsEX, is needed for cell division in *Escherichia coli*. *J Bacteriol* **186**: 785-793.
Schwedock, J., Mccormick, J.R., Angert, E.R., Nodwell, J.R., and Losick, R. (1997) assembly of the cell division protein Ftsz into ladder like structures in the aerial hyphae of *Streptomyces coelicolor*. *Mol. Microbiol.* **25**: 858.
Sharpe, M.E., and Errington, J. (1999) Upheaval in the bacterial nucleoid. An active chromosome segregation mechanism. *Trends Genet* **15**: 70-74.
Shih, Y.L., Le, T., and Rothfield, L. (2003) Division site selection in *Escherichia coli* involves dynamic redistribution of Min proteins within coiled structures that extend between the two cell poles. *Proc Natl Acad Sci U S A* **100**: 7865-7870.
Smyth, G.K., and Speed, T.P. (2003) Normalization of cDNA microarray data. *Methods*: 265-273.
Smyth, G.K. (2005) Limma: linear models for microarray data. In *Bioinformatics and Computational Biology Solutions using R and Bioconductor.* Gentleman, R., Carey, V., Dudoit, S., Irizarry, R. and Huber, W. (eds). New York: Springer, pp. 397-420.
Slovak, P.M., Wadhams, G.H., and Armitage, J.P. (2005) Localization of MreB in *Rhodobacter sphaeroides* under conditions causing changes in cell shape and membrane structure. *J Bacteriol* **187**: 54-64.
Soliveri, J.A., Gomez, J., Bishai, W.R., and Chater, K.F. (2000) Multiple paralogous genes related to the *Streptomyces coelicolor* developmental regulatory gene *whiB* are present in *Streptomyces* and other actinomycetes. *Microbiology* **146**: 333-343.
Soufo, H.J., and Graumann, P.L. (2003) Actin-like proteins MreB and Mbl from *Bacillus subtilis* are required for bipolar positioning of replication origins. *Curr Biol* **13**: 1916-1920.

Suefuji, K., Valluzzi, R., and RayChaudhuri, D. (2002) Dynamic assembly of MinD into filament bundles modulated by ATP, phospholipids, and MinE. *Proc Natl Acad Sci U S A* **99**: 16776-16781.
Takano, E., Tao, M., Long, F., Bibb, M.J., Wang, L., Li, W., Buttner, M.J., Deng, Z.X., and Chater, K.F. (2003) A rare leucine codon in adpA is implicated in the morphological defect of *bldA* mutants of *Streptomyces coelicolor*. *Mol Microbiol* **50**: 475-486.
Takano, E., Kinoshita, H., Mersinias, V., Bucca, G., Hotchkiss, G., Nihira, T., Smith, C.P., Bibb, M., Wohlleben, W., and Chater, K. (2005) A bacterial hormone (the SCB1) directly controls the expression of a pathway-specific regulatory gene in the cryptic type I polyketide biosynthetic gene cluster of *Streptomyces coelicolor*. *Mol Microbiol* **56**: 465-479.
Tan, H., Yang, H., Tian, Y., Wu, W., Whatling, C.A., Chamberlin, L.C., Buttner, M.J., Nodwell, J., and Chater, K.F. (1998) The *Streptomyces coelicolor* sporulation-specific sigma WhiG form of RNA polymerase transcribes a gene encoding a ProX-like protein that is dispensable for sporulation. *Gene* **212**: 137-146.
Tillotson, R.D., Wosten, H.A., Richter, M., and Willey, J.M. (1998) A surface active protein involved in aerial hyphae formation in the filamentous fungus *Schizophillum* commune restores the capacity of a bald mutant of the filamentous bacterium *Streptomyces coelicolor* to erect aerial structures. *Mol Microbiol* **30**: 595-602.
Traag, B.A., Kelemen, G.H., and Van Wezel, G.P. (2004) Transcription of the sporulation gene *ssgA* is activated by the IclR-type regulator SsgR in a whi-independent manner in *Streptomyces coelicolor* A3(2). *Mol Microbiol* **53**: 985-1000.
Tian, Y., Fowler, K., Findlay, K., Tan, H., and Chater, K.F. (2007) An Unusual Response Regulator Influences Sporulation at Early and Late Stages in *Streptomyces coelicolor*. *J Bacteriol* **189**: 2873-2885.
Ueda, K., Oinuma, K., Ikeda, G., Hosono, K., Ohnishi, Y., Horinouchi, S., and Beppu, T. (2002) AmfS, an extracellular peptidic morphogen in *Streptomyces griseus*. *J Bacteriol* **184**: 1488-1492.
Ukai, H., Matsuzawa, H., Ito, K., Yamada, M., and Nishimura, A. (1998) ftsE(Ts) affects translocation of K+-pump proteins into the cytoplasmic membrane of Escherichia coli. *J Bacteriol* **180**: 3663-3670.
van den Ent, F., Amos, L.A., and Lowe, J. (2001) Prokaryotic origin of the actin cytoskeleton. *Nature* **413**: 39-44.
van Wezel, G.P., van der Meulen, J., Kawamoto, S., Luiten, R.G., Koerten, H.K., and Kraal, B. (2000a) SsgA is essential for sporulation of *Streptomyces coelicolor* A3(2) and affects hyphal development by stimulating septum formation. *J Bacteriol* **182**: 5653-5662.
van Wezel, G.P., van der Meulen, J., Taal, E., Koerten, H., and Kraal, B. (2000b) Effects of increased and deregulated expression of cell division genes on the morphology and on antibiotic production of streptomycetes. *Antonie Van Leeuwenhoek* **78**: 269-276.
van Wezel, G.P., White J, Hoogvliet G, Bibb M.J. (2000c) Application of redD, the transcriptional activator gene of the undecylprodigiosin biosynthetic pathway, as a reporter for transcriptional activity in Streptomyces coelicolor A3(2) and Streptomyces lividans. *J Mol Microbiol Biotechnol* **2**:551-556.
van Wezel, G.P., and Vijgenboom, E. (2004) Novel aspects of signaling in *Streptomyces* development. *Adv Appl Microbiol* **56**: 65-88.
van Wezel, G.P., Mahr, K., Konig, M., Traag, B.A., Pimentel-Schmitt, E.F., Willimek, A., and Titgemeyer, F. (2005) GlcP constitutes the major glucose uptake system of *Streptomyces coelicolor* A3(2). *Mol Microbiol* **55**: 624-636.
van Wezel, G.P., Krabben, P., Traag, B.A., Keijser, B.J., Kerste, R., Vijgenboom, E., Heijnen, J.J., and Kraal, B. (2006) Unlocking *Streptomyces* spp. for use as sustainable industrial production platforms by morphological engineering. *Appl Environ Microbiol* **72**: 5283-5288.
Vicente, M., and Rico, A.I. (2006) The order of the ring: assembly of *Escherichia coli* cell division components. *Mol Microbiol* **61**: 5-8.
Vicente, M., Rico, A.I., Martinez-Arteaga, R., and Mingorance, J. (2006) Septum enlightenment: assembly of bacterial division proteins. *J Bacteriol* **188**: 19-27.
Vinella, D., Joseleau-Petit, D., Thevenet, D., Bouloc, P., and D'Ari, R. (1993) Penicillin-binding protein 2 inactivation in *Escherichia coli* results in cell division inhibition, which is relieved by FtsZ overexpression. *J Bacteriol* **175**: 6704-6710.
Wachi, M., and Matsuhashi, M. (1989) Negative control of cell division by *mreB*, a gene that functions in determining the rod shape of *Escherichia coli* cells. *J Bacteriol* **171**: 3123-3127.
Wang, L., Yu, Y., He, X., Zhou, X., Deng, Z., Chater, K.F., and Tao, M. (2007) Role of an FtsK-like protein in genetic stability in *Streptomyces coelicolor* A3(2). *J Bacteriol*.
Wang, X., Possoz, C., and Sherratt, D.J. (2005) Dancing around the divisome: asymmetric chromosome segregation in Escherichia coli. *Genes Dev* **19**: 2367-2377.
Ward, J.M., Janssen, G.R., Kieser, T., Bibb, M.J., and Buttner, M.J. (1986) Construction and characterisation of a series of multi-copy promoter- probe plasmid vectors for Streptomyces using the aminoglycoside phosphotransferase gene from Tn5 as indicator. *Mol Gen Genet* **203**: 468-478.
Wardell, J.N., Stocks, S.M., Thomas, C.R., and Bushell, M.E. (2002) Decreasing the hyphal branching rate of *Saccharopolyspora erythraea* NRRL 2338 leads to increased resistance to breakage and increased antibiotic production. *Biotechnol. Bioeng.* **78**: 141-146.
Wei, Y., Havasy, T., McPherson, D.C., and Popham, D.L. (2003) Rod shape determination by the *Bacillus subtilis* class B penicillin-binding proteins encoded by *pbpA* and *pbpH*. *J Bacteriol* **185**: 4717-4726.
White, J., and Bibb, M. (1997) *bldA* dependence of undecylprodigiosin production in *Streptomyces coelicolor* A3(2) involves a pathway-specific regulatory cascade. *J Bacteriol* **179**: 627-633.
Wildermuth, H. (1970) Development and organization of the aerial mycelium in *Streptomyces coelicolor*. *J Gen Microbiol* **60**: 43-50.
Wildermuth, H., and Hopwood, D.A. (1970) Septation during sporulation in *Streptomyces coelicolor*. *J Gen Microbiol* **60**: 51-59.
Willey, J., Santamaria, R., Guijarro, J., Geistlich, M., and Losick, R. (1991) Extracellular complementation of a developmental mutation implicates a small sporulation protein in aerial mycelium formation by *S. coelicolor*. *Cell* **65**: 641-650.
Withey, J.H., and Friedman, D.I. (2002) The biological roles of trans-translation. *Curr Opin Microbiol* **5**: 154-159.
Woodcock, D.M., Crowther, P.J., Doherty, J., Jefferson, S., DeCruz, E., Noyer-Weidner, M., Smith, S.S., Michael, M.Z., and Graham, M.W. (1989) Quantitative evaluation of *Escherichia coli* host strains for tolerance to cytosine methylation in plasmid and phage recombinants. *Nucleic Acids Res* **17**: 3469-3478.
Wu, L.J., and Errington, J. (2004) Coordination of cell division and chromosome segregation by a nucleoid occlusion protein in *Bacillus subtilis*. *Cell* **117**: 915-925.
Yamazaki, H., Ohnishi, Y., and Horinouchi, S. (2000) An A-factor-dependent extracytoplasmic function sigma factor (sigma(AdsA)) that is essential for morphological development in *Streptomyces griseus*. *J Bacteriol* **182**: 4596-4605.
Yamazaki, H., Ohnishi, Y., and Horinouchi, S. (2003) Transcriptional switch on of *ssgA* by A-factor, which is essential for spore septum formation in *Streptomyces griseus*. *J Bacteriol* **185**: 1273-1283.
Young, K.D. (2003) Bacterial shape. *Mol Microbiol* **49**: 571-580.
Yu, X.C., Weihe, E.K., and Margolin, W. (1998) Role of the C terminus of FtsK in *Escherichia coli* chromosome segregation. *J Bacteriol* **180**: 6424-6428.

CURRICULUM VITAE

Elke Noens was born on the 3rd of April 1979 in Kapellen (Belgium). In 1997, she obtained the diploma for secondary education at the Sint Lambertus Instituut (Ekeren, Belgium). In the same year, she started the study Medical Biochemistry at the University of Antwerp (Belgium). During the fourth and last year, she participated in an Erasmus exchange programme for six months, completing an internship in the department of Medical Microbiology, LUMC (Leiden, The Netherlands). In 2001, she obtained her Masters degree at the University of Antwerp (Belgium). During 2001-2002, she completed an internship in the Centre for Carbohydrate Chemistry, University of East Anglia (Norwich, UK) under the supervision of Prof. R.A. Field. In the summer of 2002, she started as a Ph.D. student at Leiden University. She worked under the supervision of Dr. G.P. van Wezel in Microbial Development (formerly Genexpress), LIC and Dr. H.K. Koerten in Electron Microscopy, MCB, LUMC. Prof. C.W.A. Pleij was her promotor. The work done as a Ph.D. student is presented in this thesis.

LIST OF PUBLICATIONS

BJ Keijser, **EE Noens**, B Kraal, HK Koerten and GP van Wezel. (2003) The *Streptomyces coelicolor ssgB* gene is required for early stages of sporulation. *FEMS Microbiol Lett.* **225** (1): 59-67.

A Piette, A Derouaux, P Gerkens, **EE Noens**, G Mazzucchelli, S Vion, HK Koerten, F Titgemeyer, E De Pauw, P Leprince, GP van Wezel, M Galleni, S Rigali. (2005) From dormant to germinating spores of *Streptomyces coelicolor* A3(2): new perspectives from the *crp* null mutant. *J Proteome Res.* **4** (5): 1699-708.

EE Noens, V Mersinias, BJ Traag, CP Smith, HK Koerten and GP van Wezel. (2005) SsgA-like proteins determine the fate of peptidoglycan during sporulation of *Streptomyces coelicolor. Mol. Microbiol.* **58**(4):929-44. (Including cover illustration)

P Mazza, **EE Noens**, K Schimer, N Grantcharova, AM Mommaas, HK Koerten, G Muth, K Flardh, GP van Wezel, W Wohlleben. (2006) MreB of Streptomyces coelicolor is not essential for vegetative growth but is required for the integrity of aerial hyphae and spores. *Mol Microbiol.* **60** (4):838-52.

S Rigali, L Nothaft, **EE Noens**, M Schlicht, S. Colson, M Muller, B Joris, HK Koerten, DA Hopwood, F Titgenmeyer and GP van Wezel. The sugar phosphotransferase system of *Streptomyces coelicolor* is regulated by the GntR-family regulator DasR and links N-acetylglucosamine metabolism to the control of development. *Mol. Microbiol.* **61**(5):1237-1251. (Including cover illustration)

EE Noens, V Mersinias, BA Traag, KF Chater, CP Smith, HK Koerten, GP van Wezel. *In vivo* localization and transcriptomic studies identify SsgA as an important developmental protein that controls early stages of sporulation-specific cell division in *Streptomyces coelicolor*. *Mol. Microbiol*. **64**(5): 1244-1259. (Including cover illustration)